11-17-2011

Geometric Structures on Matrix-valued Subdivision Schemes

James J. Smith
University of Missouri-St. Louis, jjsten29@gmail.com

Geometric Structures on Matrix-valued Subdivision Schemes

James J. Smith

M.A., Mathematics, University of Missouri-St. Louis, 2006

B.A., Mathematics, Washington University, St. Louis, 1972

A Thesis Submitted to The Graduate School at the University of Missouri-St. Louis in partial fulfillment of the requirements for the degree Doctor of Philosophy in Applied Mathematics

December 2011

Advisory Committee

Qingtang Jiang, Ph.D.
Chairperson

Charles K. Chui, Ph.D.

Wenjie He, Ph.D.

Henry Kang, Ph.D.

ABSTRACT

Surface subdivision schemes are used in computer graphics to generate visually smooth surfaces of arbitrary topology. Applications in computer graphics utilize surface normals and curvature. In this paper, formulas are obtained for the first and second partial derivatives of limit surfaces formed using 1-ring subdivision schemes that have 2 by 2 matrix-valued masks. Consequently, surface normals, and Gaussian and mean curvatures can be derived. Both quadrilateral and triangular schemes are considered and for each scheme both interpolatory and approximating schemes are examined. In each case, we look at both extraordinary and regular vertices. Every 3-D vertex of the refinement polyhedrons also has what is called a corresponding "shape vertex." The partial derivative formulas consist of linear combinations of surrounding polyhedron vertices as well as their corresponding shape vertices. We are able to derive detailed information on the matrix-valued masks and about the left eigenvectors of the (regular) subdivision matrix. Local parameterizations are done using these left eigenvectors and final formulas for partial derivatives are obtained after we secure detailed information about right eigenvectors of the subdivision matrix. Using specific subdivision schemes, unit normals so obtained are displayed. Also, formulas for initial shape vertices are postulated using discrete unit normals to our original polyhedron. These formulas are tested for reasonableness on surfaces using specific subdivision schemes. Obtaining a specified unit normal at a surface point is examined by changing only these shape vertices. We then describe two applications involving surface normals in the field of computer graphics that can use our results.

Acknowledgements

First and foremost, my utmost gratitude goes to Dr. Qingtang Jiang, my thesis advisor, for his kind and generous support from the very beginning. He encouraged me throughout the entire process and was a tremendous resource of knowledge in the field of subdivision surfaces. This would never have happened without him.

I also owe a big debt of thanks to Dr. Charles K. Chui for his expertise, enthusiastic support and unflagging good humor. His articles and publications proved to be absolutely invaluable.

In addition, I would like to thank the other members of my committee, Drs. Wenjie He and Henry Kang, for their generous participation and feedback.

I would be remiss if I did not mention Michael Schulte, associate teaching professor at the University of Missouri St. Louis, for his kind help in all matters related to the computer. Also, I must thank Kimberly Stanger, administrative assistant in the Mathematics and Computer Science Department, for her wise direction in navigating the roads of academia.

While she was here at The University of Missouri St. Louis, Dr. Weiwei Zhu, currently at University of Maryland Eastern Shore, was enthusiastic in her support of my research and provided great advice when I needed guidance in writing computer algorithms.

My late parents, John and Adele, instilled in me the value of learning and hard work. For that and much more, I thank them.

Finally, I wish to express my thanks to my friends and family who supported me throughout and put up with my obsessive behavior. Here I must mention my sister, Barbara Bowen, who has been a cheerleader for me for several years now. And, last of all, but certainly not least, I thank my partner, Calvin Chandler, for his patient tolerance and unwavering support.

Table of Contents

ABSTRACT i

Acknowledgements ii

List of Tables vi

List of Figures vii

Chapter 1. Introduction 1

1.1. General Background 1

1.2. Brief History of Subdivision Schemes 1

1.3. Scalar-valued Masks 4

1.4. Matrix-valued Masks 6

1.5. Dissertation Outline 7

Chapter 2. Preliminaries and Notations 8

2.1. Notations and Definitions 8

2.2. Matrix-valued Subdivision Schemes 12

2.3. Sum Rule Order and Other Assumptions 15

2.4. Sobolev Smoothness Determination 21

Chapter 3. Derivative Formulas for Interpolating Triangular Subdivision Schemes 23

3.1. Introduction 23

3.2. Development of general derivative formulas 25

3.3. First Partial Derivatives(Regular) 25

3.4. Second Partial Derivatives (Regular) 32

3.5. First Partial Derivatives (Extraordinary) 35

3.6. Partial Derivatives in Terms of Initial Control Net 43

3.7. Specific Template 49

Chapter 4. Derivative Formulas for Interpolating Quadrilateral Subdivision Schemes 56
4.1. Introduction 56
4.2. First Partial Derivatives (Regular) 58
4.3. Second Partial Derivative (Regular) 63
4.4. First Partial Derivatives (Extraordinary) 65
4.5. Partial Derivatives in Terms of Initial Control Net 76
4.6. Specific Template 83

Chapter 5. Derivative Formulas for Approximating Triangular and Approximating Quadrilateral Schemes 89
5.1. Additional Assumptions 89
5.2. Templates with Sum Rule Order 92
5.3. Development of general formulas (Regular case: Triangular and Quadrilateral) 94
5.4. Partial Derivatives as Linear Combination of Initial Control Points 110
5.5. First Partial Derivatives: Approximating Extraordinary Case 127

Chapter 6. Shape Parameters 144
6.1. Background 144
6.2. Definition based on discrete normal 145
6.3. Discrete Normal for Triangular Mesh Surfaces 146
6.4. Discrete Normal for Quadrilateral Mesh Surfaces 150
6.5. Formulation of Shape Parameters for Triangular Meshes 152
6.6. Formulation of Shape Parameters for Quadrilateral Meshes 161
6.7. Illustration of Shape Parameter Definitions Using Matlab®, 164

Chapter 7. Surface Normals and Curvature 172
7.1. Normal and Curvature Formulas 172
7.2. Achieving a specific normal at a point 173

Chapter 8. Applications Involving Surface Normals 179
8.1. Lighting and Shading Models 179
8.2. Bump Mapping 185
8.3. Potential to Use Matrix-valued Schemes for these Applications 187

Chapter 9. Conclusions and Future Work 188

References 191

Appendix A 198

Appendix B 202

Appendix C 204

Appendix D 213

Appendix E 218

Appendix F 221

Appendix G 229

List of Tables

4.1 Values of $\frac{1}{4\lambda-1}$ for several valences 74

List of Figures

2.1	Template for triangular and quad schemes	15
3.1	Three directional mesh for triangular scheme	24
3.2	Ordering of vertices in regular triangular scheme	27
3.3	Extraordinary Vertex Template (triangular)	36
3.4	Vertices around the central extraordinary vertex of valence 7	40
3.5	Representation of F_s and F_t (interp. triangular)	51
3.6	Representation of F_{ss} and F_{tt} (interp. triangular)	53
3.7	Representation of F_{st} (interp. triangular)	54
3.8	Representation of F_s and F_t (interp. tri. extraordinary)	55
4.1	Two-directional mesh for Quadrilateral subdivisions	57
4.2	Ordering of vertices in regular quadrilateral scheme	59
4.3	Extraordinary template. (quadrilateral scheme)	67
4.4	Parametrization of Quad Extraordinary Scheme	75
4.5	F_s and F_t in regular interp. quad scheme	84
4.6	F_{ss} and F_{tt} in regular interp. quad scheme	85
4.7	F_{st} in regular interp. quad scheme	85
4.8	Representation of F_s and F_t for specific quad interp extraord. scheme	87
4.9	Interpolating Quadrilateral Subdivision Scheme Figure	88
4.10	Quadrilateral interpolatory figure	88
5.1	Representation of F_s and F_t (approx. triangular)	116

5.2 Representation of F_{ss} , and F_{tt} (approx. triangular) 117
5.3 Representation of F_{st} (approx. triangular) 118
5.4 Representation of F_s and F_t (approx. quadrilateral) 124
5.5 Representation of F_{ss} and F_{tt} (approx. quadrilateral) 125
5.6 Representation of F_{st} (approx. quadrilateral) 126
5.7 Parametrization in extraordinary approx. tri case 129
5.8 Representation of F_s and F_t (Extraordinary triangular appr.) 138
5.9 Representation of F_s and F_t (Extraordinary quad approximating) 141
5.10 Approximating quadrilateral scheme: Original Polyhedron 142
5.11 Approximating quadrilateral surface 143
5.12 Approximating quadrilateral scheme: Closeup of subdivision surface 143

6.1 Drawing showing method in [**Yan05**] 146
6.2 Area Used in Adjoining Triangle in [**MDSB02**] 148
6.3 Angles opposite common side from [**MDSB02**] 149
6.4 Diagram of quadrilaterals around vertex from [**LXZ08**] 151
6.5 New edge vertex (triangular scheme) 153
6.6 Shape parameters as norma vectors [tri case 157
6.7 Original Triangular Polyhedron 158
6.8 Triangular subdivision with $\omega = .10$ 159
6.9 Triangular subdivision with $\omega = .25$ 159
6.10 Triangular subdivision with $\omega = .50$ 160
6.11 Diagram showing how central extraordinary vertex is updated. (quad extraordinary case) 163
6.12 Original polyhedron used for the following figures 165
6.13 Approximating scheme with $\omega = .25$ 165
6.14 Top view for approximating scheme where $\omega = .25$ 166

6.15	Interpolatory scheme with $\omega = .25$	166
6.16	Top view for interpolatory scheme with $\omega = .25$	167
6.17	Approximating scheme with $\omega = .4$	167
6.18	Top view of approximating scheme with $\omega = .4$	168
6.19	Interpolatory scheme with $\omega = .4$	168
6.20	Top view of interpolatory scheme with $\omega = .4$	169
6.21	Approximating scheme with $\omega = .8$	169
6.22	Top view of approximating scheme with $\omega = .8$	170
6.23	Interpolatory scheme with $\omega = .8$	170
6.24	Top view of interpolatory scheme with $\omega = .8$	171
7.1	Lattice in direct search with $n = 2$	176
8.1	Representation of Lambert and Phong Illumination	181
8.2	Bilinear Interpolation of Shading Attributes	184
9.1	"Characteristic" map for Valences 3 and 5	202
9.2	"Characteristic" map for Valences 7 and 9	202
9.3	"Characteristic" map for Valences 11 and 13	203
9.4	Values of M_{121} where first coordinate $=\pm\frac{1}{2}$	206
9.5	Box spline M_{211}	212
9.6	Box spline M_{113}	212
9.7	Box spline M_{112}	213
9.8	"Characteristic" maps for Valences 3 and 5: Quad Approx	218
9.9	"Characteristic" maps for Valences 6 and 7: Quad Approx	218
9.10	"Characteristic" maps for Valences 8 and 9: Quad Approx	219
9.11	"Characteristic" maps for Valences 10 and 11: Quad Approx	219
9.12	"Characteristic" maps for Valences 12 and 13: Quad Approx	219

9.13 “Characteristic” maps for Valences 14, 15 and 16: Quad Approx 220
9.14 Normal at regular vertex: Interp Tri 221
9.15 Normals at valence 5 vertex: Tri Interp 222
9.16 Interp Quad: Normal at regular vert 223
9.17 Interp Quad: “Top View” of nrml at reg vertex 223
9.18 Interp Quad: Normal at vertex of valence 3 224
9.19 Interp Quad: “Top View” of nrml at vertex of val 3 224
9.20 Approx tri: normal at regular vertex 225
9.21 Approx tri: Another view of normal at reg vert 225
9.22 Approx Tri: Normal at vert of valence 4 226
9.23 Approx tri: Another view of normal at vert of valence 4 226
9.24 Approx quad: Normal at regular vert 227
9.25 Approx Quad: Top view of normal at reg vert 227
9.26 Approx quad: Normal at vert of valence 3 228
9.27 Approx Quad: “Top view” of normal at vert of valence 3 228
9.28 Approximating quad scheme: Larger angle between desired and “usual” normal 229
9.29 Approximating quad figure: Smaller angle between desired normal and “usual” normal 230
9.30 Interpolatory quadrilateral figure: Larger angle between desired normal and “usual” normal. 231
9.31 Interpolatory quad figure: Smaller angle between desired normal and “usual” normal 232
9.32 Approximating triangular scheme: Larger angle between desired normal and “usual” normal 232
9.33 Approximating triangular scheme: Smaller angle between desired normal and “usual” normal 233
9.34 Interpolatory triangular figure: Larger angle between desired normal and “usual” normal 233

9.35 Interpolatory triangular figure: Smaller angle between desired normal and "usual" normal 234

CHAPTER 1

Introduction

Based on certain assumptions we will be building easy-to-implement formulas for the first and second partial derivatives of what is called a refinable function. This function can be used to quickly generate a discrete approximation to a target surface, called a subdivision surface. These formulas will be based solely on certain right eigenvectors and what are called the control and shape vertices of the original control net. From such formulas one can then obtain unit surface normals and other geometric information such as gaussian curvature. We will show a method for defining what are called the shape parameters and demonstrate how such shape parameters can change the normals of the target surface.

1.1. General Background

Subdivision is a powerful mechanism for the construction of smooth curves and surfaces. More specifically, it is an algorithmic method for surface generation that produces smooth surfaces by repetitively applying a set of rules to an initial mesh or control net. As a result of the algorithm, a sequence of meshes are produced, which generally converge to a limit surface, called the subdivision surface. Application settings range from industrial design and animation to scientific visualization and simulation. Subdivision surfaces are used increasingly in high end animation production (e.g. Pixar), game engines and are provided in many popular modeling programs (e.g. Maya, Mirai, 3D Studio Max, etc.).

1.2. Brief History of Subdivision Schemes

Subdivision schemes go back to papers published by G. de Rham in 1947 and 1956 and by G.M. Chaikin in 1974 [**PR08**],[**dR47**],[**dR56**],[**Cha74**].

Here "corner cutting" routines were applied to "smooth out" polygonal lines. Rham evenly trisected each edge to produce two new vertices and Chaikin trisected each edge in a 1:2:1 ratio to produce new vertices. In Chaikin's algorithm quadratic B-spline curves were produced [**Asp03**]. Using subdivision schemes to produce B-spline curves led to tensor-product B-spline surfaces. But in order to design surfaces that have an arbitrary topology irregular points and faces were needed in the initial control net. In the context of tensor-product spline surfaces, these would be points that had a valence other than 4 or faces that had other than 4 sides. Such surfaces were first introduced in 1978 by Edwin Catmull and Jim Clark [**CC78**] and also by Daniel Doo and Malcolm Sabin [**DS78**]. The Catmull-Clark and Doo-Sabin schemes extended to general control meshes the tensor-product cubic B-spline and quadratic B-spline schemes respectively [**PR08**]. In [**DS78**] matrix multiplication was employed to describe the subdivision process and eigenanalysis of this matrix was used to analyze the surface at the irregular (extraordinary) vertices. In 1987, Charles Loop, in his Masters' thesis, described a subdivision scheme defined over a grid of triangles (as opposed to quadrilaterals)[**Loo87**]. Loop demonstrated that eigenanalysis could be utilized to decide upon the coefficients to be used in the template of an extraordinary point.

Another significant publication in 1987 was the description by Nira Dyn, David Levin and John Gregory of their four-point curve scheme [**DLG87**]. This was new in that it was an interpolatory scheme, rather than an approximating one, and in that the limit curve did <u>not</u> consist of parametric polynomial pieces. Here, the mask of the subdivision scheme (a finite number of coefficients which defined the method of refinement) was used to determine the existence and the smoothness qualities of the limit of the scheme. We also see the use of linear combinations of eigenvectors to provide a representation of certain neighboring points on a piecewise linear approximation to a curve. Formulas for first derivatives are obtained with a method similar to what we propose to use later. See Figures 3.5, 3.6 and 3.7 on pages 51, 53 and 54 for our first partial derivative formulas for an interpolatory triangular scheme.

In 1990 Dyn et al expanded the same type of analysis to surfaces when they developed the “Butterfly” interpolatory scheme [**DGL90**].

Tools that were developed to analyze the convergence of schemes and the smoothness of limit curves and surfaces included [**PR08**]:

- the notion of “derived subdivision schemes” obtained from the differences and the divided differences of control points [**DLG91**]
- the notion of a *symbol* of a scheme that replaces the mask coefficients by a Laurent polynomial [**CDM91**]
- the notion of the “contractivity” of a subdivision scheme to check for convergence [**CDM91**]

Algebraic manipulation of the Laurent polynomials that result from these “symbols” led to *sufficient* conditions for a scheme to have a certain level of derivative continuity [**DLM90**]. (Note that, previously, the eigenanalysis had only provided *necessary* conditions.)

In [**Dyn92**] Dyn extended the analysis in [**DLG91**] to the convergence and smoothness of multivariate subdivision schemes. Such schemes used matrices instead of scalars in their masks. They converged to function vectors. In [**Str96**] multiwavelets were constructed from refinable function vectors that had matrix-valued masks.

In 1995 Ulrich Reif developed the notion of the characteristic map to assist in the analysis of the level of derivative continuity at extraordinary points [**Rei95**].

Later schemes that have been developed include Kobbelt's $\sqrt{3}$ scheme where a triangular grid becomes denser by the insertion of a new point in the middle of each triangle, the old edges disappear and are replaced by new ones joining each new point to the corners of its triangle and to the neighboring new points [**Kob00**]. This scheme has small support and is C^2 except at extraordinary points where it is C^1. Also in 2001 Luiz Velho and Denis Zorin developed the 4-8 subdivision that generalized the four-directional box spline of continuity class C^4 to surfaces of arbitrary topology [**VZ01**]. In 2004 Guiqing Li and Weiyin Ma developed the $\sqrt{2}$ subdivision scheme for quadrilateral meshes. This scheme can be regarded as an extension of the 4-8 subdivision scheme [**LMB04**]. It produces surfaces of the same smoothness and is computationally more efficient. Of course this list of subdivision schemes is not all-inclusive.

1.3. Scalar-valued Masks

Subdivision schemes are formulated in terms of certain templates of numerical (scalar) values that are used as weights for taking weighted averages of certain given "old" vertices (points in $\mathbb{R}^3$) for the purpose of generating new vertices, and perhaps to move the positions of the old vertices as well. It yields a higher resolution of some discrete approximation to the target (subdivision) surface for each application (iteration) of the weighted averages. If the old vertices are not altered for each iteration, the subdivision scheme is called an interpolatory scheme. Otherwise, it is called an approximation scheme. Subdivision templates are displayed in two dimensional space as certain triangles or quadrilaterals with certain weights attached to each vertex. For regular vertices (also called ordinary vertices) these triangles and quadrilaterals lie on 3-directional or 2-directional meshes since the valences of regular vertices are 6 and 4 respectively [**CJ03b**].

Surface subdivision templates for regular vertices are derived from the refinement equation of some bivariate refinable function with a finite refinement sequence. The refinement sequence is called the "subdivision mask" of the subdivision scheme. A refinable function ϕ is one that has the following quality:

$$\phi(\mathbf{x}) = \sum_{\mathbf{k}\in\mathbb{Z}^2} p_{\mathbf{k}} \phi(A\mathbf{x} - \mathbf{k}) \quad \mathbf{x} \in \mathbb{R}^2 \tag{1.1}$$

where A is some dilation matrix and $\{p_{\mathbf{k}}\}_{\mathbf{k}}$ is the (finite) subdivision mask. It can be shown that the subdivision mask sums to $|\det(A)|$. The selection of the dilation matrix A depends on what is commonly called the "topological rule". The most commonly used rule is the "1-to-4 split" that dictates the split of each triangle or square in the parametric domain into four sub-triangles or four sub-squares by connecting the mid-points of the appropriate edges. Also a "face point" is introduced when the mid-points of the opposite edges of a square are connected. The new vertices introduced in the parametric domain correspond to new vertices in $\mathbb{R}^3$ when the templates are applied to take weighted averages [**CJ05**]. Most of the well-known surface subdivision schemes such as Loop's scheme and the Catmull-Clark scheme use the 1-to-4 split topological rule. For the 1-to-4 split rule, the dilation matrix in the refinement equation is $2I_2$. Other topological rules are the $\sqrt{3}$ and $\sqrt{2}$ rules with dilation matrices given by

$$A_1 = \begin{bmatrix} 2 & -1 \\ 1 & -2 \end{bmatrix} \text{ and } A_2 = \begin{bmatrix} 1 & 1 \\ 1 & -1 \end{bmatrix}$$

respectively [**CJ05**].

To apply a subdivision scheme, one must first select certain desirable points in $\mathbb{R}^3$ as well as connect these points to form a triangular or quadrilateral mesh. So the points thus chosen are vertices of triangles or quadrilaterals. These points are called "control vertices" and the triangular or quad meshes are called "control meshes" or "control nets". For a control mesh with just regular initial control vertices $v^0_{\mathbf{k}}$ (i.e. their valences are equal to 6 or 4 respectively) the refinement equation (1.1 |p.4) yields a "local averaging rule":

$$v^{m+1}_{\mathbf{k}} = \sum_{\mathbf{j}} v^m_{\mathbf{j}} p_{\mathbf{k}-A\mathbf{j}} \qquad m = 0, 1, ... \tag{1.2}$$

where $v^m_{\mathbf{k}}$ denote the set of newly generated points in $\mathbb{R}^3$ after applying the local averaging rule m times (or using the corresponding subdivision templates to perform m iterations).

The target subdivision surface is precisely given by

$$f(\mathbf{x}) = \sum_{\mathbf{k}} v^0_{\mathbf{k}} \phi\left(\mathbf{x} - \mathbf{k}\right) \qquad \mathbf{x} \in \mathbb{R}^2$$

with the initial control vertices as coefficients [**CJ05**]. We can thus see that the smoothness of the limiting surface is reflected by the smoothness of the refinable function $\phi\left(\mathbf{x}\right)$.

Note that from (1.2 |p.5) one can obtain what is called the subdivision matrix S where

$$S = \left(p_{A\mathbf{j}-\mathbf{k}}\right)_{\mathbf{j},\mathbf{k}} \qquad \text{and } \mathbf{v}^{m+1} = \mathbf{v}^m S$$

A similar subdivision matrix can be constructed from the templates involving extraordinary vertices. The eigenstructure of both these matrices can tell us quite a bit about the smoothness of the subdivision scheme [**CJ06**].

1.4. Matrix-valued Masks

Since the early 90's work has been done with refinable function vectors in the field of multiwavelets [**Dyn92**], [**Str96**]. See (2.5 |p.12) for a representation of a refinement equation with a refinable function vector. Notice that the mask consists of matrices. Very briefly, wavelets (which classically use a scaling function ϕ) make large data sets more manageable. Among other areas, they have been used as a basis set of approximating functions and operators, in image processing, in processing music, speech and other acoustic signals, and for displaying 2-dimensional geographic data [**Kob98**]. Multiwavelets utilize refinable function vectors and have the advantages of shorter support and higher approximation orders than scalar wavelets [**Kei03**].

In recent years Chui and Jiang have done work on matrix-valued subdivision masks [**CJ03b**][**CJ08**][**CJ06**]. Some of the benefits they have found include:

- the introduction of a parameter (called the shape parameter) that can control and change the shape of the final subdivision surface
- the two components of a refinable vector-valued spline function can be reformulated (by taking certain linear combinations of each) in order to convert an approximation scheme into an interpolatory scheme (at the expense, however, of an increase in the template size).
- C^2 1-ring (non-spline) interpolating schemes (i.e. C^2 at regular vertices)

The schemes developed by Chui and Jiang are C^2 on regular vertices (regular surface areas) and the conditions for C^1 smoothness are maintained at the extraordinary vertices via the use of eigenanalysis of the subdivision matrix through DFT (Discrete Fourier transform) techniques.

Here we will be working exclusively with refinable function vectors and matrix-valued masks.

1.5. Dissertation Outline

In Chapter 2 we will list notations used throughout and give the assumptions used to build our formulas for first and second partial derivatives. Chapter 3 will develop these partial derivatives for a 1-ring interpolatory triangular scheme in terms of the initial control net. Chapter 4 will do likewise for a 1-ring interpolatory quadrilateral scheme. In Chapter 5 we will cover both triangular and quadrilateral *approximating* schemes.

We then proceed to a formulation of the initial shape parameters (Chapter 6) using discrete normals. Chapter 7 covers normals and curvature. In particular, it deals with achieving a specific normal at a surface point. In Chapter 8 we look at two applications of surface normals in the field of computer graphics. One is their use in surface lighting and the other is their use in texturizing a surface (bump maps). Conclusions are provided in Chapter 9. Several appendices follow.

CHAPTER 2

Preliminaries and Notations

In this chapter we will do the following:

- introduce notation used throughout the paper
- provide needed definitions
- review the notion of a refinable vector-valued function
- discuss sum rule order and provide assumptions used throughout
- outline a method to determine Sobolev smoothness

2.1. Notations and Definitions

We will now introduce some notations used in this paper. Let $\mathbb{Z}_+$ denote the set of all nonnegative integers. And so let $\mathbb{Z}_+^d$ denote the set of all d-tuples of nonnegative integers. The following multi-index notations will be adopted:

$$\omega^\beta := \omega_1^{\beta_1} \dots \omega_d^{\beta_d}, \quad \beta! := \beta_1! \dots \beta_d!, \quad |\beta| := \beta_1 + \dots + \beta_d$$

for $\omega = (\omega_1, \dots, \omega_d)^t \in \mathbb{R}^d, \beta = (\beta_1, \dots, \beta_d)^t \in \mathbb{Z}_+^d$.

If $\alpha, \beta \in \mathbb{Z}_+^d$ satisfy $\beta - \alpha \in \mathbb{Z}_+^d$ then we will say that $\alpha \le \beta$ and denote

$$\binom{\beta}{\alpha} := \frac{\beta!}{\alpha!\,(\beta-\alpha)!}$$

For $\beta = (\beta_1, \dots, \beta_d)^t \in \mathbb{Z}_+^d$ let

$$D^\beta := \frac{\partial^{\beta_1}}{\partial x_1^{\beta_1}} \dots \frac{\partial^{\beta_d}}{\partial x_d^{\beta_d}}$$

where $\partial_j = \frac{\partial}{\partial x_j}$ is the partial derivative operator with respect to the jth coordinate for $1 \le j \le d$.

For ease of notation later on define

$$D_j := \frac{\partial}{\partial x_j} \tag{2.1}$$

Hence

$$D^{\beta} := D_1^{\beta_1}...D_d^{\beta_d} \tag{2.2}$$

For $\mathbf{y} := (y_1, y_2)^T \in \mathbb{R}^2 \backslash \{\mathbf{0}\}$ denote the directional derivative in the direction of $\mathbf{y}$ as

$$D_{\mathbf{y}} := y_1 D_1 + y_2 D_2$$

and the second order directional derivative in the direction of $\mathbf{y}$ as

$$D_{\mathbf{y}}^2 := y_1^2 D_1^2 + 2y_1 y_2 D_1 D_2 + y_2^2 D_2^2$$

Note that

$$D_{(1,0)^T} = D_1 = D^{(1,0)^T}$$
$$D_{(0,1)^T} = D_2 = D^{(0,1)^T}$$

With that said, there will be instances in which the first and second partial derivative of a function F will be represented as F_s, F_t, F_{ss}, F_{st}, etc where s and t represent the variables of the first and second coordinates respectively.

For a finite collection $\mathbf{X} = \{\mathbf{x}_1, \mathbf{x}_2, ..., \mathbf{x}_n\}$ of vectors in $\mathbb{R}^s$, define the span of $\mathbf{X}$

$$\langle \mathbf{X} \rangle := \gamma_1 \mathbf{x}_1 + \gamma_2 \mathbf{x}_2 + ... + \gamma_n \mathbf{x}_n \qquad \text{where } \gamma_1, \gamma_2, ..., \gamma_n \in \mathbb{R}$$

The $d \times d$ matrix A is *isotropic* if $\exists\, \Lambda$ ($d \times d$ invertible matrix) and $\sigma = (\sigma_1, ..., \sigma_d)$ such that

$$\Lambda A \Lambda^{-1} = diag\,(\sigma_1, ..., \sigma_d) \tag{2.3}$$

where

$$|\sigma_1| = |\sigma_2| = ... |\sigma_d| := \text{spectral radius of } A$$

If A is an $m \times n$ matrix and B is a $p \times q$ matrix then we say the Kronecker product $A \otimes B$ is the $mp \times nq$ block matrix

$$A \otimes B := \begin{bmatrix} a_{11}B & \cdots & a_{1n}B \\ \vdots & \ddots & \vdots \\ a_{m1}B & \cdots & a_{mn}B \end{bmatrix}$$

Also let π_d^s denote the space of all polynomials in $\mathbb{R}^s$ of total degree d.

For $1 \leq p \leq \infty$ we denote by $L_p\left(\mathbb{R}^d\right)$ the Banach space of all (complex-valued) measurable functions f on $\mathbb{R}^d$ such that $\|f\|_p < \infty$ where

$$\|f\|_p := \left(\int_{\mathbb{R}^d} |f(x)|^p \, dx\right)^{1/p}$$

For an $r \times 1$ vector-valued function $f = (f_1 \ldots, f_r)^t$, we say that f is in some space on $\mathbb{R}^d$ if every component f_i of f is in that space. In particular, such an $f \in L_2\left(\mathbb{R}^d\right)$ means that each component $f_i \in L_2\left(\mathbb{R}^d\right)$.

Also, for such a vector-valued function f, its Fourier transform $\widehat{f} := \left(\widehat{f_1} \ldots, \widehat{f_r}\right)^t$ where

$$\widehat{f}(\xi) := \int_{\mathbb{R}^d} f(x)\, e^{-ix\cdot\xi} dx, \qquad \xi \in \mathbb{R}^d$$

and where $x \cdot \xi$ denotes the inner product of two vectors x and ξ in $\mathbb{R}^d$.

For $v \geq 0$, denote by $W_2^v(\mathbb{R}^s)$ the Sobolev space [**Jia99**] of all functions $f \in L_2(\mathbb{R}^s)$ such that

$$\int_{\mathbb{R}^s} \left|\widehat{f}(\xi)\right|^2 (1 + |\xi|^v)\, d\xi < \infty$$

The smoothness of an $r \times 1$ vector function $\Psi = (\psi_1, \psi_2, ..., \psi_r)^T$ where $\psi_i \in L_2(\mathbb{R}^s)$ is measured by the *critical exponent* $\lambda(\Psi)$ defined as [**JO03**] :

$$\lambda(\Psi) := \sup\left\{\lambda : \psi_j \in W_2^\lambda(\mathbb{R}^s) \quad \forall\, j = 1, ..., r\right\} \tag{2.4}$$

The Sobolev embedding theorem [**Mel02**] states that for $n \in \mathbb{N}_0$ and $v > \frac{s}{2} + n$ then $W_2^v(\mathbb{R}^s) \subset C^n(\mathbb{R}^s)$.

Since here $s = 2$ the Sobolev embedding theorem reverts to

$$\text{for } n \in \mathbb{N}_0 \quad \textit{and} \quad v > 1 + n \quad W_2^v\left(\mathbb{R}^2\right) \subset C^n\left(\mathbb{R}^2\right)$$

If A is a matrix of size $n \times n$ then (where I_n is the $n \times n$ identity matrix) the polynomial

$$\det(A - \lambda I_n)$$

is a polynomial of degree n. The roots of this polynomial are the eigenvalues of A. If λ_j is a root then the algebraic multiplicity of λ_j is the multiplicity of the root in the polynomial. Call this number k. If p denotes the number of linearly independent eigenvectors associated with λ_j then p is the geometric multiplicity of λ_j. It is known that $p \leq k$. But if $p < k$ then we say that the eigenvalue λ_j is defective.

In such cases, A is called a defective matrix. It has fewer linearly independent eigenvectors than eigenvalues (counting algebraic multiplicity). Generalized eigenvectors are needed to form a complete basis for A. A generalized eigenvector is a nonzero vector $\mathbf{v}$, which is associated with λ_j having algebraic multiplicity $k \geq 1$, satisfying

$$(A - \lambda_j I_n)^k \mathbf{v} = \mathbf{0}$$

The following definitions are from [**O'N06**] :

(1) We say that a *surface* in $\mathbb{R}^3$ is a subset M of $\mathbb{R}^3$ such that for each point $\mathbf{p}$ of M there exists a proper patch in M whose image contains a neighborhood of $\mathbf{p}$ in M.

(2) We say that a *proper patch* is a mapping $\mathbf{x} : D \to \mathbb{R}^3$ that is one-to-one and regular (where D is an open set of $\mathbb{R}^2$) and for which the inverse function $\mathbf{x}^{-1} : \mathbf{x}(D) \to D$ is continuous.

(3) We say that a mapping $\mathbf{x}$ is *regular* if $\mathbf{x}_u$ and $\mathbf{x}_v$ give a basis for the tangent plane of M at each point of $\mathbf{x}\,(D)$.

(4) If $\mathbf{p}$ is a point of M then for each tangent vector $\mathbf{v}$ to M at $\mathbf{p}$ then we say that the *shape operator* of M is defined as$S_p\,(\mathbf{v}) := -\nabla_v U$ where U is a unit normal vector field on a neighborhood of $\mathbf{p}$ in M and ∇_v is the directional derivative.

(5) For any unit vector $\mathbf{u}$ tangent to the surface M at point $\mathbf{p}$ we define the *normal curvature* of M in the $\mathbf{u}$ direction as: $k\,(\mathbf{u}) := S\,(\mathbf{u}) \cdot \mathbf{u}$

(6) The *Gaussian curvature* at point $\mathbf{p}$ on M is defined as $K := k_1 k_2 K := k_1 k_2$ where k_1 and k_2 are the maximum and minimum values of $k\,(\mathbf{u})$ at $\mathbf{p}$.

(7) The *quadratic approximation* of M near $\mathbf{p}$ is: $M' := \frac{1}{2}\left(k_1 u^2 + k_2 v^2\right)$.

We have *non-degenerate curvature continuity* if we have such a quadratic approximation at every point $\mathbf{p}$. [**Loo01**]

2.2. Matrix-valued Subdivision Schemes

Reformulating (1.1 | p.4) for a vector function, an r x 1 vector of functions Φ is called refinable if there exists an s x s dilation matrix A (meaning that the eigenvalues have modulus > 1) and a (finite) subdivision "mask" P_k consisting of r x r matrices such that

$$\Phi(\mathbf{x}) = \sum_{\mathbf{k}\in\mathbb{Z}^s} P_{\mathbf{k}}\Phi(A\mathbf{x} - \mathbf{k}), \quad \mathbf{x} \in \mathbb{R}^s \tag{2.5}$$

Note that we will only be working with $s = 2$, i.e. $\Phi(\mathbf{x})$ is defined on $\mathbb{R}^2$. Also the dilation matrix A will be restricted to $2I_2$. Use of $2I_2$ means that we will be using the most commonly used topological rule that we previously noted is called the "1-to-4 split" (dyadic) rule. Regular vertices in triangular schemes are vertices with valence 6 (6 adjacent vertices) and regular vertices in quad schemes are vertices with valence 4. Otherwise, the vertices are labeled "extraordinary" vertices. Both triangular and quadrilateral schemes will be examined.

For the sake of simplicity we will also restrict $r = 2$ in (2.5 |p.12). Thus $\Phi = (\phi_1, \phi_2)^T$ where ϕ_1, ϕ_2 map from $\mathbb{R}^2$ to $\mathbb{R}$. Also the support of the finite mask $P_{\mathbf{k}}$ is such that $P_{\mathbf{k}} = \mathbf{0}$, $\mathbf{k} \notin [-N, N]^2$ for some positive integer N.

Our initial control net is a collection of vertices $\{v^0_{\mathbf{k}}\}_{\mathbf{k}}$in $\mathbb{R}^3$ that belong to what is called a "simplicial complex" [**Zor00a**]. A simplicial complex is a set of vertices, edges and triangles (or quadrilaterals) in $\mathbb{R}^3$ such that for any triangle (quadrilateral) all its sides are in the complex and for any edge its endpoints are vertices in the complex. No isolated vertices or edges are assumed, that is, every vertex is an endpoint of an edge and every edge is a side of a triangle (quadrilateral). Each vertex in the initial control net is associated with a $3 \times r$ (here $r = 2$) vector $\mathbf{v}^0_{\mathbf{k}}$ where

$$\mathbf{v}^0_{\mathbf{k}} := \left[v^0_{\mathbf{k}},\, s^0_{\mathbf{k}}\right] \tag{2.6}$$

The collection of these $\{\mathbf{v}^0_{\mathbf{k}}\}_{\mathbf{k}}$ are called our "initial control vector net." We can obtain subsequent generations of vector nets using the following algorithm called the "local averaging rule."[**CJ06**] Under certain assumptions, as we shall shortly see, after m iterations of (2.7 |p.13) the first components $v_{\mathbf{k}}^m$ of these subsequent vector nets provide an accurate discrete approximation of a target (subdivision) surface (2.9 |p.13) . Thus one can effectively render a surface in three-dimensional space (3-D).

The local averaging rule is:

$$\mathbf{v}_{\mathbf{k}}^{m+1} = \sum_{\mathbf{j}\in\mathbb{Z}^2} \mathbf{v}_{\mathbf{j}}^m P_{\mathbf{k}-2\mathbf{j}}, \quad m = 0, 1, \ldots, \tag{2.7}$$

where

$$\mathbf{v}_{\mathbf{k}}^m := [v_{\mathbf{k}}^m,\, s_{\mathbf{k}}^m] \tag{2.8}$$

It is shown in [**CJ06**] that the generated subdivision surface is precisely given by

$$F(\mathbf{x}) = \sum_{\mathbf{k}} v_{\mathbf{k}}^0 \phi_1(\mathbf{x}-\mathbf{k}) + \sum_{\mathbf{k}} s_{\mathbf{k}}^0 \phi_2(\mathbf{x}-\mathbf{k}) \tag{2.9}$$

The natural question to be asked is what is the purpose of the second component of (2.6 |p.12) or (2.8 |p.13)? This second component is one of the valuable features that matrix-valued subdivision schemes allow. It is called the "shape-control parameter" and it functions just as its name implies. This parameter allows the designer to control or change the geometric shape of the surface. In Chapter 6, a method will be proposed for defining this parameter that is based on the discrete normals of the initial control polyhedron.

The local averaging rule (2.7 |p.13) gives rise to templates that visually show how new vertices are "made" and how "old" vertices are updated. Figure 2.1 shows the templates for two matrix-valued masks for 1−ring triangular [**CJ08**] and quadrilateral schemes [**CJ05**].

For the triangular scheme we have:

$$\begin{aligned} P_{0,0} &= [p_{ij}]_{1\le i,j\le 2} \qquad & D &= [d_{ij}]_{1\le i,j\le 2} \\ B &= [b_{ij}]_{1\le i,j\le 2} \qquad & C &= [c_{ij}]_{1\le i,j\le 2} \end{aligned} \tag{2.10}$$

where

$$p_{11} = 1,\ p_{21} = 0,\ d_{11} = 0,\ d_{21} = 0 \text{ in the interpolatory case}$$

and

$$B = P_{1,0} = P_{-1,0} = P_{0,1} = P_{0,-1} = P_{1,1} = P_{-1,-1}$$
$$C = P_{2,1} = P_{-2,-1} = P_{1,2} = P_{-1,-2} = P_{1,-1} = P_{-1,1}$$
$$D = P_{2,0} = P_{-2,0} = P_{0,2} = P_{0,-2} = P_{2,2} = P_{-2,-2} \tag{2.11}$$

for $P_{\mathbf{k}}$ from (2.7 |p.13)

For the quadrilateral scheme we have:

$$R_{0,0} = [r_{ij}]_{1\le i,j\le 2} \quad L = [l_{ij}]_{1\le i,j\le 2} \quad N = [n_{ij}]_{1\le i,j\le 2} \tag{2.12}$$
$$K = [k_{i\,j}]_{1\le i,j\le 2} \quad J = [j_{i\,k}]_{1\le i,j\le 2} \quad M = [m_{i\,j}]_{1\le i,j\le 2}$$

where

$r_{11} = 1,\ r_{21} = 0,\ l_{11} = 0,\ l_{21} = 0,\ n_{11} = 0,\ n_{21} = 0$ in the interpolatory case

and

$$L = P_{2,0} = P_{-2,0} = P_{0,2} = P_{0,-2}$$
$$N = P_{2,2} = P_{-2,2} = P_{2,-2} = P_{-2,-2}$$
$$K = P_{1,1} = P_{1,-1} = P_{-1,1} = P_{-1,-1}$$
$$J = P_{1,0} = P_{0,1} = P_{-1,0} = P_{0,-1}$$

(2.13)

$$M = P_{2,1} = P_{1,2} = P_{-1,-2} = P_{-2,-1} = P_{2,-1} = P_{-2,1} = P_{-1,2} = P_{1,-2}$$

for $P_{\mathbf{k}}$ from (2.7 |p.13)

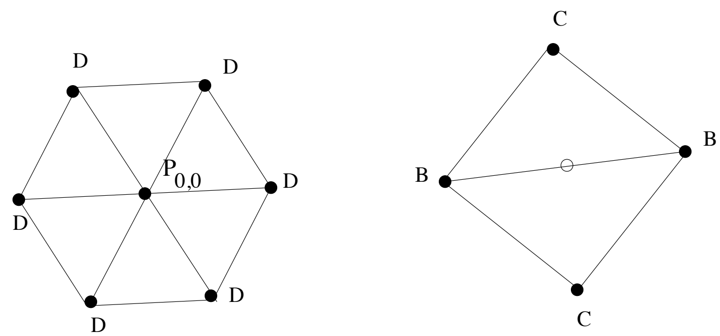

(a)

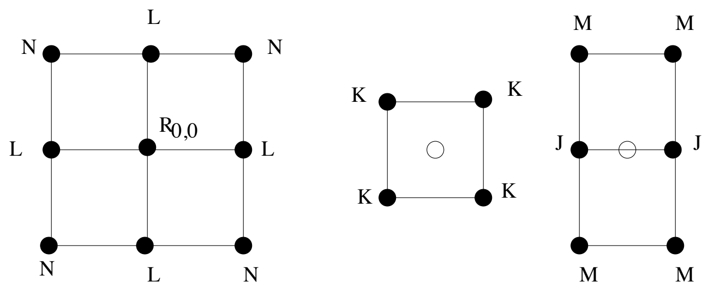

(b)

Figure 2.1. Top figure: regular template (triangular). Bottom figure: regular template (quadrilateral). These templates are 1-ring templates, meaning that the vertices involved in either forming new vertices or updating old vertices come from the immediate adjacent ring of vertices around a central vertex.

.

2.3. Sum Rule Order and Other Assumptions

We will now define [as given in [**CJ03a**]] what it means for a subdivision mask $P_{\mathbf{k}}$ to satisfy the *sum rule* of order m.

If the dilation matrix A is $2\,I_2$ [note: this will be the case used throughout] it is said that $P_{\mathbf{k}}$ satisfies the sum rule of order m if there exist 1×2 constant vectors $\mathbf{l}_0^\alpha$ with $\mathbf{l}_0^0 \neq \mathbf{0}$, such that

$$\sum_{\beta \leq \alpha} (-1)^{|\beta|} \binom{\alpha}{\beta} \mathbf{l}_0^{\alpha-\beta} \mathbf{J}_{\beta,\gamma} = 2^{-\alpha} \mathbf{l}_0^\alpha \tag{2.14}$$

for all $\gamma \in \left\{(0,0)^T, (1,0)^T, (0,1)^T, (1,1)^T\right\}$, $|\alpha| < m$, with

$$\mathbf{J}_{\beta,\gamma} := \sum_{\mathbf{k}} \left(\mathbf{k} + 2^{-1}\gamma\right)^{\beta} P_{2\mathbf{k}+\gamma}$$

The sum rule of order m is an "attractive" property since it implies (with the additional assumption that $\mathbf{l}_0^0 \widehat{\Phi}(0) = 1$) that linear combinations of integer translates of Φ will reproduce polynomials of total degree less than m:

$$\mathbf{x}^{\alpha} = \sum_{\mathbf{k}\in\mathbb{Z}^2} \left\{ \sum_{\beta\leq\alpha} \binom{\alpha}{\beta} \mathbf{k}^{\alpha-\beta} \mathbf{l}_0^{\beta} \right\} \Phi(\mathbf{x} - \mathbf{k}), \quad |\alpha| < m \tag{2.15}$$

where $\mathbf{l}_0^{\beta}$ are the same as in (2.14). Note that (2.15) is called accuracy of order m.

It can be shown that (2.14 |p.15) implies the following set of equations:

$$\sum_{\beta\leq\alpha} \binom{\alpha}{\beta} (2,2)^{\beta-\alpha} \mathbf{l}_0^{\beta} \sum_{\mathbf{k}} P_{2\mathbf{k}} (2\mathbf{k})^{\alpha-\beta} = (2,2)^{-\alpha} \mathbf{l}_0^{\alpha} \tag{2.16}$$

$$\sum_{\beta\leq\alpha} \binom{\alpha}{\beta} (2,2)^{\beta-\alpha} \mathbf{l}_0^{\beta} \sum_{\mathbf{k}} P_{2\mathbf{k}-\binom{1}{0}} \left(2\mathbf{k} - \binom{1}{0}\right)^{\alpha-\beta} = (2,2)^{-\alpha} \mathbf{l}_0^{\alpha}$$

$$\sum_{\beta\leq\alpha} \binom{\alpha}{\beta} (2,2)^{\beta-\alpha} \mathbf{l}_0^{\beta} \sum_{\mathbf{k}} P_{2\mathbf{k}-\binom{0}{1}} \left(2\mathbf{k} - \binom{0}{1}\right)^{\alpha-\beta} = (2,2)^{-\alpha} \mathbf{l}_0^{\alpha}$$

$$\sum_{\beta\leq\alpha} \binom{\alpha}{\beta} (2,2)^{\beta-\alpha} \mathbf{l}_0^{\beta} \sum_{\mathbf{k}} P_{2\mathbf{k}-\binom{1}{1}} \left(2\mathbf{k} - \binom{1}{1}\right)^{\alpha-\beta} = (2,2)^{-\alpha} \mathbf{l}_0^{\alpha}$$

where $|\alpha| < m$.

We will assume that the mask $P_{\mathbf{k}}$ satisfies (at least) sum rule of order 3. As we shall see shortly, this assumption will provide us with suitable left eigenvectors for eigenvalues $\frac{1}{2}$ and $\frac{1}{4}$.

As indicated in section 1.4, Φ is defined on $\mathbb{R}^s$ where $s = 2$ and the dilation matrix A in (2.5) is restricted to $2I_2$. Hence $\Phi = (\phi_1\, \phi_2)^T$ and the topological rule will be the commonly used one called the "1-to-4 split" (dyadic) rule.

The support of the mask $P_{\mathbf{k}}$ is assumed to be finite such that

$$P_{\mathbf{k}} = \mathbf{0}, \mathbf{k} \notin [-N, N]^2 \tag{2.17}$$

for some positive integer N.

Please note that only 1-ring templates using either triangular or quadrilateral schemes will be examined. From the 1-ring assumption it can be shown directly that $N = 2$ in (2.17). Such smaller templates do not depend on mesh orientation and avoid the unnecessary surface oscillation artifacts that larger templates have [**CJ05**]. As discussed in [**CJ05**], the schemes will have four-directional symmetry for quadrilateral scheme templates and six-directional symmetry for triangular scheme templates. Such symmetry is a very desirable quality since on surfaces it would be very difficult to keep track of mesh orientation.

Looking at the Fourier transform of both sides of (2.5 |p.12) the following is obtained:

$$\widehat{\Phi} := \mathbf{P}\left(\cdot/2\right) \widehat{\Phi}\left(\cdot/2\right) \tag{2.18}$$

where

$$\mathbf{P}\left(w\right) := \frac{1}{|\det A|} \sum_{\mathbf{k} \in \mathbb{Z}^2} P_{\mathbf{k}}\, e^{-i\mathbf{k}\omega} \tag{2.19}$$

is called the two-scale symbol of the mask $\{P_{\mathbf{k}}\}$. Note that $|\det A| = 4$.

Now one can see that if Φ satisfies (2.5 |p.12) then any scalar multiple of Φ also satisfies (2.5).

So from [**Jia99**] Φ is said to be a *normalized* solution to (2.5) if

$$\widehat{\Phi}\left(0\right) = \left(1, c\right)^T \text{ for some scalar } c \tag{2.20}$$

Note that from (2.18 |p.17)

$$\widehat{\Phi}(0) = \mathbf{P}(0)\, \widehat{\Phi}(0)$$

and so $\widehat{\Phi}(0)$ is a right eigenvector of $\mathbf{P}(0)$ for the eigenvalue 1.

Now a matrix A is said to satisfy **Condition E** [**She98**] if

- the absolute values of its eigenvalues are less than or equal to 1
- 1 is the only eigenvalue on the unit circle

- 1 is simple [geometric multiplicity = algebraic multiplicity =1].

We will assume that the symbol $\mathbf{P}$ (2.19) evaluated at $\mathbf{0}$ $[\mathbf{P}(0)]$ satisfies **Condition E**.

Since our mask $P_{\mathbf{k}}$ satisfies sum rule of order 1 (i.e. the basic sum rule), the following is obtained from (2.16):

$$\mathbf{l}_0^0 \sum_{\mathbf{k}} P_{2\mathbf{k}-\eta_j} = \mathbf{l}_0^0 \tag{2.21}$$

where $\eta_j \in \mathbb{Z}^2/2\mathbb{Z}^2$ for $j = 0, 1, 2, 3$.

Hence

$$\mathbf{l}_0^0 \sum_{\mathbf{k}} P_{\mathbf{k}} = 4\, \mathbf{l}_0^0$$

or from (2.19)

$$\mathbf{l}_0^0\, \mathbf{P}(0) = \mathbf{l}_0^0$$

We will assume that

$$\mathbf{l}_0^0 = (1, 0) \tag{2.22}$$

i.e. that the left eigenvector of $\mathbf{P}(0)$ for 1 equals $(1, 0)$.

From (2.22 |p.18) and from the normalization in (2.20 |p.17), we will obtain the following normalization of these left and right eigenvectors of $\mathbf{P}(0)$. Note that this normalization is a frequent assumption in proofs in [**JJ02**] and [**CJR02**] among others.

$$\mathbf{l}_0^0\, \widehat{\Phi}(0) = 1$$

Now if $\mathbf{l}_0^0 \neq (1, 0)$ we will do the following:

Note that since $\mathbf{P}(0)$ satisfies **Condition E** (by assumption) there exists a nonsingular matrix U such that

$$U\mathbf{P}(0)\, U^{-1} = \begin{pmatrix} 1 & 0 \\ 0 & d \end{pmatrix} \qquad \text{with } |d| < 1$$

If we define $\mathbf{P}_1 := U\mathbf{P}U^{-1}$,then $\Phi^1 := U\,\Phi$ satisfies the refinement equation

$$\widehat{\Phi^1} = \mathbf{P}_1(\cdot/2)\, \widehat{\Phi^1}(\cdot/2)$$

where Φ is a solution of (2.18 |p.17). [**She98**]

Note that the convergence and smoothness of Φ^1 are the same as Φ since its components are just linear combinations of Φ.

So if $\mathbf{l}_0^0 \neq (1,0)$ we will use Φ^1 instead of Φ and $\mathbf{P}_1$ instead of $\mathbf{P}$. With these modifications we will obtain $\mathbf{l}_0^0 = (1,0)$.

Notice from (2.15 |p.16) that

$$\mathbf{l}_0^0 \sum_{\mathbf{k}\in\mathbb{Z}^2} \Phi\left(\mathbf{x}-\mathbf{k}\right) = 1$$

which in other words means that Φ satisfies the condition of "generalized partition of unity." [**CJ06**]

Define

$$T_P := \left[B_{2\mathbf{k}-\mathbf{j}}\right]_{\mathbf{k},\,\mathbf{j}\in[-N,\,N]^2}$$

where $B_{\mathbf{j}} := \frac{1}{4}\sum\limits_{\mathbf{k},\,\mathbf{j}} P_{\mathbf{k}-\mathbf{j}} \otimes \overline{P}_{\mathbf{k}}$ and $P_{\mathbf{k}}$ is our subdivision mask.

From [**CJ06**] the sequence of piecewise linear surfaces with vertices $v_{\mathbf{j}}^m$ (2.8 |p.13) converges in the L_2-norm to the limit surface $F(\mathbf{x})$ (2.9 |p.13)

- if T_p satisfies **Condition E** and
- if (2.21 |p.18) is satisfied.

We will assume that T_P satisfies **Condition E**.

Hence only the first components of (2.8 |p.13) will be used as the vertices of the triangular or (nonplanar) quadrilateral meshes for the m^{th} iteration. And these (finer and finer) meshes will converge to the target limit surface $F(\mathbf{x})$ in (2.9).

From the assumption of sum rule of order 3, one can show that

$$\sum_{\mathbf{k}\in\mathbb{Z}^2} \mathbf{l}_{\mathbf{k}}^{\alpha} P_{2\mathbf{k}-\mathbf{j}} = (2,2)^{-\alpha}\ \mathbf{l}_{\mathbf{j}}^{\alpha} \qquad \text{for any } \mathbf{j}\in\mathbb{Z}^2 \text{ and } \quad |\alpha| < 3$$

where $\mathbf{l}_0^{\alpha}$ is the same as in (2.14) and (2.15) and where

$$\mathbf{l}_{\mathbf{j}}^{\alpha} := \sum_{0\leq\beta\leq\alpha} \binom{\alpha}{\beta} \mathbf{j}^{\alpha-\beta}\, \mathbf{l}_0^{\beta} \quad \text{for } \mathbf{j}\in\mathbb{Z}^2 \text{ and } \quad |\alpha| < 3 \tag{2.23}$$

Thus

$$\mathbf{l}^{\alpha} L = (2,2)^{-\alpha}\ \mathbf{l}^{\alpha} \tag{2.24}$$

where $|\alpha| < 3$ and L is the bi-infinite form of the regular subdivision matrix:

$$L := [P_{2\mathbf{k}-\mathbf{j}}]_{\mathbf{k},\mathbf{j}\in\mathbb{Z}^2}$$

and where

$$\mathbf{l}^{\alpha} := \left[\ldots, \mathbf{l}^{\alpha}_{\mathbf{j}}, \ldots\right]_{\mathbf{j}\in\mathbb{Z}^2} \tag{2.25}$$

So we have left eigenvectors for L corresponding to the eigenvalues $(2,2)^{-\alpha}$ for $|\alpha| < 3$.

Since the support of $P_{\mathbf{k}}$ is $\mathbf{k} \in [-2,2]^2$ there are up to 25 nonzero 2 x 2 matrices in the mask. However, a 1-ring triangular scheme will only need to use 19 of these for its finite subdivision matrix (2.11). The quadrilateral regular case will need all 25 for its finite subdivision matrix (2.13). Thus the finite (regular) triangular subdivision matrix will be a 38 x 38 matrix and the finite (regular) quadrilateral subdivision matrix will be a 50 x 50 matrix.

Denoting the required $\mathbf{k} \in [-2,2]^2$ by Q, the finite subdivision matrix S is

$$S := [P_{2\mathbf{k}-\mathbf{j}}]_{\mathbf{k},\mathbf{j}\in Q} \tag{2.26}$$

From (2.24) one sees that this subdivision matrix has eigenvalues $1, \frac{1}{2}, \frac{1}{4}$ where it can be easily demonstrated that their geometric multiplicity is at least $1, 2,$and 3 respectively. The eigenvalue 1 must be simple else the scheme will not converge [**RP06**]. The subdominant eigenvalue $\frac{1}{2}$ is assumed to have geometric and algebraic multiplicity 2 else the scheme will not be practically useful [**Zor00a**]. Finally, the subsubdominant eigenvalue $\frac{1}{4}$ is assumed to have geometric and algebraic multiplicity 3 else the curvature continuity may be degenerate [**Loo01**]. The remaining eigenvalues will be assumed to have modulus strictly less than $\frac{1}{4}$. If any of the remaining eigenvalues are defective then generalized eigenvectors will be used when it becomes necessary to construct a basis for $\mathbb{R}^{38}$ or $\mathbb{R}^{50}$ [triangular and quadrilateral cases respectively].

For the extraordinary case, we will assume that 1 is a simple eigenvalue of the (irregular or extraordinary) subdivision matrix and that its subdominant eigenvalue λ (where $\lambda < 1$) is nondefective with multiplicity 2. The modulus of the remaining eigenvalues is strictly less than λ. We will later show how this matrix is similar to a block diagonal matrix. We will assume that the subdominant eigenvalue λ is an eigenvalue of the second and last blocks of that block diagonal matrix. Cases in which this assumption is not met are not useful in practice. [**PR98**],[**Zor00a**]

Another assumption is that the limit surface F is C^2 except on extraordinary vertices where it is C^1. This is a common assumption for target surfaces of subdivision schemes.

The following question naturally arises: given a certain mask, how can the smoothness of this mask be determined? This question is answered by Jia and Jiang in [**JJ03**]. See the section that follows.

2.4. Sobolev Smoothness Determination

In [**JJ03**], Jia and Jiang develop a theorem for determining the lower bound on the Sobolev smoothness of refinable function $\Phi \in L_2\left(\mathbb{R}^d\right)^{r\times 1}$. Here we will paraphrase the theorem.

Let $\Phi \in L_2\left(\mathbb{R}^d\right)^{r\times 1}$ be a normalized solution of $\Phi\left(\mathbf{x}\right) = \sum_{\alpha\in\mathbb{Z}^d} P_\alpha \Phi\left(A\mathbf{x} - \alpha\right)$ $\mathbf{x} \in \mathbb{R}^d$ with mask P of $r\times r$ real-valued matrices and isotropic $d\times d$ dilation matrix A. Assume that P has sum rule of order k. Define

$$S_k := \text{spec } \left(T_P|_{H_\Omega}\right) \setminus \overline{S}_k$$

where

$$\overline{S}_k := \left\{\sigma^{-\alpha}\overline{\lambda_j}, \overline{\sigma^{-\alpha}}\lambda_j, \sigma^{-\beta} : \alpha, \beta \in \mathbb{Z}^d, |\alpha| < k, |\beta| < 2k, 2 \leq j \leq r\right\}$$

where σ is from (2.3) and λ_j are the eigenvalues of $\mathbf{P}\left(\mathbf{0}\right)$ where $\mathbf{P}\left(w\right) := \frac{1}{m}\sum_{\alpha\in\mathbb{Z}^d} P_\alpha\, e^{-i\alpha\cdot\omega}$ [By assumption, $\lambda_1 = 1$ and $|\lambda_j| < 1$ for $j = 2, ..., r$.] Also recall that $m := |\det A|$.

Now define $\Omega := \left\{\sum_{k=1}^{k=\infty} A^{-k}x_k : x_k \in [-N, N]^d\right\}$ where $\text{supp}(P) \subset [-N, N]^d$. Define $[\Omega] := \Omega \cap \mathbb{Z}^d$.

Jia and Jiang define H_Ω (a subspace of $C_0\left(\mathbf{T}^d\right)^{r\times r}$) as follows:

$$H_\Omega := \left\{ h(\omega) \in C_0\left(\mathbf{T}^d\right)^{r\times r} : h(\omega) = \sum_{\alpha\in[\Omega]} h_\alpha\, e^{-i\alpha\cdot\omega} \right\}$$

where $C_0\left(\mathbf{T}^d\right)^{r\times r}$ denotes the space of all $r \times r$ matrix functions with trigonometric polynomial entries.

And for a given refinement equation with symbol $\mathbf{P}(\omega) \in C_0\left(\mathbf{T}^d\right)^{r\times r}$ they define the *transition operator* T_P on $C_0\left(\mathbf{T}^d\right)^{r\times r}$ by

$$T_P X(\omega) := \sum_{j=0}^{m-1} P\left(A^{-T}(\omega + 2\pi\eta_j)\right) X\left(A^{-T}(\omega + 2\pi\eta_j)\right) P\left(A^{-T}(\omega + 2\pi\eta_j)\right)^*$$

where the complex conjugate of $P(\omega)$ is denoted by $P(\omega)^* = P(-\omega)^T$ and where $\{\eta_j\}$ is the complete set of representations of the m cosets of $\mathbb{Z}^d/M^T\mathbb{Z}^d$.

Now if we define

$$\rho_0 := \max\{|\lambda| : \lambda \in S_k\}$$

then we have the following lower bound for $\lambda(\Phi)$:

$$\lambda(\Phi) \geq -\frac{d}{2}\log_m \rho_0$$

where $\lambda(\Phi)$ is from (2.4 |p.10).

CHAPTER 3

Derivative Formulas for Interpolating Triangular Subdivision Schemes

3.1. Introduction

Here we are examining 1−ring triangular interpolating schemes. Their template is given in the upper part of Fig. 2.1 and the elements of the mask are given by 2.10. In an interpolatory scheme these matrices have the following structure: [**CJ08**]

(3.1)

$$P_{0,0} = \begin{bmatrix} 1 & * & \cdots & * \\ 0 & * & \cdots & * \\ \vdots & \vdots & \cdots & \vdots \\ 0 & * & \cdots & * \end{bmatrix}, \qquad P_{2\mathbf{j}} = \begin{bmatrix} 0 & * & \cdots & * \\ \vdots & \vdots & \cdots & \vdots \\ 0 & * & \cdots & * \end{bmatrix}, \qquad \mathbf{j} \in \mathbb{Z}^2 \setminus \{(0,0)\}$$

Note that

$$v^m_{2^m \mathbf{k}_0} = v^0_{\mathbf{k}_0} \tag{3.2}$$

follows from (2.7 |p.13) and the above matrix structures.

These regular vertices lie on a 3-directional mesh in a “so-called” parametric domain. This domain corresponds to the integer subscripts of the vertices and will be associated with the parameters of the limit surface (as we will see later). See Fig. 3.1 on p. 24.

In the following we will be using the assumptions presented in Chapter 2 to develop the first and second partial derivatives of the regular vertices of a triangular interpolating scheme We will derive from our assumptions as much information as possible about the templates $\{P_{\mathbf{k}}\}_{\mathbf{k}}$ and the 1×2 constant vectors $\mathbf{l}^{\alpha}_0$ introduced in (2.14 |p.15).

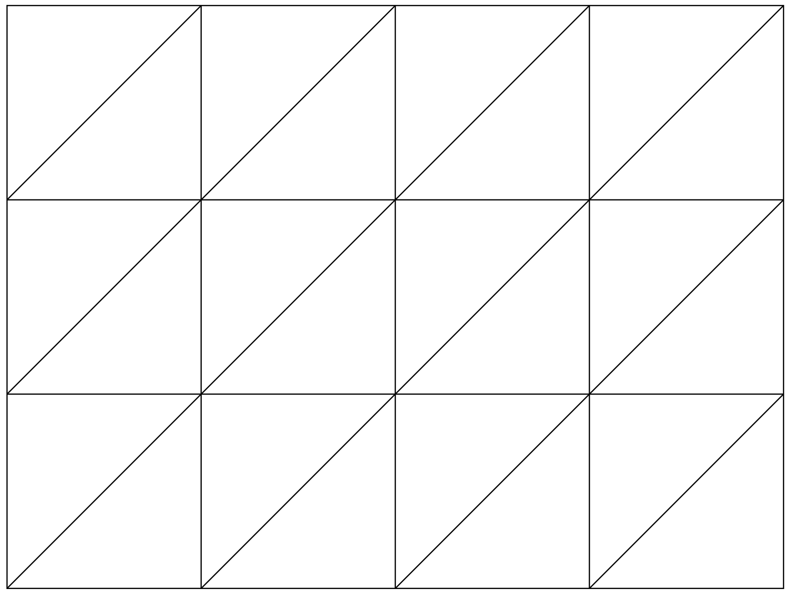

Figure 3.1. Three directional mesh for triangular scheme

Through direct calculation using the Sum rules we determined the following:

$$\begin{aligned}
\mathbf{l}_0^{(1,0)} &= \mathbf{l}_0^{(0,1)} = [0,0] \\
\mathbf{l}_0^{(2,0)} &= \mathbf{l}_0^{(0,2)} = [0,h] \\
\mathbf{l}_0^{(1,1)} &= \left[0, \frac{h}{2}\right] \qquad \text{where } h \neq 0
\end{aligned} \tag{3.3}$$

As indicated in Chapter 2, $\mathbf{l}_0^{(0,0)} = [1,0]$.

Also through direct calculation using the Sum rules we determined:

$$P_{0,0} = \begin{pmatrix} 1 & h\left(-\frac{3}{8} + 9t_3 + \frac{3}{2}t_4\right) \\ 0 & t_4 \end{pmatrix} \qquad D = \begin{pmatrix} 0 & h\left(\frac{1}{16} - \frac{3}{2}t_3 - \frac{1}{4}t_4\right) \\ 0 & t_3 \end{pmatrix} \tag{3.4}$$

$$B = \begin{pmatrix} \frac{3}{8} & 0 \\ -\frac{1}{8h} - t_1 & \frac{1}{8} - t_2 \end{pmatrix} \qquad C = \begin{pmatrix} \frac{1}{8} & 0 \\ t_1 & t_2 \end{pmatrix}$$

where t_j for $j = 1, ..., 4$ are "free" variables and h is from (3.3 |p.24). Using the techniques in ([**JO03**]), the values of these t_j will determine the Sobolev smoothness of the refinable function Φ (2.5 |p.12). See the prior section 2.4 on p. 21 for more information.

3.2. Development of general derivative formulas

We will use the same technique as found in [**SDL99**] to develop a representation of the first partial derivatives in terms of the initial control net. In [**SDL99**] the authors represented a control net around any given regular vertex (call it $v^m_{2^m\mathbf{k}_0}$) as a linear combination of right eigenvectors of the subdivision matrix. Then it was determined that in this linear combination the two first partial derivatives at $v^m_{2^m\mathbf{k}_0}$ are equal to two of the 1×3 "coefficients", namely the coefficients for the right eigenvectors (call them $\mathbf{r}_1$ and $\mathbf{r}_2$) corresponding to the multiple eigenvalue $\frac{1}{2}$. Finally by multiplying the initial control net by two normalized left eigenvectors of $\frac{1}{2}$ (call them $\mathbf{l}_1$ and $\mathbf{l}_2$) such that $\mathbf{l}_i\mathbf{r}_j = \delta(i-j)$ where $i, j = 1, 2$ they obtained a representation of the two first partial derivatives as linear combinations of the initial control net.

Here we will use this technique to develop representations of the first and second partial derivatives of the limiting surface where the initial control net is regular and then first partial derivatives corresponding to an extraordinary vertex.

3.3. First Partial Derivatives(Regular)

Here, as in [**SDL99**], we will also start at any given regular vertex $v^m_{2^m\mathbf{k}_0}$ for some $\mathbf{k}_0 \in \mathbb{Z}^2$ (after m iterations of our subdivision scheme). But in contrast we will be initially representing its surrounding control net as a linear combination of *left* eigenvectors.

In a regular interpolatory triangular scheme, the control vector net surrounding a vertex (call it $v^m_{2^m\mathbf{k}_0}$) is a 3×38 vector consisting of 19 3×1 initial control vertices and 19 3×1 initial shape control vertices. See Figure 3.2 on p. 27.

Denote each vertex surrounding $\mathbf{v}^m_{2^m\mathbf{k}_0}$ after m subdivisions by

$$\mathbf{u}^m_{\mathbf{k}_0,\mathbf{j}} := \mathbf{v}^m_{2^m\mathbf{k}_0+\mathbf{j}} \tag{3.5}$$

where $\mathbf{k}_0 \in \mathbb{Z}^2$ and $\mathbf{j} = (Q_{1,s}, Q_{2,s})^T$ for $s = 1, \ldots, 19$ and where Q is defined as the following 2×19 matrix:

(3.6)

$$Q := \begin{pmatrix} 0 & 1 & 1 & 0 & -1 & -1 & 0 & 2 & 2 & 0 & -2 & -2 & 0 & 2 & 1 & -1 & -2 & -1 & 1 \\ 0 & 0 & 1 & 1 & 0 & -1 & -1 & 0 & 2 & 2 & 0 & -2 & -2 & 1 & 2 & 1 & -1 & -2 & -1 \end{pmatrix}$$

The columns of Q reflect the ordering in Figure 3.2.

Define the following 3 x 38 matrix

$$\mathbf{U}^m_{\mathbf{k}_0} := \left\{ \mathbf{u}^m_{\mathbf{k}_0,\mathbf{j}} : \mathbf{j} = (Q_{1\,s}, Q_{2\,s})^T \text{ as above} \right\} \tag{3.7}$$

Hence

$$\mathbf{U}^{m+1}_{\mathbf{k}_0} = \mathbf{U}^m_{\mathbf{k}_0} S$$

where S is given in (2.26 |p.20).

Additionally,

$$\mathbf{U}^m_{\mathbf{k}_0} = \mathbf{U}^0_{\mathbf{k}_0} S^m \tag{3.8}$$

In other words, the m^{th} control net surrounding $\mathbf{v}^m_{2^m\mathbf{k}_0}$ is obtained by applying the subdivision matrix to our initial control net m times.

The *initial* control vector net ($\mathbf{U}^0_{\mathbf{k}_0}$) around any regular $\mathbf{v}^0_{\mathbf{k}_0}$ can be represented as a linear combination of 1×38 (generalized) left eigenvectors of our 38×38 subdivision matrix S (2.26 |p.20).

By letting $\{\mathbf{L}_j\}_{0 \le j \le 37}$ be a set of 38 (possibly generalized) linearly independent left eigenvectors of S then $\mathbf{U}^0_{\mathbf{k}_0}$ can be written as

$$\mathbf{U}^0_{\mathbf{k}_0} = \alpha^{(0)}_0 \mathbf{L}_0 + \alpha^{(0)}_1 \mathbf{L}_1 + \alpha^{(0)}_2 \mathbf{L}_2 + \alpha^{(0)}_3 \mathbf{L}_3 + \alpha^{(0)}_4 \mathbf{L}_4 + \alpha^{(0)}_5 \mathbf{L}_5 + \sum_{j=6}^{37} \alpha^{(0)}_j \mathbf{L}_j \tag{3.9}$$

where $\alpha^{(0)}_j \in \mathbb{R}^3 \quad j = 0, \ldots, 37$

By assumption (see Chapter 2) 1 is the dominant eigenvalue of S with multiplicity 1, $\frac{1}{2}$ is the subdominant eigenvalue of S with multiplicity 2 and $\frac{1}{4}$ is the subsubdominant eigenvalue with multiplicity 3. All other eigenvalues have modulus less than $\frac{1}{4}$.

In (3.9 |p.26) let $\mathbf{L}_0$ be the left eigenvector of 1, $\mathbf{L}_1$ and $\mathbf{L}_2$ be the two left eigenvectors of $\frac{1}{2}$ and $\mathbf{L}_3, \mathbf{L}_4$ and $\mathbf{L}_5$ be the three left eigenvectors of

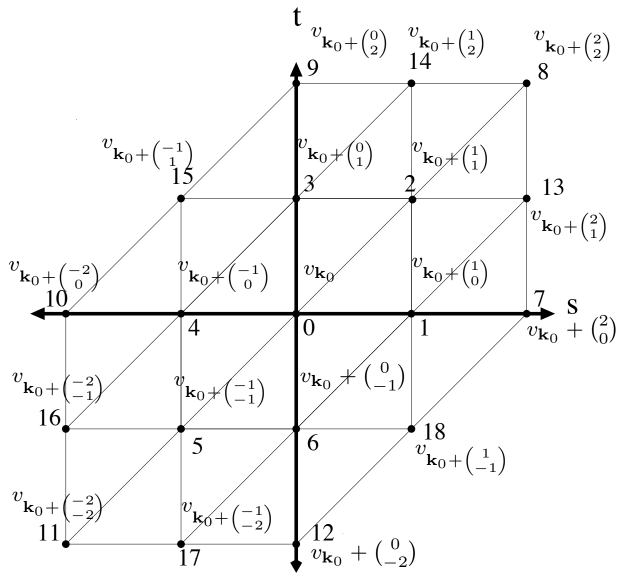

Figure 3.2. Ordering around central vertex. The intersection of grid lines are the parametric location of the vertices (the subscripts). The single numbers represent the order in which the vertices are considered. The vertex subscripts reflect the parametric domain.

$\frac{1}{4}$. For $j \geq 6$, $\mathbf{L}_j$ is a (generalized) left eigenvalue corresponding to an eigenvalue with modulus strictly less than $\frac{1}{4}$.

From (3.8 |p.26) we then have

$$\mathbf{U}^m_{\mathbf{k}_0} = \alpha_0^{(0)}\mathbf{L}_0 + 2^{-m}\alpha_1^{(0)}\mathbf{L}_1 + 2^{-m}\alpha_2^{(0)}\mathbf{L}_2 + 4^{-m}\alpha_3^{(0)}\mathbf{L}_3 + 4^{-m}\alpha_4^{(0)}\mathbf{L}_4 + 4^{-m}\alpha_5^{(0)}\mathbf{L}_5 + \sum_{j=6}^{37} \lambda_j^m \alpha_j^{(0)}\mathbf{L}_j$$

where $|\lambda_j| < \frac{1}{4}$ for $j = 6, ..., 37$.

Thus

$$\lim_{m\to\infty} \mathbf{U}^m_{\mathbf{k}_0} = \alpha_0^{(0)}\mathbf{L}_0$$
$$\lim_{m\to\infty} 2^m \left(\mathbf{U}^m_{\mathbf{k}_0} - \alpha_0^{(0)}\mathbf{L}_0\right) = \alpha_1^{(0)}\mathbf{L}_1 + \alpha_2^{(0)}\mathbf{L}_2$$

Now since

- the first component of $\mathbf{U}^m_{\mathbf{k}_0}$ is $v^m_{2^m\mathbf{k}_0}$
- $v^m_{2^m\mathbf{k}_0} = v^0_{\mathbf{k}_0}$ (see 3.2 |p.23) and
- the first component of $\mathbf{L}_0$ is 1

then we have

$$\alpha_0^{(0)} = v^0_{\mathbf{k}_0} = v^m_{2^m\mathbf{k}_0} \tag{3.10}$$

Hence we have the following:

$$\lim_{m\to\infty} 2^m \left(\mathbf{U}^m_{\mathbf{k}_0} - \left[v^0_{\mathbf{k}_0,}, 0, v^0_{\mathbf{k}_0,}, 0, v^0_{\mathbf{k}_0,}, 0..., v^0_{\mathbf{k}_0,}, 0\right]\right) = \alpha_1^{(0)}\mathbf{L}_1 + \alpha_2^{(0)}\mathbf{L}_2 \tag{3.11}$$

Now from (2.23 |p.19),(2.25 |p.20), (3.3 |p.24) and (3.6 |p.26) we can obtain the following representations of $\mathbf{L}_j$ for $j = 0, 1, ..., 5$.

$$\begin{aligned} \mathbf{L}_0 &= [1,0,1,0,1,0,1,0,...,1,0,1,0] \\ \mathbf{L}_1 &= [0,0,1,0,1,0,0,0,...,-1,0,1,0] \\ \mathbf{L}_2 &= [0,0,0,0,1,0,1,0,...,-2,0,-1,0] \\ \mathbf{L}_3 &= [0,h,1,h,1,h,0,h,...,1,h,1,h] \\ \mathbf{L}_4 &= \left[0,\frac{h}{2},0,\frac{h}{2},1,\frac{h}{2},0,\frac{h}{2},...,2,\frac{h}{2},-1,\frac{h}{2}\right] \\ \mathbf{L}_5 &= [0,h,0,h,1,h,1,h,...,4,h,1,h] \end{aligned} \tag{3.12}$$

So just looking at the odd components of the left and right sides of (3.11 |p.28) we have

$$\lim_{m\to\infty} 2^m \left(\left[v^m_{2^m\mathbf{k}_0}, v^0_{2^m\mathbf{k}_0+(1,0)^T}, v^0_{2^m\mathbf{k}_0+(1,1)^T}, ..., v^0_{2^m\mathbf{k}_0+(1,-1)^T}\right] - \left[v^0_{\mathbf{k}_0}, v^0_{\mathbf{k}_0}, v^0_{\mathbf{k}_0}, ..., v^0_{\mathbf{k}_0}\right]\right) =$$
$$\alpha_1^{(0)}\widetilde{\mathbf{L}}_1 + \alpha_2^{(0)}\widetilde{\mathbf{L}}_2 \tag{3.13}$$

where

$$\widetilde{\mathbf{L}}_1 = [0,1,1,0,-1,-1,0,2,2,0,-2,-2,0,2,1,-1,-2,-1,1]$$
$$\widetilde{\mathbf{L}}_2 = [0,0,1,1,0,-1,-1,0,2,2,0,-2,-2,1,2,1,-1,-2,-1]$$

Our goal is to connect the above formula with the 2 partial derivative of our limit surface F. First we need to locally parameterize F in the (s,t) plane as in [**SDL99**]. The (s,t) plane is drawn in Figure 3.2.

Define as follows a local parameterization of F in a neighborhood of $\mathbf{k}_0 = \left(k_0^{(1)}, k_0^{(2)}\right)^T \in \mathbb{Z}^2$

$$F\left(k_0^{(1)} + \frac{l^{(1)}}{2^m}, k_0^{(2)} + \frac{l^{(2)}}{2^m}\right) := v^m_{2^m\mathbf{k}_0+\mathbf{l}} \tag{3.14}$$

where $m \in \mathbb{Z}_+$, v^m as in (2.8 |p.13), and $\mathbf{l} = \left(l^{(1)}, l^{(2)}\right)^T = (Q_{1,j}, Q_{2,j})^T_{1\le j\le 19}$ for Q defined in (3.6 |p.26).

Since F is assumed to be C^2 at regular vertices then

$$\lim_{m\to\infty} 2^m \left\{ \begin{array}{c} F\left(k_0^{(1)}, k_0^{(2)}\right) - F\left(k_0^{(1)}, k_0^{(2)}\right),\, F\left(k_0^{(1)} + 2^{-m}\cdot 1, k_0^{(2)}\right) - F\left(k_0^{(1)}, k_0^{(2)}\right), \\ F\left(k_0^{(1)} + 2^{-m}\cdot 1, k_0^{(2)} + 2^{-m}\cdot 1\right) - F\left(k_0^{(1)}, k_0^{(2)}\right), \\ F\left(k_0^{(1)}, k_0^{(2)} + 2^{-m}\cdot 1\right) - F\left(k_0^{(1)}, k_0^{(2)}\right), ..., \\ F\left(k_0^{(1)} + 2^{-m}\cdot(-1), k_0^{(2)} + 2^{-m}\cdot(-2)\right) - F\left(k_0^{(1)}, k_0^{(2)}\right), \\ F\left(k_0^{(1)} + 2^{-m}\cdot 1, k_0^{(2)} + 2^{-m}\cdot(-1)\right) - F\left(k_0^{(1)}, k_0^{(2)}\right) \end{array} \right\} =$$

$$F_s\left(k_0^{(1)}, k_0^{(2)}\right)\widetilde{\mathbf{L}}_1 + F_t\left(k_0^{(1)}, k_0^{(2)}\right)\widetilde{\mathbf{L}}_2 \tag{3.15}$$

So from the local parametrization (3.14 |p.29) we have

$$\lim_{m\to\infty} 2^m \left(\left[v^m_{2^m\mathbf{k}_0}, v^m_{2^m\mathbf{k}_0+(1,0)^T}, v^m_{2^m\mathbf{k}_0+(1,1)^T}, ..., v^m_{2^m\mathbf{k}_0+(1,-1)^T}\right] - \left[v^0_{\mathbf{k}_0}, v^0_{\mathbf{k}_0}, v^0_{\mathbf{k}_0}, ..., v^0_{\mathbf{k}_0}\right]\right) =$$
$$F_s\left(k_0^{(1)}, k_0^{(2)}\right)\widetilde{\mathbf{L}}_1 + F_t\left(k_0^{(1)}, k_0^{(2)}\right)\widetilde{\mathbf{L}}_2$$

By the linear independence of $\widetilde{\mathbf{L}}_1$ and $\widetilde{\mathbf{L}}_2$ we have

$$F_s\left(k_0^{(1)}, k_0^{(2)}\right) = \alpha_1^{(0)} \tag{3.16}$$
$$F_t\left(k_0^{(1)}, k_0^{(2)}\right) = \alpha_2^{(0)}$$

Proposition 3.1. *Suppose that an interpolatory triangular scheme is convergent with limiting surface F in C^1 where for $\mathbf{k}_0 = \left[k_0^{(1)}, k_0^{(2)}\right]^T \in \mathbb{Z}^2$ the initial control vector surrounding $\mathbf{v}_{\mathbf{k}_0}$ is given as in Figure 3.2. Also assume its mask $\{P_{\mathbf{k}}\}_{\mathbf{k}}$ has Sum Rule of at least order 3. Let $\alpha_1^{(0)}$,$\alpha_2^{(0)} \in \mathbb{R}^3$ be the column vectors in (3.9 |p.26). Then*

$$F_s\left(k_0^{(1)}, k_0^{(2)}\right) = \alpha_1^{(0)}, \qquad F_t\left(k_0^{(1)}, k_0^{(2)}\right) = \alpha_2^{(0)}$$

Similarly we can obtain the derivative of F at a point $\left(k_0^{(1)} + \frac{i^{(1)}}{2^n}, k_0^{(2)} + \frac{i^{(2)}}{2^n}\right)$ for $\mathbf{k}_0, \mathbf{i} \in \mathbb{Z}^2$ and $n \in \mathbb{Z}_+$.

In this case denote each vertex surrounding $\mathbf{v}^n_{2^n\mathbf{k}_0+\mathbf{i}}$ after m additional subdivisions by

$$\begin{aligned}\mathbf{u}^{n+m}_{\mathbf{k}_0,\mathbf{i},\mathbf{j}} &:= \mathbf{v}^{n+m}_{2^{n+m}\mathbf{k}_0+2^m\mathbf{i}+\mathbf{j}} \quad for\ m \neq 0\\ \mathbf{u}^{n}_{\mathbf{k}_0,\,\mathbf{i},\mathbf{j}} &:= \mathbf{v}^{n}_{2^{n}\mathbf{k}_0+\mathbf{i}+\mathbf{j}} \quad for\ m = 0\end{aligned}$$

where $\mathbf{j} = (Q_{1,\,s}, Q_{2,\,s})^T_{1\leq s\leq 19}$ for Q defined in (3.6 |p.26).

Let

$$\mathbf{U}^{n+m}_{\mathbf{k}_0,\mathbf{i}} := \left\{\mathbf{u}^{n+m}_{\mathbf{k}_0,\mathbf{i},\mathbf{j}} : \mathbf{j} = (Q_{1,\,s}, Q_{2,\,s})^T_{1\leq s\leq 19} \text{ as above}\right\} \tag{3.17}$$

Similar to what was done earlier, we can represent $\mathbf{U}^{n+0}_{\mathbf{k}_0,\mathbf{i}}$ as

$$\mathbf{U}^{n+0}_{\mathbf{k}_0,\mathbf{i}} = \alpha_0^{(n)}\mathbf{L}_0 + \alpha_1^{(n)}\mathbf{L}_1 + \alpha_2^{(n)}\mathbf{L}_2 + \alpha_3^{(n)}\mathbf{L}_3 + \alpha_4^{(n)}\mathbf{L}_4 + \alpha_5^{(n)}\mathbf{L}_5 + \sum_{j=7}^{37} \alpha_j^{(n)}\mathbf{L}_j \tag{3.18}$$

where $\mathbf{L}_j$ are defined in (3.12 |p.28) and $\alpha_j^{(n)} \in \mathbb{R}^3$.

As in (3.10 |p.28) we have

$$\alpha_0^{(n)} = v^n_{2^n\mathbf{k}_0+\mathbf{i}} = v^{n+m}_{2^{n+m}\mathbf{k}_0+2^m\mathbf{i}}$$

Likewise as in (3.11 |p.28) we obtain:

$$\lim_{m\to\infty} 2^m\left(\mathbf{U}^{n+m}_{\mathbf{k}_0,\mathbf{i}} - \left[v^n_{2^n\mathbf{k}_0+\mathbf{i},}, 0, v^n_{2^n\mathbf{k}_0+\mathbf{i},}, 0, v^n_{2^n\mathbf{k}_0+\mathbf{i},}, 0..., v^n_{2^n\mathbf{k}_0+\mathbf{i},}, 0\right]\right) = \alpha_1^{(n)}\mathbf{L}_1 + \alpha_2^{(n)}\mathbf{L}_2$$

This in turn leads to (like in (3.13 |p.28)):

$$\lim_{m\to\infty} 2^m \left(\begin{bmatrix} v^{n+m}_{2^{n+m}\mathbf{k}_0+2^m\mathbf{i}}, v^{n+m}_{2^{n+m}\mathbf{k}_0+2^m\mathbf{i}+(1,0)^T}, \\ v^{n+m}_{2^{n+m}\mathbf{k}_0+2^m\mathbf{i}+(1,1)^T}, \dots, v^{n+m}_{2^{n+m}\mathbf{k}_0+2^m\mathbf{i}+(1,-1)^T} \end{bmatrix} - \atop \left[v^n_{2^n\mathbf{k}_0+\mathbf{i},}, v^n_{2^n\mathbf{k}_0+\mathbf{i},}, v^n_{2^n\mathbf{k}_0+\mathbf{i},}, \dots, v^n_{2^n\mathbf{k}_0+\mathbf{i},}\right] \right) = \tag{3.19}$$
$$\alpha_1^{(n)}\widetilde{\mathbf{L}}_1 + \alpha_2^{(n)}\widetilde{\mathbf{L}}_2$$

Our local parameterization of F in a neighborhood of $\left(k_0^{(1)} + \frac{i^{(1)}}{2^n}, k_0^{(2)} + \frac{i^{(2)}}{2^n}\right)$ is

(3.20)
$$F\left(k_0^{(1)} + \frac{i^{(1)}}{2^n} + 2^{-(n+m)}l^{(1)}, k_0^{(2)} + \frac{i^{(2)}}{2^n} + 2^{-(n+m)}l^{(2)}\right) := v^{m+n}_{2^{m+n}\mathbf{k}_0+2^m\mathbf{i}+\mathbf{l}}$$

where $m, n \in \mathbb{Z}_+$, v^{m+n} as in (2.8 |p.13), and $\mathbf{l} = \left(l^{(1)}, l^{(2)}\right)^T = (Q_{1,j}, Q_{2,j})^T_{1\le j\le 19}$ for Q defined in (3.6 |p.26).

As in (3.15)

(3.21)
$$\lim_{m\to\infty} 2^m \left\{ \begin{array}{l} F\left(k_0^{(1)} + \frac{i^{(1)}}{2^n}, k_0^{(2)} + \frac{i^{(2)}}{2^n}\right) - F\left(k_0^{(1)} + \frac{i^{(1)}}{2^n}, k_0^{(2)} + \frac{i^{(2)}}{2^n}\right), \\ F\left(k_0^{(1)} + \frac{i^{(1)}}{2^n} + 2^{-(n+m)}\cdot 1, k_0^{(2)} + \frac{i^{(2)}}{2^n}\right) - F\left(k_0^{(1)} + \frac{i^{(1)}}{2^n}, k_0^{(2)} + \frac{i^{(2)}}{2^n}\right), \\ F\left(k_0^{(1)} + \frac{i^{(1)}}{2^n} + 2^{-(n+m)}\cdot 1, k_0^{(2)} + \frac{i^{(2)}}{2^n} + 2^{-(n+m)}\cdot 1\right) - F\left(k_0^{(1)} + \frac{i^{(1)}}{2^n}, k_0^{(2)} + \frac{i^{(2)}}{2^n}\right), \\ F\left(k_0^{(1)} + \frac{i^{(1)}}{2^n}, k_0^{(2)} + \frac{i^{(2)}}{2^n} + 2^{-(n+m)}\cdot 1\right) - F\left(k_0^{(1)} + \frac{i^{(1)}}{2^n}, k_0^{(2)} + \frac{i^{(2)}}{2^n}\right), \dots, \\ F\left(k_0^{(1)} + \frac{i^{(1)}}{2^n} + 2^{-(m+n)}\cdot(-1), k_0^{(2)} + \frac{i^{(2)}}{2^n} + 2^{-(n+m)}\cdot(-2)\right) - \\ F\left(k_0^{(1)} + \frac{i^{(1)}}{2^n}, k_0^{(2)} + \frac{i^{(2)}}{2^n}\right), \\ F\left(k_0^{(1)} + \frac{i^{(1)}}{2^n} + 2^{-(m+n)}\cdot(1), k_0^{(2)} + \frac{i^{(2)}}{2^n} + 2^{-(n+m)}\cdot(-1)\right) - \\ F\left(k_0^{(1)} + \frac{i^{(1)}}{2^n}, k_0^{(2)} + \frac{i^{(2)}}{2^n}\right) \end{array} \right\}$$
$$= \frac{1}{2^n}F_s\left(k_0^{(1)} + \frac{i^{(1)}}{2^n}, k_0^{(2)} + \frac{i^{(2)}}{2^n}\right)\widetilde{\mathbf{L}}_1 + \frac{1}{2^n}F_t\left(k_0^{(1)} + \frac{i^{(1)}}{2^n}, k_0^{(2)} + \frac{i^{(2)}}{2^n}\right)\widetilde{\mathbf{L}}_2$$

by the Chain Rule.

Using (3.20) we can equate the right sides of 3.19 and 3.21

$$\alpha_1^{(n)}\widetilde{\mathbf{L}}_1+\alpha_2^{(n)}\widetilde{\mathbf{L}}_2 = \frac{1}{2^n}F_s\left(k_0^{(1)} + \frac{i^{(1)}}{2^n}, k_0^{(2)} + \frac{i^{(2)}}{2^n}\right)\widetilde{\mathbf{L}}_1+\frac{1}{2^n}F_t\left(k_0^{(1)} + \frac{i^{(1)}}{2^n}, k_0^{(2)} + \frac{i^{(2)}}{2^n}\right)\widetilde{\mathbf{L}}_2$$

So by linear independence

$$F_s\left(k_0^{(1)}+\frac{i^{(1)}}{2^n},k_0^{(2)}+\frac{i^{(2)}}{2^n}\right)=2^n\alpha_1^{(n)} \tag{3.22}$$

$$F_t\left(k_0^{(1)}+\frac{i^{(1)}}{2^n},k_0^{(2)}+\frac{i^{(2)}}{2^n}\right)=2^n\alpha_2^{(n)}$$

Proposition 3.2. *Suppose that an interpolatory triangular scheme is convergent with limiting surface F in C^1 where for $\mathbf{k}_0=\left[k_0^{(1)},k_0^{(2)}\right]^T\in\mathbb{Z}^2$ the n^{th} control net surrounding $\mathbf{v}_{2^n\mathbf{k}_0+\mathbf{i}}$ for $\mathbf{i}\in\mathbb{Z}^2\setminus(0,0)^T$ (after n subdivisions of the initial control vector net) is given as in (3.17 |p.30). Also assume its mask $\{P_\mathbf{k}\}_\mathbf{k}$ has Sum Rule of at least order 3. Let $\alpha_1^{(n)}$,$\alpha_2^{(n)}\in\mathbb{R}^3$ be the column vectors in (3.18 |p.30). Then*

$$F_s\left(k_0^{(1)}+\frac{i^{(1)}}{2^n},k_0^{(2)}+\frac{i^{(2)}}{2^n}\right)=2^n\alpha_1^{(n)},\qquad F_t\left(k_0^{(1)}+\frac{i^{(1)}}{2^n},k_0^{(2)}+\frac{i^{(2)}}{2^n}\right)=2^n\alpha_2^{(n)}$$

3.4. Second Partial Derivatives (Regular)

The procedure for obtaining the second partial derivatives of our limit surface F is similar. Again we will first consider vertex $v^m_{2^m\mathbf{k}_0}\left(=v^0_{\mathbf{k}_0}\right)$ from the initial control net after m subdivisions.

Define J^* as the 38×38 "picking" matrix that for odd j between 3 and 31 replaces the j and $j+1$ columns with the $j+6$ and $j+7$ columns (and vice versa) of any 3×38 matrix. To illustrate, $U^m_{\mathbf{k}_0}J^*$ replaces $\mathbf{u}^m_{\mathbf{k}_0+(1,0)^T}$ with $\mathbf{u}^m_{\mathbf{k}_0+(-1,0)^T}$ and vice versa. It also replaces $\mathbf{u}^m_{\mathbf{k}_0+(1,1)^T}$ with $\mathbf{u}^m_{\mathbf{k}_0+(-1,-1)^T}$ and vice versa.

We then obtain the following set of equalities:

(3.23)

$$\lim_{m\to\infty} 2^{2m}\left[\mathbf{U}^m_{\mathbf{k}_0}+\mathbf{U}^m_{\mathbf{k}_0}J^*-2\left[v^0_{\mathbf{k}_0,},0,v^0_{\mathbf{k}_0,},0,v^0_{\mathbf{k}_0,},0...,v^0_{\mathbf{k}_0,},0\right]\right]=$$

$$\lim_{m\to\infty} 2^{2m}\left\{\begin{array}{c}\left[\begin{array}{c}\alpha^{(0)}_0\mathbf{L}_0+2^{-m}\alpha^{(0)}_1\mathbf{L}_1+2^{-m}\alpha^{(0)}_2\mathbf{L}_2+4^{-m}\alpha^{(0)}_3\mathbf{L}_3...\\+4^{-m}\alpha^{(0)}_4\mathbf{L}_4+4^{-m}\alpha^{(0)}_5\mathbf{L}_5+o\left(2^{-2m}\right)\end{array}\right]+\\ \left[\begin{array}{c}\alpha^{(0)}_0\mathbf{L}_0+2^{-m}\alpha^{(0)}_1\mathbf{L}_1+2^{-m}\alpha^{(0)}_2\mathbf{L}_2+4^{-m}\alpha^{(0)}_3\mathbf{L}_3...\\+4^{-m}\alpha^{(0)}_4\mathbf{L}_4+4^{-m}\alpha^{(0)}_5\mathbf{L}_5+o\left(2^{-2m}\right)\end{array}\right]J^*-\\ 2\left[v^0_{\mathbf{k}_0,},0,v^0_{\mathbf{k}_0,},0,v^0_{\mathbf{k}_0,},0...,v^0_{\mathbf{k}_0,},0\right]\end{array}\right\}=$$

$$\lim_{m\to\infty} 2^{2m}\left\{\begin{array}{c}\left[4^{-m}\alpha^{(0)}_3\mathbf{L}_3+4^{-m}\alpha^{(0)}_4\mathbf{L}_4+4^{-m}\alpha^{(0)}_5\mathbf{L}_5+o\left(2^{-2m}\right)\right]+\\ \left[4^{-m}\alpha^{(0)}_3\mathbf{L}_3+4^{-m}\alpha^{(0)}_4\mathbf{L}_4+4^{-m}\alpha^{(0)}_5\mathbf{L}_5+o\left(2^{-2m}\right)\right]J^*\end{array}\right\}=$$

$$\lim_{m\to\infty} 2^{2m}\left\{2\cdot 4^{-m}\alpha^{(0)}_3\mathbf{L}_3+2\cdot 4^{-m}\alpha^{(0)}_4\mathbf{L}_4+2\cdot 4^{-m}\alpha^{(0)}_5\mathbf{L}_5+o\left(2^{-2m}\right)\right\}=$$

$$2\alpha^{(0)}_3\mathbf{L}_3+2\alpha^{(0)}_4\mathbf{L}_4+2\alpha^{(0)}_5\mathbf{L}_5$$

Now we look at the second order directional derivatives in the direction of each of the 18 surrounding vertices and derive:

(3.24)

$$\lim_{m\to\infty} 2^{2m}\left\{\begin{array}{c}0,F\left(k^{(1)}_0+2^{-m}\left(1\right),k^{(2)}_0\right)+F\left(k^{(1)}_0+2^{-m}\left(-1\right),k^{(2)}_0\right)\\-2F\left(k^{(1)}_0,k^{(2)}_0\right),\\ F\left(k^{(1)}_0+2^{-m}\left(1\right),k^{(2)}_0+2^{-m}\left(1\right)\right)+F\left(k^{(1)}_0+2^{-m}\left(-1\right),k^{(2)}_0+2^{-m}\left(-1\right)\right)\\-2F\left(k^{(1)}_0,k^{(2)}_0\right),...,\\ F\left(k^{(1)}_0+2^{-m}\left(-1\right),k^{(2)}_0+2^{-m}\left(-2\right)\right)+F\left(k^{(1)}_0+2^{-m}\left(1\right),k^{(2)}_0+2^{-m}\left(2\right)\right)\\-2F\left(k^{(1)}_0,k^{(2)}_0\right),\\ F\left(k^{(1)}_0+2^{-m}\left(1\right),k^{(2)}_0+2^{-m}\left(-1\right)\right)+F\left(k^{(1)}_0+2^{-m}\left(-1\right),k^{(2)}_0+2^{-m}\left(1\right)\right)\\-2F\left(k^{(1)}_0,k^{(2)}_0\right)\end{array}\right\}=$$

$$F_{ss}\left(k^{(1)}_0,k^{(2)}_0\right)\widetilde{\mathbf{L}}_3+2F_{st}\left(k^{(1)}_0,k^{(2)}_0\right)\widetilde{\mathbf{L}}_4+F_{tt}\left(k^{(1)}_0,k^{(2)}_0\right)\widetilde{\mathbf{L}}_5$$

where

$$\widetilde{\mathbf{L}}_3 = \left[0, 1^2, 1^2, 0, (-1)^2, (-1)^2, ..., (-1)^2, 1^2\right]$$
$$\widetilde{\mathbf{L}}_4 = \left[0, 1 \cdot 0, 1 \cdot 1, 0 \cdot 1, (-1) \cdot 0, (-1)^2 ...., (-1)(-2), 1(-1)\right]$$
$$\widetilde{\mathbf{L}}_5 = \left[0, 0, 1^2, 1^2, 0, (-1)^2, ..., (-2)^2, (-1)^2\right]$$

which are the odd components of $\mathbf{L}_3$, $\mathbf{L}_4$, and $\mathbf{L}_5$ respectively.

Using (3.14 |p.29) we then can equate the right sides of (3.23 |p.33) and (3.24 |p.33) to obtain:

$$2\alpha_3^{(0)}\widetilde{\mathbf{L}}_3+2\alpha_4^{(0)}\widetilde{\mathbf{L}}_4+2\alpha_5^{(0)}\widetilde{\mathbf{L}}_5 = F_{ss}\left(k_0^{(1)}, k_0^{(2)}\right)\widetilde{\mathbf{L}}_3+2F_{st}\left(k_0^{(1)}, k_0^{(2)}\right)\widetilde{\mathbf{L}}_4+F_{tt}\left(k_0^{(1)}, k_0^{(2)}\right)\widetilde{\mathbf{L}}_5$$

By linear independence we have:

$$\begin{aligned} F_{ss}\left(k_0^{(1)}, k_0^{(2)}\right) &= 2\alpha_3^{(0)} \\ F_{st}\left(k_0^{(1)}, k_0^{(2)}\right) &= \alpha_4^{(0)} \\ F_{tt}\left(k_0^{(1)}, k_0^{(2)}\right) &= 2\alpha_5^{(0)} \end{aligned} \tag{3.25}$$

Proposition 3.3. *Suppose that an interpolatory triangular scheme is convergent with limiting surface F in C^2 where for $\mathbf{k}_0 = \left[k_0^{(1)}, k_0^{(2)}\right]^T \in \mathbb{Z}^2$ the initial control vector surrounding $\mathbf{v}_{\mathbf{k}_0}$ is given as in Figure 3.2. Also assume its mask $\{P_\mathbf{k}\}_\mathbf{k}$ has Sum Rule of at least order 3. Let $\alpha_3^{(0)}$,$\alpha_4^{(0)}$, $\alpha_5^{(0)}$ $\in \mathbb{R}^3$ be the column vectors in (3.9 |p.26). Then*

$$\begin{aligned} F_{ss}\left(k_0^{(1)}, k_0^{(2)}\right) &= 2\alpha_3^{(0)} \\ F_{st}\left(k_0^{(1)}, k_0^{(2)}\right) &= \alpha_4^{(0)} \\ F_{tt}\left(k_0^{(1)}, k_0^{(2)}\right) &= 2\alpha_5^{(0)} \end{aligned}$$

Similar to the proof of Proposition 3.2 we have the following

Proposition 3.4. *Suppose that an interpolatory triangular scheme is convergent with limiting surface F in C^2 where for $\mathbf{k}_0 = \left[k_0^{(1)}, k_0^{(2)}\right]^T \in \mathbb{Z}^2$ the n^{th} control net surrounding $\mathbf{v}_{2^n\mathbf{k}_0+\mathbf{i}}$ for $\mathbf{i} \in \mathbb{Z}^2 \backslash (0,0)^T$ (after n subdivisions of the initial control vector net) is given as in (3.17 |p.30). Also assume its mask $\{P_\mathbf{k}\}_\mathbf{k}$ has Sum Rule of at least order 3. Let $\alpha_1^{(n)}$,$\alpha_2^{(n)} \in \mathbb{R}^3$ be the* *column vectors in (3.18 |p.30). Then*

$$F_{ss}\left(k_0^{(1)}+\frac{i^{(1)}}{2^n},k_0^{(2)}+\frac{i^{(2)}}{2^n}\right)=2^{2n+1}\alpha_3^{(n)} \tag{3.26}$$
$$F_{st}\left(k_0^{(1)}+\frac{i^{(1)}}{2^n},k_0^{(2)}+\frac{i^{(2)}}{2^n}\right)=2^{2n}\alpha_4^{(n)}$$
$$F_{tt}\left(k_0^{(1)}+\frac{i^{(1)}}{2^n},k_0^{(2)}+\frac{i^{(2)}}{2^n}\right)=2^{2n+1}\alpha_5^{(n)}$$

3.5. First Partial Derivatives (Extraordinary)

The scheme is assumed to be C^1 at the extraordinary vertices. So in a similar fashion, first partial derivatives at an extraordinary vertex (valence $n \neq 6$) will be developed. As before, we will start by developing the left eigenvectors of the subdominant eigenvalue λ. We assume

- λ has multiplicity 2 and
- the subdominant eigenvalue λ is an eigenvalue of the second and last blocks of a block diagonal matrix that is similar to the subdivision matrix for the extraordinary vertex.

Please note that since our subdivision matrix has real entries only then by the above assumptions λ must be real.

First we introduce some notation from [**CJ08**]. Let $\mathcal{C}$ be a $2n \times 2n$ cyclic block matrix with 2×2 submatrix blocks C_j. We have

$$\mathcal{C}=\begin{bmatrix} C_0 & C_1 & \cdots & C_{n-1} \\ C_{n-1} & C_0 & \cdots & C_{n-2} \\ \cdots & \cdots & \cdots & \cdots \\ C_1 & C_2 & \cdots & C_0 \end{bmatrix} \tag{3.27}$$

Let $\mathcal{C}\left(C_0, C_1; C_{n-1}\right)$ denote the above matrix $\mathcal{C}$ but with $C_j = 0,\ j \neq 0, 1, n-1$.

Define the $2n \times 2n$ matrix U_n

$$U_n := \left[z^{k\,j} I_2\right]_{k=0,\ldots,n-1,\quad j=0,\ldots,n-1} \tag{3.28}$$

where

$$z := e^{\frac{2\pi i}{n}} \tag{3.29}$$

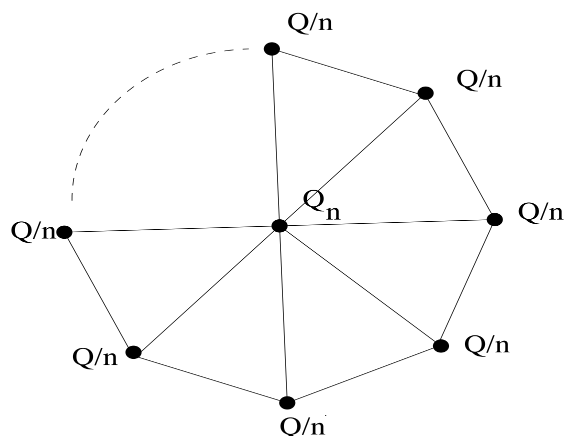

Figure 3.3. Extraordinary Vertex Template (triangular)

By direct calculation, the DFT (Discrete Fourier Transform) of $\mathcal{C}$, defined by $\widehat{\mathcal{C}} := U_n C U_n^{-1}$, can be written as

$$\widehat{\mathcal{C}} = diag\left(\widehat{C}_0,\widehat{C}_1,\ldots,\widehat{C}_{n-1}\right)$$

where $\widehat{C}_j := \sum_{k=0}^{n-1} C_k z^{-jk}$

Let S_n be the following $(6n+2)\times(6n+2)$ subdivision matrix around an extraordinary vertex of valence n

$$\begin{bmatrix} Q_n & \begin{bmatrix} B & B & \cdots & B \end{bmatrix} & \begin{bmatrix} D & D & \cdots & D \end{bmatrix} & \begin{bmatrix} C & C & \cdots & C \end{bmatrix} \\ \frac{1}{n}\begin{bmatrix} Q \\ Q \\ \vdots \\ Q \end{bmatrix} & \mathcal{C}\left(B,C;C\right) & \mathcal{C}\left(P_{0,0},D;D\right) & \mathcal{C}\left(B,\mathbf{0};\mathbf{B}\right) \\ \mathbf{0} & \mathbf{0} & diag\left(D\right) & \mathbf{0} \\ \mathbf{0} & \mathbf{0} & \mathcal{C}\left(D,D;\mathbf{0}\right) & diag\left(C\right) \end{bmatrix} \tag{3.30}$$

where B, C are as in (2.10 |p.13) and Q_n, Q are from the template for the extraordinary vertex given in Figure 3.3:

In Figure 3.3

$$Q_n = \begin{bmatrix} 1 & w_{1,2} \\ 0 & w_{2,2} \end{bmatrix} \qquad Q = \begin{bmatrix} 0 & q_{1,2} \\ 0 & q_{2,2} \end{bmatrix} \tag{3.31}$$

where we will assume that

$$w_{1,2} = -q_{1,2} \tag{3.32}$$

Note that S_n is a matrix on a 2-ring neighborhood of our central extraordinary vertex just as S (2.26 |p.20) is a matrix on a 2-ring neighborhood of our central vertex v_0.

Define

$$U := \operatorname{diag}(I_2,\, U_n, U_n, U_n) \quad (6n+2) \;\; \times \;\; (6n+2) \;\text{ matrix}$$

Let $\mathcal{L}$ represent the $(6n+2)\times(6n+2)$ "picking" matrix that exchanges the $j+nk$ block row with the $3\,(j-2)+k+2$ block row where $0 \le k \le 2$ and $2 \le j \le n+1$. Then as in [**Zor00a**] and [**CJ08**], $\widetilde{S}_n := \mathcal{L} U S_n\,(U_n)^{-1}\,\mathcal{L}^{-1}$ is a $(6n+2)\times(6n+2)$ block diagonal matrix that is similar to S_n and hence has the same eigenvalues. $\widetilde{S}_n$ has the following representation:

$$\widetilde{S}_n = \begin{bmatrix} M_0 & \mathbf{0} & \mathbf{0} & \mathbf{0} & \mathbf{0} & \mathbf{0} \\ \mathbf{0} & M_1 & \mathbf{0} & \mathbf{0} & \mathbf{0} & \mathbf{0} \\ \mathbf{0} & \mathbf{0} & M_2 & \cdots & \mathbf{0} & \mathbf{0} \\ \vdots & \vdots & \vdots & \ddots & \vdots & \vdots \\ \mathbf{0} & \mathbf{0} & \mathbf{0} & \cdots & M_{n-2} & \mathbf{0} \\ \mathbf{0} & \mathbf{0} & \mathbf{0} & \cdots & \mathbf{0} & M_{n-1} \end{bmatrix}$$

where

$$M_0 = \begin{bmatrix} Q_n & B & D & C \\ Q & B+2C & P_{0,0}+2D & 2B \\ \mathbf{0} & \mathbf{0} & D & \mathbf{0} \\ \mathbf{0} & \mathbf{0} & 2D & C \end{bmatrix}$$

and for $j = 1, 2, ..., n-1$

$$M_j = \begin{bmatrix} B + C\left(z^j + \frac{1}{z^j}\right) & P_{0,0} + D\left(z^j + \frac{1}{z^j}\right) & B\left(1 + z^j\right) \\ \mathbf{0} & D & \mathbf{0} \\ \mathbf{0} & D\left(1 + \frac{1}{z^j}\right) & C \end{bmatrix}$$

Our real subdominant eigenvalue (call it λ) of multiplicity 2 is assumed to be an eigenvalue of the second block $M_{1.}$ So it must either be an eigenvalue of $B+C\left(z+\frac{1}{z}\right)$ or it must be an eigenvalue of $\begin{bmatrix} D & \mathbf{0} \\ D\left(1+\frac{1}{z}\right) & C \end{bmatrix}$. If it were an eigenvalue of the latter then its multiplicity would not be 2. Hence, it is an eigenvalue of $B + C\left(z + \frac{1}{z}\right)$.

So if we further restrict our subdivision matrix to a 1-ring neighborhood around the central extraordinary vertex we get the $(2n+2)\times(2n+2)$ matrix $S1_n$ where

$$S1_n := \begin{bmatrix} Q_n & \begin{bmatrix} B & B & \cdots & B \end{bmatrix} \\ \frac{1}{n}\begin{bmatrix} Q \\ Q \\ \vdots \\ Q \end{bmatrix} & \mathcal{C}\left(B, C; C\right) \end{bmatrix} \tag{3.33}$$

If we define $(2n+2)\times(2n+2)$ matrix $\widetilde{U} := diag\left(I_2,\, U_n\right)$ we can then define $\widetilde{S1}_n := \widetilde{U}\, S1_n \left(\widetilde{U}\right)^{-1}$ (here we do not need the "picking" matrix to obtain the desired form we want):

$$\widetilde{S1}_n = \begin{pmatrix} Q_n & B & \mathbf{0} & \cdots & \mathbf{0} \\ Q & B+2C & \mathbf{0} & \cdots & \mathbf{0} \\ \mathbf{0} & \mathbf{0} & B+C\left(z+\frac{1}{z}\right) & \cdots & \vdots \\ \vdots & \vdots & \ddots & \ddots & \mathbf{0} \\ \mathbf{0} & \mathbf{0} & \mathbf{0} & \cdots & B+C\left(z^{n-1}+\frac{1}{z^{n-1}}\right) \end{pmatrix} \tag{3.34}$$

Note that the subdominant eigenvalue of $\widetilde{S1}_n$ is λ.

Lemma 3.1. *Claim that if* t_2 *(from 3.4 |p.24) is such that* $\left|\frac{1}{8} - t_2 + t_2\left(z + z^{-1}\right)\right| < \frac{3}{8} + \frac{1}{8}\left(z + z^{-1}\right)$ *then* $\lambda = \frac{3}{8} + \frac{1}{8}\left(z + z^{-1}\right)$ *and a left eigenvector for* λ *of* $B + C\left(z + \frac{1}{z}\right)$ *is* $[1,\ 0]$.

Proof. From (3.4 |p.24), we see that

$$B + C\left(z + \frac{1}{z}\right) = \begin{bmatrix} \frac{3}{8} + \frac{1}{8}\left(z + z^{-1}\right) & 0 \\ -\frac{1}{8h} - t_1 + t_1\left(z + z^{-1}\right) & \frac{1}{8} - t_2 + t_2\left(z + z^{-1}\right) \end{bmatrix}$$

So its 2 eigenvalues are $\frac{3}{8} + \frac{1}{8}\left(z + z^{-1}\right)$ and $\frac{1}{8} - t_2 + t_2\left(z + z^{-1}\right)$. We know that λ is an eigenvalue of this matrix. Hence by our modulus assumption, $\lambda = \frac{3}{8} + \frac{1}{8}\left(z + z^{-1}\right)$. We can then readily see that $[1,\ 0]$ is a left eigenvector for λ. □

Since t_2 is a free variable, we can assume in the following that $\left|\frac{1}{8} - t_2 + t_2\left(z + z^{-1}\right)\right| < \frac{3}{8} + \frac{1}{8}\left(z + z^{-1}\right)$.

We can readily see that the $2n + 2$ row vector $(0, 0, 0, 0, 1, 0, 0, \ldots, 0)$ is a left eigenvector of $\widetilde{S1}_n$ for λ and thus $(0, 0, 0, 0, 1, 0, 0, \ldots, 0)\,\widetilde{U}$ is a left eigenvector of $S1_n$ for λ.

So we have

$$\mathbf{L}_1 = (0, 0, 0, 0, 1, 0, 0, \ldots, 0)\,\widetilde{U} = \left(0, 0, 1, 0, z, 0, \ldots, z^{n-1}, 0\right)$$

where $\mathbf{L}_1$ is a complex left eigenvector of $S1_n$ for λ

Note that $\lambda \in \mathbb{R}$. Hence the real and imaginary parts $\left(\widetilde{\mathbf{L}}_1 \text{ and } \widetilde{\mathbf{L}}_2 \text{ respectively}\right)$ are two real left eigenvectors of the real matrix $S1_n$ for λ.

$$\widetilde{\mathbf{L}}_1 = \left(0, 0, 1, 0, \cos\left(\frac{2\pi}{n}\right), 0, \ldots, \cos\left(\frac{2\left(n-1\right)\pi}{n}\right), 0\right)$$

$$\widetilde{\mathbf{L}}_2 = \left(0, 0, 0, 0, \sin\left(\frac{2\pi}{n}\right), 0, \ldots, \sin\left(\frac{2\left(n-1\right)\pi}{n}\right), 0\right) \tag{3.35}$$

Lemma 3.2. $\widetilde{\mathbf{L}}_1$ *and* $\widetilde{\mathbf{L}}_2$ *are linearly independent over* $\mathbb{C}$.

Proof. Suppose $\exists\ c_1, c_2 \in \mathbb{C}$ such that $c_1\widetilde{\mathbf{L}}_1 + c_2\widetilde{\mathbf{L}}_2 = \mathbf{0}$. Then immediately we can see that $c_1 = 0$. Thus $c_2\widetilde{\mathbf{L}}_2 = \mathbf{0}$. Hence $c_2 \sin\left(\frac{2\pi k}{n}\right) = 0$ for $k = 1, ..., n-1$. Thus since $n \geq 3$, $c_2 = 0$. □

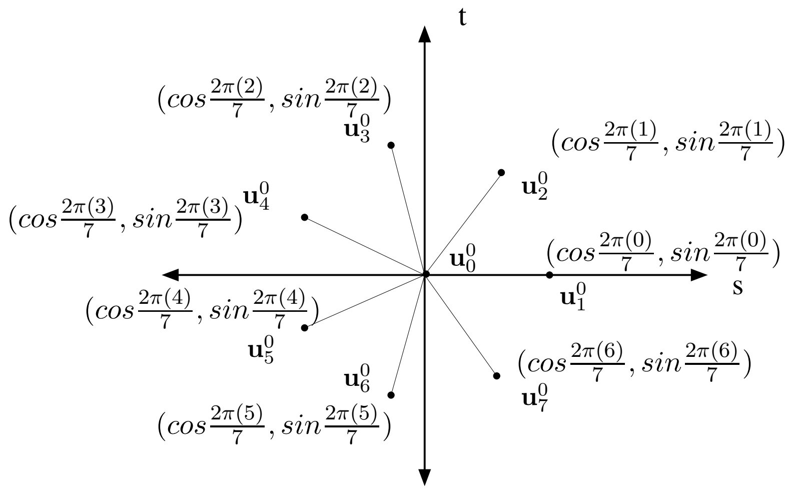

Figure 3.4. Initial control vector net of extraordinary vertex of valence 7 and the 7 vertices adjacent to it. The parameters of the surrounding 7 vertices are given. Note the s and t axis.

As in the regular case we will be representing an initial control vector net around an extraordinary vertex (having valence n) as a linear combination of left eigenvectors.

Let us denote the extraordinary vertex by v_0^0 (the first component of $\mathbf{u}_0^0 := [v_0^0, s_0^0]$). The initial control vector net that includes $\mathbf{u}_0^0$ and the vertices immediately adjacent to $\mathbf{u}_0^0$ is a $3 \times (2n+2)$ vector of $n+1$ initial control vertices and $n+1$ initial shape control vertices. See Figure 3.4 where $n = 7$.

Denote the vector net immediately surrounding (and including) the extraordinary vertex after $m \geq 0$ subdivisions by

$$\mathbf{U}^m := [\mathbf{u}_0^m, \mathbf{u}_1^m, \mathbf{u}_2^m, ..., \mathbf{u}_n^m]$$

where for $j = 0, 1, 2, ..., n$, $\mathbf{u}_j^m := \left[v_j^m, s_j^m\right]$ (the block vertex consisting of new vertices and new shape control vertices).

Hence

$$\mathbf{U}^{m+1} = \mathbf{U}^m S1_n$$
$$\mathbf{U}^m = \mathbf{U}^0 \left(S1_n\right)^m$$

where $S1_n$ is given in (3.33 |p.38).

The $3 \times (2n+2)$ *initial* control vector net ($\mathbf{U}^0$) around this irregular $\mathbf{v}_\mathbf{0}^0$ can be represented as a linear combination of $1 \times (2n+2)$ (possibly generalized) left eigenvectors of our $(2n+2) \times (2n+2)$ subdivision matrix $S1_n$ (3.33 |p.38).

So by letting $\left\{\widetilde{\mathbf{L}}_j : 0 \le j \le 2n+1\right\}$ be a set of $2n+2$ (possibly generalized) linearly independent left eigenvectors of $S1_n$ $\mathbf{U}^0$ can be written as

$$\mathbf{U}^0 = \widetilde{\alpha}_0^{(0)}\widetilde{\mathbf{L}}_0 + \widetilde{\alpha}_1^{(0)}\widetilde{\mathbf{L}}_1 + \widetilde{\alpha}_2^{(0)}\widetilde{\mathbf{L}}_2 + \sum_{j=3}^{2n+1} \widetilde{\alpha}_j^{(0)}\widetilde{\mathbf{L}}_j \tag{3.36}$$

where for $j = 0, \ldots, 2n+1$ $\widetilde{\alpha}_j^{(0)} \in \mathbb{R}^3$ where $\widetilde{\mathbf{L}}_1, \widetilde{\mathbf{L}}_2$ are the left eigenvectors for λ from (3.35 |p.39).

Note that the left eigenvector for 1 is $\widetilde{\mathbf{L}}_0 = [1, 0, 1, 0, ..., 1, 0]$ due to the assumption (3.32 |p.37).

Recall that by assumption the eigenvalues for $\widetilde{\mathbf{L}}_j$ $(j = 3, ..., 2n+1)$ have modulus less than λ.

Hence

$$\mathbf{U}^m = \widetilde{\alpha}_0^{(0)}\widetilde{\mathbf{L}}_0 + \lambda^m\widetilde{\alpha}_1^{(0)}\widetilde{\mathbf{L}}_1 + \lambda^m\widetilde{\alpha}_2^{(0)}\widetilde{\mathbf{L}}_2 + o\left(\lambda^m\right)$$
$$\lim_{m\to\infty} \lambda^{-m}\left(\mathbf{U}^m - \widetilde{\alpha}_0^{(0)}\widetilde{\mathbf{L}}_0\right) = \widetilde{\alpha}_1^{(0)}\widetilde{\mathbf{L}}_1 + \widetilde{\alpha}_2^{(0)}\widetilde{\mathbf{L}}_2$$

Since

- $\lim_{m\to\infty} \mathbf{U}^m = \widetilde{\alpha}_0^{(0)}\widetilde{\mathbf{L}}_0$
- the first component of $\widetilde{\mathbf{L}}_0$ being 1 and
- the scheme being interpolatory

we derive $\widetilde{\alpha}_0^{(0)} = v_0^0 = v_0^m$ for $m = 1, 2, ...$

So we have

$$\lim_{m\to\infty} \lambda^{-m}\left(\mathbf{U}^m - \left[v_{\mathbf{0},}^0, 0, v_{\mathbf{0},}^0, 0, v_{\mathbf{0},}^0, 0..., v_{\mathbf{0},}^0, 0\right]\right) = \widetilde{\alpha}_1^{(0)}\widetilde{\mathbf{L}}_1 + \widetilde{\alpha}_2^{(0)}\widetilde{\mathbf{L}}_2 \tag{3.37}$$

Looking at the odd components of the left and right sides we obtain:

(3.38)
$$\lim_{m\to\infty} \lambda^{-m}\left(\left[v_0^m, v_1^m, v_2^m, ..., v_n^m\right] - \left[v_{\mathbf{0},}^0, v_{\mathbf{0},}^0, v_{\mathbf{0},}^0, ..., v_{\mathbf{0},}^0\right]\right) = \widetilde{\alpha}_1^{(0)}\widetilde{\widetilde{\mathbf{L}}}_1 + \widetilde{\alpha}_2^{(0)}\widetilde{\widetilde{\mathbf{L}}}_2$$

where

$$\widetilde{\widetilde{\mathbf{L}}}_1 = \left[0, \cos(\frac{2\cdot 0\cdot\pi}{n}), \cos\left(\frac{2\cdot 1\cdot\pi}{n}\right), \cos\left(\frac{2\cdot 2\cdot\pi}{n}\right), ..., \cos\left(\frac{2\cdot(n-1)\cdot\pi}{n}\right)\right]$$

$$\widetilde{\widetilde{\mathbf{L}}}_2 = \left[0, \sin(\frac{2\cdot 0\cdot\pi}{n}), \sin\left(\frac{2\cdot 1\cdot\pi}{n}\right), \sin\left(\frac{2\cdot 2\cdot\pi}{n}\right), ..., \sin\left(\frac{2\cdot(n-1)\cdot\pi}{n}\right)\right]$$

Now we will use (3.37 |p.41) to get a representation of the two first partial derivatives at the point on the surface corresponding to the extraordinary vertex.

Let us parametrize F locally around this point (see Figure 3.4) where

$$F(0,0) := v_0^0$$

$$F\left(\cos\left(\frac{2j\pi}{n}\right), \sin\left(\frac{2j\pi}{n}\right)\right) := v_{j+1}^0 \quad \text{for } j = 0, 1, ..., n-1$$

$$F\left(\lambda^m \cos\left(\frac{2j\pi}{n}\right), \lambda^m \sin\left(\frac{2j\pi}{n}\right)\right) := v_{j+1}^m \quad \text{after } m \text{ subdivisions}$$

Since F is assumed to be C^1 at extraordinary vertices then

$$\lim_{m\to\infty} \lambda^{-m} \left\{ \begin{array}{c} F(0,0) - F(0,0),\ F\left(\lambda^m \cos\left(\frac{2\cdot 0\cdot\pi}{n}\right), \lambda^m \sin\left(\frac{2\cdot 0\cdot\pi}{n}\right)\right) - F(0,0), \\ F\left(\lambda^m \cos\left(\frac{2\cdot 1\cdot\pi}{n}\right), \lambda^m \sin\left(\frac{2\cdot 1\cdot\pi}{n}\right)\right) - F(0,0), \\ F\left(\lambda^m \cos\left(\frac{2\cdot 2\cdot\pi}{n}\right), \lambda^m \sin\left(\frac{2\cdot 2\cdot\pi}{n}\right)\right) - F(0.0), ..., \\ F\left(\lambda^m \cos\left(\frac{2\cdot(n-2)\cdot\pi}{n}\right), \lambda^m \sin\left(\frac{2\cdot(n-2)\cdot\pi}{n}\right)\right) - F(0,0)\ , \\ F\left(\lambda^m \cos\left(\frac{2\cdot(n-1)\cdot\pi}{n}\right), \lambda^m \sin\left(\frac{2\cdot(n-1)\cdot\pi}{n}\right)\right) - F(0,0) \end{array} \right\} =$$

$$F_s(0,0)\,\widetilde{\widetilde{\mathbf{L}}}_1 + F_t(0,0)\,\widetilde{\widetilde{\mathbf{L}}}_2$$

So from the local parametrization we have

$$\lim_{m\to\infty} \lambda^{-m} \left([v_0^m, v_1^m, v_2^m, ..., v_n^m] - \left[v_0^0, v_0^0, v_0^0, ..., v_0^0\right]\right) = F_s(0,0)\,\widetilde{\widetilde{\mathbf{L}}}_1 + F_t(0,0)\,\widetilde{\widetilde{\mathbf{L}}}_2 \tag{3.39}$$

From (3.38 |p.41) and (3.39 |p.42) and the linear independence of $\widetilde{\widetilde{\mathbf{L}}}_1$ and $\widetilde{\widetilde{\mathbf{L}}}_2$

$$F_s(0,0) = \widetilde{\alpha}_1^{(0)}$$
$$F_t(0,0) = \widetilde{\alpha}_2^{(0)}$$

Proposition 3.5. *Suppose that an interpolatory triangular scheme is convergent with limiting surface F that is C^1 at points corresponding to extraordinary vertices. Let $F(0,0)$ be such a point. Let $\widetilde{\alpha}_1^{(0)}, \widetilde{\alpha}_2^{(0)} \in \mathbb{R}^3$ be the column vectors in (3.36 |p.41). Then*

$$F_s(0,0) = \widetilde{\alpha}_1^{(0)}, \qquad F_t(0,0) = \widetilde{\alpha}_2^{(0)}$$

3.6. Partial Derivatives in Terms of Initial Control Net

So far we have partial derivatives in terms of coefficients of the linear combinations of left eigenvectors. Here we will obtain a much more specific representation of the partial derivatives. They will be given in terms of the initial control vector net. First looking at the regular case, we will use right eigenvectors of the subdivision matrix to achieve this.

3.6.1. Regular Case

We are first going to obtain the right eigenvectors of S (2.26 |p.20).

As in [**Zor00a**] and [**CJ08**], we can derive the following 6 diagonal block matrix $\widetilde{B}$ that is similar to the subdivision matrix S where

$$\widetilde{B} = \mathfrak{L} U S U^{-1} \mathfrak{L}^{-1} \tag{3.40}$$

and

$$U := \operatorname{diag}(I_2, U_6, U_6, U_6) \qquad 38 \times 38 \quad \text{matrix} \tag{3.41}$$

where U_6 is defined in (3.28 |p.35).

$\mathfrak{L}$ denotes the 38×38 "picking" matrix that exchanges the $6k + j$ and $(j-2)\,3 + k + 2$ (block matrix) rows where $0 \le k \le 2$ and $2 \le j \le 7$

One gets

$$\widetilde{B} = \begin{pmatrix} M_0 & & & & & \\ & M_1 & & & & \\ & & M_2 & & & \\ & & & M_3 & & \\ & & & & M_4 & \\ & & & & & M_5 \end{pmatrix}$$

where

(3.42)

$$M_0 = \begin{pmatrix} P_{0,0} & B & D & C \\ 6D & B+2C & P_{0,0}+2D & 2B \\ 0 & 0 & D & 0 \\ 0 & 0 & 2D & C \end{pmatrix}, \quad 8 \times 8 \text{ matrix}$$

$$M_j = \begin{pmatrix} B + C\left(z^j + \frac{1}{z^j}\right) & P_{0,0} + D\left(z^j + \frac{1}{z^j}\right) & B\left(1+z^j\right) \\ 0 & D & 0 \\ 0 & D\left(1+\frac{1}{z^j}\right) & C \end{pmatrix}, \quad 6 \times 6 \text{ matrix for } j = 1, \dots, 5$$

The eigenvalues of the blocks M_j for $j = 0, \dots, 5$ are the eigenvalues of S since $\widetilde{B}$ is similar to S.

We can show through direct calculations using a computer algebra system that

- 1 and $\frac{1}{4}$ are eigenvalues of M_0,
- $\frac{1}{2}$ is only an eigenvalue of M_1 and M_5, and
- $\frac{1}{4}$ is also an eigenvalue of M_2 and M_4.

The corresponding right eigenvectors are

(3.43) $$\mathbf{r}_{1/2} = [-3h, 1, 0, 0, 0, 0]^T \qquad \text{for blocks } M_1 \text{ and } M_5$$

$$\mathbf{r}_{1/4} = \left[\frac{-h\left(16t_2+1\right)}{1+16ht_1}, 1, 0, 0, 0, 0\right]^T \qquad \text{for block } M_2 \text{ and } M_4$$

$$\mathbf{r}_{1/4} = \left[-hq, 1, hq, -\frac{m}{p}, 0, 0, 0, 0\right]^T \qquad \text{for block } M_0$$

where $q = -1 + 24t_3 + 4t_4$, $m = -4t_4 + 1 + 192ht_1t_3 + 32ht_1t_4 + 24t_3 - 8ht_1$, $p = -1 + 8t_2$ (see 3.4 |p.24). Note that h is from (3.3 |p.24).

We then "pad" the top and bottom components with the appropriate number of zeros and obtain right eigenvectors for $\widetilde{B}$ above. If we then multiply by $U^{-1}\mathfrak{L}^{-1}$ (3.40 |p.43) we obtain right eigenvectors for our subdivision matrix S.

Again using a computer algebra system we can obtain the following 38×1 right eigenvectors for $\frac{1}{2}$ and $\frac{1}{4}$ that are orthonormal to our left eigenvectors in (3.12 |p.28); i.e. we have $\mathbf{L}_i\mathbf{R}_j = \delta(i-j) \quad i,j = 1,2,3,4,5$:

$$\mathbf{R}_1 := \left[0, 0, \frac{1}{3}, \frac{-1}{9h}, \frac{1}{6}, \frac{-1}{18h}, \frac{-1}{6}, \frac{1}{18h}, \frac{-1}{3}, \frac{1}{9h}, \frac{-1}{6}, \frac{1}{18h}, \frac{1}{6}, \frac{-1}{18h}, 0, ..., 0\right]^T$$

$$\mathbf{R}_2 := \left[0, 0, \frac{-1}{6}, \frac{1}{18h}, \frac{1}{6}, \frac{-1}{18h}, \frac{1}{3}, \frac{-1}{9h}, \frac{1}{6}, \frac{-1}{18h}, \frac{-1}{6}, \frac{1}{18h}, \frac{-1}{3}, \frac{1}{9h}, 0, ..., 0\right]^T$$

$$\mathbf{R}_3 := \left[\begin{array}{c} 2d_1, 2d_2, -\frac{1}{3}(d_1-1), \frac{1}{3}(d_3+w), -\frac{1}{6}(2d_1+1), \frac{1}{6}(2d_3-w), -\frac{1}{6}(2d_1+1), \frac{1}{6}(2d_3-w), \\ -\frac{1}{3}(d_1-1), \frac{1}{3}(d_3+w), -\frac{1}{6}(2d_1+1), \frac{1}{6}(2d_3-w), -\frac{1}{6}(2d_1+1), \frac{1}{6}(2d_3-w), 0, ..., 0 \end{array}\right]^T$$

$$\mathbf{R}_4 := \left[\begin{array}{c} -2d_1, -2d_2, \frac{1}{3}(d_1-1), -\frac{1}{3}(d_3+w), \frac{1}{3}(d_1+2), -\frac{1}{3}(d_3-2w), \frac{1}{3}(d_1-1), -\frac{1}{3}(d_3+w), \\ \frac{1}{3}(d_1-1), -\frac{1}{3}(d_3+w), \frac{1}{3}(d_1+2), -\frac{1}{3}(d_3-2w), \frac{1}{3}(d_1-1), -\frac{1}{3}(d_3+w), 0, ..., 0 \end{array}\right]^T$$

$$\mathbf{R}_5 := \left[\begin{array}{c} 2d_1, 2d_2, -\frac{1}{6}(2d_1+1), \frac{1}{6}(2d_3-w), -\frac{1}{6}(2d_1+1), \frac{1}{6}(2d_3-w), \\ -\frac{1}{3}(d_1-1), \frac{1}{3}(d_3+w), -\frac{1}{6}(2d_1+1), \\ \frac{1}{6}(2d_3-w), -\frac{1}{6}(2d_1+1), \frac{1}{6}(2d_3-w), -\frac{1}{3}(d_1-1), \frac{1}{3}(d_3+w), 0, ..., 0 \end{array}\right]^T$$

where

$$\begin{aligned} d_1 &:= \frac{1}{4}\left(\frac{pq}{\widetilde{r}}\right) \\ d_2 &:= -\frac{1}{4h}\left(\frac{p}{\widetilde{r}}\right) \\ d_3 &:= \frac{1}{4h}\left(\frac{m}{\widetilde{r}}\right) \\ w &:= -\frac{(1+16ht_1)}{h(1+16t_2)} \end{aligned}$$

and where p, q, and m are from (3.43 |p.44) and $\widetilde{r} := 1 - 2t_2 + 30t_3 - 96t_2t_3 - t_4 - 16t_2t_4 + 144ht_1t_3 + 24ht_1t_4 - 6ht_1$. See (3.4 |p.24) and (3.3 |p.24).

Note that by direct calculation the following are true:

- if $1 + 16t_2 = 0$ then the eigenvalue $\frac{1}{4}$ will have multiplicity >3
- if $q = 0$ then $\frac{1}{2}$ is no longer the subdominant eigenvalue

Since right and left eigenvectors that correspond to *different* eigenvalues are orthogonal we can multiply both sides of (3.9 |p.26) by each $\mathbf{R}_j$ and so obtain (using (3.16 |p.29) and (3.25 |p.34)) the following representations for the first and second partial derivatives at a point locally parameterized as $\left(k_0^{(1)}, k_0^{(2)}\right)$:

$$
\begin{aligned}
F_s\left(k_0^{(1)}, k_0^{(2)}\right) &= \alpha_1^{(0)} = \mathbf{U}^0_{\mathbf{k}_0}\mathbf{R}_1 \\
F_t\left(k_0^{(1)}, k_0^{(2)}\right) &= \alpha_2^{(0)} = \mathbf{U}^0_{\mathbf{k}_0}\mathbf{R}_2 \\
F_{ss}\left(k_0^{(1)}, k_0^{(2)}\right) &= 2\alpha_3^{(0)} = 2\mathbf{U}^0_{\mathbf{k}_0}\mathbf{R}_3 \\
F_{st}\left(k_0^{(1)}, k_0^{(2)}\right) &= \alpha_4^{(0)} = \mathbf{U}^0_{\mathbf{k}_0}\mathbf{R}_4 \\
F_{tt}\left(k_0^{(1)}, k_0^{(2)}\right) &= 2\alpha_5^{(0)} = 2\mathbf{U}^0_{\mathbf{k}_0}\mathbf{R}_5
\end{aligned}
\tag{3.44}
$$

Note that the 15^{th} through 38^{th} components of the above right eigenvectors equal 0. So define $\mathbf{R}_j^*$ as the 14×1 column vector whose components are the first 14 components of $\mathbf{R}_j$ $(j = 1, 2, ..., 5)$. Also define $\widetilde{\mathbf{U}}^0_{\mathbf{k}_0}$ as the 3×14 vector consisting of the first 14 elements of $\mathbf{U}^0_{\mathbf{k}_0}$.

We can then rewrite (3.44) as:

$$
\begin{aligned}
F_s\left(k_0^{(1)}, k_0^{(2)}\right) &= \alpha_1^{(0)} = \widetilde{\mathbf{U}}^0_{\mathbf{k}_0}\mathbf{R}_1^* \\
F_t\left(k_0^{(1)}, k_0^{(2)}\right) &= \alpha_2^{(0)} = \widetilde{\mathbf{U}}^0_{\mathbf{k}_0}\mathbf{R}_2^* \\
F_{ss}\left(k_0^{(1)}, k_0^{(2)}\right) &= 2\alpha_3^{(0)} = 2\widetilde{\mathbf{U}}^0_{\mathbf{k}_0}\mathbf{R}_3^* \\
F_{st}\left(k_0^{(1)}, k_0^{(2)}\right) &= \alpha_4^{(0)} = \widetilde{\mathbf{U}}^0_{\mathbf{k}_0}\mathbf{R}_4^* \\
F_{tt}\left(k_0^{(1)}, k_0^{(2)}\right) &= 2\alpha_5^{(0)} = 2\widetilde{\mathbf{U}}^0_{\mathbf{k}_0}\mathbf{R}_5^*
\end{aligned}
$$

Similarly we then obtain from (3.22 |p.32) and (3.26 |p.35) the following representations for the first and second partial derivatives of a point locally parameterized as $\left(k_0^{(1)} + \frac{i^{(1)}}{2^n}, k_0^{(2)} + \frac{i^{(2)}}{2^n}\right)$on the surface F:

$$
\begin{aligned}
F_s\left(k_0^{(1)} + \frac{i^{(1)}}{2^n}, k_0^{(2)} + \frac{i^{(2)}}{2^n}\right) &= 2^n \alpha_1^{(n)} = 2^n \widetilde{\mathbf{U}}^n_{\mathbf{k}_0,\mathbf{i}} \mathbf{R}_1^* \\
F_t\left(k_0^{(1)} + \frac{i^{(1)}}{2^n}, k_0^{(2)} + \frac{i^{(2)}}{2^n}\right) &= 2^n \alpha_2^{(n)} = 2^n \widetilde{\mathbf{U}}^n_{\mathbf{k}_0,\mathbf{i}} \mathbf{R}_2^* \\
F_{ss}\left(k_0^{(1)} + \frac{i^{(1)}}{2^n}, k_0^{(2)} + \frac{i^{(2)}}{2^n}\right) &= 2^{2n+1} \alpha_3^{(n)} = 2^{2n+1} \widetilde{\mathbf{U}}^n_{\mathbf{k}_0,\mathbf{i}} \mathbf{R}_3^* \\
F_{st}\left(k_0^{(1)} + \frac{i^{(1)}}{2^n}, k_0^{(2)} + \frac{i^{(2)}}{2^n}\right) &= 2^{2n} \alpha_4^{(n)} = 2^{2n} \widetilde{\mathbf{U}}^n_{\mathbf{k}_0,\mathbf{i}} \mathbf{R}_4^* \\
F_{tt}\left(k_0^{(1)} + \frac{i^{(1)}}{2^n}, k_0^{(2)} + \frac{i^{(2)}}{2^n}\right) &= 2^{2n+1} \alpha_5^{(n)} = 2^{2n+1} \widetilde{\mathbf{U}}^n_{\mathbf{k}_0,\mathbf{i}} \mathbf{R}_5^*
\end{aligned}
\tag{3.45}
$$

where $\widetilde{\mathbf{U}}^n_{\mathbf{k}_0,\mathbf{i}}$ is the 3×14 vector consisting of the first 14 elements of $\mathbf{U}^n_{\mathbf{k}_0,\mathbf{i}}$ (3.17 |p.30).

Thus we see that once we are working with a *specific* subdivision scheme we only need to compute the above right eigenvectors *one* time, and so all that is needed to compute the partial derivatives is the surrounding control net.

3.6.2. Extraordinary Case

Likewise we will obtain a similar representation of the first partial derivatives of the limit surface at an extraordinary vertex. So we need to get the right eigenvectors of S_n (3.30 |p.36) for the subdominant eigenvalue λ.

Lemma 3.3. *Claim that if* t_2 *(from 3.4 |p.24) is such that* $\left|\frac{1}{8} - t_2 + t_2\left(z + z^{-1}\right)\right| < \frac{3}{8} + \frac{1}{8}\left(z + z^{-1}\right)$ *then* $\lambda = \frac{3}{8} + \frac{1}{8}\left(z + z^{-1}\right)$ *and a right eigenvector of* λ *for* $B + C\left(z + \frac{1}{z}\right)$ *is* $[1, d_2]^T$ *where* $d_2 = \frac{-\frac{1}{8h} - t_1 + t_1\left(z + z^{-1}\right)}{\lambda - \left(\frac{1}{8} - t_2 + t_2\left(z + z^{-1}\right)\right)}$.

Proof. We have the same assumption as in Lemma 3.1. And so from that lemma we have $\lambda = \frac{3}{8} + \frac{1}{8}\left(z + z^{-1}\right)$. Recall that λ is an eigenvalue of

$$
B + C\left(z + \frac{1}{z}\right) = \begin{bmatrix} \frac{3}{8} + \frac{1}{8}\left(z + z^{-1}\right) & 0 \\ -\frac{1}{8h} - t_1 + t_1\left(z + z^{-1}\right) & \frac{1}{8} - t_2 + t_2\left(z + z^{-1}\right) \end{bmatrix}
$$

Let $[d_1, d_2]^T$ be a *right* eigenvector for λ. So we obtain the following two equations:

$$\left(\frac{3}{8}+\frac{1}{8}\left(z+z^{-1}\right)\right)d_1=\lambda d_1$$
$$\left(-\frac{1}{8h}-t_1+t_1\left(z+z^{-1}\right)\right)d_1+\left(\frac{1}{8}-t_2+t_2\left(z+z^{-1}\right)\right)d_2=\lambda d_2$$

If $d_1 = 0$ we must have $d_2 \neq 0$ and so $\lambda = \frac{1}{8} - t_2 + t_2\left(z + z^{-1}\right)$ by the second equation. Contradiction. Thus $d_1 \neq 0$and can be normalized so that it equals 1. From the second equation we have:

$$d_2=\frac{-\frac{1}{8h}-t_1+t_1\left(z+z^{-1}\right)}{\lambda-\left(\frac{1}{8}-t_2+t_2\left(z+z^{-1}\right)\right)} \tag{3.46}$$

□

As said previously, we will assume that the free variable t_2 is such that $\left|\frac{1}{8} - t_2 + t_2\left(z + z^{-1}\right)\right| < \frac{3}{8} + \frac{1}{8}\left(z + z^{-1}\right)$. Hence $[1, d_2]$ is a right eigenvector of $B + C\left(z + \frac{1}{z}\right)$ corresponding to λ.

Padding with zeros we have that the $2n+2$ column vector $[0, 0, 0, 0, 1, d_2, 0, ..., 0]^T$ is a right eigenvector of λ for $\widetilde{S1}_n$ (3.34 |p.38) and thus $\widetilde{U}^{-1}[0, 0, 0, 0, 1, d_2, 0, ..., 0]^T$ is a right eigenvector of λ for $S1_n$.

By direct calculation

$$\mathbf{R}_1=\left[0,0,1,d_2,\overline{z},d_2\overline{z},\overline{z}^2,d_2\overline{z}^2,...,\overline{z}^{n-1},d_2\overline{z}^{n-1}\right]$$

is a complex right eigenvector of λ for $S1_n$ where z is from (3.29 |p.35) and $\overline{z}$ is the complex conjugate of z.

Since λ and $S1_n$ are both real then the real and imaginary parts of $\mathbf{R}_1$ are also real right eigenvectors of λ for $S1_n$:

$$\widetilde{\mathbf{R}}_1=\begin{bmatrix} 0,0,1,d_2,\cos\left(\frac{2\cdot1\cdot\pi}{n}\right),d_2\cos\left(\frac{2\cdot1\cdot\pi}{n}\right),..., \\ \cos\left(\frac{2\cdot(n-1)\cdot\pi}{n}\right),d_2\cos\left(\frac{2\cdot(n-1)\cdot\pi}{n}\right)\end{bmatrix}^T \tag{3.47}$$
$$\widetilde{\mathbf{R}}_2=\begin{bmatrix} 0,0,0,0,\sin\left(\frac{2\cdot1\cdot\pi}{n}\right),d_2\sin\left(\frac{2\cdot1\cdot\pi}{n}\right),..., \\ \sin\left(\frac{2\cdot(n-1)\cdot\pi}{n}\right),d_2\sin\left(\frac{2\cdot(n-1)\cdot\pi}{n}\right)\end{bmatrix}^T$$

Note that $\widetilde{\mathbf{R}}_1$ and $\widetilde{\mathbf{R}}_2$ are linearly independent and the proof mirrors the proof of Lemma 3.2 on page 39.

Through direct calculation and using the fact that $\sum_{j=0}^{n-1} \sin\left(\frac{2\pi j}{n}\right)\cos\left(\frac{2\pi j}{n}\right) = 0$, we obtain the following 2 right eigenvectors $\{\widehat{\mathbf{R}}_1, \widehat{\mathbf{R}}_2\}$ such that $\widetilde{\mathbf{L}}_i\widehat{\mathbf{R}}_j = \delta(i-j)$ for $\widetilde{\mathbf{L}}_i$ in (3.35 |p.39) where $i, j = 1, 2$:

$$\widehat{\mathbf{R}}_1 = \frac{1}{\widetilde{\mathbf{L}}_1\widetilde{\mathbf{R}}_1}\left(\widetilde{\mathbf{R}}_1\right)$$
$$\widehat{\mathbf{R}}_2 = \frac{1}{\widetilde{\mathbf{L}}_2\widetilde{\mathbf{R}}_2}\left(\widetilde{\mathbf{R}}_2\right)$$

Furthermore, since $\widetilde{\mathbf{L}}_1\widetilde{\mathbf{R}}_1 = \sum_{j=0}^{n-1} \cos^2\left(\frac{2\pi j}{n}\right) = \frac{n}{2}$ and $\widetilde{\mathbf{L}}_2\widetilde{\mathbf{R}}_2 = \sum_{j=1}^{n-1} \sin^2\left(\frac{2\pi j}{n}\right) = \frac{n}{2}$

$$\widehat{\mathbf{R}}_1 = \frac{2}{n}\widetilde{\mathbf{R}}_1 \tag{3.48}$$
$$\widehat{\mathbf{R}}_2 = \frac{2}{n}\widetilde{\mathbf{R}}_2$$

From Proposition 3.5 on page 43 and from (3.36 |p.41) we now have a representation of the first partial derivatives of the limit surface at an extraordinary vertex in terms of the surrounding block vertices:

$$F_s(0,0) = \mathbf{U}^0\widehat{\mathbf{R}}_1$$
$$F_t(0,0) = \mathbf{U}^0\widehat{\mathbf{R}}_2$$

Proposition 3.6. *Suppose that an interpolatory triangular scheme is convergent with limiting surface F that is C^1 at points corresponding to extraordinary vertices. Let $F(0,0)$ be such a point. Assume that $\lambda = \frac{3}{8} + \frac{1}{8}\left(z + z^{-1}\right)$. Then for $\widehat{\mathbf{R}}_1, \widehat{\mathbf{R}}_2$ in (3.48)*

$$F_s(0,0) = \mathbf{U}^0\widehat{\mathbf{R}}_1, \qquad F_t(0,0) = \mathbf{U}^0\widehat{\mathbf{R}}_2$$

3.7. Specific Template

Let's now apply these formulas to a specific 1-ring triangular interpolatory scheme that was developed by Chui and Jiang in [**CJ05**]. The scheme is given by (3.4 |p.24) where

$$[t_1, t_2, t_3, t_4] = \frac{1}{512}[-17, -5, -45, -182] \tag{3.49}$$
$$h = 1$$

These values result in Φ being in $W^{3.03450}$.

Substituting these values into our formulas for the right eigenvectors (regular case) we get:

$$\mathbf{R}_1^* = \left[0, 0, \frac{1}{3}, -\frac{1}{9}, \frac{1}{6}, -\frac{1}{18}, -\frac{1}{6}, \frac{1}{18}, -\frac{1}{3}, \frac{1}{9}, -\frac{1}{6}, \frac{1}{18}, \frac{1}{6}, -\frac{1}{18}\right]^T$$
$$\mathbf{R}_2^* = \left[0, 0, -\frac{1}{6}, \frac{1}{18}, \frac{1}{6}, -\frac{1}{18}, \frac{1}{3}, -\frac{1}{9}, \frac{1}{6}, -\frac{1}{18}, -\frac{1}{6}, \frac{1}{18}, -\frac{1}{3}, \frac{1}{9}\right]^T$$
$$\mathbf{R}_3^* = \left[-\frac{290}{59}, -\frac{64}{59}, \frac{68}{59}, -\frac{700}{1593}, \frac{77}{118}, -\frac{515}{3186}, \frac{77}{118}, -\frac{515}{3186}, \frac{68}{59}, -\frac{700}{1593}, \frac{77}{118}, -\frac{515}{3186}, \frac{77}{118}, -\frac{515}{3186}\right]^T$$
$$\mathbf{R}_4^* = \left[\frac{290}{59}, \frac{64}{59}, -\frac{68}{59}, \frac{700}{1593}, -\frac{9}{59}, -\frac{185}{1593}, -\frac{68}{59}, \frac{700}{1593}, -\frac{68}{59}, \frac{700}{1593}, -\frac{9}{59}, -\frac{185}{1593}, -\frac{68}{59}, \frac{700}{1593}\right]^T$$
$$\mathbf{R}_5^* = \left[-\frac{290}{59}, -\frac{64}{59}, \frac{77}{118}, -\frac{515}{3186}, \frac{77}{118}, -\frac{515}{3186}, \frac{68}{59}, -\frac{700}{1593}, \frac{77}{118}, -\frac{515}{3186}, \frac{77}{118}, -\frac{515}{3186}, \frac{68}{59}, -\frac{700}{1593}\right]^T$$

3.7.1. Corresponding specific derivative formulas

Note that for any particular scheme, the above calculations only need to be done once. If we insert these values into either (3.44 |p.46) or (3.45 |p.47) we then get the first and second partial derivatives as linear combinations of the block vectors that surround the regular vertex.

Figures 3.5 , 3.6 and 3.7 visually show the symmetry that these formulas have.

3.7.2. "Visual C^1" for extraordinary case

In [**CJ08**], Chui/Jiang develop a template for an extraordinary vertex of a 1-ring interpolatory scheme. Referring to Q_n and Q in (3.31 |p.37)

$$Q := \begin{bmatrix} 0 & \frac{145}{512}\beta \\ 0 & -\frac{45}{512}\beta \end{bmatrix} \qquad Q_n := \begin{bmatrix} 1 & -\frac{145}{512}\beta \\ 0 & x_1 \end{bmatrix}$$

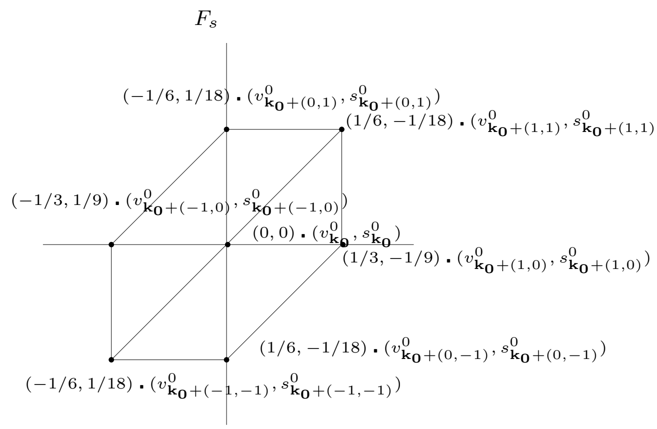

(a)

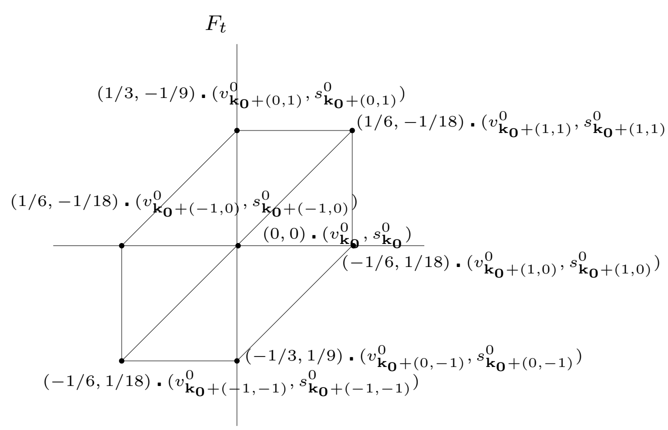

(b)

Figure 3.5. The above diagrams represents F_s and F_t. Each block vertex has both a "regular" vertex and a shape control vertex. Each is multiplied by the respective numbers. Note the symmetry in each diagram around the central vertex. F_t only differs from F_s by a rotation of the $s-t$ axes.

They found that the eigenvalues of the upper left block in M_0 in (3.42 |p.44) would be given by 1, $\frac{59}{512}$, and $\widetilde{\lambda}_{\pm} := \frac{5}{16} + \frac{x_1}{2} \pm \frac{1}{64}\sqrt{400 - 1280x_1 + 1024x_1^2 - 155\beta}$. Choices can be made for x_1 and β such that the eigenvalues of the subdivision matrix $S1_n$ (3.33 |p.38) satisfy $\lambda_0 = 1$, $\lambda_1 = \lambda_2$, with $|\lambda_1 < 1|$ and $|\lambda_j| < |\lambda_1|$, $j = 3, 4, ...$

Meshes are formed by subdividing an initial control set of points in $\mathbb{R}^2$ whose coordinates are the *2 left eigenvectors* of the subdominant eigenvalue λ. The extraordinary scheme is shown to be "visually" C^1 in the sense that these 2-D meshes suggest the regularity and injectivity of the characteristic map.

From Lemma **3.3** and from (3.48) we can get specific right eigenvectors of λ by using appropriate values of t_1,t_2 and h [from (3.4 |p.24)].

We obtain:

$$d_2 = \frac{-17\left(z+z^{-1}\right)-47}{123+69\left(z+z^{-1}\right)}$$

where z is from (3.29 |p.35).

So from (3.47 |p.48) and (3.48 |p.49) and using the values from (3.49 |p.50) we get for $n=5$

$$\widehat{\mathbf{R}}_1 = \frac{2}{5}\left[0,0,1,d_2,\cos\left(\frac{2\pi}{5}\right),d_2\cos\left(\frac{2\pi}{5}\right),...,\cos\left(\frac{8\pi}{5}\right),d_2\cos\left(\frac{8\pi}{5}\right)\right]$$
$$\widehat{\mathbf{R}}_2 = \frac{2}{5}\left[0,0,0,0,\sin\left(\frac{2\pi}{5}\right),d_2\sin\left(\frac{2\pi}{5}\right),...,\sin\left(\frac{8\pi}{5}\right),d_2\sin\left(\frac{8\pi}{5}\right)\right]$$

where

$$d_2 = \frac{-17\left(z+z^{-1}\right)-47}{123+69\left(z+z^{-1}\right)} \approx -.3471689765$$

See Figure 3.8 on p. 55 for a visual representation of these two partial derivatives.

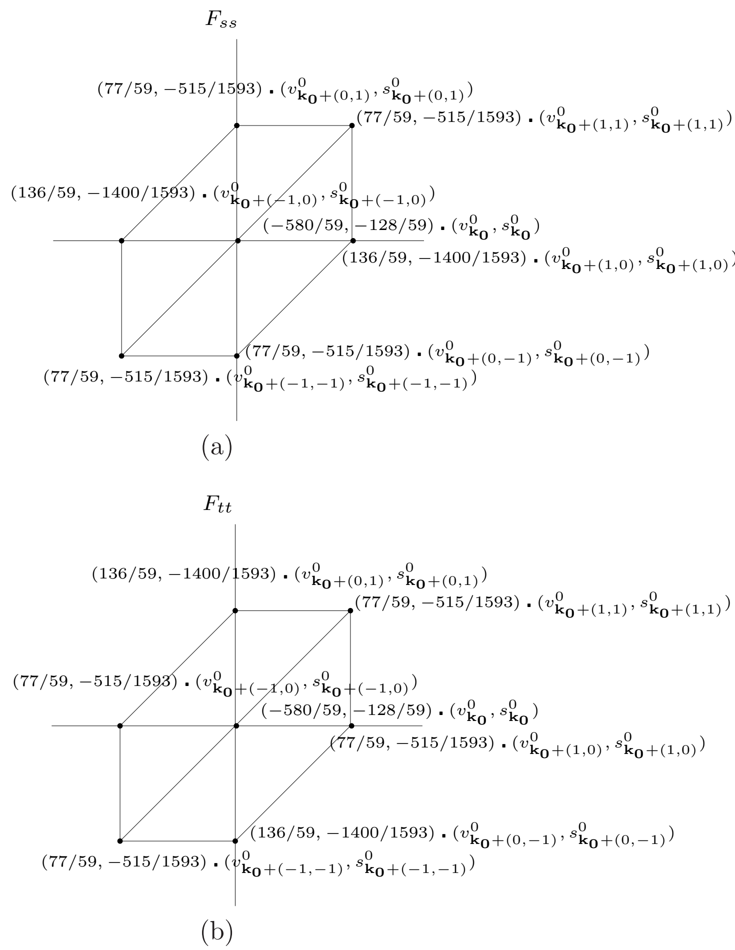

Figure 3.6. The above diagrams represents F_{ss} and F_{tt}. Each block vertex has both a "regular" vertex and a shape control vertex. Each is multiplied by the respective numbers. Observe the symmetry in each diagram around the central vertex. F_{tt} only differs from F_{ss} by a rotation of the $s-t$ axes. Note that the central vertex is multiplied by factors. Also note that the factors have been multiplied by 2 as required by (3.44 |p.46).

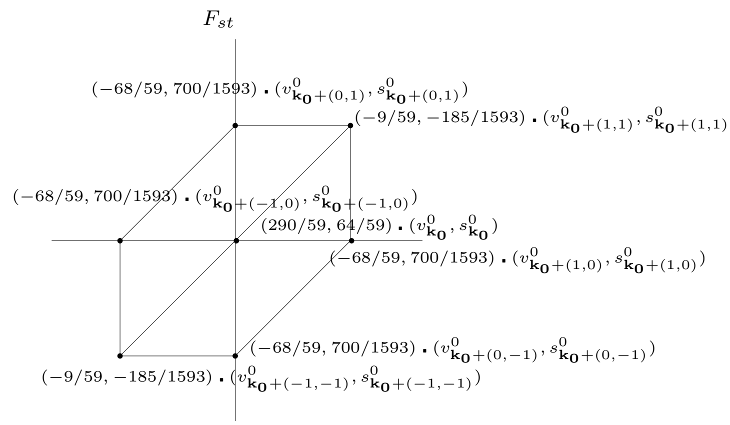

(a)

Figure 3.7. The above diagram represents F_{st}. Each block vertex has both a "regular" vertex and a shape control vertex. Each is multiplied by the respective numbers. Observe the symmetry in each diagram around the central vertex. Note that the central vertex is multiplied by factors.

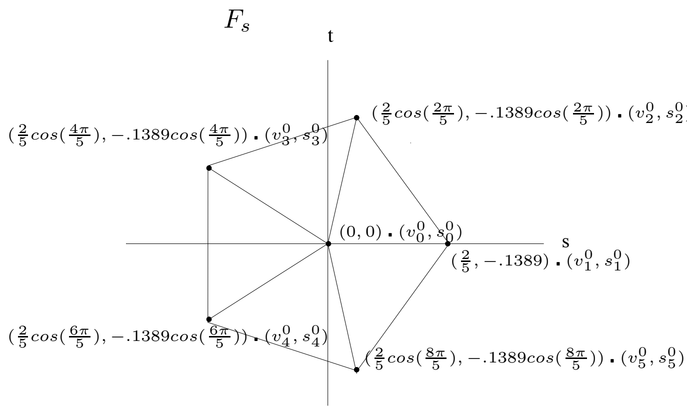

(a)

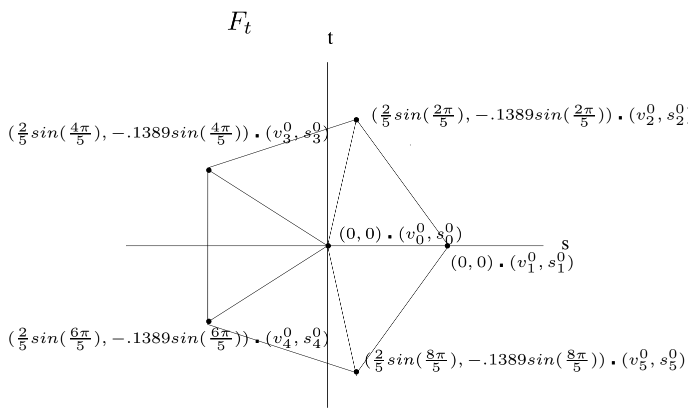

(b)

Figure 3.8. The above diagrams represents F_s and F_t at an extraordinary vertex of valence 5. We use the scheme in Subsection 3.7.2. Each block vertex has both a "regular" vertex and a shape control vertex. Each is multiplied by the respective numbers.

CHAPTER 4

Derivative Formulas for Interpolating Quadrilateral Subdivision Schemes

4.1. Introduction

Here we are examining 1−ring quadrilateral interpolating schemes. Their template is at the lower part of Fig. (2.1 |p.15) and the elements of the mask are given by (2.12 |p.14). As in the triangular interpolatory case, the structure of these matrices corresponds to the algebraic structure of an interpolatory mask given in [**CJ08**] and shown in (3.1 |p.23).

For the quadrilateral scheme, the regular vertices lie on a 2-directional mesh in the "so-called" parametric domain. This domain corresponds to the integer subscripts of the vertices and will be associated with the parameters of the limit surface (as we will see later). See Fig. 4.1 on p. 57.

In the following we will be using the assumptions presented in Chapter 2 to develop the first and second partial derivatives of the regular vertices of a quadrilateral interpolating scheme

We will derive as much information as we can regarding the templates $\{P_{\mathbf{k}}\}_{\mathbf{k}}$ and the 1×2 constant vectors $\mathbf{l}_0^{\alpha}$ introduced in (2.14 |p.15).

Through direct calculation using the Sum rules we determined the following:

$$\begin{aligned} \mathbf{l}_0^{(1,0)} &= \mathbf{l}_0^{(0,1)} = [0,0] \\ \mathbf{l}_0^{(2,0)} &= \mathbf{l}_0^{(0,2)} = [0,h] \\ \mathbf{l}_0^{(1,1)} &= [0,0] \end{aligned} \tag{4.1}$$

where $h \neq 0$

As indicated in Chapter 2 $\mathbf{l}_0^{(0,0)} = [1,0]$.

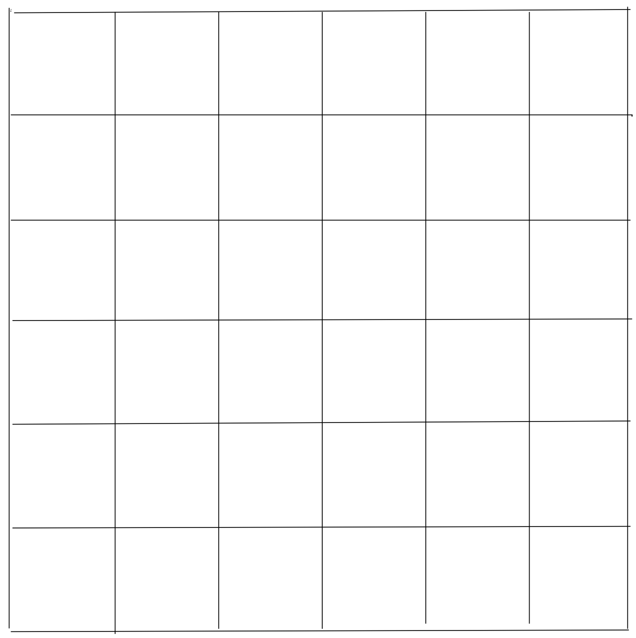

Figure 4.1. Two-directional mesh for Quadrilateral subdivisions

Also through direct calculation using the Sum rules we determined:

(4.2)

$$R_{0,0} = \begin{pmatrix} 1 & 4t_3 + h\left(-\frac{1}{2} + 8t_4 + 8t_5 + 2t_6\right) \\ 0 & t_6 \end{pmatrix}$$

$$L = \begin{pmatrix} 0 & -t_3 - \frac{1}{4}\left(4t_3 + h\left(-\frac{1}{2} + 8t_4 + 8t_5 + 2t_6\right)\right) \\ 0 & t_5 \end{pmatrix} \qquad N = \begin{pmatrix} 0 & t_3 \\ 0 & t_4 \end{pmatrix}$$

$$J = \begin{pmatrix} \frac{3}{8} & 0 \\ -\frac{1}{8h} - 2t_1 & \frac{1}{8} - 2t_2 \end{pmatrix} \qquad K = \begin{pmatrix} \frac{1}{4} & 0 \\ -\frac{1}{16h} & \frac{1}{16} \end{pmatrix} \qquad M = \begin{pmatrix} \frac{1}{16} & 0 \\ t_1 & t_2 \end{pmatrix}$$

where t_j are "free" variables for $j = 1, ..., 6$. Using the techniques in ([**JO03**]), the values of the t_j will determine the Sobolev smoothness of the refinable function Φ (2.5 |p.12). See section 2.4.

4.2. First Partial Derivatives (Regular)

We will use the same technique as in the triangular regular case to develop a representation of the first partial derivatives in terms of the initial control net.

Again we start at any given regular vertex $v^m_{2^m\mathbf{k}_0}$ for some $\mathbf{k}_0 \in \mathbb{Z}^2$ (after m iterations of our subdivision scheme). Also we will be initially representing its surrounding control net as a linear combination of left eigenvectors.

For the regular interpolatory quadrilateral scheme, the control vector net surrounding a vertex (call it $v^m_{2^m\mathbf{k}_0}$) is a 3×50 vector of 25 3×1 control vertices and 25 3×1 shape control vertices. See Figure 4.2.

As before, we define Q as the matrix whose column entries represent the subscripts of the vertices (Q is now a 2×25 matrix):

$$Q := \begin{bmatrix} 0 & 1 & 0 & -1 & 0 & 1 & -1 & -1 & 1 & 2 & 0 & -2 & \cdots \\ 0 & 0 & 1 & 0 & -1 & 1 & 1 & -1 & -1 & 0 & 2 & 0 & \cdots \end{bmatrix} \tag{4.3}$$

$$\begin{matrix} 0 & 2 & -1 & -2 & 1 & 2 & -2 & -2 & 2 & 1 & -2 & -1 & 2 \\ -2 & 1 & 2 & -1 & -2 & 2 & 2 & -2 & -2 & 2 & 1 & -2 & -1 \end{matrix} \Bigg]$$

The columns of Q reflect the ordering in Figure 4.2.

Define the following 3 x 50 matrix that represents the vertices surrounding $v^m_{2^m\mathbf{k}_0}$ in a 2-ring neighborhood:

$$\mathbf{U}^m_{\mathbf{k}_0} := \left\{ \mathbf{u}^m_{\mathbf{k}_0,\mathbf{j}} : \mathbf{j} = (Q_{1\,s}, Q_{2\,s})^T_{1 \le s \le 25} \text{ as above} \right\} \tag{4.4}$$

where $\mathbf{k}_0 \in \mathbb{Z}^2$ and $\mathbf{u}^m_{\mathbf{k}_0,\mathbf{j}}$ is defined as in (3.5 |p.25).

Again

$$\mathbf{U}^m_{\mathbf{k}_0} = \mathbf{U}^0_{\mathbf{k}_0} S^m$$

where S is from (2.26 |p.20).

The *initial* control vector net ($\mathbf{U}^0_{\mathbf{k}_0}$) around any regular $\mathbf{v}^0_{\mathbf{k}_0}$ can be represented as a linear combination of 1×50 (generalized) left eigenvectors of our 50×50 subdivision matrix S.

By letting $\{\mathbf{L}_j : 0 \le j \le 49\}$ be a set of 50 (possibly generalized) linearly independent left eigenvectors of S then $\mathbf{U}^0_{\mathbf{k}_0}$ can be written as

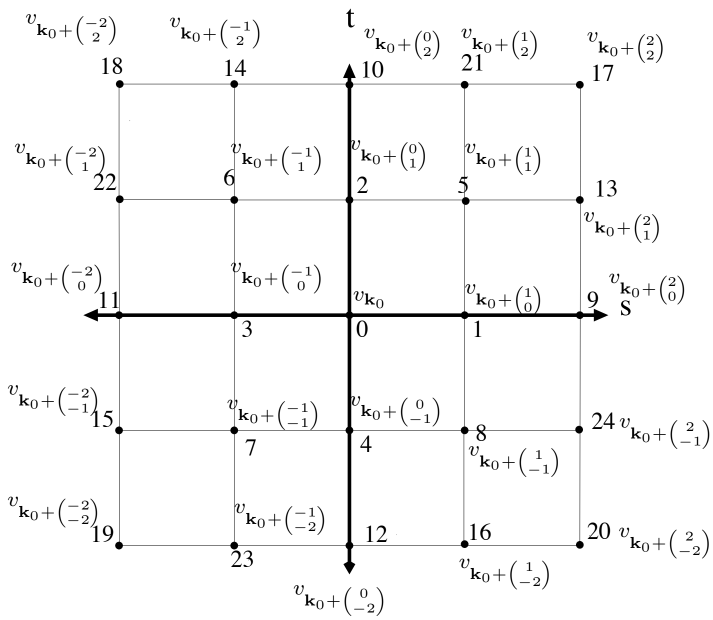

Figure 4.2. Ordering around central vertex. The intersection of grid lines are the parametric location of the vertices (the subscripts). The single numbers represent the order in which the vertices are considered. The vertex subscripts reflect the parametric domain.

$$\mathbf{U}^0_{\mathbf{k}_0} = \alpha^{(0)}_0\mathbf{L}_0+\alpha^{(0)}_1\mathbf{L}_1+\alpha^{(0)}_2\mathbf{L}_2+\alpha^{(0)}_3\mathbf{L}_3+\alpha^{(0)}_4\mathbf{L}_4+\alpha^{(0)}_5\mathbf{L}_5+\sum_{j=6}^{49}\alpha^{(0)}_j\mathbf{L}_j \tag{4.5}$$

where $\alpha^{(0)}_j \in \mathbb{R}^3 \quad j = 0, \ldots, 49$

We have the same assumptions regarding the eigenvalues as for the triangular scheme, and in (4.5) $\mathbf{L}_0$, $\mathbf{L}_1$, $\mathbf{L}_2$, $\mathbf{L}_3, \mathbf{L}_4$ and $\mathbf{L}_5$ are defined as before.

We thus get (after m subdivisions)

$$\mathbf{U}_{\mathbf{k}_0}^m = \alpha_0^{(0)}\mathbf{L}_0+2^{-m}\alpha_1^{(0)}\mathbf{L}_1+2^{-m}\alpha_2^{(0)}\mathbf{L}_2+4^{-m}\alpha_3^{(0)}\mathbf{L}_3+4^{-m}\alpha_4^{(0)}\mathbf{L}_4+4^{-m}\alpha_5^{(0)}\mathbf{L}_5+\sum_{j=6}^{49} \lambda_j^m\alpha_j^{(0)}\mathbf{L}_j$$

where $|\lambda_j| < \frac{1}{4}$ for $j = 6, ..., 49$.

Hence

$$\lim_{m\to\infty} \mathbf{U}_{\mathbf{k}_0}^m = \alpha_0^{(0)}\mathbf{L}_0$$

$$\lim_{m\to\infty} 2^m \left(\mathbf{U}_{\mathbf{k}_0}^m - \alpha_0^{(0)}\mathbf{L}_0\right) = \alpha_1^{(0)}\mathbf{L}_1 + \alpha_2^{(0)}\mathbf{L}_2$$

Now since

- the first component of $\mathbf{U}_{\mathbf{k}_0}^m$ is $v_{2^m\mathbf{k}_0}^m$,
- $v_{2^m\mathbf{k}_0}^m = v_{\mathbf{k}_0}^0$ (see 3.2) and
- the first component of $\mathbf{L}_0$ is 1

then we can derive

$$\alpha_0^{(0)} = v_{\mathbf{k}_0}^0$$

Hence we have the following

$$\lim_{m\to\infty} 2^m \left(\mathbf{U}_{\mathbf{k}_0}^m - \left[v_{\mathbf{k}_0,}^0, 0, v_{\mathbf{k}_0,}^0, 0, v_{\mathbf{k}_0,}^0, 0..., v_{\mathbf{k}_0,}^0, 0\right]\right) =\alpha_1^{(0)}\mathbf{L}_1 + \alpha_2^{(0)}\mathbf{L}_2 \tag{4.6}$$

Now from (2.23 |p.19),(2.25 |p.20), (4.1 |p.56) and (4.3 |p.58) we obtain the following representations of $\mathbf{L}_j$ for $j = 0, 1, ..., 5$

$$\begin{aligned}
\mathbf{L}_0 &= [1, 0, 1, 0, 1, 0, 1, 0, ..., 1, 0, 1, 0] \\
\mathbf{L}_1 &= [0, 0, 1, 0, 0, 0, -1, 0, ..., -1, 0, 2, 0] \\
\mathbf{L}_2 &= [0, 0, 0, 0, 1, 0, 0, 0, ..., -2, 0, -1, 0] \\
\mathbf{L}_3 &= [0, h, 1, h, 0, h, 1, h, ..., 1, h, 4, h] \\
\mathbf{L}_4 &= [0, 0, 0, 0, 0, 0, 0, 0, ..., 2, 0, -2, 0] \\
\mathbf{L}_5 &= [0, h, 0, h, 1, h, 0, h, ..., 4, h, 1, h]
\end{aligned} \tag{4.7}$$

So just looking at the odd components of the left and right sides of (4.6) we have

$$\lim_{m\to\infty} 2^m \left(\left[v^m_{2^m\mathbf{k}_0}, v^0_{2^m\mathbf{k}_0+(1,0)^T}, v^0_{2^m\mathbf{k}_0+(0,1)^T}, \ldots, v^0_{2^m\mathbf{k}_0+(2,-1)^T} \right] - \left[v^0_{\mathbf{k}_0}, v^0_{\mathbf{k}_0}, v^0_{\mathbf{k}_0}, \ldots, v^0_{\mathbf{k}_0} \right] \right) = \alpha_1^{(0)} \widetilde{\mathbf{L}}_1 + \alpha_2^{(0)} \widetilde{\mathbf{L}}_2$$

where

$$\widetilde{\mathbf{L}}_1 = [0, 1, 0, -1, 0, 1, -1, -1, 1, 2, 0, -2, 0, 2, -1, -2, 1, 2, -2, -2, 2, 1, -2, -1, 2]$$

$$\widetilde{\mathbf{L}}_2 = [0, 0, 1, 0, -1, 0, 0, -1, -1, 0, 2, 0, -2, 1, 2, -1, -2, 2, 2, -2, -2, 2, 1, -2, -1]$$

Again the goal is to connect the above formula with the 2 partial derivatives of our limit surface F. So we need to locally parameterize F in the (s, t) plane as in [**SDL99**]. The (s, t) plane is drawn in Figure 4.2.

We will use the same local parameterization of F in a neighborhood of $\mathbf{k}_0 = \left(k_0^{(1)}, k_0^{(1)}\right)^T \in \mathbb{Z}^2$

$$F\left(k_0^{(1)} + \frac{l^{(1)}}{2^m}, k_0^{(2)} + \frac{l^{(2)}}{2^m}\right) := v^m_{2^m\mathbf{k}_0+\mathbf{l}} \tag{4.8}$$

where $m \in \mathbb{Z}_+$, v^m as in (2.8 |p.13), and $\mathbf{l} = \left(l^{(1)}, l^{(2)}\right)^T = \left(Q_{1,j}, Q_{2,j}\right)^T_{1\le j\le 25}$ for Q defined in (4.3 |p.58).

Using the same argument as in Section 3.3 we arrive at:

$$\lim_{m\to\infty} 2^m \left(\left[v^m_{2^m\mathbf{k}_0}, v^m_{2^m\mathbf{k}_0+(1,0)^T}, v^m_{2^m\mathbf{k}_0+(0,1)^T}, \ldots, v^m_{2^m\mathbf{k}_0+(2,-1)^T} \right] - \left[v^0_{\mathbf{k}_0}, v^0_{\mathbf{k}_0}, v^0_{\mathbf{k}_0}, \ldots, v^0_{\mathbf{k}_0} \right] \right) = F_s\left(k_0^{(1)}, k_0^{(2)}\right) \widetilde{\mathbf{L}}_1 + F_t\left(k_0^{(1)}, k_0^{(2)}\right) \widetilde{\mathbf{L}}_2$$

By the linear independence of $\widetilde{\mathbf{L}}_1$ and $\widetilde{\mathbf{L}}_2$ we have

$$\begin{aligned} F_s\left(k_0^{(1)}, k_0^{(2)}\right) &= \alpha_1^{(0)} \\ F_t\left(k_0^{(1)}, k_0^{(2)}\right) &= \alpha_2^{(0)} \end{aligned} \tag{4.9}$$

Proposition 4.1. *Suppose that an interpolatory quadrilateral scheme is convergent with limiting surface F in C^1 where for $\mathbf{k}_0 = \left[k_0^{(1)}, k_0^{(2)}\right]^T \in \mathbb{Z}^2$ the initial control vector surrounding $\mathbf{v}_{\mathbf{k}_0}$ is given as in Figure 4.2. Also assume its mask $\{P_\mathbf{k}\}_\mathbf{k}$ has Sum Rule of at least order 3. Let $\alpha_1^{(0)}, \alpha_2^{(0)} \in \mathbb{R}^3$*

be the column vectors in (4.5 |p.59). Then

$$F_s\left(k_0^{(1)}, k_0^{(2)}\right) = \alpha_1^{(0)}, \qquad F_t\left(k_0^{(1)}, k_0^{(2)}\right) = \alpha_2^{(0)}$$

As we did in the triangular case, denote each vertex surrounding $\mathbf{v}^n_{2^n\mathbf{k}_0+\mathbf{i}}$ after m additional subdivisions by

$$\mathbf{u}^{n+m}_{\mathbf{k}_0,\mathbf{i},\mathbf{j}} := \mathbf{v}^{n+m}_{2^{n+m}\mathbf{k}_0+2^m\mathbf{i}+\mathbf{j}} \quad for\ m \neq 0$$
$$\mathbf{u}^{n}_{\mathbf{k}_0,\,\mathbf{i},\mathbf{j}} := \mathbf{v}^{n}_{2^{n}\mathbf{k}_0+\mathbf{i}+\mathbf{j}} \quad for\ m = 0$$

where $\mathbf{j} = (Q_{1,\,s}, Q_{2,\,s})^T_{1\leq s\leq 25}$ for Q defined in (4.3 |p.58).

Let

$$\mathbf{U}^{n+m}_{\mathbf{k}_0,\mathbf{i}} := \left\{\mathbf{u}^{n+m}_{\mathbf{k}_0,\mathbf{i},\mathbf{j}} : \mathbf{j} = (Q_{1,\,s}, Q_{2,\,s})^T_{1\leq s\leq 25}\right\} \tag{4.10}$$

In the case where we have not done *any* additional subdivisions, we can represent the n^{th} control net surrounding the regular vertex $\mathbf{v}_{2^n\mathbf{k}_0+\mathbf{i}}$ as a linear combination of $\mathbf{L}_j$ (4.7 |p.60)

$$\mathbf{U}^{n+0}_{\mathbf{k}_0,\mathbf{i}} = \alpha_0^{(n)}\mathbf{L}_0 + \alpha_1^{(n)}\mathbf{L}_1 + \alpha_2^{(n)}\mathbf{L}_2 + \alpha_3^{(n)}\mathbf{L}_3 + \alpha_4^{(n)}\mathbf{L}_4 + \alpha_5^{(n)}\mathbf{L}_5 + \sum_{j=6}^{49} \alpha_j^{(n)}\mathbf{L}_j \tag{4.11}$$

where $\alpha_j^{(n)} \in \mathbb{R}^3$.

We obtain the following proposition:

Proposition 4.2. *Suppose that an interpolatory quadrilateral scheme is convergent with limiting surface F in C^1 where for $\mathbf{k}_0 = \left[k_0^{(1)}, k_0^{(2)}\right]^T \in \mathbb{Z}^2$ the n^{th} control net surrounding $\mathbf{v}_{2^n\mathbf{k}_0+\mathbf{i}}$ for $\mathbf{i} \in \mathbb{Z}^2 \setminus (0,0)^T$ (after n subdivisions of the initial control vector net) is given as in (4.10 |p.62). Also assume its mask $\{P_\mathbf{k}\}_\mathbf{k}$ has Sum Rule of at least order 3. Let $\alpha_1^{(n)}$,$\alpha_2^{(n)}$ $\in \mathbb{R}^3$ be the column vectors in (4.11 |p.62). Then*

$$F_s\left(k_0^{(1)} + \frac{i^{(1)}}{2^n}, k_0^{(2)} + \frac{i^{(2)}}{2^n}\right) = 2^n\alpha_1^{(n)}, \qquad F_t\left(k_0^{(1)} + \frac{i^{(1)}}{2^n}, k_0^{(2)} + \frac{i^{(2)}}{2^n}\right) = 2^n\alpha_2^{(n)} \tag{4.12}$$

Proof. The proof is the same as in section 3.3 for obtaining the first partials at a regular point on the surface after n subdivisions. □

4.3. Second Partial Derivative (Regular)

The procedure for obtaining the second partial derivatives of our limit surface F is similar is to the triangular case. Again we will first consider regular vertex $v^m_{2^m\mathbf{k}_0}$ $\left(= v^0_{\mathbf{k}_0}\right)$ from the initial control net after m subdivisions.

Again define a "picking" matrix $\widetilde{J}$ (50×50 this time) that for odd j between 3 and 31 replaces the j and $j+1$ column with the $j+4$ and $j+5$ column (and vice versa) of any $3{\times}50$ matrix. To illustrate, using the column vectors of Q (4.3 |p.58) for the ordering of subscripts in $U^m_{\mathbf{k}_0}$ (4.4 |p.58), then $U^m_{\mathbf{k}_0}\widetilde{J}$ replaces $\mathbf{u}^m_{\mathbf{k}_0+(1,0)^T}$ with $\mathbf{u}^m_{\mathbf{k}_0+(-1,0)^T}$ and vice versa and $\mathbf{u}^m_{\mathbf{k}_0+(1,1)^T}$ with $\mathbf{u}^m_{\mathbf{k}_0+(-1,-1)^T}$ and vice versa.

We then derive the following set of equalities:

$$\lim_{m\to\infty} 2^{2m}\left[\mathbf{U}^m_{\mathbf{k}_0} + \mathbf{U}^m_{\mathbf{k}_0}\widetilde{J} - 2\left[v^0_{\mathbf{k}_0,}, 0, v^0_{\mathbf{k}_0,}, 0, v^0_{\mathbf{k}_0,}, 0..., v^0_{\mathbf{k}_0,}, 0\right]\right] = \tag{4.13}$$

$$\lim_{m\to\infty} 2^{2m}\left\{\begin{array}{c} \left[\begin{array}{c}\alpha^{(0)}_0\mathbf{L}_0 + 2^{-m}\alpha^{(0)}_1\mathbf{L}_1 + 2^{-m}\alpha^{(0)}_2\mathbf{L}_2 + 4^{-m}\alpha^{(0)}_3\mathbf{L}_3... \\ +4^{-m}\alpha^{(0)}_4\mathbf{L}_4 + 4^{-m}\alpha^{(0)}_5\mathbf{L}_5 + o\left(2^{-2m}\right)\end{array}\right] \\ +\left[\begin{array}{c}\alpha^{(0)}_0\mathbf{L}_0 + 2^{-m}\alpha^{(0)}_1\mathbf{L}_1 + 2^{-m}\alpha^{(0)}_2\mathbf{L}_2 + 4^{-m}\alpha^{(0)}_3\mathbf{L}_3... \\ +4^{-m}\alpha^{(0)}_4\mathbf{L}_4 + 4^{-m}\alpha^{(0)}_5\mathbf{L}_5 + o\left(2^{-2m}\right)\end{array}\right]\widetilde{J} \\ -2\left[v^0_{\mathbf{k}_0,}, 0, v^0_{\mathbf{k}_0,}, 0, v^0_{\mathbf{k}_0,}, 0..., v^0_{\mathbf{k}_0,}, 0\right]\end{array}\right\} =$$

$$\lim_{m\to\infty} 2^{2m}\left\{\begin{array}{c}\left[4^{-m}\alpha^{(0)}_3\mathbf{L}_3 + 4^{-m}\alpha^{(0)}_4\mathbf{L}_4 + 4^{-m}\alpha^{(0)}_5\mathbf{L}_5 + o\left(2^{-2m}\right)\right] \\ +\left[4^{-m}\alpha^{(0)}_3\mathbf{L}_3 + 4^{-m}\alpha^{(0)}_4\mathbf{L}_4 + 4^{-m}\alpha^{(0)}_5\mathbf{L}_5 + o\left(2^{-2m}\right)\right]\widetilde{J}\end{array}\right\} =$$

$$\lim_{m\to\infty} 2^{2m}\left\{2\cdot 4^{-m}\alpha^{(0)}_3\mathbf{L}_3 + 2\cdot 4^{-m}\alpha^{(0)}_4\mathbf{L}_4 + 2\cdot 4^{-m}\alpha^{(0)}_5\mathbf{L}_5 + o\left(2^{-2m}\right)\right\} =$$

$$2\alpha^{(0)}_3\mathbf{L}_3 + 2\alpha^{(0)}_4\mathbf{L}_4 + 2\alpha^{(0)}_5\mathbf{L}_5$$

Looking at the second order directional derivatives in the direction of each of the 24 surrounding vertices, we have:

(4.14)

$$\lim_{m\to\infty} 2^{2m} \left\{ \begin{array}{c} 0, F\left(k_0^{(1)} + 2^{-m}(1), k_0^{(2)}\right) + F\left(k_0^{(1)} + 2^{-m}(-1), k_0^{(2)}\right) \\ -2F\left(k_0^{(1)}, k_0^{(2)}\right), \\ F\left(k_0^{(1)} + 2^{-m}(0), k_0^{(2)} + 2^{-m}(1)\right) + F\left(k_0^{(1)} + 2^{-m}(0), k_0^{(2)} + 2^{-m}(-1)\right) \\ -2F\left(k_0^{(1)}, k_0^{(2)}\right), \ldots, \\ F\left(k_0^{(1)} + 2^{-m}(-1), k_0^{(2)} + 2^{-m}(-2)\right) + F\left(k_0^{(1)} + 2^{-m}(1), k_0^{(2)} + 2^{-m}(2)\right) \\ -2F\left(k_0^{(1)}, k_0^{(2)}\right), \\ F\left(k_0^{(1)} + 2^{-m}(2), k_0^{(2)} + 2^{-m}(-1)\right) + F\left(k_0^{(1)} + 2^{-m}(-2), k_0^{(2)} + 2^{-m}(1)\right) \\ -2F\left(k_0^{(1)}, k_0^{(2)}\right) \end{array} \right\} =$$

$$F_{ss}\left(k_0^{(1)}, k_0^{(2)}\right)\widetilde{\mathbf{L}}_3 + 2F_{st}\left(k_0^{(1)}, k_0^{(2)}\right)\widetilde{\mathbf{L}}_4 + F_{tt}\left(k_0^{(1)}, k_0^{(2)}\right)\widetilde{\mathbf{L}}_5$$

where

$\widetilde{\mathbf{L}}_3 = \left[(0)^2, (1)^2, (0)^2, (-1)^2, (0)^2, (1)^2, \ldots, (-1)^2, (2)^2\right]$

$\widetilde{\mathbf{L}}_4 = \left[(0)^2, (1)\cdot(0), (0)\cdot(1), (-1)\cdot 0, 0\cdot(-1), (1)^2 \ldots, (-1)(-2), (2)(-1)\right]$

$\widetilde{\mathbf{L}}_5 = \left[(0)^2, (0)^2, (1)^2, (0)^2, (-1)^2, (1)^2, \ldots, (-2)^2, (-1)^2\right]$

which are the odd components of $\mathbf{L}_3$, $\mathbf{L}_4$, and $\mathbf{L}_5$ (4.7) respectively.

So using our parametrization (4.8 |p.61) we can equate the last expression in 4.13 and the right side of 4.14:

$$2\alpha_3^{(0)}\widetilde{\mathbf{L}}_3 + 2\alpha_4^{(0)}\widetilde{\mathbf{L}}_4 + 2\alpha_5^{(0)}\widetilde{\mathbf{L}}_5 = F_{ss}\left(k_0^{(1)}, k_0^{(2)}\right)\widetilde{\mathbf{L}}_3 + 2F_{st}\left(k_0^{(1)}, k_0^{(2)}\right)\widetilde{\mathbf{L}}_4 + F_{tt}\left(k_0^{(1)}, k_0^{(2)}\right)\widetilde{\mathbf{L}}_5$$

By linear independence

(4.15)
$$\begin{aligned} F_{ss}\left(k_0^{(1)}, k_0^{(2)}\right) &= 2\alpha_3^{(0)} \\ F_{st}\left(k_0^{(1)}, k_0^{(2)}\right) &= \alpha_4^{(0)} \\ F_{tt}\left(k_0^{(1)}, k_0^{(2)}\right) &= 2\alpha_5^{(0)} \end{aligned}$$

Proposition 4.3. *Suppose that an interpolatory quadrilateral scheme is convergent with limiting surface F in C^2 where for $\mathbf{k}_0 = \left[k_0^{(1)}, k_0^{(2)}\right]^T \in \mathbb{Z}^2$ the initial control vector surrounding $\mathbf{v}_{\mathbf{k}_0}$ is given as in Figure 4.2 on p. 59. Also assume its mask $\{P_{\mathbf{k}}\}_{\mathbf{k}}$ has Sum Rule of at least order 3. Let $\alpha_3^{(0)}$,$\alpha_4^{(0)}$, $\alpha_5^{(0)} \in \mathbb{R}^3$ be the column vectors in (4.5 |p.59). Then*

$$F_{ss}\left(k_0^{(1)}, k_0^{(2)}\right) = 2\alpha_3^{(0)}$$
$$F_{st}\left(k_0^{(1)}, k_0^{(2)}\right) = \alpha_4^{(0)}$$
$$F_{tt}\left(k_0^{(1)}, k_0^{(2)}\right) = 2\alpha_5^{(0)}$$

Proposition 4.4. *Suppose that an interpolatory quadrilateral scheme is convergent with limiting surface F in C^2 where for $\mathbf{k}_0 = \left[k_0^{(1)}, k_0^{(2)}\right]^T \in \mathbb{Z}^2$ the n^{th} control net surrounding $\mathbf{v}_{2^n\mathbf{k}_0+\mathbf{i}}$ for $\mathbf{i} \in \mathbb{Z}^2 \setminus (0,0)^T$ (after n subdivisions of the initial control vector net) is given as in (4.10 |p.62). Also assume its mask $\{P_{\mathbf{k}}\}_{\mathbf{k}}$ has Sum Rule of at least order 3. Let $\alpha_1^{(n)}$,$\alpha_2^{(n)}$ $\in \mathbb{R}^3$ be the column vectors in (4.11 |p.62). Then*

$$F_{ss}\left(k_0^{(1)} + \frac{i^{(1)}}{2^n}, k_0^{(2)} + \frac{i^{(2)}}{2^n}\right) = 2^{2n+1}\alpha_3^{(n)} \tag{4.16}$$
$$F_{st}\left(k_0^{(1)} + \frac{i^{(1)}}{2^n}, k_0^{(2)} + \frac{i^{(2)}}{2^n}\right) = 2^{2n}\alpha_4^{(n)}$$
$$F_{tt}\left(k_0^{(1)} + \frac{i^{(1)}}{2^n}, k_0^{(2)} + \frac{i^{(2)}}{2^n}\right) = 2^{2n+1}\alpha_5^{(n)}$$

Proof. Proof is similar to the proof of Proposition 3.2 on p. 32. □

4.4. First Partial Derivatives (Extraordinary)

Here we will obtain a representation of the first partial derivatives in a similar fashion as in 3.5 starting on p. 35. Using the notation in (3.27 |p.35), the following is the $(12n + 2) \times (12n + 2)$ subdivision matrix

S_n around an extraordinary vertex of valence $n \neq 4$:

$$\begin{bmatrix} W_n & [J \,...\, J] & [K \,...\, K] & [L \,...\, L] & [M \,...\, M] & [N \,...\, N] & [M \,...\, M] \\ \frac{1}{n}\begin{bmatrix} W \\ W \\ \vdots \\ W \end{bmatrix} & \mathcal{C}\,(J, M; M) & \mathcal{C}\,(K, 0; K) & \mathcal{C}\,(R_{0,0}, N; N) & \mathcal{C}\,(J, 0; M) & \mathcal{C}\,(L, 0; L) & \mathcal{C}\,(M, 0; J) \\ \frac{1}{n}\begin{bmatrix} w \\ w \\ \vdots \\ w \end{bmatrix} & \mathcal{C}\,(M, M; 0) & diag\,(K) & \mathcal{C}\,(L, L; 0) & diag\,(J) & diag\,(R_{0,0}) & diag\,(J) \\ \mathbf{0} & \mathbf{0} & \mathbf{0} & diag\,(L) & diag\,(M) & \mathcal{C}\,(N, 0; N) & \mathcal{C}\,(0, 0; M) \\ \mathbf{0} & \mathbf{0} & \mathbf{0} & diag\,(N) & diag\,(M) & diag\,(L) & \mathbf{0} \\ \mathbf{0} & \mathbf{0} & \mathbf{0} & \mathbf{0} & \mathbf{0} & diag\,(N) & \mathbf{0} \\ \mathbf{0} & \mathbf{0} & \mathbf{0} & \mathcal{C}\,(0, N; 0) & \mathbf{0} & diag\,(L) & diag\,(M) \end{bmatrix}$$

where J, K, L, M, N and $R_{0,0}$ are all from (2.12 |p.14) and (4.2 |p.57) and W_n, W, and w are from the template for the extraordinary vertex given in Figure 4.3 on p. 67.

In this template, W_n, W, and w are given by:

$$W_n := \begin{bmatrix} 1 & \widetilde{n}_{1,2} \\ 0 & \widetilde{n}_{2,2} \end{bmatrix} \qquad W := \begin{bmatrix} 0 & W_{1,2} \\ 0 & W_{2,2} \end{bmatrix} \qquad w := \begin{bmatrix} 0 & w_{1,2} \\ 0 & w_{2,2} \end{bmatrix} \tag{4.17}$$

where we will assume that

$$\widetilde{n}_{1,2} + W_{1,2} + w_{1,2} = 0 \tag{4.18}$$

Note that S_n is a matrix of a 2-ring neighborhood around our central extraordinary vertex just as S (2.26 |p.20) is a matrix on a 2-ring neighborhood of our central vertex $v_{\mathbf{0}}$.

We now define

$$U := \text{diag}\,(I_2,\, U_n, U_n, U_n, U_n, U_n, U_n) \quad (12n+2) \;\times\; (12n+2) \text{ matrix}$$

with U_n as in (3.28 |p.35).

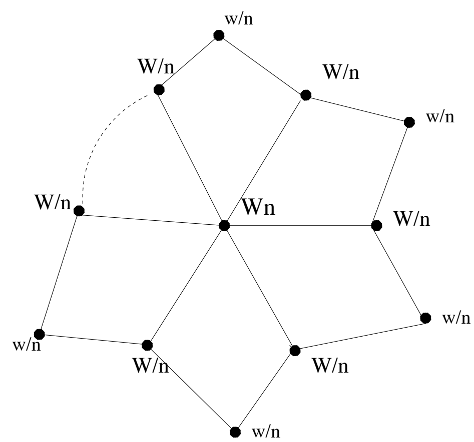

Figure 4.3. Extraordinary template. (quadrilateral scheme)

Let $\mathcal{L}$ represent the $(12n+2) \times (12n+2)$ "picking" matrix that exchanges the $j+nk$ block row with the $6(j-2)+k+2$ block row where $0 \leq k \leq 5$ and $2 \leq j \leq n+1$. Then as in [**Zor00a**] and [**CJ08**] $\widetilde{S}_n := \mathcal{L} U S_n (U_n)^{-1} \mathcal{L}^{-1}$ is a $(12n+2) \times (12n+2)$ block diagonal matrix that is similar to S_n and hence has the same eigenvalues. $\widetilde{S}_n$ has the following representation:

$$\widetilde{S}_n = \begin{bmatrix} M_0 & \mathbf{0} & \mathbf{0} & \mathbf{0} & \mathbf{0} & \mathbf{0} \\ \mathbf{0} & M_1 & \mathbf{0} & \mathbf{0} & \mathbf{0} & \mathbf{0} \\ \mathbf{0} & \mathbf{0} & M_2 & \cdots & \mathbf{0} & \mathbf{0} \\ \vdots & \vdots & \vdots & \ddots & \vdots & \vdots \\ \mathbf{0} & \mathbf{0} & \mathbf{0} & \cdots & M_{n-2} & \mathbf{0} \\ \mathbf{0} & \mathbf{0} & \mathbf{0} & \cdots & \mathbf{0} & M_{n-1} \end{bmatrix}$$

where

$$M_0 = \begin{bmatrix} W_n & J & K & L & M & N & M \\ W & J+2M & 2K & R_{0,0}+2N & J+M & 2L & M+J \\ w & 2M & K & 2L & J & R_{0,0} & J \\ 0 & 0 & 0 & L & M & 2N & M \\ 0 & 0 & 0 & N & M & L & 0 \\ 0 & 0 & 0 & 0 & 0 & N & 0 \\ 0 & 0 & 0 & N & 0 & L & M \end{bmatrix}$$

and for $j = 1, 2, ..., n-1$ and $z := e^{\frac{2\pi i}{n}}$

$$M_j = \begin{bmatrix} J + M\left(z^j + \frac{1}{z^j}\right) & K\left(1 + z^j\right) & R_{0,0} + N\left(z^j + \frac{1}{z^j}\right) & J + M\left(z^j\right) & L\left(1 + z^j\right) & M + J\left(z^j\right) \\ M\left(1 + \frac{1}{z^j}\right) & K & L\left(1 + \frac{1}{z^j}\right) & J & R_{0,0} & J \\ 0 & 0 & L & M & N\left(1 + z^j\right) & M\left(z^j\right) \\ 0 & 0 & N & M & L & 0 \\ 0 & 0 & 0 & 0 & N & 0 \\ 0 & 0 & N\left(\frac{1}{z^j}\right) & 0 & L & M \end{bmatrix}$$

For $j = 0$, M_j has an upper left 6×6 block and for $j = 1, 2, ..., n-1$ M_j has an upper left 4×4 block. For $j = 0, 1, 2, ..., n-1$, M_j has a lower right 8×8 block. Through direct calculation using a computer algebra system, the eight eigenvalues of each of these *lower* blocks are:

$$0, 0, t_2, t_4, \frac{1}{16} \text{ and the 3 roots of a cubic characteristic polynomial}$$

where t_2 and t_4 are from (4.2 |p.57).

Now the second block M_1 [where we are considering M_0 as the first block] has for one of its eigenvalues the subdominant eigenvalue λ. From the structure of M_1, λ is either an eigenvalue of either the 4×4 upper block

$$\begin{bmatrix} J + M\left(z + \frac{1}{z}\right) & K\left(1 + z\right) \\ M\left(1 + \frac{1}{z}\right) & K \end{bmatrix} \text{ or the } 8 \times 8 \text{ lower block } \begin{bmatrix} L & M & N\left(1 + z\right) & M\left(z\right) \\ N & M & L & 0 \\ 0 & 0 & N & 0 \\ N\left(\frac{1}{z}\right) & 0 & L & M \end{bmatrix}.$$

Since by assumption λ has multiplicity 2, it will have to be either an eigenvalue of the 4×4 upper block or a root of the cubic characteristic polynomial. We will assume that λ is an eigenvalue of the upper 4×4 block.

Again by direct calculation, the 4 eigenvalues of the upper block of M_1 are:

$$\frac{10 + 2\cos\left(\frac{2\pi}{n}\right) \pm \sqrt{38 + 40\cos\left(\frac{2\pi}{n}\right) + 2\cos\left(\frac{4\pi}{n}\right)}}{32}$$

$$\frac{3 + 32t_2\left(\cos\left(\frac{2\pi}{n}\right) - 1\right) \pm \sqrt{\begin{array}{c} 1 + t_2\left[256 + 192\left(\cos\left(\frac{2\pi}{n} - 1\right)\right)\right] \\ +1024\left(t_2\right)^2\left[\cos^2\left(\frac{2\pi}{n}\right) - 2\cos\left(\frac{2\pi}{n}\right) + 1\right] \end{array}}}{32}$$

Since t_2 is a free variable that can be small we have that the subdominant eigenvalue λ is:

$$\lambda = \frac{10 + 2\cos\left(\frac{2\pi}{n}\right) + \sqrt{38 + 40\cos\left(\frac{2\pi}{n}\right) + 2\cos\left(\frac{4\pi}{n}\right)}}{32} \tag{4.19}$$

Via direct calculation, a left eigenvector for λ of this 4×4 upper block is

$$\widetilde{l_1} = [1, 0, e_3, 0] \tag{4.20}$$

where

$$e_3 = \frac{1+z}{4\lambda - 1}$$

Now if we restrict our subdivision matrix to a 1-ring neighborhood around the central extraordinary vertex we get the following $4n+2 \times 4n+2$ matrix $S1_n$:

$$S1_n := \begin{bmatrix} W_n & \begin{bmatrix} J & \cdots & J \end{bmatrix} & \begin{bmatrix} K & \cdots & K \end{bmatrix} \\ \frac{1}{n}\begin{bmatrix} W \\ W \\ \vdots \\ W \end{bmatrix} & \mathcal{C}(J, M; M) & \mathcal{C}(K, 0; K) \\ \frac{1}{n}\begin{bmatrix} w \\ w \\ \vdots \\ w \end{bmatrix} & \mathcal{C}(M, M; 0) & diag(K) \end{bmatrix} \tag{4.21}$$

If we define $\widetilde{U} := diag(I_2, U_n, U_n)$ [a $(4n+2) \times (4n+2)$ matrix] and L as a “picking” matrix that exchanges the $kn + j$ and $2(j-2) + k + 2$ (block matrix) rows where $2 \le j \le n+1$ and $0 \le k \le 1$ then $\widetilde{S1_n} := L\widetilde{U}(S1_n)\widetilde{U}^{-1}L^{-1}$ is a similar matrix with the same eigenvalues as $S1_n$ and the following form:

$$\widetilde{S1}_n = \begin{bmatrix} \widetilde{M}_0 & \mathbf{0} & \mathbf{0} & \mathbf{0} & \mathbf{0} & \mathbf{0} \\ \mathbf{0} & \widetilde{M}_1 & \mathbf{0} & \mathbf{0} & \mathbf{0} & \mathbf{0} \\ \mathbf{0} & \mathbf{0} & \widetilde{M}_2 & \cdots & \mathbf{0} & \mathbf{0} \\ \vdots & \vdots & \vdots & \ddots & \vdots & \vdots \\ \mathbf{0} & \mathbf{0} & \mathbf{0} & \cdots & \widetilde{M}_{n-2} & \mathbf{0} \\ \mathbf{0} & \mathbf{0} & \mathbf{0} & \cdots & \mathbf{0} & \widetilde{M}_{n-1} \end{bmatrix} \tag{4.22}$$

where

$$\widetilde{M}_0 = \begin{bmatrix} W_n & J & K \\ W & J+2M & 2K \\ w & 2M & K \end{bmatrix} \text{ and}$$

$$\widetilde{M}_j = \begin{bmatrix} J + M\left(z^j + \frac{1}{z^j}\right) & K\left(1+z^j\right) \\ M\left(1+\frac{1}{z^j}\right) & K \end{bmatrix} \quad j = 1, 2, ..., n-1.$$

By our assumption that λ is an eigenvalue of $\begin{bmatrix} J + M\left(z+\frac{1}{z}\right) & K\left(1+z\right) \\ M\left(1+\frac{1}{z}\right) & K \end{bmatrix}$ we see that λ is an eigenvalue of the second block $\widetilde{M}_1$ and from (4.20 |p.69) $\widetilde{l}_1 = \left[1, 0, \frac{1+z}{4\lambda-1}, 0\right]$ is a corresponding left eigenvector.

By padding the 1×4 $rowvector \widetilde{l}_1$ with 6 initial zeros and $4(n-1)$ trailing zeros and we obtain a left eigenvector $\widetilde{\widetilde{\mathbf{L}}}_1$ for λ of $\widetilde{S1}_n$. Hence, $\widehat{\mathbf{L}}_1 := \widetilde{\widetilde{\mathbf{L}}}_1 L\widetilde{U}$ is a left eigenvector for λ of $S1_n$. Through direct computation

$$\widehat{\mathbf{L}}_1 = \left[\begin{array}{c} 0,0,1,0,z,0,z^2,0,...,z^{n-1},0,\frac{1+z}{4\lambda-1},0,\left(\frac{1+z}{4\lambda-1}\right)z,0, \\ \left(\frac{1+z}{4\lambda-1}\right)z^2,0,...,\left(\frac{1+z}{4\lambda-1}\right)z^{n-1},0 \end{array} \right] \qquad 1\times(4n+2) \text{ vector}$$

By considering the real and imaginary parts we get 2 real left eigenvectors for λ of $S1_n$:

(4.23)

$$\widetilde{\mathbf{L}}_1 := \left[\begin{array}{c} 0,0,1,0,\cos\left(\frac{2\pi}{n}\right),0,\cos\left(\frac{2\pi\cdot 2}{n}\right),0,...,\cos\left(\frac{2\pi\cdot(n-1)}{n}\right),0,\frac{1}{4\lambda-1}\left(1+\cos\left(\frac{2\pi}{n}\right)\right),0, \\ \frac{1}{4\lambda-1}\left(\cos\left(\frac{2\pi}{n}\right)+\cos\left(\frac{2\pi\cdot 2}{n}\right)\right),0,...,\frac{1}{4\lambda-1}\left(\cos\left(\frac{2\pi(n-1)}{n}\right)+\cos\left(\frac{2\pi\cdot n}{n}\right)\right),0 \end{array}\right]$$

$$\widetilde{\mathbf{L}}_2 := \left[\begin{array}{c} 0,0,0,0,\sin\left(\frac{2\pi}{n}\right),0,\sin\left(\frac{2\pi\cdot 2}{n}\right),0,...,\sin\left(\frac{2\pi\cdot(n-1)}{n}\right),0,\frac{1}{4\lambda-1}\left(\sin\left(\frac{2\pi}{n}\right)\right),0, \\ \frac{1}{4\lambda-1}\left(\sin\left(\frac{2\pi}{n}\right)+\sin\left(\frac{2\pi\cdot 2}{n}\right)\right),0,...,\frac{1}{4\lambda-1}\left(\sin\left(\frac{2\pi(n-1)}{n}\right)+\sin\left(\frac{2\pi\cdot n}{n}\right)\right),0 \end{array}\right]$$

As was done with the triangular interpolatory extraordinary case, the *initial* $1-$ring control vector net ($\mathbf{U}^0$) around this irregular $\mathbf{v}_{\mathbf{0}}^0$ can be represented as a linear combination of $1\times(4n+2)$ (possibly generalized) left eigenvectors of our $(4n+2)\times(4n+2)$ subdivision matrix $S1_n$ (4.21).

By letting $\left\{\widetilde{\mathbf{L}}_j\right\}_{0\le j\le 4n+1}$ be a set of $4n+2$ (possibly generalized) linearly independent left eigenvectors of $S1_n$, then $\mathbf{U}^0$ can be written as

$$\mathbf{U}^0 = \widetilde{\alpha}_0^{(0)}\widetilde{\mathbf{L}}_0 + \widetilde{\alpha}_1^{(0)}\widetilde{\mathbf{L}}_1 + \widetilde{\alpha}_2^{(0)}\widetilde{\mathbf{L}}_2 + \sum_{j=3}^{4n+1} \widetilde{\alpha}_j^{(0)}\widetilde{\mathbf{L}}_j \tag{4.24}$$

where $\widetilde{\alpha}_j^{(0)} \in \mathbb{R}^3$ $\ j = 0,\dots,4n+1$ and

- the left eigenvector for 1 is $\widetilde{\mathbf{L}}_0 = [1,0,1,0,...,1,0]$ due (4.18 |p.66) and

- $\widetilde{\mathbf{L}}_1, \widetilde{\mathbf{L}}_2$ are the left eigenvectors for λ from (4.23 |p.71).

By assumption the eigenvalues for $\widetilde{\mathbf{L}}_j$ $(j = 3,...,4n+1)$ have modulus less than λ.

Hence

$$\mathbf{U}^m = \widetilde{\alpha}_0^{(0)}\widetilde{\mathbf{L}}_0 + \lambda^m\widetilde{\alpha}_1^{(0)}\widetilde{\mathbf{L}}_1 + \lambda^m\widetilde{\alpha}_2^{(0)}\widetilde{\mathbf{L}}_2 + o\left(\lambda^m\right)$$

$$\lim_{m\to\infty}\lambda^{-m}\left(\mathbf{U}^m - \widetilde{\alpha}_0^{(0)}\widetilde{\mathbf{L}}_0\right) = \widetilde{\alpha}_1^{(0)}\widetilde{\mathbf{L}}_1 + \widetilde{\alpha}_2^{(0)}\widetilde{\mathbf{L}}_2$$

Due to

- $\lim\limits_{m\to\infty}\mathbf{U}^m = \widetilde{\alpha}_0^{(0)}\widetilde{\mathbf{L}}_0$

- the first component of $\widetilde{\mathbf{L}}_0$ being 1 and

- the scheme being interpolatory

then $\widetilde{\alpha}_0^{(0)} = v_0^0 = v_0^m$ for $m = 1, 2, ...$

So we have

$$\lim_{m\to\infty} \lambda^{-m} \left(\mathbf{U}^m - \left[v_{\mathbf{0},}^0, 0, v_{\mathbf{0},}^0, 0, v_{\mathbf{0},}^0, 0..., v_{\mathbf{0},}^0, 0\right]\right) = \widetilde{\alpha}_1^{(0)}\widetilde{\mathbf{L}}_1 + \widetilde{\alpha}_2^{(0)}\widetilde{\mathbf{L}}_2 \tag{4.25}$$

If we just look at the odd components of the left and right sides of (4.25) then we get

(4.26)

$$\lim_{m\to\infty} \lambda^{-m} \left(\left[v_0^m, v_1^m, v_2^m, ..., v_n^m\right] - \left[v_{\mathbf{0},}^0, v_{\mathbf{0},}^0, v_{\mathbf{0},}^0, ..., v_{\mathbf{0},}^0\right]\right) = \widetilde{\alpha}_1^{(0)}\widetilde{\widetilde{\mathbf{L}}}_1 + \widetilde{\alpha}_2^{(0)}\widetilde{\widetilde{\mathbf{L}}}_2$$

where

$$\widetilde{\widetilde{\mathbf{L}}}_1 := \left[\begin{array}{c} 0, 1, \cos\left(\frac{2\pi}{n}\right), \cos\left(\frac{2\pi\cdot 2}{n}\right), ..., \cos\left(\frac{2\pi\cdot(n-1)}{n}\right), \frac{1}{4\lambda-1}\left(1+\cos\left(\frac{2\pi}{n}\right)\right), \\ \frac{1}{4\lambda-1}\left(\cos\left(\frac{2\pi}{n}\right)+\cos\left(\frac{2\pi\cdot 2}{n}\right)\right), ..., \frac{1}{4\lambda-1}\left(\cos\left(\frac{2\pi(n-1)}{n}\right)+\cos\left(\frac{2\pi\cdot n}{n}\right)\right) \end{array}\right]$$

$$\widetilde{\widetilde{\mathbf{L}}}_2 := \left[\begin{array}{c} 0, 0, \sin\left(\frac{2\pi}{n}\right), \sin\left(\frac{2\pi\cdot 2}{n}\right), ..., \sin\left(\frac{2\pi\cdot(n-1)}{n}\right), \frac{1}{4\lambda-1}\left(\sin\left(\frac{2\pi}{n}\right)\right), \\ \frac{1}{4\lambda-1}\left(\sin\left(\frac{2\pi}{n}\right)+\sin\left(\frac{2\pi\cdot 2}{n}\right)\right), ..., \frac{1}{4\lambda-1}\left(\sin\left(\frac{2\pi(n-1)}{n}\right)+\sin\left(\frac{2\pi\cdot n}{n}\right)\right) \end{array}\right]$$

Now we will use (4.26) to get a representation of the two first partial derivatives at the point on the surface corresponding to the extraordinary vertex.

Let us parametrize F locally around this point. Let

$$F(0,0) := v_0^0$$

$$F\left(\cos\left(\frac{2j\pi}{n}\right), \sin\left(\frac{2j\pi}{n}\right)\right) := v_{j+1}^0 \text{ for } j = 0, 1, ..., n-1$$

$$F\left(\begin{array}{c} \frac{1}{4\lambda-1}\left(\cos\left(\frac{2\pi j}{n}\right)+\cos\left(\frac{2\pi(j+1)}{n}\right)\right), \\ \frac{1}{4\lambda-1}\left(\sin\left(\frac{2\pi j}{n}\right)+\sin\left(\frac{2\pi(j+1)}{n}\right)\right) \end{array}\right) := v_{n+j+1}^0$$

$$\text{for } j = 0, 1, ..., n-1$$

After m subdivisions the $2n$ surrounding vertices are parametrized as follows;

$$F\left(\lambda^m\left[\cos\left(\frac{2j\pi}{n}\right)\right], \lambda^m\left[\sin\left(\frac{2j\pi}{n}\right)\right]\right) := v_{j+1}^m \text{ for } j = 0, 1, ..., n-1$$

$$F\left(\begin{array}{c} \frac{\lambda^m}{4\lambda-1}\left(\cos\left(\frac{2\pi j}{n}\right) + \cos\left(\frac{2\pi(j+1)}{n}\right)\right), \\ \frac{\lambda^m}{4\lambda-1}\left(\sin\left(\frac{2\pi j}{n}\right) + \sin\left(\frac{2\pi(j+1)}{n}\right)\right) \end{array}\right) := v_{n+j+1}^m$$

$$\text{for } j = 0, 1, ..., n-1$$

Notice that there is a factor $\frac{1}{4\,\lambda-1}$ in the parametrization of the last n surrounding vertices. These vertices are the ones in the quadrilaterals that are "opposite" from the central extraordinary vertex. Their parametrization is essentially this factor multiplied by the sum of the parametrization of the *other* 2 vertices that *adjoin* the central vertex. See Figure 4.4. Also see Table 4.1 that displays these factors for various valences and shows them to be positive in value. In particular, see that if the central vertex were really a regular vertex (i.e. having valence 4) then $\frac{1}{4\,\lambda-1} = 1$.

valence	$\frac{1}{4\,\lambda-1}$
3	1.5616
4	1
5	.8334
6	.7583
7	.7173
8	.6923
9	.6758
10	.6643
11	.6559
12	.6497
13	.6449
14	.6411
15	.6381
16	.6356
17	.6336

Table 4.1. Values of $\frac{1}{4\lambda-1}$ for several valences

Since F is assumed to be C^1 at extraordinary vertices then

(4.27)

$$\lim_{m\to\infty}\lambda^{-m}\left\{\begin{array}{c}
F\left(0,0\right)-F\left(0,0\right),\ F\left(\lambda^m\cos\left(\frac{2\cdot 0\cdot\pi}{n}\right),\lambda^m\sin\left(\frac{2\cdot 0\cdot\pi}{n}\right)\right)-F\left(0,0\right),\\
F\left(\lambda^m\cos\left(\frac{2\cdot 1\cdot\pi}{n}\right),\lambda^m\sin\left(\frac{2\cdot 1\cdot\pi}{n}\right)\right)-F\left(0,0\right),\\
F\left(\lambda^m\cos\left(\frac{2\cdot 2\cdot\pi}{n}\right),\lambda^m\sin\left(\frac{2\cdot 2\cdot\pi}{n}\right)\right)-F\left(0.0\right),\\
\vdots\\
F\left(\lambda^m\cos\left(\frac{2\cdot(n-1)\cdot\pi}{n}\right),\lambda^m\sin\left(\frac{2\cdot(n-1)\cdot\pi}{n}\right)\right)-F\left(0,0\right)\ ,\\
F\left(\frac{\lambda^m}{4\lambda-1}\left[\cos\left(\frac{2\pi\cdot 0}{n}\right)+\cos\left(\frac{2\pi(0+1)}{n}\right)\right],\frac{\lambda^m}{4\lambda-1}\left[\sin\left(\frac{2\pi\cdot 0}{n}\right)+\sin\left(\frac{2\pi(0+1)}{n}\right)\right]\right)\\
-F\left(0,0\right),\\
F\left(\frac{\lambda^m}{4\lambda-1}\left[\cos\left(\frac{2\pi\cdot 1}{n}\right)+\cos\left(\frac{2\pi(1+1)}{n}\right)\right],\frac{\lambda^m}{4\lambda-1}\left[\sin\left(\frac{2\pi\cdot 1}{n}\right)+\sin\left(\frac{2\pi(1+1)}{n}\right)\right]\right)\\
-F\left(0,0\right),\\
\vdots\\
F\left(\frac{\lambda^m}{4\lambda-1}\left[\cos\left(\frac{2\pi\cdot(n-1)}{n}\right)+\cos\left(\frac{2\pi(n)}{n}\right)\right],\frac{\lambda^m}{4\lambda-1}\left[\sin\left(\frac{2\pi\cdot(n-1)}{n}\right)+\sin\left(\frac{2\pi(n)}{n}\right)\right]\right)\\
-F\left(0,0\right)
\end{array}\right\}=$$

$$F_s\left(0,0\right)\tilde{\tilde{\tilde{\mathbf{L}}}}_1+F_t\left(0,0\right)\tilde{\tilde{\tilde{\mathbf{L}}}}_2$$

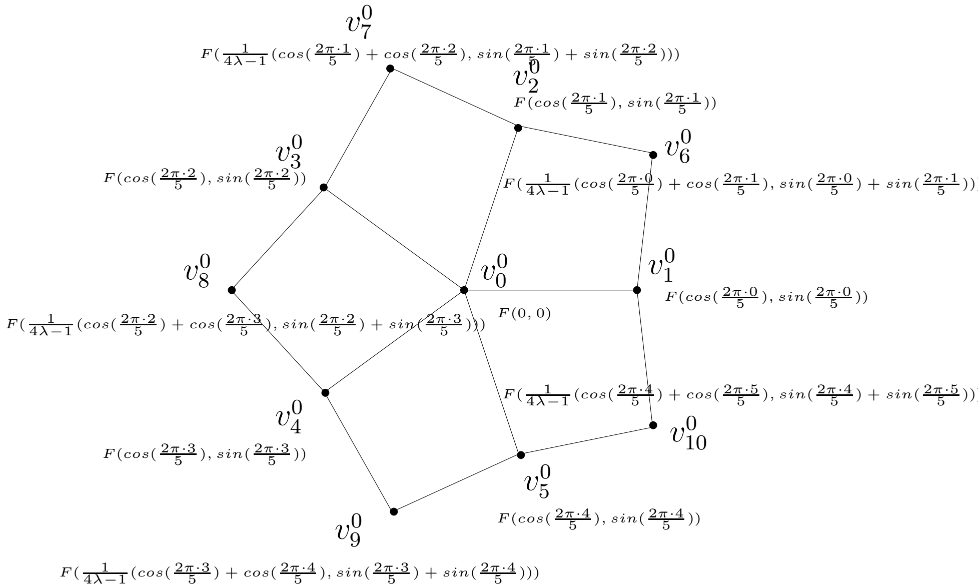

Figure 4.4. Figure shows the parametrization around a vertex of valence 5 for an interpolatory quadrilateral scheme. Note that the vertices were placed on the figure using the actual values of the parameters.

So from the local parametrization we can equate the right sides of (4.25 |p.72) and (4.27):

$$\widetilde{\alpha}_1^{(0)}\widetilde{\widetilde{\mathbf{L}}}_1+\widetilde{\alpha}_2^{(0)}\widetilde{\widetilde{\mathbf{L}}}_2= F_s\left(0,0\right)\widetilde{\widetilde{\mathbf{L}}}_1+F_t\left(0,0\right)\widetilde{\widetilde{\mathbf{L}}}_2$$

By linear independence this gives us

$$F_s\left(0,0\right)=\widetilde{\alpha}_1^{(0)}$$
$$F_t\left(0,0\right)=\widetilde{\alpha}_2^{(0)}$$

Proposition 4.5. *Suppose that an interpolatory quadrilateral scheme is convergent with limiting surface F that is C^1 at points corresponding to extraordinary vertices. Let $F\left(0,0\right)$ be such a point. Let $\widetilde{\alpha}_1^{(0)},\widetilde{\alpha}_2^{(0)}\in\mathbb{R}^3$ be the column vectors in (4.24 |p.71). Then*

$$F_s\left(0,0\right)=\widetilde{\alpha}_1^{(0)},\qquad F_t\left(0,0\right)=\widetilde{\alpha}_2^{(0)}$$

4.5. Partial Derivatives in Terms of Initial Control Net

As in the triangular case, we now have partial derivatives in terms of coefficients of the linear combinations of left eigenvectors. We will again obtain a much more specific representation of the partial derivatives. They will be given in terms of the initial control vector net. Initially looking at the regular case, we will use right eigenvectors of the subdivision matrix to achieve this.

4.5.1. Regular Case

We will obtain the right eigenvectors of S (2.26 |p.20) for the eigenvalues $\frac{1}{2}$ and $\frac{1}{4}$.

We can derive the following 4 diagonal block matrix $\widetilde{D}$ that is similar to the subdivision matrix S where

$$\widetilde{D} := \mathfrak{L} U S U^{-1} \mathfrak{L}^{-1}$$

and where

$$U := diag\left(I_{2,} U_4, U_4, U_4, U_4, U_4, U_4\right) \qquad 50 \times 50 \text{ matrix}$$

for U_4 defined in (3.41 |p.43).

$\mathfrak{L}$ is the 50×50 "picking" matrix that exchanges the $4k+j$ and $(j-2)\,6+k+2$ (block matrix) rows where $0 \leq k \leq 5$ and $2 \leq j \leq 5$.

We obtain

$$\widetilde{D} = \begin{pmatrix} M_0 & & & \\ & M_1 & & \\ & & M_2 & \\ & & & M_3 \end{pmatrix}$$

where

$$M_0 = \begin{bmatrix} R_{0,0} & J & K & L & M & N & M \\ 4L & J+2M & 2K & R_{0,0}+2N & J+M & 2L & M+J \\ 4N & 2M & K & 2L & J & R_{0,0} & J \\ 0 & 0 & 0 & L & M & 2N & M \\ 0 & 0 & 0 & N & M & L & 0 \\ 0 & 0 & 0 & 0 & 0 & N & 0 \\ 0 & 0 & 0 & N & 0 & L & M \end{bmatrix} \qquad 14{\times}14 \text{ matrix}$$

and for $j = 1, 2, 3$ the following 12×12 matrices

$$M_j = \begin{bmatrix} J + M\left(z^j + \frac{1}{z^j}\right) & K\left(1+z^j\right) & R_{0,0} + N\left(z^j + \frac{1}{z^j}\right) & J + M\left(z^j\right) & L\left(1+z^j\right) & M + J\left(z^j\right) \\ M\left(1+\frac{1}{z^j}\right) & K & L\left(1+\frac{1}{z^j}\right) & J & R_{0,0} & J \\ 0 & 0 & L & M & N\left(1+z^j\right) & M\left(z^j\right) \\ 0 & 0 & N & M & L & 0 \\ 0 & 0 & 0 & 0 & N & 0 \\ 0 & 0 & N\left(\frac{1}{z^j}\right) & 0 & L & M \end{bmatrix}$$

where $z = e^{\frac{2\pi i}{4}} = \sqrt{-1}$.

We can show through direct calculations that:

- 1 and $\frac{1}{4}$ are eigenvalues of M_0
- $\frac{1}{2}$ is an eigenvalue of M_1 and M_3
- $\frac{1}{4}$ is a double eigenvalue of M_2.

.

The right eigenvectors of $\frac{1}{2}$ for M_1, $\frac{1}{4}$ for M_0 and $\frac{1}{4}$ for M_2 are (respectively)

$$r_{1/2} = \left[1, w_0, \frac{1}{4}(1-i), w_1(1-i), 0, ..., 0\right]^T \qquad 12 \times 1$$

$$r_{1/4} = [w_2, w_3, w_4, w_5, w_6, w_7, 0, ..., 0]^T \qquad 14 \times 1$$

$$r_{1/4} = [1, w_8, 0, 0, 0, ..., 0]^T \qquad 12 \times 1$$

$$r_{1/4} = \left[0, 0, 1, -\frac{1}{3h}, 0, ..., 0\right]^T \qquad 12 \times 1$$

where

$$w_0 = \frac{-\left(3+32t_1h\right)}{h\left(32t_2+7\right)}$$

$$w_1 = -\frac{\left(32t_2-64ht_1+1\right)}{4h\left(32t_2+7\right)}$$

$$w_2 = h\left(1-16t_4-16t_5-4t_6\right)$$

$$w_3 = 1$$

$$w_4 = -32t_3$$

$$w_5 = \frac{8\left(2t_6+\frac{4}{h}t_3+128t_1t_3-\frac{1}{2}-4t_5\right)}{32t_2-3}$$

$$w_6 = -h+4ht_6+32t_3+16ht_4+16ht_5$$

$$w_7 = \frac{-1-32t_2+16t_5-512t_2t_5-48t_4+512t_2t_4+4t_6+128t_2t_6+\frac{32}{h}t_3+1024t_1t_3}{32t_2-3}$$

$$w_8 = -\left(\frac{\frac{1}{h}+32t_1}{1+32t_2}\right)$$

where $t_1, t_2, t_3, t_4, t_5, t_6$ and h are from (4.2 |p.57).

It can be directly shown that

- $t_2 \neq \frac{3}{32}$ and $t_2 \neq \frac{-1}{32}$ else the subsubdominant eigenvalue, $\frac{1}{4}$, has multiplicity 4 and
- if $32t_2+7=0$ then the eigenvalue 1 has multiplicity greater than 1.

We then insert the appropriate number of leading and trailing zeros to obtain right eigenvectors for $\widetilde{D}$ above. By multiplying by $U^{-1}\mathfrak{L}^{-1}$ we derive right eigenvectors for our subdivision matrix S.

Again using a computer algebra system we can obtain the following 50×1 right eigenvectors for $\frac{1}{2}$ and $\frac{1}{4}$ such that $\mathbf{L}_i\mathbf{R}_j = \delta\left(i-j\right) \quad j = 1,2,...,5$

where the $\mathbf{L}_i$ are from (4.7 |p.60):

(4.28)

$$\mathbf{R}_1 = \begin{bmatrix} 0,0,\tfrac{1}{3},\tfrac{1}{3}w_0,0,0,-\tfrac{1}{3},-\tfrac{1}{3}w_0,0,0,\tfrac{1}{12},\tfrac{1}{3}w_1,-\tfrac{1}{12},-\tfrac{1}{3}w_1,-\tfrac{1}{12},-\tfrac{1}{3}w_1,\tfrac{1}{12}, \\ \tfrac{1}{3}w_1,0,...,0 \end{bmatrix}^T$$

$$\mathbf{R}_2 = \begin{bmatrix} 0,0,0,0,\tfrac{1}{3},\tfrac{1}{3}w_0,0,0,-\tfrac{1}{3},-\tfrac{1}{3}w_0,\tfrac{1}{12},\tfrac{1}{3}w_1,\tfrac{1}{12},\tfrac{1}{3}w_1,-\tfrac{1}{12},-\tfrac{1}{3}w_1,-\tfrac{1}{12}, \\ -\tfrac{1}{3}w_1,0,...,0 \end{bmatrix}^T$$

$$\mathbf{R}_3 = \begin{bmatrix} \tfrac{w_2}{2w_7},\tfrac{1}{2w_7},\tfrac{1}{4}+\tfrac{w_4}{8w_7},\tfrac{w_8}{4}+\tfrac{w_5}{8w_7},-\tfrac{1}{4}+\tfrac{w_4}{8w_7},-\tfrac{w_8}{4}+\tfrac{w_5}{8w_7},\tfrac{1}{4}+\tfrac{w_4}{8w_7}, \\ \tfrac{w_8}{4}+\tfrac{w_5}{8w_7},-\tfrac{1}{4}+\tfrac{w_4}{8w_7},-\tfrac{w_8}{4}+\tfrac{w_5}{8w_7},\tfrac{w_6}{8w_7},\tfrac{1}{8},\tfrac{w_6}{8w_7},\tfrac{1}{8},\tfrac{w_6}{8w_7},\tfrac{1}{8},\tfrac{w_6}{8w_7},\tfrac{1}{8},0,...,0 \end{bmatrix}^T$$

$$\mathbf{R}_4 = \left[0,0,0,0,0,0,0,0,0,0,\frac{1}{4},-\frac{1}{12h},-\frac{1}{4},\frac{1}{12h},\frac{1}{4},-\frac{1}{12h},-\frac{1}{4},\frac{1}{12h},0,...,0\right]^T$$

$$\mathbf{R}_5 = \begin{bmatrix} \tfrac{w_2}{2w_7},\tfrac{1}{2w_7},-\tfrac{1}{4}+\tfrac{w_4}{8w_7},-\tfrac{w_8}{4}+\tfrac{w_5}{8w_7},\tfrac{1}{4}+\tfrac{w_4}{8w_7},\tfrac{w_8}{4}+\tfrac{w_5}{8w_7},-\tfrac{1}{4}+\tfrac{w_4}{8w_7}, \\ -\tfrac{w_8}{4}+\tfrac{w_5}{8w_7},\tfrac{1}{4}+\tfrac{w_4}{8w_7},\tfrac{w_8}{4}+\tfrac{w_5}{8w_7},\tfrac{w_6}{8w_7},\tfrac{1}{8},\tfrac{w_6}{8w_7},\tfrac{1}{8},\tfrac{w_6}{8w_7},\tfrac{1}{8},\tfrac{w_6}{8w_7},\tfrac{1}{8},0,...,0 \end{bmatrix}^T$$

Since right and left eigenvectors that correspond to *different* eigenvalues are orthogonal we can multiply both sides of (4.5 |p.59) by each $\mathbf{R}_j$ and so obtain (using (4.9 |p.61) and (4.15 |p.64)) the following representations for the first and second partial derivatives at a point locally parameterized as $\left(k_0^{(1)},k_0^{(2)}\right)$:

$$\begin{aligned} F_s\left(k_0^{(1)},k_0^{(2)}\right) &= \alpha_1^{(0)} &&= \mathbf{U}^0_{\mathbf{k}_0}\mathbf{R}_1 \\ F_t\left(k_0^{(1)},k_0^{(2)}\right) &= \alpha_2^{(0)} &&= \mathbf{U}^0_{\mathbf{k}_0}\mathbf{R}_2 \\ F_{ss}\left(k_0^{(1)},k_0^{(2)}\right) &= 2\alpha_3^{(0)} &&= 2\mathbf{U}^0_{\mathbf{k}_0}\mathbf{R}_3 \\ F_{st}\left(k_0^{(1)},k_0^{(2)}\right) &= \alpha_4^{(0)} &&= \mathbf{U}^0_{\mathbf{k}_0}\mathbf{R}_4 \\ F_{tt}\left(k_0^{(1)},k_0^{(2)}\right) &= 2\alpha_5^{(0)} &&= 2\mathbf{U}^0_{\mathbf{k}_0}\mathbf{R}_5 \end{aligned} \tag{4.29}$$

Note that the 19^{th} through 50^{th} components of the above right eigenvectors equal 0. So define $\mathbf{R}_j^*$ as the 18×1 column vector whose components are the first 18 components of $\mathbf{R}_j$ $(j=1,2,...,5)$. Also define $\widetilde{\mathbf{U}}^0_{\mathbf{k}_0}$ as the 3×18 vector consisting of the first 18 elements of $\mathbf{U}^0_{\mathbf{k}_0}$(4.4 |p.58).

We can then rewrite (4.29) as:

$$\begin{aligned} F_s\left(k_0^{(1)}, k_0^{(2)}\right) &= \alpha_1^{(0)} &&= \widetilde{\mathbf{U}}^0_{\mathbf{k}_0}\widetilde{\mathbf{R}}^*_1 \\ F_t\left(k_0^{(1)}, k_0^{(2)}\right) &= \alpha_2^{(0)} &&= \widetilde{\mathbf{U}}^0_{\mathbf{k}_0}\widetilde{\mathbf{R}}^*_2 \\ F_{ss}\left(k_0^{(1)}, k_0^{(2)}\right) &= 2\alpha_3^{(0)} &&= 2\widetilde{\mathbf{U}}^0_{\mathbf{k}_0}\widetilde{\mathbf{R}}^*_3 \\ F_{st}\left(k_0^{(1)}, k_0^{(2)}\right) &= \alpha_4^{(0)} &&= \widetilde{\mathbf{U}}^0_{\mathbf{k}_0}\widetilde{\mathbf{R}}^*_4 \\ F_{tt}\left(k_0^{(1)}, k_0^{(2)}\right) &= 2\alpha_5^{(0)} &&= 2\widetilde{\mathbf{U}}^0_{\mathbf{k}_0}\widetilde{\mathbf{R}}^*_5 \end{aligned} \tag{4.30}$$

Similarly we then obtain from (4.12 |p.62) and (4.16 |p.65) the following representations for the first and second partial derivatives of a point locally parameterized as $\left(k_0^{(1)} + \frac{i^{(1)}}{2^n}, k_0^{(2)} + \frac{i^{(2)}}{2^n}\right)$ on the surface F

$$\begin{aligned} F_s\left(k_0^{(1)} + \tfrac{i^{(1)}}{2^n}, k_0^{(2)} + \tfrac{i^{(2)}}{2^n}\right) &= 2^n\alpha_1^{(n)} &&= 2^n\widetilde{\mathbf{U}}^n_{\mathbf{k}_0,\mathbf{i}}\widetilde{\mathbf{R}}^*_1 \\ F_t\left(k_0^{(1)} + \tfrac{i^{(1)}}{2^n}, k_0^{(2)} + \tfrac{i^{(2)}}{2^n}\right) &= 2^n\alpha_2^{(n)} &&= 2^n\widetilde{\mathbf{U}}^n_{\mathbf{k}_0,\mathbf{i}}\widetilde{\mathbf{R}}^*_2 \\ F_{ss}\left(k_0^{(1)} + \tfrac{i^{(1)}}{2^n}, k_0^{(2)} + \tfrac{i^{(2)}}{2^n}\right) &= 2^{2n+1}\alpha_3^{(n)} &&= 2^{2n+1}\widetilde{\mathbf{U}}^n_{\mathbf{k}_0,\mathbf{i}}\widetilde{\mathbf{R}}^*_3 \\ F_{st}\left(k_0^{(1)} + \tfrac{i^{(1)}}{2^n}, k_0^{(2)} + \tfrac{i^{(2)}}{2^n}\right) &= 2^{2n}\alpha_4^{(n)} &&= 2^{2n}\widetilde{\mathbf{U}}^n_{\mathbf{k}_0,\mathbf{i}}\widetilde{\mathbf{R}}^*_4 \\ F_{tt}\left(k_0^{(1)} + \tfrac{i^{(1)}}{2^n}, k_0^{(2)} + \tfrac{i^{(2)}}{2^n}\right) &= 2^{2n+1}\alpha_5^{(n)} &&= 2^{2n+1}\widetilde{\mathbf{U}}^n_{\mathbf{k}_0,\mathbf{i}}\widetilde{\mathbf{R}}^*_5 \end{aligned} \tag{4.31}$$

where $\widetilde{\mathbf{U}}^n_{\mathbf{k}_0,\mathbf{i}}$ is the 3×18 vector consisting of the first 18 elements of $\mathbf{U}^n_{\mathbf{k}_0,\mathbf{i}}$ (4.10 |p.62).

So again we see that once we are working with a *specific* subdivision scheme we only need to compute the above right eigenvectors *one* time, and thus all that is needed to compute the partial derivatives is the surrounding control net.

4.5.2. Extraordinary Case

We will obtain a similar representation of the first partial derivatives of the limit surface at an extraordinary vertex with valence $n \neq 4$. Therefore, we need to get the right eigenvectors of $S1_n$ (4.21 |p.69) for the subdominant eigenvalue λ.

Through direct calculations the following is a right eigenvector of subdominant λ for $\widetilde{M_1}$ in $\widetilde{S1}_n$ (4.22 |p.70):

$$\begin{bmatrix} 1 \\ d_2 \\ d_3 \\ d_4 \end{bmatrix}$$

where

(4.32)

$$d_2 := \frac{-\left(\frac{16\lambda-1}{2+2re(z)}\right)\left(\frac{-8(4\lambda-1)+128h(4\lambda-1)(re(z)-1)t_1-2-2re(z)}{64h(4\lambda-1)}\right)-\frac{64h(4\lambda-1)t_1-1}{64h(4\lambda-1)}}{t_2+\left[\frac{16\lambda-1}{16+16re(z)}\right][1+16t_2(re(z)-1)-8\lambda]} \in \mathbb{R}$$

$$d_3 := \frac{1+z^{-1}}{16\lambda-4} \notin \mathbb{R}$$

$$d_4 := \left(\frac{256t_2(1+re(z))}{[1+z][-16t_2(1+re(z))-\{16\lambda-1\}\{1+16t_2(re(z)-1)-8\lambda\}]}\right) \times \left(-\frac{1}{8h}+2t_1\left(re\left(z\right)-1\right)-\frac{2+2re(z)}{64h(4\lambda-1)}-\left[\frac{t_1}{t_2}-\frac{1}{64ht_2(4\lambda-1)}\right]\left[\frac{1}{8}+2t_2\left(re\left(z\right)-1\right)-\lambda\right]\right) \notin \mathbb{R}$$

and where $z := e^{\frac{2\pi i}{n}}$, t_1, t_2, h are from (4.2 |p.57) and λ is from (4.19 |p.69).

The following will be needed shortly:

$$re\left(d_3\right) = \frac{1+re(z)}{16\lambda-4}$$

$$im\left(d_3\right) = \frac{-im(z)}{16\lambda-4}$$

$$re\left(d_4\right) = \left(\frac{1+re(z)}{2+2re(z)}\right) \times \left(\frac{256t_2(1+re(z))}{[-16t_2(1+re(z))-\{16\lambda-1\}\{1+16t_2(re(z)-1)-8\lambda\}]}\right) \times \left(-\frac{1}{8h}+2t_1\left(re\left(z\right)-1\right)-\frac{2+2re(z)}{64h(4\lambda-1)}-\left[\frac{t_1}{t_2}-\frac{1}{64ht_2(4\lambda-1)}\right]\left[\frac{1}{8}+2t_2\left(re\left(z\right)-1\right)-\lambda\right]\right)$$

$$im\left(d_4\right) = \left(\frac{-im(z)}{2+2re(z)}\right) \times \left(\frac{256t_2(1+re(z))}{[-16t_2(1+re(z))-\{16\lambda-1\}\{1+16t_2(re(z)-1)-8\lambda\}]}\right) \times \left(-\frac{1}{8h}+2t_1\left(re\left(z\right)-1\right)-\frac{2+2re(z)}{64h(4\lambda-1)}-\left[\frac{t_1}{t_2}-\frac{1}{64ht_2(4\lambda-1)}\right]\left[\frac{1}{8}+2t_2\left(re\left(z\right)-1\right)-\lambda\right]\right)$$

Now we will insert 6 leading zeros and $4\left(n-2\right)$ trailing zeros to get a right eigenvector of λ for $\widetilde{S1}_n$. Then multiplying by $\widetilde{U}^{-1}L^{-1}$ we get the following $4n+2$ right eigenvector of λ for $S1_n$ (4.21 |p.69):

$$\left[0, 0, 1, d_2, \overline{z}, d_2\overline{z}, \overline{z}^2, d_2\overline{z}^2, ..., \overline{z}^{n-1}, d_2\overline{z}^{n-1}, d_3, d_4, d_3\overline{z}, d_4\overline{z}, d_3\overline{z}^2, d_4\overline{z}^2, ..., d_3\overline{z}^{n-1}, d_4\overline{z}^{n-1}\right]^T$$

Separating the real and imaginary parts we have 2 real right eigenvectors of λ:

$$\widetilde{\mathbf{R}}_1 = \begin{bmatrix} 0,0,1,d_2,\cos\left(\frac{2\pi}{n}\right),d_2\cos\left(\frac{2\pi}{n}\right),...,\cos\left(\frac{2\pi(n-1)}{n}\right),d_2\cos\left(\frac{2\pi(n-1)}{n}\right),re\left(d_3\right),re\left(d_4\right), \\ re\left(d_3\right)\cos\left(\frac{2\pi}{n}\right)+im\left(d_3\right)\sin\left(\frac{2\pi}{n}\right),re\left(d_4\right)\cos\left(\frac{2\pi}{n}\right)+im\left(d_4\right)\sin\left(\frac{2\pi}{n}\right),..., \\ re\left(d_3\right)\cos\left(\frac{2\pi(n-1)}{n}\right)+im\left(d_3\right)\sin\left(\frac{2\pi(n-1)}{n}\right), \\ re\left(d_4\right)\cos\left(\frac{2\pi(n-1)}{n}\right)+im\left(d_4\right)\sin\left(\frac{2\pi(n-1)}{n}\right) \end{bmatrix}^T$$

$$\widetilde{\mathbf{R}}_2 = \begin{bmatrix} 0,0,0,0,\sin\left(\frac{2\pi}{n}\right),d_2\sin\left(\frac{2\pi}{n}\right),...,\sin\left(\frac{2\pi(n-1)}{n}\right),d_2\sin\left(\frac{2\pi(n-1)}{n}\right),im\left(d_3\right),im\left(d_4\right), \\ im\left(d_3\right)\cos\left(\frac{2\pi}{n}\right)-re\left(d_3\right)\sin\left(\frac{2\pi}{n}\right),im\left(d_4\right)\cos\left(\frac{2\pi}{n}\right)-re\left(d_4\right)\sin\left(\frac{2\pi}{n}\right),..., \\ im\left(d_3\right)\cos\left(\frac{2\pi(n-1)}{n}\right)-re\left(d_3\right)\sin\left(\frac{2\pi(n-1)}{n}\right), \\ im\left(d_4\right)\cos\left(\frac{2\pi(n-1)}{n}\right)-re\left(d_4\right)\sin\left(\frac{2\pi(n-1)}{n}\right) \end{bmatrix}^T$$

Through direct calculation using a computer algebra system we obtain the following 2 right eigenvectors $\left[\widehat{\mathbf{R}}_1,\widehat{\mathbf{R}}_2\right]$ such that for $i,j=1,2:\ \widetilde{\mathbf{L}}_i\widehat{\mathbf{R}}_j = \delta\left(i-j\right)$ where $\widetilde{\mathbf{L}}_i$ is from (4.23 |p.71) for

$$\widehat{\mathbf{R}}_1 = \frac{2\beta}{n\cdot\gamma}\widetilde{\mathbf{R}}_1+\frac{2\alpha}{n\cdot\gamma}\widetilde{\mathbf{R}}_2 \qquad (4.33)$$
$$\widehat{\mathbf{R}}_2 = \frac{2\alpha}{n\cdot\gamma}\widetilde{\mathbf{R}}_1-\frac{2\beta}{n\cdot\gamma}\widetilde{\mathbf{R}}_2$$

and where

$$\begin{aligned} \gamma &:= -1-2re\left(e_3\right)re\left(d_3\right)+2im\left(e_3\right)im\left(d_3\right) \\ &\quad -\left[re\left(e_3\right)re\left(d_3\right)\right]^2-\left[im\left(e_3\right)im\left(d_3\right)\right]^2-\left[re\left(e_3\right)im\left(d_3\right)\right]^2-\left[im\left(e_3\right)re\left(d_3\right)\right]^2 \\ \beta &:= -1-re\left(e_3\right)re\left(d_3\right)+im\left(e_3\right)im\left(d_3\right) \\ \alpha &:= -re\left(e_3\right)im\left(d_3\right)-im\left(e_3\right)re\left(d_3\right) \end{aligned}$$

So by Proposition 4.5 on p. 75 and by (4.24 |p.71) we now have a representation of the first partial derivatives of the limit surface at an extraordinary vertex in terms of the surrounding block vertices:

$$F_s\left(0,0\right) = \mathbf{U}^0\widehat{\mathbf{R}}_1 \qquad (4.34)$$
$$F_t\left(0,0\right) = \mathbf{U}^0\widehat{\mathbf{R}}_2$$

Proposition 4.6. *Suppose that an interpolatory quadrilateral scheme is convergent with limiting surface F that is C^1 at points corresponding to* *extraordinary vertices. Let $F(0,0)$ be such a point. Assume that $\lambda = \frac{3}{8} + \frac{1}{8}(z + z^{-1})$. Then for $\widehat{\mathbf{R}}_1, \widehat{\mathbf{R}}_2$ in (4.33 |p.82)*

$$F_s(0,0) = \mathbf{U}^0 \widehat{\mathbf{R}}_1, \qquad F_t(0,0) = \mathbf{U}^0 \widehat{\mathbf{R}}_2$$

4.6. Specific Template

Let's now apply these formulas to a specific 1-ring quadrilateral interpolatory scheme that was developed by Chui/Jiang in [**CJ05**]. The scheme is given by (4.2 |p.57) where

$$[t_1, t_2, t_3, t_4, t_5, t_6] = \frac{1}{256}[5, -1, -30, -9, -33, -86]$$
$$h = -1$$

These values result in Φ being in $W^{3.27720}$.

Plugging these values into our formulas for the right eigenvectors (regular case) (4.28 |p.79) we get:

$$\mathbf{R}_1 = \left[0, 0, \frac{1}{3}, \frac{19}{165}, 0, 0, -\frac{1}{3}, -\frac{19}{165}, 0, 0, \frac{1}{12}, \frac{17}{660}, -\frac{1}{12}, -\frac{17}{660}, -\frac{1}{12}, -\frac{17}{660}, \frac{1}{12}, \frac{17}{660}\right]^T$$

$$\mathbf{R}_2 = \left[0, 0, 0, 0, \frac{1}{3}, \frac{19}{165}, 0, 0, -\frac{1}{3}, -\frac{19}{165}, \frac{1}{12}, \frac{17}{660}, \frac{1}{12}, \frac{17}{660}, -\frac{1}{12}, -\frac{17}{660}, -\frac{1}{12}, -\frac{17}{660}\right]^T$$

$$\mathbf{R}_3 = \left[\begin{array}{l} -\frac{3975}{764}, \frac{200}{191}, \frac{941}{764}, \frac{2295}{5348}, \frac{559}{764}, \frac{1149}{5348}, \frac{941}{764}, \frac{2295}{5348}, \frac{559}{764}, \frac{1149}{5348}, \\ \frac{975}{3056}, \frac{309}{3056}, \frac{975}{3056}, \frac{309}{3056}, \frac{975}{3056}, \frac{309}{3056}, \frac{975}{3056}, \frac{309}{3056} \end{array}\right]^T$$

$$\mathbf{R}_4 = \left[0, 0, 0, 0, 0, 0, 0, 0, 0, 0, \frac{1}{4}, \frac{1}{12}, -\frac{1}{4}, -\frac{1}{12}, \frac{1}{4}, \frac{1}{12}, -\frac{1}{4}, -\frac{1}{12}\right]^T$$

$$\mathbf{R}_5 = \left[\begin{array}{l} -\frac{3975}{764}, \frac{200}{191}, \frac{559}{764}, \frac{1149}{5348}, \frac{941}{764}, \frac{2295}{5348}, \frac{559}{764}, \frac{1149}{5348}, \frac{941}{764}, \frac{2295}{5348}, \\ \frac{975}{3056}, \frac{309}{3056}, \frac{975}{3056}, \frac{309}{3056}, \frac{975}{3056}, \frac{309}{3056}, \frac{975}{3056}, \frac{309}{3056} \end{array}\right]^T$$

4.6.1. Corresponding specific derivative formulas

Note that for any particular scheme, the above calculations only need to be done once. If we insert these values into either (4.30 |p.80) or (4.31 |p.80) then we get the first and second partial derivatives as linear combinations of the block vectors that surround the regular vertex.

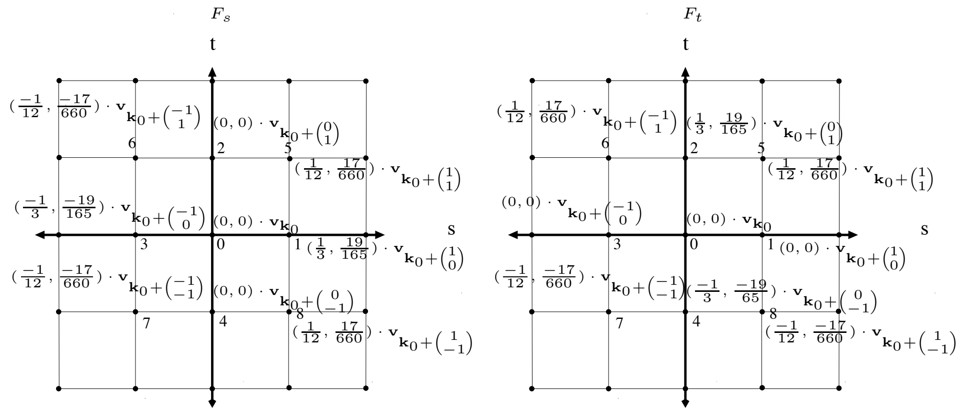

Figure 4.5. Partial derivatives in interpolatory quadrilateral scheme. Note the symmetry around the central axis. Observe the symmetry between F_s and F_t

The following charts (Figures 4.5, 4.6 and 4.7) visually show the symmetry that these formulas have:

4.6.2. "Visual C^1" for extraordinary case

To accompany this specific regular template, we propose the following template for an extraordinary vertex. Referring to the matrices in (4.17 |p.66), let

(4.35)

$$W_n := \begin{bmatrix} 1 & \frac{\beta}{4}\left[4t_3 + h\left(-\frac{1}{2} + 8t_4 + 8t_5 + 2t_6\right)\right] \\ 0 & \frac{\beta}{4}\left(t_6\right) \end{bmatrix} \qquad W := \beta \begin{bmatrix} 0 & -2t_3 + h\left(\frac{1}{8} - 2t_4 - 2t_5 - \frac{1}{2}t_6\right) \\ 0 & t_5 \end{bmatrix}$$

$$w := \beta \begin{bmatrix} 0 & t_3 \\ 0 & t_4 \end{bmatrix}$$

where $\beta = 4$ if $n = 3$ else $\beta = \frac{16}{n}$. Note that if $n = 4$ then these revert to the matrices for the regular mask.

This template appears satisfactory for three reasons. The first is that the leading eigenvalues of the subdivision matrix $S1_n$ (4.21 |p.69) satisfy

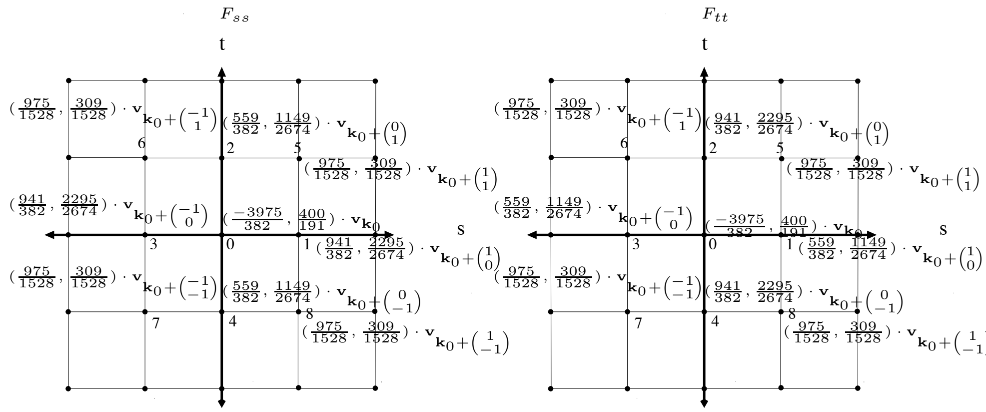

Figure 4.6. Second partial derivatives F_{ss} and F_{tt} in interpolatory quadrilateral scheme. Note the symmetry around the central axis. Observe the symmetry between F_{ss} and F_{tt}

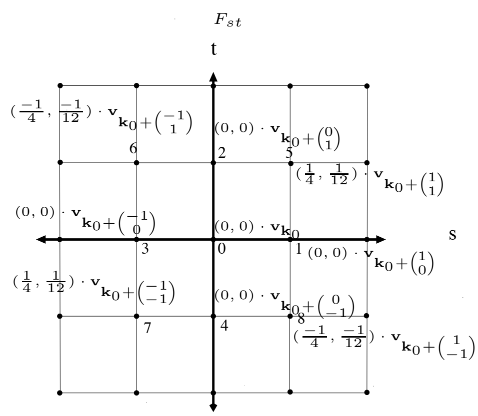

Figure 4.7. Note the extremely simple form of F_{st}. Also symmetric around central vertex.

the conditions

$$\lambda_0 = 1 \qquad \lambda_1 = \lambda_2 \qquad |\lambda_j| < |\lambda_1| \quad j = 3, 4, ... \tag{4.36}$$

for valences 3 to (at least) 16. See Appendix A for a listing of the eigenvalues for each of these valences.

The second is the appearance of the 2-D meshes formed by performing 4 subdivisions on an initial control set of points in $\mathbb{R}^2$ whose coordinates are the two left eigenvectors of the subdominant eigenvalue λ. These meshes were first introduced in [**Rei95**] and were seen again in [**CJ08**]. The meshes in Figures 9.1 through 9.3 shown in Appendix B suggest the regularity and injectivity of the characteristic map.

The background for the above second reason is that in [**Rei95**] Reif introduced sufficient conditions for C^1 continuity at an extraordinary vertex. Namely, if the leading eigenvalues satisfied (4.36 |p.86) and if the characteristic map is regular and injective then almost all surfaces generated by the subdivision are C^1 continuous. Briefly, the characteristic map is the map $\phi : U \to \mathbb{R}^2$ that is the subdivision surface generated from U (a 2-D initial control net whose coordinates are the two left eigenvectors of the subdominant eigenvalue λ).

The third reason is that actual subdivision surfaces generated using the templates in (4.17 |p.66) and (4.35 |p.84) appear good. See Figures 4.9 and 4.10.

From (4.32 |p.81) and (4.33 |p.82) we can derive specific right eigenvectors $\widehat{\mathbf{R}}_1, \widehat{\mathbf{R}}_2$ of λ by using the values of t_j and h from the regular case. For valence = 5 we obtain the following:

$$\widehat{\mathbf{R}}_1 = \begin{bmatrix} 0, 0, .2749, .0934, .08492, .02887, -.2224, -.0756, -.2224, -.0756, .08492, \\ .02887, .07497, .02305, -.02864, -.008798, -.09266, -.02850, -.02864, \\ -.008804, .0794, .02304 \end{bmatrix}^T$$

$$\widehat{\mathbf{R}}_2 = \begin{bmatrix} 0, 0, 0, 0, .2614, .0888, .1616, .05492, -.1616, -.05492, -.2614, -.08888, .05447, \\ .01675, .08816, .02711, 0, 0, -.08816, -.02710, -.05447, -.01675 \end{bmatrix}^T$$

If we insert these values into (4.34 |p.82) then we get the partial derivatives as linear combinations of the block vectors that surround the extraordinary vertex.

The following diagrams [Figure 4.8] visually demonstrate these formulas:

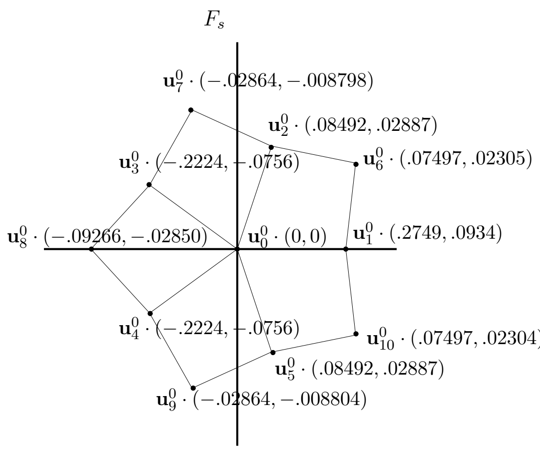

(a)

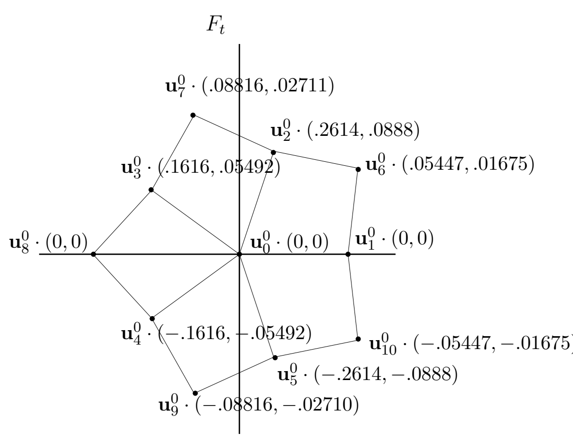

(b)

Figure 4.8. The above diagrams represents F_s and F_t at a vertex of valence 5 for our specific interpolatory quadrilateral scheme.

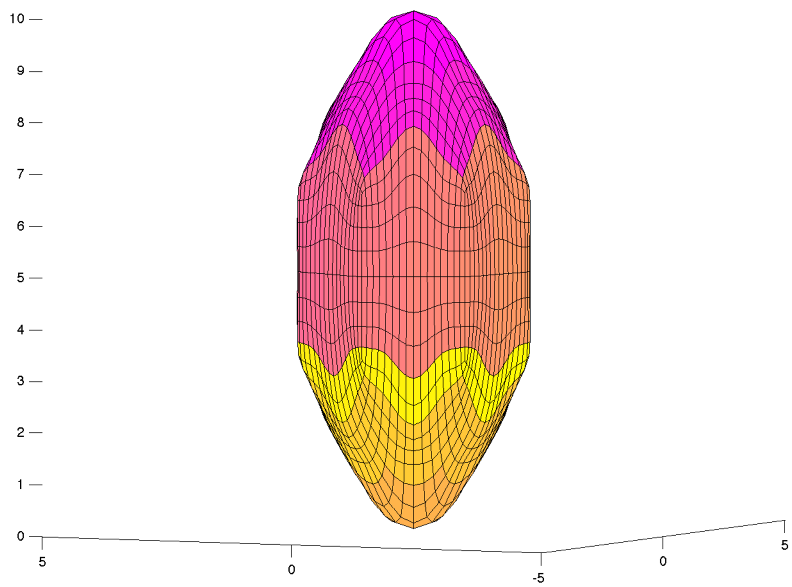

Figure 4.9. Figure created using our interpolating quadrilateral subdivision scheme There are several extraordinary vertices of valence 3 and 7.

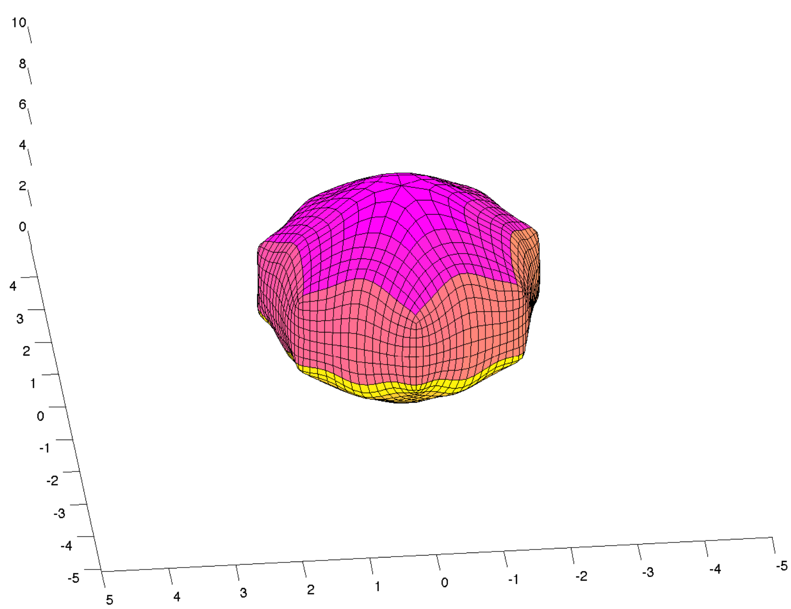

Figure 4.10. Another view of the figure created with the interpolating quadrilateral scheme

CHAPTER 5

Derivative Formulas for Approximating Triangular and Approximating Quadrilateral Schemes

With approximating schemes initial and subsequent control vertices do not lay on the limit surface F. Instead these vertices converge to the limit surface. In other words, for $\mathbf{v}_{\mathbf{k}}^{m} = (v_{\mathbf{k}}^{m}, s_{\mathbf{k}}^{m})$ generated after m subdivisions or for $\mathbf{v}_{\mathbf{k}}^{n+m} = \left(v_{\mathbf{k}}^{n+m}, s_{\mathbf{k}}^{n+m}\right)$ generated after $n+m$ subdivisions by the local averaging rule (2.7 |p.13) we have

$$\lim_{m\to\infty} \sup_{\mathbf{k}} \left|v_{2^m\mathbf{k}}^{m} - F(\mathbf{k})\right| = 0 \tag{5.1}$$

$$\lim_{m\to\infty} \sup_{\mathbf{k}} \left|v_{2^{n+m}\mathbf{k}+2^m\mathbf{i}}^{n+m} - F\left(\mathbf{k} + \frac{\mathbf{i}}{2^n}\right)\right| = 0$$

A benefit of approximating schemes is that the quality of the surface produced is generally better than that produced by interpolatory schemes [**Zor00b**]. A drawback is that vertices are not points on the limit surface and thus we have the limit above (5.1) instead of the following equality that we have for the interpolatory case:

$$v_{2^m\mathbf{k}}^{m} = F(\mathbf{k}) \qquad m = 0, 1, 2, ... \quad \mathbf{k} \in \mathbb{Z}^2$$

As a result we require an additional assumption so that we can derive the partial derivatives as for interpolatory schemes.

5.1. Additional Assumptions

We will assume that the cascade algorithm converges in $C^1(\mathbb{R}^2)$ and in $C^2(\mathbb{R}^2)$. Basically we are proposing to extend Jiang/Smith's 1-D work on deriving formulas of first and second derivatives for approximating schemes for curves to the 2-D surface case. (See [**JS09**].) B-splines were used there. We will be using box-splines.

The cascade operator $Q_P\, f$ for some nontrivial 2×1 vector of compactly supported functions $\Phi_0 \in C^k(\mathbb{R}^2)$ and a refinement mask P is defined as

$$Q_P\,\Phi_0 := \sum_{\mathbf{k}\in\mathbb{Z}^2} P_{\mathbf{k}}\,\Phi_0\,(2\cdot - \mathbf{k})$$

The iteration scheme $\Phi_m := Q_P\,\Phi_{m-1}$ is called a cascade algorithm. Note that $\Phi_m = Q_P^m\,\Phi_0$. Also the refinable Φ associated with P is a fixed point for the cascade algorithm (i.e. $\Phi := Q_P\,\Phi$). In addition note that if the cascade algorithm converges then the limit function is Φ.

We also have the following relation from [**Jia02**]:

$$\sum_{\mathbf{k}} \mathbf{v}_{\mathbf{k}}^0\,(Q_P^m\,\Phi_0)\,(\mathbf{x}-\mathbf{k}) = \sum_{\mathbf{k}} \mathbf{v}_{\mathbf{k}}^m\,\Phi_0\,(2^m\mathbf{x}-\mathbf{k}) \tag{5.2}$$

From [**JJL02**] we say that the cascade algorithm converges in $C^k(\mathbb{R}^2)$ if

$$\lim_{m\to\infty} \sum_{|\mu|\le k} \left\| D^\mu\,(Q_P^m\Phi_0) - D^\mu\Phi \right\|_\infty = 0 \quad \text{for } |\mu| \le k \tag{5.3}$$

holds for any $\Phi_0 \in C^k(\mathbb{R}^2)$ where Φ_0 is compactly supported and has accuracy order of at least $k+1$

Note that (5.3) implies

$$\lim_{m\to\infty} \left\| D^\mu\,(Q_P^m\Phi_0) - D^\mu\Phi \right\|_\infty = 0 \quad \text{for } |\mu| \le k$$

5.1.1. Characterization of C^k Convergence

Before we proceed further, we wish to give the characterization of C^k convergence provided by Chen, Jia and Riemenschneider in [**CJR02**]. Here is their theorem:

> The subdivision scheme associated with a mask a ($r\times r$ matrices) and a ($s\times s$) dilation matrix M converges in $C^k(\mathbb{R}^s)$ if and only if (1) V_k is invariant under A_ε for every $\varepsilon \in E$ and (2) $\rho_\infty\left(\{A_\varepsilon|_V : \varepsilon \in E\}\right) < m^{-k/s}$

In what follows we will define (as in [**CJR02**]) the terms in the above theorem.

The matrix M is the same as matrix A in (1.1 |p.4). In their paper, M is also assumed to be isotropic which means that $\exists\Lambda$ ($s \times s$ invertible matrix) such that $\Lambda M \Lambda^{-1} = diag\left(\sigma_1, ..., \sigma_s\right)$ where $|\sigma_1| = |\sigma_2| = ... |\sigma_s| :=$ spectral radius of M. Note that $m := |\det M|$.

E is the complete set of representations of the cosets of $\mathbb{Z}^s / M\mathbb{Z}^s$. We include $\mathbf{0}$. There are m elements in E.

A_ε is a linear operator on $\left(\ell_0\left(\mathbb{Z}^s\right)\right)^r$ [finitely supported $r \times 1$ sequences on $\mathbb{Z}^s$] where

$$A_\varepsilon v\left(\alpha\right) := \sum_{\beta \in \mathbb{Z}^s} a\left(\varepsilon + M\alpha - \beta\right) v\left(\beta\right) \qquad \alpha \in \mathbb{Z}^s \text{ and } v \in \left(\ell_0\left(\mathbb{Z}^s\right)\right)^r$$

Define U_k as the linear span of u_μ ($|\mu| \leq k$) where

$$u_\mu\left(\alpha\right) := \sum_{\nu \leq \mu} \binom{\mu}{\nu} \left(\Lambda\alpha\right)^\nu B_{\mu-\nu} \qquad \alpha \in \mathbb{Z}^s$$

where we have the following recursive definition

$$B_\mu := \sum_{\nu \leq \mu} \binom{\mu}{\nu} \sigma^{\mu-\nu} B_{\mu-\nu} q_\nu\left(-iD\right) A\left(\mathbf{0}\right)$$

where

$$q_\nu\left(\mathbf{x}\right) := \left(\Lambda\mathbf{x}\right)^\nu \qquad \mathbf{x} \in \mathbb{R}^s$$

$$A\left(\omega\right) := \frac{1}{|\det M|} \sum_{\alpha \in \mathbb{Z}^s} a\left(\alpha\right) e^{-i\alpha\cdot\omega}$$

$$B_{\mathbf{0}} := \text{ left eigenvector of } A\left(\mathbf{0}\right) \text{ corresponding to eigenvalue } 1$$

The linear space V_k is defined using U_k :

$$V_k := \left\{v \in \left(\ell_0\left(Z^s\right)\right)^{r\times 1} : \langle u, v\rangle = 0\right\} \quad \forall u \in U_k$$

where for $u \in \left(\ell\left(Z^s\right)\right)^{1\times r}$, $v \in \left(\ell_0\left(Z^s\right)\right)^{r\times 1}$

$$\langle u, v\rangle := \sum_{\alpha \in \mathbb{Z}^s} u\left(-\alpha\right) v\left(\alpha\right)$$

We now obtain V (a subspace of V_k) defined as:

$$V := V_k \cap \left(\ell\left(K\right)\right)^r$$

where $(\ell(K))^r$ is the linear space of $r \times 1$ sequences supported on the following set K:

$$K \subset \mathbb{Z}^s := \sum_{n=1}^{n=\infty} M^{-n} G$$

where

$$G := (\text{supp } a \cup \{\mathbf{0}\}) - E + [-1,1]^s$$

Regarding the second condition of the theorem in [**CJR02**], if $\mathcal{A}$ is a finite multiset of linear operators on V then $\mathcal{A}^n := \{(A_1, A_2, ..., A_n) : A_1, A_2, ..., A_n \in \mathcal{A}\}$

We define

$$\|\mathcal{A}^n\|_\infty := \max\left\{\|A_1 A_2 ... A_n\|_\infty : (A_1, A_2, ..., A_n) \in \mathcal{A}^n\right\}$$

where for any $m \times n$ matrix P

$$\|P\|_\infty = \max_i \left(\sum_j |p_{ij}|\right) = \text{ the maximum of the row sums (using absolute values)}$$

Now we can define $\rho_\infty(\mathcal{A})$:

$$\rho_\infty(\mathcal{A}) := \lim_{n\to\infty} \|\mathcal{A}^n\|_\infty^{1/n}$$

So for that second condition of the theorem, we use the finite multiset $\{A_\varepsilon|_V : \varepsilon \in E\}$ in place of $\mathcal{A}$ used above in the definitions.

5.2. Templates with Sum Rule Order

5.2.1. Triangular Scheme

We again will derive as much information about the templates $\{P_{\mathbf{k}}\}_{\mathbf{k}}$ and the 1×2 constant vectors $\mathbf{l}_0^\alpha$ introduced in (2.14). This time we will no longer have the interpolatory format given in (3.1) and (3.2). As a result we will have more free variables. The number of free variables increases from 4 to 6.

Through direct calculation using the Sum rules we can determine the following:

$$
\begin{aligned}
\mathbf{l}_0^{(1,0)} &= \mathbf{l}_0^{(0,1)} = [0,0] \\
\mathbf{l}_0^{(2,0)} &= \mathbf{l}_0^{(0,2)} = [0,h] \\
\mathbf{l}_0^{(1,1)} &= \left[0, \frac{h}{2}\right] \qquad \text{where } h \neq 0
\end{aligned} \tag{5.4}
$$

As indicated in Chapter 2, $\mathbf{l}_0^{(0,0)} = [1,0]$.

Also per direct calculation using the Sum rules we can determine:

$$
P_{0,0} = \begin{pmatrix} 1 + 6h\left(\frac{3}{2}t_6 + \frac{1}{4}t_5\right) & h\left(-\frac{3}{8} + 9t_3 + \frac{3}{2}t_4\right) \\ t_5 & t_4 \end{pmatrix} \qquad D = \begin{pmatrix} -h\left(\frac{3}{2}t_6 + \frac{1}{4}t_5\right) & h\left(\frac{1}{16} - \frac{3}{2}t_3 - \frac{1}{4}t_4\right) \\ t_6 & t_3 \end{pmatrix}
$$

(5.5)

$$
B = \begin{pmatrix} \frac{3}{8} & 0 \\ -\frac{1}{8h} - t_1 & \frac{1}{8} - t_2 \end{pmatrix} \qquad C = \begin{pmatrix} \frac{1}{8} & 0 \\ t_1 & t_2 \end{pmatrix}
$$

where t_j for $j = 1, ..., 6$ are "free" variables. Using the techniques in [**JO03**], the values of the t_j will determine the Sobolev smoothness of the refinable function Φ (2.5 |p.12). See section 2.4.

5.2.2. Quadrilateral Scheme

Again we will have more free variables than for the interpolatory quad scheme. The number of free variables increases from 6 to 10.

Through direct calculation using the Sum rules we can determine the following:

$$
\begin{aligned}
\mathbf{l}_0^{(1,0)} &= \mathbf{l}_0^{(0,1)} = [0,0] \\
\mathbf{l}_0^{(2,0)} &= \mathbf{l}_0^{(0,2)} = [0,h] \\
\mathbf{l}_0^{(1,1)} &= [0,0] \qquad \text{where } h \neq 0
\end{aligned} \tag{5.6}
$$

As indicated in Chapter 2 $\mathbf{l}_0^{(0,0)} = [1,0]$.

Through direct calculation using the Sum rules we determine:

(5.7)

$$R_{0,0} = \begin{pmatrix} 1-4t_9-4t_{10} & 4t_3+h\left(-\frac{1}{2}+8t_4+8t_5+2t_6\right) \\ -\frac{4}{h}t_{10}-\frac{2}{h}t_9-4t_8-4t_7 & t_6 \end{pmatrix}$$

$$L = \begin{pmatrix} t_9 & -t_3-\frac{1}{4}\left(4t_3+h\left(-\frac{1}{2}+8t_4+8t_5+2t_6\right)\right) \\ t_7 & t_5 \end{pmatrix} \qquad N = \begin{pmatrix} t_{10} & t_3 \\ t_8 & t_4 \end{pmatrix}$$

$$J = \begin{pmatrix} \frac{3}{8} & 0 \\ -\frac{1}{8h}-2t_1 & \frac{1}{8}-2t_2 \end{pmatrix} \qquad K = \begin{pmatrix} \frac{1}{4} & 0 \\ -\frac{1}{16h} & \frac{1}{16} \end{pmatrix} \qquad M = \begin{pmatrix} \frac{1}{16} & 0 \\ t_1 & t_2 \end{pmatrix}$$

where t_j for $j = 1, ..., 10$ are "free" variables. Using the techniques in [**JO03**], the values of the t_j will determine the Sobolev smoothness of the refinable function Φ (2.5 |p.12). See section 2.4.

5.3. Development of general formulas (Regular case: Triangular and Quadrilateral)

Here we will find representation of the first and second partial derivatives of the limiting surface in terms of limits of linear combinations of surrounding vertices as the number of subdivisions goes to ∞. To do this we will be using box splines. So we will first introduce what box splines are.

5.3.1. Box Splines

As in [**CDV10**] define the following set of direction vectors in $\mathbb{R}^2$:

$$\mathcal{D}_n := \left\{ \underbrace{\mathbf{e}_1, ..., \mathbf{e}_1}_{n_1}, \underbrace{\mathbf{e}_2, ..., \mathbf{e}_2}_{n_2}, \underbrace{\mathbf{e}_3, ..., \mathbf{e}_3}_{n_3}, \underbrace{\mathbf{e}_4, ..., \mathbf{e}_4}_{n_4} \right\} \subset \mathbb{Z}^2 \backslash \{\mathbf{0}\} \tag{5.8}$$

where

$$\mathbf{e}_1 := (1,0)^T, \mathbf{e}_2 := (0,1)^T, \mathbf{e}_3 := \mathbf{e}_1 + \mathbf{e}_2 = (1,1)^T, \mathbf{e}_4 := \mathbf{e}_1 - \mathbf{e}_2 = (1,-1)^T$$

and where n_1, n_2 are positive, n_3, n_4 may be zero and $n := n_1+n_2+n_3+n_4$.

Now relabel the direction vectors in (5.8) with superscripts and define

$$\mathcal{D}_m := \left\{ \mathbf{e}^1, \mathbf{e}^2, ..., \mathbf{e}^m \right\} \subset \mathcal{D}_n \quad \text{above} \tag{5.9}$$

where

$$
\begin{aligned}
\mathbf{e}^1 &:= \mathbf{e}_1 \\
\mathbf{e}^2 &:= \mathbf{e}_2 \\
\mathbf{e}^m &\in \{\mathbf{e}_1, \mathbf{e}_2, \mathbf{e}_3, \mathbf{e}_4\} \qquad 2 \le m \le n
\end{aligned} \tag{5.10}
$$

Now define the box spline $M(\mathbf{x}|\mathcal{D}_2)$:

$$M(\mathbf{x}|\mathcal{D}_2) := \chi_{[0,1)^2}(\mathbf{x}), \qquad \mathbf{x} \in \mathbb{R}^2$$

and similar to [**Chu98**] define the box spline $M(\mathbf{x}|\mathcal{D}_m)$ inductively for $m = 3, ...n$:

$$M(\mathbf{x}|\mathcal{D}_m) := \int_{-\frac{1}{2}}^{\frac{1}{2}} M(\mathbf{x} - t\mathbf{e}^m|\mathcal{D}_{m-1})\, dt \qquad \mathbf{x} \in \mathbb{R}^2$$

For convenience of notation, write

$$
\begin{aligned}
M_{n_1 n_2 n_3 n_4} &:= M(\cdot|\mathcal{D}_n) \\
M_{n_1 n_2} &:= M_{n_1 n_2 00} \quad \text{if } n_3 = n_4 = 0 \\
M_{n_1 n_2 n_3} &:= M_{n_1 n_2 n_3 0} \quad \text{if } n_4 = 0
\end{aligned}
$$

where $\mathcal{D}_n$ is from (5.8 |p.94) or (5.9 |p.94).

As shown in [**Chu98**] the directional derivative of a box spline can be given in terms of a forward difference:

$$D_{\mathbf{e}^j} M(\cdot|\mathcal{D}_n) = \triangle_{\mathbf{e}^j} M\left(\cdot|\mathcal{D}_n \backslash \left\{\mathbf{e}^j\right\}\right) \qquad \text{for any } j \text{ such that } \left\langle \mathcal{D}_n \backslash \left\{\mathbf{e}^j\right\}\right\rangle = \mathbb{R}^2 \tag{5.11}$$

where $\mathcal{D}_n$ is given in (5.9 |p.94), $\mathbf{e}^j$ is given in (5.10 |p.95) and where

$$\triangle_{\mathbf{y}} f := f\left(\cdot + \frac{\mathbf{y}}{2}\right) - f\left(\cdot - \frac{\mathbf{y}}{2}\right)$$

Now let $\triangle^2$ be the 2-directional mesh with vertices in $\mathbb{Z}^2$ as given in Figure 4.1 on p. 57 and let $\triangle^3$ be the 3-directional mesh over $\mathbb{Z}^2$ as given in Figure 3.2 on p.27.

Define

$$n^* := \min\{n_1 + n_2 + n_3, n_1 + n_2 + n_4, n_1 + n_3 + n_4, n_2 + n_3 + n_4\} - 2$$

We have the following facts from [**CDV10**]:

- $M(\mathbf{x}|\mathcal{D}_n) \in C^{n^*}(\mathbb{R}^2)$
- The restriction of $M_{n_1 n_2}$ on each square of $\triangle^2$ is in $\pi^2_{n_1+n_2-2}$
- The restriction of $M_{n_1 n_2 n_3}$ on each triangle of $\triangle^3$ is in $\pi^2_{n_1+n_2+n_3-2}$
- The closure of the support of $M(\mathbf{x}|\mathcal{D}_n)$ is: $[\mathcal{D}_n] = \sum_{i=1}^{n} t_i \mathbf{e}^i \quad -\frac{1}{2} \leq t_i \leq \frac{1}{2}$

5.3.2. Partial Derivatives as Limits of Surrounding Vertices

With the background given above we can now proceed to develop a representation of partial derivative of the limiting surface as a *limit* of linear combinations of surrounding vertices. The proofs are provided in Appendix C.

Theorem 5.1. *Assume that the subdivision scheme is an approximating scheme and that the cascade algorithm given by $\Phi_m := Q_P\,\Phi_{m-1}$ converges in $C^1(\mathbb{R})$. Then for $\mathbf{k}_0 \in \mathbb{Z}^2$*

$$D_1 F(\mathbf{k}_0) = \lim_{m\to\infty} 2^m \left\{ \frac{1}{8} \begin{pmatrix} 3v^m_{2^m\mathbf{k}_0+(1,0)^T} - 3v^m_{2^m\mathbf{k}_0+(-1,0)^T} + v^m_{2^m\mathbf{k}_0+(1,1)^T} \\ -v^m_{2^m\mathbf{k}_0+(0,1)^T} + v^m_{2^m\mathbf{k}_0+(0,-1)^T} - v^m_{2^m\mathbf{k}_0+(-1,-1)^T} \end{pmatrix} \right\}$$

$$D_2 F(\mathbf{k}_0) = \lim_{m\to\infty} 2^m \left\{ \frac{1}{8} \begin{pmatrix} v^m_{2^m\mathbf{k}_0+(1,1)^T} - v^m_{2^m\mathbf{k}_0+(1,0)^T} + v^m_{2^m\mathbf{k}_0+(-1,0)^T} \\ -v^m_{2^m\mathbf{k}_0+(-1,-1)^T} + 3v^m_{2^m\mathbf{k}_0+(0,1)^T} - 3v^m_{2^m\mathbf{k}_0+(0,-1)^T} \end{pmatrix} \right\}$$

where $F(\cdot) := \sum_{\mathbf{k}\in\mathbb{Z}^2} \mathbf{v}^0_{\mathbf{k}} \Phi(\cdot - \mathbf{k})$ is the limiting surface for the subdivision scheme and Φ is from (2.5 |p.12).

Corollary 5.1. *Assume that the subdivision scheme is an approximating scheme and that the cascade algorithm given by $\Phi_m := Q_P\,\Phi_{m-1}$ converges* *in* $C^1(\mathbb{R})$. *Then for* $\mathbf{k}_0, \mathbf{i} \in \mathbb{Z}^2$, $n \in \mathbb{Z}_+$

$$D_1 F\left(\mathbf{k}_0 + \frac{\mathbf{i}}{2^n}\right) = 2^n \lim_{m\to\infty} 2^m \left\{ \frac{1}{8} \left(\begin{array}{c} 3v^{n+m}_{2^{n+m}\mathbf{k}_0+2^m\mathbf{i}+(1,0)^T} - 3v^{n+m}_{2^{n+m}\mathbf{k}_0+2^m\mathbf{i}+(-1,0)^T} \\ +v^{n+m}_{2^{n+m}\mathbf{k}_0+2^m\mathbf{i}+(1,1)^T} - v^{n+m}_{2^{n+m}\mathbf{k}_0+2^m\mathbf{i}+(0,1)^T} \\ +v^{n+m}_{2^{n+m}\mathbf{k}_0+2^m\mathbf{i}+(0,-1)^T} - v^{n+m}_{2^{n+m}\mathbf{k}_0+2^m\mathbf{i}+(-1,-1)^T} \end{array} \right) \right\}$$

$$D_2 F\left(\mathbf{k}_0 + \frac{\mathbf{i}}{2^n}\right) = 2^n \lim_{m\to\infty} 2^m \left\{ \frac{1}{8} \left(\begin{array}{c} v^{n+m}_{2^{n+m}\mathbf{k}_0+2^m\mathbf{i}+(1,1)^T} - v^{n+m}_{2^{n+m}\mathbf{k}_0+2^m\mathbf{i}+(1,0)^T} \\ +v^{n+m}_{2^{n+m}\mathbf{k}_0+2^m\mathbf{i}+(-1,0)^T} - v^{n+m}_{2^{n+m}\mathbf{k}_0+2^m\mathbf{i}+(-1,-1)^T} \\ +3v^{n+m}_{2^{n+m}\mathbf{k}_0+2^m\mathbf{i}+(0,1)^T} - 3v^{n+m}_{2^{n+m}\mathbf{k}_0+2^m\mathbf{i}+(0,-1)^T} \end{array} \right) \right\}$$

where $F(\cdot) := \sum_{\mathbf{k}\in\mathbb{Z}^2} \mathbf{v}^0_{\mathbf{k}} \Phi(\cdot - \mathbf{k})$ *is the limiting surface for the subdivision scheme and* Φ *is from (2.5 |p.12).*

Theorem 5.2. *Assume that the subdivision scheme is an approximating scheme and that the cascade algorithm given by* $\Phi_m := Q_P\,\Phi_{m-1}$ *converges in* $C^2(\mathbb{R})$. *Then for* $\mathbf{k}_0 \in \mathbb{Z}^2$

$$D_1^2 F(\mathbf{k}_0) = \lim_{m\to\infty} 2^{2m} \left\{ \frac{1}{6} \begin{pmatrix} -8v^m_{2^m\mathbf{k}_0+(0,0)^T} + 4v^m_{2^m\mathbf{k}_0+(1,0)^T} + 4v^m_{2^m\mathbf{k}_0+(-1,0)^T} \\ -2v^m_{2^m\mathbf{k}_0+(1,1)^T} + v^m_{2^m\mathbf{k}_0+(2,1)^T} + v^m_{2^m\mathbf{k}_0+(0,1)^T} \\ -2v^m_{2^m\mathbf{k}_0+(-1,-1)^T} + v^m_{2^m\mathbf{k}_0+(0,-1)^T} + v^m_{2^m\mathbf{k}_0+(-2,-1)^T} \end{pmatrix} \right\}$$

$$D_2 D_1 F(\mathbf{k}_0) = \lim_{m\to\infty} 2^{2m} \left\{ \frac{1}{2} \begin{pmatrix} 2v^m_{2^m\mathbf{k}_0+(0,0)^T} - v^m_{2^m\mathbf{k}_0+(1,0)^T} - v^m_{2^m\mathbf{k}_0+(-1,0)^T} \\ +v^m_{2^m\mathbf{k}_0+(1,1)^T} - v^m_{2^m\mathbf{k}_0+(0,1)^T} \\ +v^m_{2^m\mathbf{k}_0+(-1,-1)^T} - v^m_{2^m\mathbf{k}_0+(0,-1)^T} \end{pmatrix} \right\}$$

$$D_2^2 F(\mathbf{k}_0) = \lim_{m\to\infty} 2^{2m} \left\{ \frac{1}{6} \begin{pmatrix} -8v^m_{2^m\mathbf{k}_0+(0,0)^T} + 4v^m_{2^m\mathbf{k}_0+(0,1)^T} + 4v^m_{2^m\mathbf{k}_0+(0,-1)^T} \\ -2v^m_{2^m\mathbf{k}_0+(1,1)^T} + v^m_{2^m\mathbf{k}_0+(1,2)^T} + v^m_{2^m\mathbf{k}_0+(1,0)^T} \\ -2v^m_{2^m\mathbf{k}_0+(-1,-1)^T} + v^m_{2^m\mathbf{k}_0+(-1,0)^T} + v^m_{2^m\mathbf{k}_0+(-1,-2)^T} \end{pmatrix} \right\}$$

where $F(\cdot) := \sum_{\mathbf{k}\in\mathbb{Z}^2} \mathbf{v}^0_{\mathbf{k}} \Phi(\cdot - \mathbf{k})$ *is the limiting surface for the subdivision scheme and* Φ *is from (2.5 |p.12).*

Corollary 5.2. *Assume that the subdivision scheme is an approximating scheme and that the cascade algorithm given by $\Phi_m := Q_P \, \Phi_{m-1}$ converges in $C^2(\mathbb{R})$. Then for $\mathbf{k}_0, \mathbf{i} \in \mathbb{Z}^2$, $n \in \mathbb{Z}_+$*

$$D_1^2 F\left(\mathbf{k}_0 + \frac{\mathbf{i}}{2^n}\right) = 2^{2n} \lim_{m\to\infty} 2^{2m} \left\{ \frac{1}{6} \left(\begin{array}{c} -8v^{n+m}_{2^{n+m}\mathbf{k}_0+2^m\mathbf{i}+(0,0)^T} + 4v^{n+m}_{2^{n+m}\mathbf{k}_0+(1,0)^T} \\ +4v^{n+m}_{2^{n+m}\mathbf{k}_0+2^m\mathbf{i}+(-1,0)^T} - 2v^{n+m}_{2^{n+m}\mathbf{k}_0+2^m\mathbf{i}+(1,1)^T} \\ +v^{n+m}_{2^{n+m}\mathbf{k}_0+2^m\mathbf{i}+(2,1)^T} + v^{n+m}_{2^{n+m}\mathbf{k}_0+2^m\mathbf{i}+(0,1)^T} \\ -2v^{n+m}_{2^{n+m}\mathbf{k}_0+2^m\mathbf{i}+(-1,-1)^T} + v^{n+m}_{2^{n+m}\mathbf{k}_0+2^m\mathbf{i}+(0,-1)^T} \\ +v^{n+m}_{2^{n+m}\mathbf{k}_0+2^m\mathbf{i}+(-2,-1)^T} \end{array} \right) \right\}$$

$$D_2 D_1 F\left(\mathbf{k}_0 + \frac{\mathbf{i}}{2^n}\right) = 2^{2n} \lim_{m\to\infty} 2^{2m} \left\{ \frac{1}{2} \left(\begin{array}{c} 2v^{n+m}_{2^{n+m}\mathbf{k}_0+2^m\mathbf{i}+(0,0)^T} - v^{n+m}_{2^{n+m}\mathbf{k}_0+2^m\mathbf{i}+(1,0)^T} \\ -v^{n+m}_{2^{n+m}\mathbf{k}_0+2^m\mathbf{i}+(-1,0)^T} + v^{n+m}_{2^{n+m}\mathbf{k}_0+2^m\mathbf{i}+(1,1)^T} \\ -v^{n+m}_{2^{n+m}\mathbf{k}_0+2^m\mathbf{i}+(0,1)^T} + v^{n+m}_{2^{n+m}\mathbf{k}_0+2^m\mathbf{i}+(-1,-1)^T} \\ -v^{n+m}_{2^{n+m}\mathbf{k}_0+2^m\mathbf{i}+(0,-1)^T} \end{array} \right) \right\}$$

$$D_2^2 F\left(\mathbf{k}_0 + \frac{\mathbf{i}}{2^n}\right) = 2^{2n} \lim_{m\to\infty} 2^{2m} \left\{ \frac{1}{6} \left(\begin{array}{c} -8v^{n+m}_{2^{n+m}\mathbf{k}_0+2^m\mathbf{i}+(0,0)^T} + 4v^{n+m}_{2^{n+m}\mathbf{k}_0+2^m\mathbf{i}+(0,1)^T} \\ +4v^{n+m}_{2^{n+m}\mathbf{k}_0+2^m\mathbf{i}+(0,-1)^T} - 2v^{n+m}_{2^{n+m}\mathbf{k}_0+2^m\mathbf{i}+(1,1)^T} \\ +v^{n+m}_{2^{n+m}\mathbf{k}_0+2^m\mathbf{i}+(1,2)^T} + v^{n+m}_{2^{n+m}\mathbf{k}_0+2^m\mathbf{i}+(1,0)^T} \\ -2v^{n+m}_{2^{n+m}\mathbf{k}_0+2^m\mathbf{i}+(-1,-1)^T} + v^{n+m}_{2^{n+m}\mathbf{k}_0+2^m\mathbf{i}+(-1,0)^T} \\ +v^{n+m}_{2^{n+m}\mathbf{k}_0+2^m\mathbf{i}+(-1,-2)^T} \end{array} \right) \right\}$$

where $F(\cdot) := \sum_{\mathbf{k}\in\mathbb{Z}^2} \mathbf{v}^0_{\mathbf{k}} \Phi(\cdot - \mathbf{k})$ is the limiting surface for the subdivision scheme and Φ is from (2.5 |p.12).

Proof. Proof follows the same method as Corollary 5.1. □

5.3.3. Partial Derivatives as Linear Combination of Eigenvectors

We will now get a representation of the partial derivatives as linear combinations of left eigenvectors as we had done for the interpolating scheme.

5.3.3.1. Triangular Approximating Scheme. Our sum rule assumption (2.14 |p.15) provides us with specific left eigenvectors of our subdivision matrix for eigenvalues 1, $\frac{1}{2}$ and $\frac{1}{4}$ [see(2.23 |p.19),(2.25 |p.20), (5.4 |p.93)]. So for a 1-ring neighborhood around a regular vertex $\mathbf{v}^0_{\mathbf{k}_0}$ where $\mathbf{k}_0 \in \mathbb{Z}^2$ we have the following representation of this 3×14 ring of vectors:

$$\begin{bmatrix} v^0_{\mathbf{k}_0}, s^0_{\mathbf{k}_0}, v^0_{\mathbf{k}_0+(1,0)^T}, s^0_{\mathbf{k}_0+(1,0)^T}, v^0_{\mathbf{k}_0+(1,1)^T}, s^0_{\mathbf{k}_0+(1,1)^T}, \\ ..., v^0_{\mathbf{k}_0+(-1,-1)^T}, s^0_{\mathbf{k}_0+(-1,-1)^T}, v^0_{\mathbf{k}_0+(0,-1)^T}, s^0_{\mathbf{k}_0+(0,-1)^T} \end{bmatrix} = \alpha_0^{(0)}\mathbf{L}_0 + \alpha_1^{(0)}\mathbf{L}_1 + \alpha_2^{(0)}\mathbf{L}_2 + \sum_{i=3}^{13}\alpha_i^{(0)}\mathbf{L}_i$$

where we have the following 3×14 (possibly generalized) linearly independent left eigenvectors of a 14×14 subdivision matrix S:

$$\mathbf{L}_0 = [1,0,1,0,...,1,0] \qquad \text{for eigenvalue } 1$$

$$\mathbf{L}_1 = [0,0,1,0,1,0,0,0,...,-1,0,0,0] \qquad \text{for eigenvalue } \frac{1}{2}$$

$$\mathbf{L}_2 = [0,0,0,0,1,0,1,0,...,-1,0,-1,0] \qquad \text{for eigenvalue } \frac{1}{2}$$

$$\mathbf{L}_i = \text{left eigenvectors for eigenvalues } \gamma_i \text{ where } |\gamma_i| < \frac{1}{2}$$

Let J be the 14×2 matrix defined as

$$J := \begin{bmatrix} 0 & 0 & \frac{3}{8} & 0 & \frac{1}{8} & 0 & -\frac{1}{8} & 0 & -\frac{3}{8} & 0 & -\frac{1}{8} & 0 & \frac{1}{8} & 0 \\ 0 & 0 & -\frac{1}{8} & 0 & \frac{1}{8} & 0 & \frac{3}{8} & 0 & \frac{1}{8} & 0 & -\frac{1}{8} & 0 & -\frac{3}{8} & 0 \end{bmatrix}^T$$

By direct calculation:

$$\begin{aligned} \begin{bmatrix} v^0_{\mathbf{k}_0}, s^0_{\mathbf{k}_0}, v^0_{\mathbf{k}_0+(1,0)^T}, s^0_{\mathbf{k}_0+(1,0)^T}, \\ v^0_{\mathbf{k}_0+(1,1)^T}, s^0_{\mathbf{k}_0+(1,1)^T}, ..., v^0_{\mathbf{k}_0+(-1,-1)^T}, s^0_{\mathbf{k}_0+(-1,-1)^T}, \\ v^0_{\mathbf{k}_0+(0,-1)^T}, s^0_{\mathbf{k}_0+(0,-1)^T} \end{bmatrix} J &= \begin{bmatrix} \alpha_0^{(0)}\mathbf{L}_0 + \alpha_1^{(0)}\mathbf{L}_1 \\ +\alpha_2^{(0)}\mathbf{L}_2 + \sum_{i=3}^{13}\alpha_i^{(0)}\mathbf{L}_i \end{bmatrix} J \\ &= \alpha_0^{(0)}\mathbf{L}_0 J + \alpha_1^{(0)}\mathbf{L}_1 J + \alpha_2^{(0)}\mathbf{L}_2 J \\ &\quad + \sum_{i=3}^{13}\alpha_i^{(0)}\mathbf{L}_i J \\ &= \alpha_0^{(0)}[0,0] + \alpha_1^{(0)}[1,0] + \alpha_2^{(0)}[0,1] \\ &\quad + \sum_{i=3}^{13}\alpha_i^{(0)}\mathbf{L}_i J \end{aligned}$$

After m subdivisions we have:

$$\begin{aligned}
&\begin{bmatrix} v^m_{2^m\mathbf{k}_0}, s^m_{2^m\mathbf{k}_0}, v^m_{2^m\mathbf{k}_0+(1,0)^T}, s^m_{2^m\mathbf{k}_0+(1,0)^T}, \\ v^m_{2^m\mathbf{k}_0+(1,1)^T}, s^m_{2^m\mathbf{k}_0+(1,1)^T}, \ldots, \\ v^m_{2^m\mathbf{k}_0+(-1,-1)^T}, s^m_{2^m\mathbf{k}_0+(-1,-1)^T}, \\ v^m_{2^m\mathbf{k}_0+(0,-1)^T}, s^m_{2^m\mathbf{k}_0+(0,-1)^T} \end{bmatrix} J = \begin{bmatrix} \alpha_0^{(0)}\mathbf{L}_0 + 2^{-m}\alpha_1^{(0)}\mathbf{L}_1 \\ +2^{-m}\alpha_2^{(0)}\mathbf{L}_2 + \sum_{i=3}^{13}\gamma_i^m\alpha_i^{(0)}\mathbf{L}_i \end{bmatrix} J \\
&\qquad = \alpha_0^{(0)}\mathbf{L}_0 J + 2^{-m}\alpha_1^{(0)}\mathbf{L}_1 J + 2^{-m}\alpha_2^{(0)}\mathbf{L}_2 J \\
&\qquad\quad + \sum_{i=3}^{13}\gamma_i^m\alpha_i^{(0)}\mathbf{L}_i J \\
&\qquad = \alpha_0^{(0)}\,[0,0] + 2^{-m}\alpha_1^{(0)}\,[1,0] + 2^{-m}\alpha_2^{(0)}\,[0,1] \\
&\qquad\quad + \sum_{i=3}^{13}\gamma_i^m\alpha_i^{(0)}\mathbf{L}_i J
\end{aligned} \tag{5.12}$$

Now note that

$$\begin{bmatrix} v^m_{2^m\mathbf{k}_0}, s^m_{2^m\mathbf{k}_0}, v^m_{2^m\mathbf{k}_0+(1,0)^T}, s^m_{2^m\mathbf{k}_0+(1,0)^T}, \\ v^m_{2^m\mathbf{k}_0+(1,1)^T}, s^m_{2^m\mathbf{k}_0+(1,1)^T}, \ldots, \\ v^m_{2^m\mathbf{k}_0+(-1,-1)^T}, s^m_{2^m\mathbf{k}_0+(-1,-1)^T}, \\ v^m_{2^m\mathbf{k}_0+(0,-1)^T}, s^m_{2^m\mathbf{k}_0+(0,-1)^T} \end{bmatrix} J = \begin{bmatrix} \frac{3}{8}v^m_{2^m\mathbf{k}_0+(1,0)^T} + \frac{1}{8}v^m_{2^m\mathbf{k}_0+(1,1)^T} \\ -\frac{1}{8}v^m_{2^m\mathbf{k}_0+(0,1)^T} - \frac{3}{8}v^m_{2^m\mathbf{k}_0+(-1,0)^T} \\ -\frac{1}{8}v^m_{2^m\mathbf{k}_0+(-1,-1)^T} + \frac{1}{8}v^m_{2^m\mathbf{k}_0+(0,-1)^T} \\ \\ -\frac{1}{8}v^m_{2^m\mathbf{k}_0+(1,0)^T} + \frac{1}{8}v^m_{2^m\mathbf{k}_0+(1,1)^T} \\ +\frac{3}{8}v^m_{2^m\mathbf{k}_0+(0,1)^T} + \frac{1}{8}v^m_{2^m\mathbf{k}_0+(-1,0)^T} \\ -\frac{1}{8}v^m_{2^m\mathbf{k}_0+(-1,-1)^T} - \frac{3}{8}v^m_{2^m\mathbf{k}_0+(0,-1)^T} \end{bmatrix}^T$$

Hence taking the limit as the number of subdivisions goes to infinity:

$$\lim_{m\to\infty} 2^m \begin{bmatrix} v^m_{2^m\mathbf{k}_0}, s^m_{2^m\mathbf{k}_0}, \\ v^m_{2^m\mathbf{k}_0+(1,0)^T}, s^m_{2^m\mathbf{k}_0+(1,0)^T}, \\ v^m_{2^m\mathbf{k}_0+(1,1)^T}, s^m_{2^m\mathbf{k}_0+(1,1)^T}, \ldots, \\ v^m_{2^m\mathbf{k}_0+(-1,-1)^T}, s^m_{2^m\mathbf{k}_0+(-1,-1)^T}, \\ v^m_{2^m\mathbf{k}_0+(0,-1)^T}, s^m_{2^m\mathbf{k}_0+(0,-1)^T} \end{bmatrix} J = \lim_{m\to\infty} 2^m \begin{bmatrix} \frac{3}{8}v^m_{2^m\mathbf{k}_0+(1,0)^T} + \frac{1}{8}v^m_{2^m\mathbf{k}_0+(1,1)^T} \\ -\frac{1}{8}v^m_{2^m\mathbf{k}_0+(0,1)^T} - \frac{3}{8}v^m_{2^m\mathbf{k}_0+(-1,0)^T} \\ -\frac{1}{8}v^m_{2^m\mathbf{k}_0+(-1,-1)^T} + \frac{1}{8}v^m_{2^m\mathbf{k}_0+(0,-1)^T} \\ \\ -\frac{1}{8}v^m_{2^m\mathbf{k}_0+(1,0)^T} + \frac{1}{8}v^m_{2^m\mathbf{k}_0+(1,1)^T} \\ +\frac{3}{8}v^m_{2^m\mathbf{k}_0+(0,1)^T} + \frac{1}{8}v^m_{2^m\mathbf{k}_0+(-1,0)^T} \\ -\frac{1}{8}v^m_{2^m\mathbf{k}_0+(-1,-1)^T} - \frac{3}{8}v^m_{2^m\mathbf{k}_0+(0,-1)^T} \end{bmatrix}^T$$

$$\begin{aligned} &= \alpha_1^{(0)}\,[1,0] + \alpha_2^{(0)}\,[0,1] \\ &= D_1F\,(\mathbf{k}_0)\,[1,0] + D_2F\,(\mathbf{k}_0)\,[0,1] \\ &= F_s\,(\mathbf{k}_0)\,[1,0] + F_t\,(\mathbf{k}_0)\,[0,1] \end{aligned}$$

by Theorem 5.1 on p.96 and by (5.12).

And so by linear independence:

$$F_s\,(\mathbf{k}_0) = \alpha_1^{(0)}$$
$$F_t\,(\mathbf{k}_0) = \alpha_2^{(0)}$$

For the second partial derivatives we will need to go to a 2-ring neighborhood around regular vertex $\mathbf{v}^0_{\mathbf{k}_0}$ where $\mathbf{k}_0 \in \mathbb{Z}^2$ and where this 3×38 ring of vectors $\mathbf{U}^m_{\mathbf{k}_0}$ is defined the same way as in the *interpolatory* triangular scheme (3.7 |p.26).

$\mathbf{U}^0_{\mathbf{k}_0}$ can be written as a linear combination of left eigenvectors of the subdivision matrix:

$$\text{(5.13)}\quad \mathbf{U}^0_{\mathbf{k}_0} = \alpha_0^{(0)}\mathbf{L}_0 + \alpha_1^{(0)}\mathbf{L}_1 + \alpha_2^{(0)}\mathbf{L}_2 + \alpha_3^{(0)}\mathbf{L}_3 + \alpha_4^{(0)}\mathbf{L}_4 + \alpha_5^{(0)}\mathbf{L}_5 + \sum_{j=6}^{37} \alpha_j^{(0)}\mathbf{L}_j$$

From (5.4 |p.93) we see that L_j for $j = 0, 1, , , , .5$ are the same as the L_j for $j = 0, 1, , , , .5$ (3.12 |p.28) in the interpolatory triangular scheme.

Let J^* be the 38×3 matrix defined as

$$J^* := \begin{bmatrix} J_1 \\ J_2 \\ J_3 \end{bmatrix}$$

where we have

$$14 \times 3 \text{ matrix } J_1 := \begin{bmatrix} -\frac{4}{3} & 0 & \frac{2}{3} & 0 & -\frac{1}{3} & 0 & \frac{1}{6} & 0 & \frac{2}{3} & 0 & -\frac{1}{3} & 0 & \frac{1}{6} & 0 \\ -\frac{8}{3} & 0 & -\frac{2}{3} & 0 & \frac{4}{3} & 0 & -\frac{2}{3} & 0 & -\frac{2}{3} & 0 & \frac{4}{3} & 0 & -\frac{2}{3} & 0 \\ -\frac{8}{3} & 0 & -\frac{2}{3} & 0 & \frac{1}{3} & 0 & \frac{5}{6} & 0 & -\frac{2}{3} & 0 & \frac{1}{3} & 0 & \frac{5}{6} & 0 \end{bmatrix}^T$$

$$12 \times 3 \text{ zero matrix } := J_2$$

$$12 \times 3 \text{ matrix } J_3 := \begin{bmatrix} \frac{1}{6} & 0 & 0 & 0 & 0 & 0 & \frac{1}{6} & 0 & 0 & 0 & 0 & 0 \\ \frac{2}{3} & 0 & \frac{2}{3} & 0 & 0 & 0 & \frac{2}{3} & 0 & \frac{2}{3} & 0 & 0 & 0 \\ \frac{1}{6} & 0 & \frac{2}{3} & 0 & 0 & 0 & \frac{1}{6} & 0 & \frac{2}{3} & 0 & 0 & 0 \end{bmatrix}^T$$

By direct calculation we obtain the following representation of the 3×3 matrix $\mathbf{U}^0_{\mathbf{k}_0} J^*$:

$$\begin{aligned} \mathbf{U}^0_{\mathbf{k}_0} J^* &= \left\{ \alpha_0^{(0)} \mathbf{L}_0 + \alpha_1^{(0)} \mathbf{L}_1 + \alpha_2^{(0)} \mathbf{L}_2 + \alpha_3^{(0)} \mathbf{L}_3 + \alpha_4^{(0)} \mathbf{L}_4 + \alpha_5^{(0)} \mathbf{L}_5 + \sum_{j=6}^{37} \alpha_j^{(0)} \mathbf{L}_j \right\} J^* \\ &= 2\alpha_3^{(0)} \begin{bmatrix} 1 & 4 & 1 \end{bmatrix} + 2\alpha_4^{(0)} \begin{bmatrix} 0 & 4 & 1 \end{bmatrix} + 2\alpha_5^{(0)} \begin{bmatrix} 0 & 4 & 4 \end{bmatrix} + \left\{ \sum_{j=6}^{37} \alpha_j^{(0)} \mathbf{L}_j \right\} J^* \end{aligned}$$

After m subdivisions we have:

$$\begin{aligned} \mathbf{U}^m_{\mathbf{k}_0} J^* &= \left\{ \begin{array}{c} \alpha_0^{(0)} \mathbf{L}_0 + 2^{-m}\, \alpha_1^{(0)} \mathbf{L}_1 + 2^{-m}\, \alpha_2^{(0)} \mathbf{L}_2 \\ +2^{-2m}\, \alpha_3^{(0)} \mathbf{L}_3 + 2^{-2m}\, \alpha_4^{(0)} \mathbf{L}_4 + 2^{-2m}\, \alpha_5^{(0)} \mathbf{L}_5 \\ + \sum_{j=6}^{37} \gamma^m\, \alpha_j^{(0)} \mathbf{L}_j \end{array} \right\} J^* \\ &= 2 \cdot 2^{-2m}\, \alpha_3^{(0)} \begin{bmatrix} 1 & 4 & 1 \end{bmatrix} + 2 \cdot 2^{-2m}\, \alpha_4^{(0)} \begin{bmatrix} 0 & 4 & 1 \end{bmatrix} + 2 \cdot 2^{-2m}\, \alpha_5^{(0)} \begin{bmatrix} 0 & 4 & 4 \end{bmatrix} \\ &\quad + \left\{ \sum_{j=6}^{37} \gamma^m\, \alpha_j^{(0)} \mathbf{L}_j \right\} J^* \end{aligned}$$

Hence

$$\lim_{m \to \infty} 2^{2m} \mathbf{U}^m_{\mathbf{k}_0} J^* = 2\alpha_3^{(0)} \begin{bmatrix} 1 & 4 & 1 \end{bmatrix} + 2\alpha_4^{(0)} \begin{bmatrix} 0 & 4 & 2 \end{bmatrix} + 2\alpha_5^{(0)} \begin{bmatrix} 0 & 4 & 4 \end{bmatrix}$$

Furthermore, using Theorem 5.2 on p. 98, direct calculations show that

$$\lim_{m \to \infty} 2^{2m} \mathbf{U}^m_{\mathbf{k}_0} J^* = D_1^2 F(\mathbf{k}_0) \begin{bmatrix} 1 & 4 & 1 \end{bmatrix} + 2 D_2 D_1 F(\mathbf{k}_0) \begin{bmatrix} 0 & 4 & 2 \end{bmatrix} + D_2^2 F(\mathbf{k}_0) \begin{bmatrix} 0 & 4 & 4 \end{bmatrix}$$

Thus by linear independence

$$D_1^2 F(\mathbf{k}_0) = 2\alpha_3^{(0)}$$
$$D_2 D_1 F(\mathbf{k}_0) = \alpha_4^{(0)}$$
$$D_2^2 F(\mathbf{k}_0) = 2\alpha_5^{(0)}$$

Theorem 5.3. *Assume that the subdivision scheme is an approximating triangular scheme and that the cascade algorithm given by $\Phi_m := Q_P\,\Phi_{m-1}$ converges in $C^1(\mathbb{R})$. Then for $\mathbf{k}_0 \in \mathbb{Z}^2$*

$$D_1 F(\mathbf{k}_0) = \alpha_1^{(0)}$$
$$D_2 F(\mathbf{k}_0) = \alpha_2^{(0)}$$

where $F(\cdot) := \sum_{\mathbf{k}\in\mathbb{Z}^2} \mathbf{v}_{\mathbf{k}}^0 \Phi(\cdot - \mathbf{k})$ is the limiting surface for the subdivision scheme, Φ is from (2.5 |p.12) and α_1, α_2 are from (5.12 |p.100). If in addition the cascade algorithm converges in $C^2(\mathbb{R})$

$$D_1^2 F(\mathbf{k}_0) = 2\alpha_3^{(0)}$$
$$D_2 D_1 F(\mathbf{k}_0) = \alpha_4^{(0)}$$
$$D_2^2 F(\mathbf{k}_0) = 2\alpha_5^{(0)}$$

where $\alpha_3^{(0)}$, $\alpha_{4,}^{(0)}$ $\alpha_5^{(0)}$ are from (5.13 |p.102).

Corollary 5.3. *Assume that the subdivision scheme is an approximating triangular scheme and that the cascade algorithm given by $\Phi_m := Q_P\,\Phi_{m-1}$ converges in $C^1(\mathbb{R})$. Then for $\mathbf{k}_0, \mathbf{i} \in \mathbb{Z}^2$, $n \in \mathbb{Z}_+$*

$$D_1 F\left(\mathbf{k}_0 + \frac{\mathbf{i}}{2^n}\right) = 2^n \alpha_1^{(n)}$$
$$D_2 F\left(\mathbf{k}_0 + \frac{\mathbf{i}}{2^n}\right) = 2^n \alpha_2^{(n)}$$

where $F(\cdot) := \sum_{\mathbf{k}\in\mathbb{Z}^2} \mathbf{v}_{\mathbf{k}}^0 \Phi(\cdot - \mathbf{k})$ is the limiting surface for the subdivision scheme, Φ is from (2.5 |p.12).and $\alpha_1^{(n)}$, $\alpha_2^{(n)}$ are from (3.18 |p.30). If in *addition the cascade algorithm converges in* $C^2(\mathbb{R})$

$$D_1^2 F\left(\mathbf{k}_0 + \frac{\mathbf{i}}{2^n}\right) = 2^{2n+1}\alpha_3^{(n)}$$
$$D_2 D_1 F\left(\mathbf{k}_0 + \frac{\mathbf{i}}{2^n}\right) = 2^{2n}\alpha_4^{(n)}$$
$$D_2^2 F\left(\mathbf{k}_0 + \frac{\mathbf{i}}{2^n}\right) = 2^{2n+1}\alpha_5^{(n)}$$

where $\alpha_3^{(n)}$, $\alpha_{4,}^{(n)}$ $\alpha_5^{(n)}$ *are from (3.18 |p.30).*

5.3.3.2. Quadrilateral Approximating Scheme. Our sum rule assumption (2.14 |p.15) provides us with specific left eigenvectors of our subdivision matrix for eigenvalues 1, $\frac{1}{2}$ and $\frac{1}{4}$ [see(2.23 |p.19),(2.25 |p.20), (5.6 |p.93)]. So for a 1-ring neighborhood around a regular vertex $\mathbf{v}_{\mathbf{k}_0}^0$ where $\mathbf{k}_0 \in \mathbb{Z}^2$ we have the following representation of this 3×18 ring of vectors:

$$\begin{bmatrix} v_{\mathbf{k}_0}^0, s_{\mathbf{k}_0}^0, v_{\mathbf{k}_0+(1,0)^T}^0, s_{\mathbf{k}_0+(1,0)^T}^0, v_{\mathbf{k}_0+(0,1)^T}^0, s_{\mathbf{k}_0+(0,1)^T}^0, \\ v_{\mathbf{k}_0+(-1,0)^T}^0, s_{\mathbf{k}_0+(-1,0)^T}^0, v_{\mathbf{k}_0+(0,-1)^T}^0, s_{\mathbf{k}_0+(0,-1)^T}^0, \\ v_{\mathbf{k}_0+(1,1)^T}^0, s_{\mathbf{k}_0+(1,1)^T}^0, v_{\mathbf{k}_0+(-1,1)^T}^0, s_{\mathbf{k}_0+(-1,1)^T}^0, \\ v_{\mathbf{k}_0+(-1,-1)^T}^0, s_{\mathbf{k}_0+(-1,-1)^T}^0, v_{\mathbf{k}_0+(1,-1)^T}^0, s_{\mathbf{k}_0+(1,-1)^T}^0 \end{bmatrix} = \alpha_0^{(0)}\mathbf{L}_0 + \alpha_1^{(0)}\mathbf{L}_1 + \alpha_2^{(0)}\mathbf{L}_2 + \sum_{i=3}^{17}\alpha_i^{(0)}\mathbf{L}_i$$

where we have the following 3×18 (possibly generalized) linearly independent left eigenvectors of a 18×18 subdivision matrix S

$$\mathbf{L}_0 = [1, 0, 1, 0, ..., 1, 0] \qquad \text{for eigenvalue } 1$$
$$\mathbf{L}_1 = [0, 0, 1, 0, 0, 0, -1, 0, ..., -1, 0, 1, 0] \qquad \text{for eigenvalue } \frac{1}{2}$$
$$\mathbf{L}_2 = [0, 0, 0, 0, 1, 0, 0, 0, ..., -1, 0, -1, 0] \qquad \text{for eigenvalue } \frac{1}{2}$$
$$\mathbf{L}_i = \text{left eigenvectors for eigenvalues } \gamma_i \text{ where } |\gamma_i| < \frac{1}{2}$$

Let J be the 18×2 matrix defined as

$$J := \begin{bmatrix} 0 & 0 & \frac{3}{8} & 0 & -\frac{1}{8} & 0 & -\frac{3}{8} & 0 & \frac{1}{8} & 0 & \frac{1}{8} & 0 & 0 & 0 & -\frac{1}{8} & 0 & 0 & 0 \\ 0 & 0 & -\frac{1}{8} & 0 & \frac{3}{8} & 0 & \frac{1}{8} & 0 & -\frac{3}{8} & 0 & \frac{1}{8} & 0 & 0 & 0 & -\frac{1}{8} & 0 & 0 & 0 \end{bmatrix}^T$$

By direct calculation:

$$\begin{bmatrix} v^0_{\mathbf{k}_0}, s^0_{\mathbf{k}_0}, v^0_{\mathbf{k}_0+(1,0)^T}, s^0_{\mathbf{k}_0+(1,0)^T}, \\ v^0_{\mathbf{k}_0+(0,1)^T}, s^0_{\mathbf{k}_0+(0,1)^T}, ..., v^0_{\mathbf{k}_0+(-1,-1)^T}, s^0_{\mathbf{k}_0+(-1,-1)^T}, \\ v^0_{\mathbf{k}_0+(1,-1)^T}, s^0_{\mathbf{k}_0+(1,-1)^T} \end{bmatrix} J = \begin{bmatrix} \alpha_0^{(0)}\mathbf{L}_0 + \alpha_1^{(0)}\mathbf{L}_1 \\ +\alpha_2^{(0)}\mathbf{L}_2 + \sum_{i=3}^{17}\alpha_i^{(0)}\mathbf{L}_i \end{bmatrix} J$$
$$= \alpha_0^{(0)}\mathbf{L}_0 J + \alpha_1^{(0)}\mathbf{L}_1 J + \alpha_2^{(0)}\mathbf{L}_2 J + \sum_{i=3}^{17}\alpha_i^{(0)}\mathbf{L}_i J$$
$$= \alpha_0^{(0)}[0,0] + \alpha_1^{(0)}[1,0] + \alpha_2^{(0)}[0,1] + \sum_{i=3}^{17}\alpha_i^{(0)}\mathbf{L}_i J$$

After m subdivisions we have:

$$\begin{bmatrix} v^m_{2^m\mathbf{k}_0}, s^m_{2^m\mathbf{k}_0}, v^m_{2^m\mathbf{k}_0+(1,0)^T}, s^m_{2^m\mathbf{k}_0+(1,0)^T}, \\ v^m_{2^m\mathbf{k}_0+(0,1)^T}, s^m_{2^m\mathbf{k}_0+(0,1)^T}, ..., \\ v^m_{2^m\mathbf{k}_0+(-1,-1)^T}, s^m_{2^m\mathbf{k}_0+(-1,-1)^T}, \\ v^m_{2^m\mathbf{k}_0+(1,-1)^T}, s^m_{2^m\mathbf{k}_0+(1,-1)^T} \end{bmatrix} J = \begin{bmatrix} \alpha_0^{(0)}\mathbf{L}_0 + 2^{-m}\alpha_1^{(0)}\mathbf{L}_1 \\ +2^{-m}\alpha_2^{(0)}\mathbf{L}_2 + \sum_{i=3}^{17}\gamma_i^m\alpha_i^{(0)}\mathbf{L}_i \end{bmatrix} J$$
$$= \alpha_0^{(0)}\mathbf{L}_0 J + 2^{-m}\alpha_1^{(0)}\mathbf{L}_1 J + 2^{-m}\alpha_2^{(0)}\mathbf{L}_2 J + \sum_{i=3}^{17}\gamma_i^m\alpha_i^{(0)}\mathbf{L}_i J$$
$$= \alpha_0^{(0)}[0,0] + 2^{-m}\alpha_1^{(0)}[1,0] + 2^{-m}\alpha_2^{(0)}[0,1] + \sum_{i=3}^{17}\gamma_i^m\alpha_i^{(0)}\mathbf{L}_i J \tag{5.14}$$

Now note that

$$\begin{bmatrix} v^m_{2^m\mathbf{k}_0}, s^m_{2^m\mathbf{k}_0}, \\ v^m_{2^m\mathbf{k}_0+(1,0)^T}, s^m_{2^m\mathbf{k}_0+(1,0)^T}, \\ v^m_{2^m\mathbf{k}_0+(0,1)^T}, s^m_{2^m\mathbf{k}_0+(0,1)^T}, ..., \\ v^m_{2^m\mathbf{k}_0+(-1,-1)^T}, s^m_{2^m\mathbf{k}_0+(-1,-1)^T}, \\ v^m_{2^m\mathbf{k}_0+(1,-1)^T}, s^m_{2^m\mathbf{k}_0+(1,-1)^T} \end{bmatrix} J = \begin{bmatrix} \frac{3}{8}v^m_{2^m\mathbf{k}_0+(1,0)^T} + \frac{1}{8}v^m_{2^m\mathbf{k}_0+(1,1)^T} - \frac{1}{8}v^m_{2^m\mathbf{k}_0+(0,1)^T} \\ -\frac{3}{8}v^m_{2^m\mathbf{k}_0+(-1,0)^T} - \frac{1}{8}v^m_{2^m\mathbf{k}_0+(-1,-1)^T} + \frac{1}{8}v^m_{2^m\mathbf{k}_0+(0,-1)^T} \\ \\ -\frac{1}{8}v^m_{2^m\mathbf{k}_0+(1,0)^T} + \frac{1}{8}v^m_{2^m\mathbf{k}_0+(1,1)^T} + \frac{3}{8}v^m_{2^m\mathbf{k}_0+(0,1)^T} \\ +\frac{1}{8}v^m_{2^m\mathbf{k}_0+(-1,0)^T} - \frac{1}{8}v^m_{2^m\mathbf{k}_0+(-1,-1)^T} - \frac{3}{8}v^m_{2^m\mathbf{k}_0+(0,-1)^T} \end{bmatrix}^T$$

Hence taking the limit as the number of subdivisions goes to infinity:

$$\lim_{m\to\infty} 2^m \begin{bmatrix} v^m_{2^m\mathbf{k}_0}, s^m_{2^m\mathbf{k}_0}, \\ v^m_{2^m\mathbf{k}_0+(1,0)^T}, s^m_{2^m\mathbf{k}_0+(1,0)^T}, \\ v^m_{2^m\mathbf{k}_0+(0,1)^T}, s^m_{2^m\mathbf{k}_0+(0,1)^T},..., \\ v^m_{2^m\mathbf{k}_0+(-1,-1)^T}, s^m_{2^m\mathbf{k}_0+(-1,-1)^T}, \\ v^m_{2^m\mathbf{k}_0+(1,-1)^T}, s^m_{2^m\mathbf{k}_0+(1,-1)^T} \end{bmatrix} J = \lim_{m\to\infty} 2^m \begin{bmatrix} \frac{3}{8}v^m_{2^m\mathbf{k}_0+(1,0)^T} + \frac{1}{8}v^m_{2^m\mathbf{k}_0+(1,1)^T} \\ -\frac{1}{8}v^m_{2^m\mathbf{k}_0+(0,1)^T} - \frac{3}{8}v^m_{2^m\mathbf{k}_0+(-1,0)^T} \\ -\frac{1}{8}v^m_{2^m\mathbf{k}_0+(-1,-1)^T} + \frac{1}{8}v^m_{2^m\mathbf{k}_0+(0,-1)^T} \\ \\ -\frac{1}{8}v^m_{2^m\mathbf{k}_0+(1,0)^T} + \frac{1}{8}v^m_{2^m\mathbf{k}_0+(1,1)^T} \\ +\frac{3}{8}v^m_{2^m\mathbf{k}_0+(0,1)^T} + \frac{1}{8}v^m_{2^m\mathbf{k}_0+(-1,0)^T} \\ -\frac{1}{8}v^m_{2^m\mathbf{k}_0+(-1,-1)^T} - \frac{3}{8}v^m_{2^m\mathbf{k}_0+(0,-1)^T} \end{bmatrix}^T$$

$$= \alpha_1^{(0)}[1,0] + \alpha_2^{(0)}[0,1]$$
$$= D_1F(\mathbf{k}_0)[1,0] + D_2F(\mathbf{k}_0)[0,1]$$
$$= F_s(\mathbf{k}_0)[1,0] + F_t(\mathbf{k}_0)[0,1]$$

by Theorem 5.1 on p.96 and by (5.14).

And so by linear independence

$$F_s(\mathbf{k}_0) = \alpha_1^{(0)}$$
$$F_t(\mathbf{k}_0) = \alpha_2^{(0)}$$

For the second partial derivatives we will need to go to a 2-ring neighborhood around regular vertex $\mathbf{v}^0_{\mathbf{k}_0}$ where $\mathbf{k}_0 \in \mathbb{Z}^2$ and where this 3×50 ring of vectors $\mathbf{U}^m_{\mathbf{k}_0}$ is defined the same way as in the *interpolatory* quadrilateral scheme (4.4 |p.58).

$\mathbf{U}^0_{\mathbf{k}_0}$ can be written as a linear combination of left eigenvectors of the subdivision matrix:

$$\text{(5.15)}\quad \mathbf{U}^0_{\mathbf{k}_0} = \alpha_0^{(0)}\mathbf{L}_0 + \alpha_1^{(0)}\mathbf{L}_1 + \alpha_2^{(0)}\mathbf{L}_2 + \alpha_3^{(0)}\mathbf{L}_3 + \alpha_4^{(0)}\mathbf{L}_4 + \alpha_5^{(0)}\mathbf{L}_5 + \sum_{j=6}^{49} \alpha_j^{(0)}\mathbf{L}_j$$

From (5.6 |p.93) we see that L_j for $j = 0, 1, , , , .5$ are the same as the L_j for $j = 0, 1, , , , .5$ (4.7 |p.60) in the interpolatory quadrilateral scheme.

Let J^* be defined the 50×3 matrix defined as

$$J^* := \begin{bmatrix} J_1 \\ J_2 \\ J_3 \\ J_4 \\ J_5 \end{bmatrix}$$

where we have

$$10 \times 3 \text{ matrix } J_1 := \begin{bmatrix} -\frac{4}{3} & 0 & \frac{2}{3} & 0 & \frac{1}{6} & 0 & \frac{2}{3} & 0 & \frac{1}{6} & 0 \\ -\frac{4}{3} & 0 & \frac{1}{6} & 0 & \frac{2}{3} & 0 & \frac{1}{6} & 0 & \frac{2}{3} & 0 \\ -\frac{2}{3} & 0 & -\frac{1}{6} & 0 & -\frac{1}{6} & 0 & -\frac{1}{6} & 0 & -\frac{1}{6} & 0 \end{bmatrix}^T$$

$$10 \times 3 \text{ matrix } J_2 := \begin{bmatrix} -\frac{1}{3} & 0 & 0 & 0 & -\frac{1}{3} & 0 & 0 & 0 & 0 & 0 \\ -\frac{1}{3} & 0 & 0 & 0 & -\frac{1}{3} & 0 & 0 & 0 & 0 & 0 \\ \frac{1}{3} & 0 & 0 & 0 & \frac{1}{3} & 0 & 0 & 0 & 0 & 0 \end{bmatrix}^T$$

$$10 \times 3 \text{ matrix } J_3 := \begin{bmatrix} 0 & 0 & 0 & 0 & 0 & 0 & \frac{1}{6} & 0 & 0 & 0 \\ 0 & 0 & 0 & 0 & 0 & 0 & 0 & 0 & 0 & 0 \\ 0 & 0 & 0 & 0 & 0 & 0 & \frac{1}{6} & 0 & 0 & 0 \end{bmatrix}^T$$

$$10 \times 3 \text{ matrix } J_4 := \begin{bmatrix} \frac{1}{6} & 0 & 0 & 0 & 0 & 0 & 0 & 0 & 0 & 0 \\ 0 & 0 & 0 & 0 & 0 & 0 & 0 & 0 & 0 & 0 \\ \frac{1}{6} & 0 & 0 & 0 & 0 & 0 & 0 & 0 & 0 & 0 \end{bmatrix}^T$$

$$10 \times 3 \text{ matrix } J_5 := \begin{bmatrix} 0 & 0 & 0 & 0 & 0 & 0 & 0 & 0 & 0 & 0 \\ 0 & 0 & \frac{1}{6} & 0 & 0 & 0 & \frac{1}{6} & 0 & 0 & 0 \\ 0 & 0 & \frac{1}{6} & 0 & 0 & 0 & \frac{1}{6} & 0 & 0 & 0 \end{bmatrix}^T$$

By direct calculation we obtain the following representation of the 3×3 matrix $\mathbf{U}^0_{\mathbf{k}_0} J^*$:

$$\begin{aligned} \mathbf{U}^0_{\mathbf{k}_0} J^* &= \left\{ \alpha_0^{(0)} \mathbf{L}_0 + \alpha_1^{(0)} \mathbf{L}_1 + \alpha_2^{(0)} \mathbf{L}_2 + \alpha_3^{(0)} \mathbf{L}_3 + \alpha_4^{(0)} \mathbf{L}_4 + \alpha_5^{(0)} \mathbf{L}_5 + \sum_{j=6}^{49} \alpha_j^{(0)} \mathbf{L}_j \right\} J^* \\ &= 2\alpha_3^{(0)} \begin{bmatrix} 1 & 0 & 1 \end{bmatrix} + 2\alpha_4^{(0)} \begin{bmatrix} 0 & 0 & 2 \end{bmatrix} + 2\alpha_5^{(0)} \begin{bmatrix} 0 & 1 & 1 \end{bmatrix} + \left\{ \sum_{j=6}^{49} \alpha_j^{(0)} \mathbf{L}_j \right\} J^* \end{aligned}$$

After m subdivisions we have:

$$\mathbf{U}_{\mathbf{k}_0}^{m} J^* = \left\{ \begin{array}{c} \alpha_0^{(0)}\mathbf{L}_0 + 2^{-m}\ \alpha_1^{(0)}\mathbf{L}_1 + 2^{-m}\ \alpha_2^{(0)}\mathbf{L}_2 \\ +2^{-2m}\ \alpha_3^{(0)}\mathbf{L}_3 + 2^{-2m}\ \alpha_4^{(0)}\mathbf{L}_4 + 2^{-2m}\ \alpha_5^{(0)}\mathbf{L}_5 \\ +\sum_{j=6}^{49} \gamma^m\ \alpha_j^{(0)}\mathbf{L}_j \end{array} \right\} J^*$$

$$= 2 \cdot 2^{-2m}\ \alpha_3^{(0)} \begin{bmatrix} 1 & 0 & 1 \end{bmatrix} + 2 \cdot 2^{-2m}\ \alpha_4^{(0)} \begin{bmatrix} 0 & 0 & 2 \end{bmatrix} + 2 \cdot 2^{-2m}\ \alpha_5^{(0)} \begin{bmatrix} 0 & 1 & 1 \end{bmatrix}$$

$$+ \left\{ \sum_{j=6}^{49} \gamma^m\ \alpha_j^{(0)}\mathbf{L}_j \right\} J^*$$

Hence

$$\lim_{m\to\infty} 2^{2m}\mathbf{U}_{\mathbf{k}_0}^{m} J^* = 2\alpha_3^{(0)} \begin{bmatrix} 1 & 0 & 1 \end{bmatrix} + 2\alpha_4^{(0)} \begin{bmatrix} 0 & 0 & 2 \end{bmatrix} + 2\alpha_5^{(0)} \begin{bmatrix} 0 & 1 & 1 \end{bmatrix}$$

Furthermore, using Theorem 5.2 on p. 98, direct calculations show that

$$\lim_{m\to\infty} 2^{2m}\mathbf{U}_{\mathbf{k}_0}^{m} J^* = D_1^2 F\left(\mathbf{k}_0\right) \begin{bmatrix} 1 & 0 & 1 \end{bmatrix} + 2 D_2 D_1 F\left(\mathbf{k}_0\right) \begin{bmatrix} 0 & 0 & 2 \end{bmatrix} + D_2^2 F\left(\mathbf{k}_0\right) \begin{bmatrix} 0 & 1 & 1 \end{bmatrix}$$

Thus by linear independence

$$\begin{aligned} D_1^2 F\left(\mathbf{k}_0\right) &= 2\alpha_3^{(0)} \\ D_2 D_1 F\left(\mathbf{k}_0\right) &= \alpha_4^{(0)} \\ D_2^2 F\left(\mathbf{k}_0\right) &= 2\alpha_5^{(0)} \end{aligned}$$

Theorem 5.4. *Assume that the subdivision scheme is an approximating quadrilateral scheme and that the cascade algorithm given by $\Phi_m := Q_P\, \Phi_{m-1}$ converges in $C^1(\mathbb{R})$. Then for $\mathbf{k}_0 \in \mathbb{Z}^2$*

$$\begin{aligned} D_1 F\left(\mathbf{k}_0\right) &= \alpha_1^{(0)} \\ D_2 F\left(\mathbf{k}_0\right) &= \alpha_2^{(0)} \end{aligned}$$

where $F(\cdot) := \sum_{\mathbf{k}\in\mathbb{Z}^2} \mathbf{v}_{\mathbf{k}}^0 \Phi(\cdot - \mathbf{k})$ is the limiting surface for the subdivision scheme, Φ is from (2.5 |p.12) and α_1, α_2 are from (5.14 |p.105). If in *addition the cascade algorithm converges in* $C^2(\mathbb{R})$

$$D_1^2 F(\mathbf{k}_0) = 2\alpha_3^{(0)}$$
$$D_2 D_1 F(\mathbf{k}_0) = \alpha_4^{(0)}$$
$$D_2^2 F(\mathbf{k}_0) = 2\alpha_5^{(0)}$$

where $\alpha_3^{(0)}$, $\alpha_{4,}^{(0)}$ $\alpha_5^{(0)}$ *are from (5.15 |p.107).*

Corollary 5.4. *Assume that the subdivision scheme is an approximating quadrilateral scheme and that the cascade algorithm given by* $\Phi_m := Q_P\,\Phi_{m-1}$ *converges in* $C^1(\mathbb{R})$. *Then for* $\mathbf{k}_0, \mathbf{i} \in \mathbb{Z}^2$, $n \in \mathbb{Z}_+$

$$D_1 F\left(\mathbf{k}_0 + \frac{\mathbf{i}}{2^n}\right) = 2^n \alpha_1^{(n)}$$
$$D_2 F\left(\mathbf{k}_0 + \frac{\mathbf{i}}{2^n}\right) = 2^n \alpha_2^{(n)}$$

where $F(\cdot) := \sum_{\mathbf{k}\in\mathbb{Z}^2} \mathbf{v}_{\mathbf{k}}^0 \Phi(\cdot - \mathbf{k})$ *is the limiting surface for the subdivision scheme,* Φ *is from (2.5 |p.12).and* $\alpha_1^{(n)}$, $\alpha_2^{(n)}$ *are from (4.11 |p.62). If in addition the cascade algorithm converges in* $C^2(\mathbb{R})$

$$D_1^2 F\left(\mathbf{k}_0 + \frac{\mathbf{i}}{2^n}\right) = 2^{2n+1} \alpha_3^{(n)}$$
$$D_2 D_1 F\left(\mathbf{k}_0 + \frac{\mathbf{i}}{2^n}\right) = 2^{2n} \alpha_4^{(n)}$$
$$D_2^2 F\left(\mathbf{k}_0 + \frac{\mathbf{i}}{2^n}\right) = 2^{2n+1} \alpha_5^{(n)}$$

where $\alpha_3^{(n)}$, $\alpha_{4,}^{(n)}$ $\alpha_5^{(n)}$ *are from (4.11 |p.62).*

5.4. Partial Derivatives as Linear Combination of Initial Control Points

As with the interpolatory cases we will now derive right eigenvectors for $\frac{1}{2}$ and $\frac{1}{4}$ of our subdivision matrix that are orthonormal to their corresponding left eigenvectors. Again this is done using direct calculations with a computer algebra system in the same manner as subsections 3.6.1 and 4.5.1.

5.4.1. Triangular Approximating Case

We can obtain via direct calculations the following 38×1 right eigenvectors for $\frac{1}{2}$ and $\frac{1}{4}$ such that $\mathbf{L}_i\mathbf{R}_j = \delta(i-j)\ i,j = 1,...,5$ where $\mathbf{L}_i$ are from (3.12 |p.28):

(5.16)

$$\mathbf{R}_1 := \left[0, 0, \frac{1}{3}, \frac{-1}{9h}, \frac{1}{6}, \frac{-1}{18h}, \frac{-1}{6}, \frac{1}{18h}, \frac{-1}{3}, \frac{1}{9h}, \frac{-1}{6}, \frac{1}{18h}, \frac{1}{6}, \frac{-1}{18h}, 0, ..., 0\right]^T$$

$$\mathbf{R}_2 := \left[0, 0, \frac{-1}{6}, \frac{1}{18h}, \frac{1}{6}, \frac{-1}{18h}, \frac{1}{3}, \frac{-1}{9h}, \frac{1}{6}, \frac{-1}{18h}, \frac{-1}{6}, \frac{1}{18h}, \frac{-1}{3}, \frac{1}{9h}, 0, ..., 0\right]^T$$

$$\mathbf{R}_3 := \left[\begin{array}{c} 2d_1, 2d_2, -\frac{1}{3}(d_1-1), \frac{1}{3}(d_3+w), -\frac{1}{6}(2d_1+1), \frac{1}{6}(2d_3-w), -\frac{1}{6}(2d_1+1), \frac{1}{6}(2d_3-w), \\ -\frac{1}{3}(d_1-1), \frac{1}{3}(d_3+w), -\frac{1}{6}(2d_1+1), \frac{1}{6}(2d_3-w), -\frac{1}{6}(2d_1+1), \frac{1}{6}(2d_3-w), 0, ..., 0 \end{array}\right]^T$$

$$\mathbf{R}_4 := \left[\begin{array}{c} -2d_1, -2d_2, \frac{1}{3}(d_1-1), -\frac{1}{3}(d_3+w), \frac{1}{3}(d_1+2), -\frac{1}{3}(d_3-2w), \frac{1}{3}(d_1-1), -\frac{1}{3}(d_3+w), \\ \frac{1}{3}(d_1-1), -\frac{1}{3}(d_3+w), \frac{1}{3}(d_1+2), -\frac{1}{3}(d_3-2w), \frac{1}{3}(d_1-1), -\frac{1}{3}(d_3+w), 0, ..., 0 \end{array}\right]^T$$

$$\mathbf{R}_5 := \left[\begin{array}{c} 2d_1, 2d_2, -\frac{1}{6}(2d_1+1), \frac{1}{6}(2d_3-w), -\frac{1}{6}(2d_1+1), \frac{1}{6}(2d_3-w), \\ -\frac{1}{3}(d_1-1), \frac{1}{3}(d_3+w), -\frac{1}{6}(2d_1+1), \\ \frac{1}{6}(2d_3-w), -\frac{1}{6}(2d_1+1), \frac{1}{6}(2d_3-w), -\frac{1}{3}(d_1-1), \frac{1}{3}(d_3+w), 0, ..., 0 \end{array}\right]^T$$

where

$$d_1 := \frac{1}{4}\left(\frac{\widetilde{Y}\widetilde{Q}}{\widetilde{X}}\right)$$

$$d_2 := -\frac{1}{4h}\left(\frac{\widetilde{Y}}{\widetilde{X}}\right)$$

$$d_3 := \frac{1}{4h}\left(\frac{\widetilde{Z}}{\widetilde{X}}\right)$$

$$w := -\frac{(1+16ht_1)}{h(1+16t_2)}$$

for

$$\widetilde{Y} := -1 + 8t_2 + 192ht_2t_6 + 32ht_2t_5 - 4ht_5 - 24ht_6 = (-1 + 8t_2)(1 + 4ht_5 + 24ht_6)$$

(5.17)

$$\widetilde{Q} := \frac{-1 + 24t_3 + 4t_4}{1 + 4ht_5 + 24ht_6}$$

$$\widetilde{X} := 144ht_3t_5 + 3ht_5 - 24ht_2t_5 + 54ht_6 - 144ht_4t_6$$
$$- 144ht_2t_6 + 1 - 2t_2 + 30t_3 - 96t_2t_3 - t_4 - 16t_2t_4 + 144ht_1t_3 + 24ht_1t_4 - 6ht_1$$

$$\widetilde{Z} := 48ht_6 + 192ht_5t_3 - 192ht_4t_6 - 4t_4 + 1 + 192ht_1t_3 + 32ht_1t_4 + 24t_3 - 8ht_1$$

where t_j for $j = 1, ..., 6$ and h are from (5.5 |p.93).

Note the following facts that can be shown with direct calculation:

- if $1 + 16t_2 = 0$ then eigenvalue $\frac{1}{4}$ has multiplicity greater than 3
- if $-1 + 24t_3 + 4t_4 = 0$ then $t_5 + 6t_6 < -\frac{1}{12h}$ or else $\frac{1}{2}$ is not the subdominant eigenvalue

Since right and left eigenvectors that correspond to *different* eigenvalues are orthogonal we can multiply both sides of (5.13 |p.102) by each $\mathbf{R}_j$ and so obtain (using Theorem 5.3 on p.104) the following representations for the first and second partial derivatives at a point locally parameterized as $\left(k_0^{(1)}, k_0^{(2)}\right)$:

$$F_s\left(k_0^{(1)}, k_0^{(2)}\right) = \alpha_1^{(0)} = \mathbf{U}^0_{\mathbf{k}_0}\mathbf{R}_1 \tag{5.18}$$
$$F_t\left(k_0^{(1)}, k_0^{(2)}\right) = \alpha_2^{(0)} = \mathbf{U}^0_{\mathbf{k}_0}\mathbf{R}_2$$
$$F_{ss}\left(k_0^{(1)}, k_0^{(2)}\right) = 2\alpha_3^{(0)} = 2\mathbf{U}^0_{\mathbf{k}_0}\mathbf{R}_3$$
$$F_{st}\left(k_0^{(1)}, k_0^{(2)}\right) = \alpha_4^{(0)} = \mathbf{U}^0_{\mathbf{k}_0}\mathbf{R}_4$$
$$F_{tt}\left(k_0^{(1)}, k_0^{(2)}\right) = 2\alpha_5^{(0)} = 2\mathbf{U}^0_{\mathbf{k}_0}\mathbf{R}_5$$

Note that the 15^{th} through 38^{th} components of the above right eigenvectors equal 0. So define $\mathbf{R}^*_j$ as the 14×1 column vector whose components are the first 14 components of $\mathbf{R}_j$ $(j = 1, 2, ..., 5)$. Also define $\widetilde{\mathbf{U}}^0_{\mathbf{k}_0}$ as the 3×14 vector consisting of the first 14 elements of $\mathbf{U}^0_{\mathbf{k}_0}$.

We can then rewrite (5.18) as:

$$F_s\left(k_0^{(1)},k_0^{(2)}\right)=\alpha_1^{(0)}=\widetilde{\mathbf{U}}_{\mathbf{k}_0}^0\mathbf{R}_1^*$$
$$F_t\left(k_0^{(1)},k_0^{(2)}\right)=\alpha_2^{(0)}=\widetilde{\mathbf{U}}_{\mathbf{k}_0}^0\mathbf{R}_2^*$$
$$F_{ss}\left(k_0^{(1)},k_0^{(2)}\right)=2\alpha_3^{(0)}=2\widetilde{\mathbf{U}}_{\mathbf{k}_0}^0\mathbf{R}_3^*$$
$$F_{st}\left(k_0^{(1)},k_0^{(2)}\right)=\alpha_4^{(0)}=\widetilde{\mathbf{U}}_{\mathbf{k}_0}^0\mathbf{R}_4^*$$
$$F_{tt}\left(k_0^{(1)},k_0^{(2)}\right)=2\alpha_5^{(0)}=2\widetilde{\mathbf{U}}_{\mathbf{k}_0}^0\mathbf{R}_5^*$$

Theorem 5.5. *Assume that the subdivision scheme is an approximating triangular scheme and that the cascade algorithm given by* $\Phi_m := Q_P\,\Phi_{m-1}$ *converges in* $C^1(\mathbb{R})$. *Then for* $\mathbf{k}_0\in\mathbb{Z}^2$

$$D_1F(\mathbf{k}_0)=F_s\left(k_0^{(1)},k_0^{(2)}\right)=\widetilde{\mathbf{U}}_{\mathbf{k}_0}^0\mathbf{R}_1^*$$
$$D_2F(\mathbf{k}_0)=F_t\left(k_0^{(1)},k_0^{(2)}\right)=\widetilde{\mathbf{U}}_{\mathbf{k}_0}^0\mathbf{R}_2^*$$

where $F(\cdot):=\sum_{\mathbf{k}\in\mathbb{Z}^2}\mathbf{v}_{\mathbf{k}}^0\Phi(\cdot-\mathbf{k})$ *is the limiting surface for the subdivision scheme,* Φ *is from (2.5 |p.12),* $\widetilde{\mathbf{U}}_{\mathbf{k}_0}^0$ *is the* 3×14 *vector consisting of the first 14 elements of* $\mathbf{U}_{\mathbf{k}_0}^0$ *and* $\mathbf{R}_1^*$, $\mathbf{R}_2^*$ *are as above. If in addition the cascade algorithm converges in* $C^2(\mathbb{R})$

$$D_1^2F(\mathbf{k}_0)=F_{ss}\left(k_0^{(1)},k_0^{(2)}\right)=2\widetilde{\mathbf{U}}_{\mathbf{k}_0}^0\mathbf{R}_3^*$$
$$D_2D_1F(\mathbf{k}_0)=F_{st}\left(k_0^{(1)},k_0^{(2)}\right)=\widetilde{\mathbf{U}}_{\mathbf{k}_0}^0\mathbf{R}_4^*$$
$$D_2^2F(\mathbf{k}_0)=F_{tt}\left(k_0^{(1)},k_0^{(2)}\right)=2\widetilde{\mathbf{U}}_{\mathbf{k}_0}^0\mathbf{R}_5^*$$

where $\mathbf{R}_3^*$, $\mathbf{R}_4^*,\mathbf{R}_5^*$ *are as above.*

And from Corollary 5.3 on p. 104:

Corollary 5.5. *Assume that the subdivision scheme is an approximating triangular scheme and that the cascade algorithm given by* $\Phi_m := Q_P\,\Phi_{m-1}$

converges in $C^1(\mathbb{R})$. *Then for* $\mathbf{k}_0, \mathbf{i} \in \mathbb{Z}^2$, $n \in \mathbb{Z}_+$

$$D_1 F\left(\mathbf{k}_0 + \frac{\mathbf{i}}{2^n}\right) = 2^n \widetilde{\mathbf{U}}^n_{\mathbf{k}_0,\mathbf{i}} \mathbf{R}_1^*$$

$$D_2 F\left(\mathbf{k}_0 + \frac{\mathbf{i}}{2^n}\right) = 2^n \widetilde{\mathbf{U}}^n_{\mathbf{k}_0,\mathbf{i}} \mathbf{R}_2^*$$

where $F(\cdot) := \sum_{\mathbf{k}\in\mathbb{Z}^2} \mathbf{v}^0_{\mathbf{k}} \Phi(\cdot - \mathbf{k})$ *is the limiting surface for the subdivision scheme,* Φ *is from (2.5 |p.12), and* $\widetilde{\mathbf{U}}^n_{\mathbf{k}_0}$ *is the* 3×14 *vector consisting of the first 14 elements of* $\mathbf{U}^n_{\mathbf{k}_0,\mathbf{i}}$ *(3.17 |p.30). If in addition the cascade algorithm converges in* $C^2(\mathbb{R})$

$$D_1^2 F\left(\mathbf{k}_0 + \frac{\mathbf{i}}{2^n}\right) = 2^{2n+1} \widetilde{\mathbf{U}}^n_{\mathbf{k}_0,\mathbf{i}} \mathbf{R}_3^*$$

$$D_2 D_1 F\left(\mathbf{k}_0 + \frac{\mathbf{i}}{2^n}\right) = 2^{2n} \widetilde{\mathbf{U}}^n_{\mathbf{k}_0,\mathbf{i}} \mathbf{R}_4^*$$

$$D_2^2 F\left(\mathbf{k}_0 + \frac{\mathbf{i}}{2^n}\right) = 2^{2n+1} \widetilde{\mathbf{U}}^n_{\mathbf{k}_0,\mathbf{i}} \mathbf{R}_5^*$$

If the denominator $1 + 4ht_5 + 24ht_6$ for $\widetilde{Q}$ in (5.17 |p.112) equals zero then through direct calculations we can arrive at the following three 38×1 right eigenvectors of $\frac{1}{4}$, $\{\mathbf{R}_j\}_{j=3,4,5}$, such that $\mathbf{L}_i \mathbf{R}_j = \delta(i-j)$ $i, j = 3, 4, 5$

$$\mathbf{R}_3 := \begin{bmatrix} 2\alpha, 0, -\frac{1}{3}\alpha + \frac{1}{3}, \frac{1}{3}\beta - \frac{1}{3}\gamma, -\frac{1}{3}\alpha - \frac{1}{6}, \frac{1}{3}\beta + \frac{1}{6}\gamma, -\frac{1}{3}\alpha - \frac{1}{6}, \frac{1}{3}\beta + \frac{1}{6}\gamma, \\ -\frac{1}{3}\alpha + \frac{1}{3}, \frac{1}{3}\beta - \frac{1}{3}\gamma, -\frac{1}{3}\alpha - \frac{1}{6}, \frac{1}{3}\beta + \frac{1}{6}\gamma, -\frac{1}{3}\alpha - \frac{1}{6}, \frac{1}{3}\beta + \frac{1}{6}\gamma, 0, ..., 0 \end{bmatrix}^T$$

$$\mathbf{R}_4 := \begin{bmatrix} -2\alpha, 0, \frac{1}{3}\alpha - \frac{1}{3}, -\frac{1}{3}\beta + \frac{1}{3}\gamma, \frac{1}{3}\alpha + \frac{2}{3}, -\frac{1}{3}\beta - \frac{2}{3}\gamma, \frac{1}{3}\alpha - \frac{1}{3}, -\frac{1}{3}\beta + \frac{1}{3}\gamma, \\ \frac{1}{3}\alpha - \frac{1}{3}, -\frac{1}{3}\beta + \frac{1}{3}\gamma, \frac{1}{3}\alpha + \frac{2}{3}, -\frac{1}{3}\beta - \frac{2}{3}\gamma, \frac{1}{3}\alpha - \frac{1}{3}, -\frac{1}{3}\beta + \frac{1}{3}\gamma, 0, ..., 0 \end{bmatrix}^T$$

(5.19)

$$\mathbf{R}_5 := \begin{bmatrix} 2\alpha, 0, -\frac{1}{3}\alpha - \frac{1}{6}, \frac{1}{3}\beta + \frac{1}{6}\gamma, -\frac{1}{3}\alpha - \frac{1}{6}, \frac{1}{3}\beta + \frac{1}{6}\gamma, -\frac{1}{3}\alpha + \frac{1}{3}, \frac{1}{3}\beta - \frac{1}{3}\gamma, \\ -\frac{1}{3}\alpha - \frac{1}{6}, \frac{1}{3}\beta + \frac{1}{6}\gamma, -\frac{1}{3}\alpha - \frac{1}{6}, \frac{1}{3}\beta + \frac{1}{6}\gamma, -\frac{1}{3}\alpha + \frac{1}{3}, \frac{1}{3}\beta - \frac{1}{3}\gamma, 0, ..., 0 \end{bmatrix}^T$$

where

$$\alpha := \frac{8t_2 - 1}{-16t_2 - 1 + 24ht_1 - 144ht_6}$$
$$\beta := \frac{8ht_1 - 1 - 48ht_6}{h\left(-16t_2 - 1 + 24ht_1 - 144ht_6\right)}$$
$$\gamma := \frac{1 + 16ht_1}{h\left(1 + 16t_2\right)}$$

The 14×1 shortened version of these eigenvectors would then be used in Theorem 5.5 and Corollary 5.5.

5.4.1.1. Specific Triangular Approximating Scheme (Regular). In [**CJ08**] and [**CJ03b**] Chui/Jiang devised a spline-based 1-ring triangular approximating scheme that was labelled the S_3^2-subdivision. The notation indicates that the splines are C^2 functions whose restrictions on each triangle are polynomials of total degree ≤ 3. Here

$$h = -\frac{1}{3} \tag{5.20}$$
$$[t_1, t_2, t_3, t_4, t_5, t_6] = \frac{1}{16}\left[2, 0, -1, -2, 6, 1\right]$$

where we note that $1 + 4ht_5 + 24ht_6 = 0$.

We will use the right eigenvectors for $\frac{1}{4}$ from (5.19) and the right eigenvectors for $\frac{1}{2}$ from (5.16).

We obtain:

$$\mathbf{R}_1^* := \left[0, 0, \frac{1}{3}, \frac{1}{3}, \frac{1}{6}, \frac{1}{6}, -\frac{1}{6}, -\frac{1}{6}, -\frac{1}{3}, -\frac{1}{3}, -\frac{1}{6}, -\frac{1}{6}, \frac{1}{6}, \frac{1}{6}\right]^T$$
$$\mathbf{R}_2^* := \left[0, 0, -\frac{1}{6}, -\frac{1}{6}, \frac{1}{6}, \frac{1}{6}, \frac{1}{3}, \frac{1}{3}, \frac{1}{6}, \frac{1}{6}, -\frac{1}{6}, -\frac{1}{6}, -\frac{1}{3}, -\frac{1}{3}\right]^T$$
$$\mathbf{R}_3^* := \left[-2, 0, \frac{2}{3}, \frac{2}{3}, \frac{1}{6}, \frac{1}{6}, \frac{1}{6}, \frac{1}{6}, \frac{2}{3}, \frac{2}{3}, \frac{1}{6}, \frac{1}{6}, \frac{1}{6}, \frac{1}{6}\right]^T$$
$$\mathbf{R}_4^* := \left[2, 0, -\frac{2}{3}, -\frac{2}{3}, \frac{1}{3}, \frac{1}{3}, -\frac{2}{3}, -\frac{2}{3}, -\frac{2}{3}, -\frac{2}{3}, \frac{1}{3}, \frac{1}{3}, -\frac{2}{3}, -\frac{2}{3}\right]^T$$
$$\mathbf{R}_5^* := \left[-2, 0, \frac{1}{6}, \frac{1}{6}, \frac{1}{6}, \frac{1}{6}, \frac{2}{3}, \frac{2}{3}, \frac{1}{6}, \frac{1}{6}, \frac{1}{6}, \frac{1}{6}, \frac{2}{3}, \frac{2}{3}\right]^T$$

Figures 5.1 , ,5.2 and 5.3 visually show the symmetry that these formulas have.

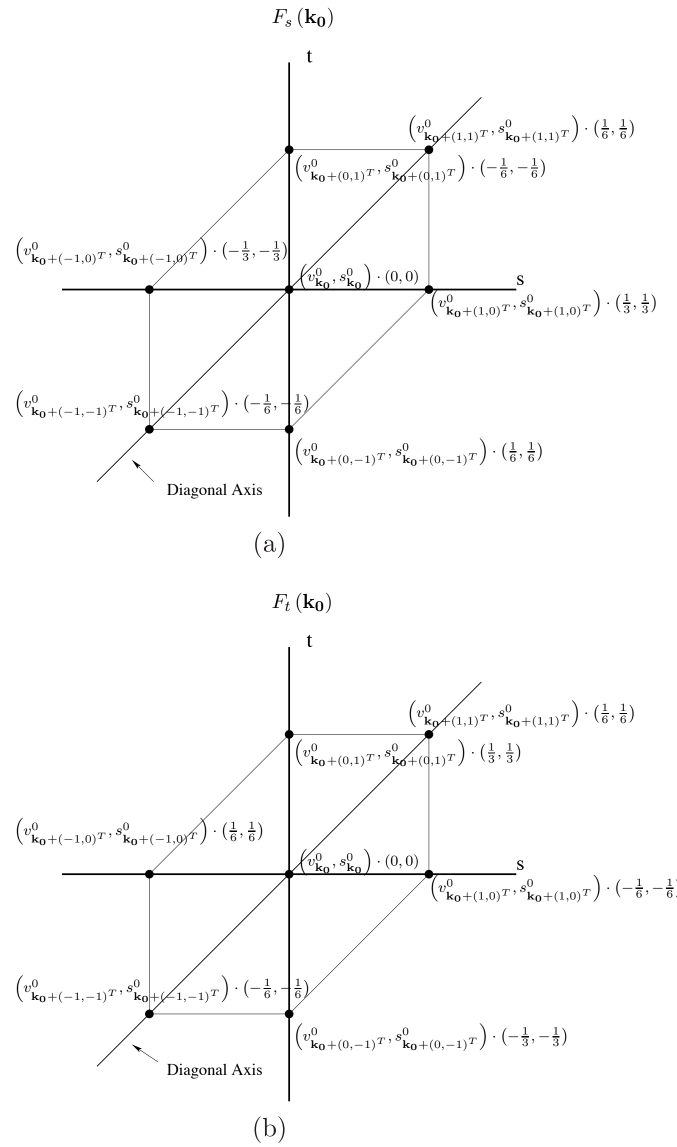

Figure 5.1. The above diagrams represent F_s and F_t. Note the symmetry between each diagram around the diagonal axis.

$F_{ss}(\mathbf{k_0})$

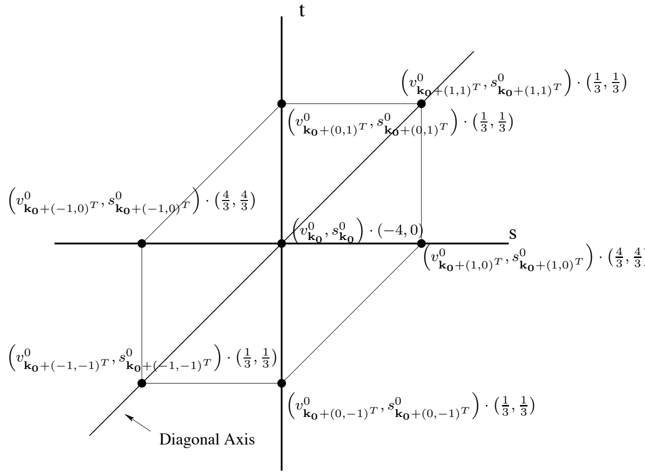

(a)

$F_{tt}(\mathbf{k_0})$

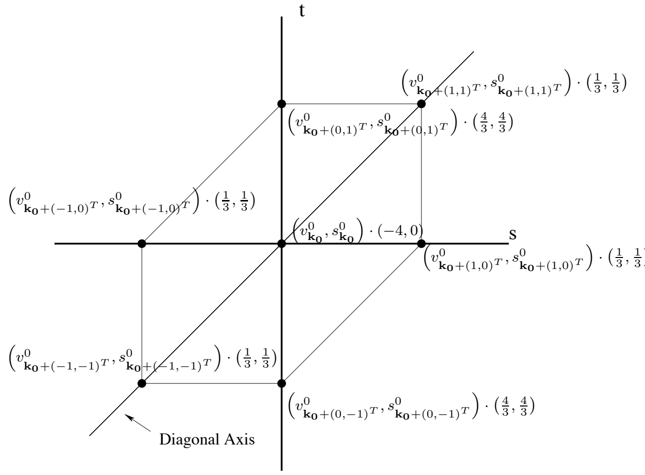

(b)

Figure 5.2. The above diagrams represent F_{ss} and F_{tt}. Note the symmetry between each diagram around the diagonal axis.

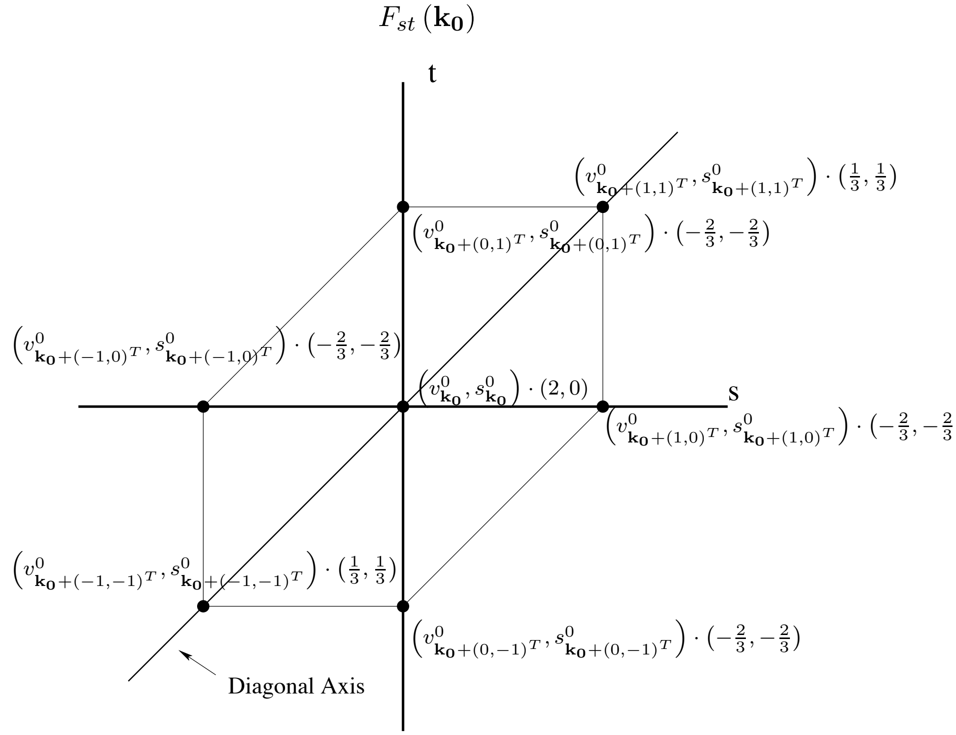

Figure 5.3. The above diagram represents F_{st}. Note the symmetry around the diagonal axis.

5.4.2. Quadrilateral Approximating Case

As indicated at the beginning of section 5.4 on p. 110, we can use the same techniques as for the interpolating case and obtain the following 50×1 right eigenvectors for $\frac{1}{2}$ and $\frac{1}{4}$, $\{R_j\}_{j=1,...,5}$, such that $\mathbf{L}_i \mathbf{R}_j = \delta(i-j)\ i,j = 1,...,5$ where $\mathbf{L}_i$ are from (4.7 |p.60):

(5.21)

$$\mathbf{R}_1 := \begin{bmatrix} 0,0,\frac{1}{3},-\frac{1}{3}\frac{3+32ht_1}{h(7+32t_2)},0,0,-\frac{1}{3},\frac{1}{3}\frac{3+32ht_1}{h(7+32t_2)},0,0,\frac{1}{12},\frac{1}{12}\frac{-32t_2+64ht_1-1}{h(7+32t_2)}, \\ -\frac{1}{12},-\frac{1}{12}\frac{-32t_2+64ht_1-1}{h(7+32t_2)},-\frac{1}{12},-\frac{1}{12}\frac{-32t_2+64ht_1-1}{h(7+32t_2)},\frac{1}{12},\frac{1}{12}\frac{-32t_2+64ht_1-1}{h(7+32t_2)},0,...,0 \end{bmatrix}^T$$

$$\mathbf{R}_2 := \begin{bmatrix} 0,0,0,0,\frac{1}{3},-\frac{1}{3}\frac{3+32ht_1}{h(7+32t_2)},0,0,-\frac{1}{3},\frac{1}{3}\frac{3+32ht_1}{h(7+32t_2)},\frac{1}{12},\frac{1}{12}\frac{-32t_2+64ht_1-1}{h(7+32t_2)}, \\ \frac{1}{12},\frac{1}{12}\frac{-32t_2+64ht_1-1}{h(7+32t_2)},-\frac{1}{12},-\frac{1}{12}\frac{-32t_2+64ht_1-1}{h(7+32t_2)},-\frac{1}{12},-\frac{1}{12}\frac{-32t_2+64ht_1-1}{h(7+32t_2)},0,...,0 \end{bmatrix}^T$$

$$\mathbf{R}_3 := \begin{bmatrix} \frac{1}{2}\frac{E(16t_5+4t_6+16t_4-1)}{C\cdot F},\frac{1}{2h}\frac{E}{C},-\frac{1}{2h}\frac{E\cdot D}{C\cdot F}+\frac{1}{4},\frac{1}{2h}\frac{G}{C}-\frac{1}{4}\frac{1+32ht_1}{h(1+32t_2)}, \\ -\frac{1}{2h}\frac{E\cdot D}{C\cdot F}-\frac{1}{4},\frac{1}{2h}\frac{G}{C}+\frac{1}{4}\frac{1+32ht_1}{h(1+32t_2)},-\frac{1}{2h}\frac{E\cdot D}{C\cdot F}+\frac{1}{4},\frac{1}{2h}\frac{G}{C}-\frac{1}{4}\frac{1+32ht_1}{h(1+32t_2)}, \\ -\frac{1}{2h}\frac{E\cdot D}{C\cdot F}-\frac{1}{4},\frac{1}{2h}\frac{G}{C}+\frac{1}{4}\frac{1+32ht_1}{h(1+32t_2)},\frac{1}{8h}\frac{E\cdot H}{C\cdot F},\frac{1}{8h}\frac{J}{C}, \\ \frac{1}{8h}\frac{E\cdot H}{C\cdot F},\frac{1}{8h}\frac{J}{C},\frac{1}{8h}\frac{E\cdot H}{C\cdot F},\frac{1}{8h}\frac{J}{C},\frac{1}{8h}\frac{E\cdot H}{C\cdot F},\frac{1}{8h}\frac{J}{C},0,...,0 \end{bmatrix}^T$$

$$\mathbf{R}_4 := \left[0,0,0,0,0,0,0,0,0,0,\frac{1}{4},-\frac{1}{12h},-\frac{1}{4},\frac{1}{12h},\frac{1}{4},-\frac{1}{12h},-\frac{1}{4},\frac{1}{12h},0,...0\right]^T$$

$$\mathbf{R}_5 := \begin{bmatrix} \frac{1}{2}\frac{E(16t_5+4t_6+16t_4-1)}{C\cdot F},\frac{1}{2h}\frac{E}{C},-\frac{1}{2h}\frac{E\cdot D}{C\cdot F}-\frac{1}{4},\frac{1}{2h}\frac{G}{C}+\frac{1}{4}\frac{1+32ht_1}{h(1+32t_2)}, \\ -\frac{1}{2h}\frac{E\cdot D}{C\cdot F}+\frac{1}{4},\frac{1}{2h}\frac{G}{C}-\frac{1}{4}\frac{1+32ht_1}{h(1+32t_2)},-\frac{1}{2h}\frac{E\cdot D}{C\cdot F}-\frac{1}{4},\frac{1}{2h}\frac{G}{C}+\frac{1}{4}\frac{1+32ht_1}{h(1+32t_2)}, \\ -\frac{1}{2h}\frac{E\cdot D}{C\cdot F}+\frac{1}{4},\frac{1}{2h}\frac{G}{C}-\frac{1}{4}\frac{1+32ht_1}{h(1+32t_2)},\frac{1}{8h}\frac{E\cdot H}{C\cdot F},\frac{1}{8h}\frac{J}{C}, \\ \frac{1}{8h}\frac{E\cdot H}{C\cdot F},\frac{1}{8h}\frac{J}{C},\frac{1}{8h}\frac{E\cdot H}{C\cdot F},\frac{1}{8h}\frac{J}{C},\frac{1}{8h}\frac{E\cdot H}{C\cdot F},\frac{1}{8h}\frac{J}{C},0,...,0 \end{bmatrix}^T$$

Here we have

$$
\begin{aligned}
C :=& -64ht_{10} + 5h - 16t_3 + 128t_3t_9 - 1280ht_5t_{10} + 64ht_6t_{10} - 1792ht_4t_{10} - 2048h^2t_4t_8 \\
& - 2048h^2t_1t_{10} - 768ht_5t_9 - 1024ht_4t_9 - 2048h^2t_5t_8 - 512h^2t_6t_8 - 2048ht_1t_3 - 384h^2t_6t_7 \\
& - 1536h^2t_5t_7 - 1536h^2t_4t_7 + 1024h^2t_2t_7 - 1024ht_2t_4 - 256ht_2t_6 + 8192ht_2t_4t_{10} + 2048ht_2t_6t_{10} \\
& + 8192t_2t_3t_{10} + 4096t_2t_3t_9 + 256ht_2t_9 + 96ht_4 + 64ht_5 - 8ht_6 + 16384ht_1t_3t_9 + 32768ht_1t_3t_{10} \\
& + 32768h^2t_1t_5t_{10} + 8192h^2t_1t_6t_{10} + 32768h^2t_1t_4t_{10} - 8192ht_2t_5t_{10} - 8192ht_2t_5t_9 - 16384h^2t_2t_5t_7 \\
& - 4096h^2t_2t_6t_7 - 16384h^2t_2t_4t_7 - 512t_2t_3 - 24ht_9 + 256t_3t_{10} + 128h^2t_8 + 96h^2t_7 + 32ht_2 \\
D :=& \, 8\left(16ht_5t_{10} - ht_{10} + 4ht_6t_{10} + 16ht_4t_{10} - t_3 + 8t_3t_9 + 16t_3t_{10}\right) \\
E :=& \, h\left(3 - 48t_{10} - 32t_2 + 512t_2t_{10} + 256t_2t_9 - 24t_9\right) \\
F :=& -1 + 8t_9 + 16t_{10} \\
G :=& -8ht_{10} + h - 8t_3 + 64t_3t_9 - 256ht_5t_{10} + 32ht_6t_{10} - 128ht_4t_{10} - 256h^2t_4t_8 \\
& - 256h^2t_1t_{10} - 192ht_5t_9 - 128ht_4t_9 - 256h^2t_5t_8 - 64h^2t_6t_8 - 256ht_1t_3 - 96h^2t_6t_7 - 384h^2t_5t_7 \\
& - 384h^2t_4t_7 + 8ht_5 - 4ht_6 + 2048ht_1t_3t_9 + 4096ht_1t_3t_{10} + 4096h^2t_1t_5t_{10} + 1024h^2t_1t_6t_{10} \\
& + 4096h^2t_1t_4t_{10} + 128t_3t_{10} + 16h^2t_8 + 24h^2t_7 \\
H :=& \, 256t_3t_9 - 32t_3 - 16ht_4 + 512t_3t_{10} + 128ht_6t_{10} - 4ht_6 \\
& - 32ht_{10} + 512ht_5t_{10} + h - 16ht_5 + 512ht_4t_{10} \\
J :=& -32ht_{10} + h - 32t_3 + 256t_3t_9 + 512ht_5t_{10} + 128ht_6t_{10} - 512ht_4t_{10} - 1024h^2t_4t_8 \\
& - 1024h^2t_1t_{10} - 512ht_4t_9 - 1024h^2t_5t_8 - 256h^2t_6t_8 - 1024ht_1t_3 + 1024h^2t_2t_7 - 512ht_2t_4 \\
& - 128ht_2t_6 + 512ht_2t_5 + 48ht_4 - 16ht_5 - 4ht_6 + 8192ht_1t_3t_9 + 16384ht_1t_3t_{10} \\
& + 16384h^2t_1t_5t_{10} + 4096h^2t_1t_6t_{10} + 16384h^2t_1t_4t_{10} - 16384ht_2t_5t_{10} \\
& - 8192ht_2t_5t_9 - 16384h^2t_2t_5t_7 - 4096h^2t_2t_6t_7 - 16384h^2t_2t_4t_7 \\
& + 512t_3t_{10} + 64h^2t_8 + 32ht_2
\end{aligned}
$$

where h and t_j for $j = 1, ..., 10$ are from (5.7 |p.94)

It can be directly shown that:

- $t_2 \neq \frac{-1}{32}$ else the subsubdominant eigenvalue, $\frac{1}{4}$, has multiplicity 4.
- if $7 + 32t_2 = 0$ then the eigenvalue 1 has multiplicity greater than 1.

Since right and left eigenvectors that correspond to *different* eigenvalues are orthogonal we can multiply both sides of (5.15 |p.107) by each $\mathbf{R}_j$ and so obtain (using Theorem 5.4 on p.109) the following representations for the first and second partial derivatives at a point locally parameterized as $\left(k_0^{(1)}, k_0^{(2)}\right)$:

$$\begin{aligned}
F_s\left(k_0^{(1)}, k_0^{(2)}\right) &= \alpha_1^{(0)} = \mathbf{U}_{\mathbf{k}_0}^0 \mathbf{R}_1 \\
F_t\left(k_0^{(1)}, k_0^{(2)}\right) &= \alpha_2^{(0)} = \mathbf{U}_{\mathbf{k}_0}^0 \mathbf{R}_2 \\
F_{ss}\left(k_0^{(1)}, k_0^{(2)}\right) &= 2\alpha_3^{(0)} = 2\mathbf{U}_{\mathbf{k}_0}^0 \mathbf{R}_3 \\
F_{st}\left(k_0^{(1)}, k_0^{(2)}\right) &= \alpha_4^{(0)} = \mathbf{U}_{\mathbf{k}_0}^0 \mathbf{R}_4 \\
F_{tt}\left(k_0^{(1)}, k_0^{(2)}\right) &= 2\alpha_5^{(0)} = 2\mathbf{U}_{\mathbf{k}_0}^0 \mathbf{R}_5
\end{aligned} \tag{5.22}$$

Note that the 19^{th} through 50^{th} components of the above right eigenvectors equal 0. So define $\mathbf{R}_j^*$ as the 18×1 column vector whose components are the first 18 components of $\mathbf{R}_j$ $(j = 1, 2, ..., 5)$. Also define $\widetilde{\mathbf{U}}_{\mathbf{k}_0}^0$ as the 3×18 vector consisting of the first 18 elements of $\mathbf{U}_{\mathbf{k}_0}^0$.

We can then rewrite (5.22) as:

$$\begin{aligned}
F_s\left(k_0^{(1)}, k_0^{(2)}\right) &= \alpha_1^{(0)} = \widetilde{\mathbf{U}}_{\mathbf{k}_0}^0 \mathbf{R}_1^* \\
F_t\left(k_0^{(1)}, k_0^{(2)}\right) &= \alpha_2^{(0)} = \widetilde{\mathbf{U}}_{\mathbf{k}_0}^0 \mathbf{R}_2^* \\
F_{ss}\left(k_0^{(1)}, k_0^{(2)}\right) &= 2\alpha_3^{(0)} = 2\widetilde{\mathbf{U}}_{\mathbf{k}_0}^0 \mathbf{R}_3^* \\
F_{st}\left(k_0^{(1)}, k_0^{(2)}\right) &= \alpha_4^{(0)} = \widetilde{\mathbf{U}}_{\mathbf{k}_0}^0 \mathbf{R}_4^* \\
F_{tt}\left(k_0^{(1)}, k_0^{(2)}\right) &= 2\alpha_5^{(0)} = 2\widetilde{\mathbf{U}}_{\mathbf{k}_0}^0 \mathbf{R}_5^*
\end{aligned}$$

Theorem 5.6. *Assume that the subdivision scheme is an approximating quadrilateral scheme and that the cascade algorithm given by $\Phi_m := Q_P\,\Phi_{m-1}$ converges in $C^1(\mathbb{R})$. Then for $\mathbf{k}_0 \in \mathbb{Z}^2$*

$$\begin{aligned}
D_1 F(\mathbf{k}_0) &= F_s\left(k_0^{(1)}, k_0^{(2)}\right) = \widetilde{\mathbf{U}}_{\mathbf{k}_0}^0 \mathbf{R}_1^* \\
D_2 F(\mathbf{k}_0) &= F_t\left(k_0^{(1)}, k_0^{(2)}\right) = \widetilde{\mathbf{U}}_{\mathbf{k}_0}^0 \mathbf{R}_2^*
\end{aligned}$$

where $F(\cdot) := \sum_{\mathbf{k}\in\mathbb{Z}^2} \mathbf{v}_{\mathbf{k}}^0 \Phi(\cdot - \mathbf{k})$ *is the limiting surface for the subdivision scheme,* Φ *is from (2.5 |p.12),* $\widetilde{\mathbf{U}}_{\mathbf{k}_0}^0$ *is the* 3×18 *vector consisting of the first 18 elements of* $\mathbf{U}_{\mathbf{k}_0}^0$ *and* $\mathbf{R}_1^*$, $\mathbf{R}_2^*$ *are as above. If in addition the cascade algorithm converges in* $C^2(\mathbb{R})$

$$D_1^2 F(\mathbf{k}_0) = F_{ss}\left(k_0^{(1)}, k_0^{(2)}\right) = 2\widetilde{\mathbf{U}}_{\mathbf{k}_0}^0 \mathbf{R}_3^*$$
$$D_2 D_1 F(\mathbf{k}_0) = F_{st}\left(k_0^{(1)}, k_0^{(2)}\right) = \widetilde{\mathbf{U}}_{\mathbf{k}_0}^0 \mathbf{R}_4^*$$
$$D_2^2 F(\mathbf{k}_0) = F_{tt}\left(k_0^{(1)}, k_0^{(2)}\right) = 2\widetilde{\mathbf{U}}_{\mathbf{k}_0}^0 \mathbf{R}_5^*$$

where $\mathbf{R}_3^*$, $\mathbf{R}_4^*, \mathbf{R}_5^*$ *are as above.*

From Corollary 5.4 on p. 110:

Corollary 5.6. *Assume that the subdivision scheme is an approximating quadrilateral scheme and that the cascade algorithm given by* $\Phi_m := Q_P \Phi_{m-1}$ *converges in* $C^1(\mathbb{R})$*. Then for* $\mathbf{k}_0, \mathbf{i} \in \mathbb{Z}^2$, $n \in \mathbb{Z}_+$

$$D_1 F\left(\mathbf{k}_0 + \frac{\mathbf{i}}{2^n}\right) = 2^n \alpha_1^{(n)}$$
$$D_2 F\left(\mathbf{k}_0 + \frac{\mathbf{i}}{2^n}\right) = 2^n \alpha_2^{(n)}$$

where $F(\cdot) := \sum_{\mathbf{k}\in\mathbb{Z}^2} \mathbf{v}_{\mathbf{k}}^0 \Phi(\cdot - \mathbf{k})$ *is the limiting surface for the subdivision scheme,* Φ *is from (2.5 |p.12).and* $\alpha_1^{(n)}$, $\alpha_2^{(n)}$ *are from (4.11). If in addition the cascade algorithm converges in* $C^2(\mathbb{R})$

$$D_1^2 F\left(\mathbf{k}_0 + \frac{\mathbf{i}}{2^n}\right) = 2^{2n+1} \alpha_3^{(n)}$$
$$D_2 D_1 F\left(\mathbf{k}_0 + \frac{\mathbf{i}}{2^n}\right) = 2^{2n} \alpha_4^{(n)}$$
$$D_2^2 F\left(\mathbf{k}_0 + \frac{\mathbf{i}}{2^n}\right) = 2^{2n+1} \alpha_5^{(n)}$$

where $\alpha_3^{(n)}$, $\alpha_{4,}^{(n)}$ $\alpha_5^{(n)}$ *are from (4.11 |p.62).*

5.4.2.1. Specific Quadrilateral Approximating Scheme (Regular). The following specific template for a 1-ring quadrilateral approximating scheme was developed using the Jiang/Oswald Matlab® routines (see [**JO01**]) for determining the Sobolev smoothness of refinable functions. Here we have

$$h = 1 \tag{5.23}$$
$$[t_1, t_2, t_3, t_4, t_5, t_6, t_7, t_8, t_9, t_{10}] := \frac{1}{256}\,[-5, 8, 36, -16, -24, 12, -12, -5, 30, 10]$$
$$\Phi \in W^{3.91577948}$$

We use the right eigenvectors from (5.21 |p.119) and obtain the following 50×1 column vectors:

$$\mathbf{R}_1 := \left[0, 0, \frac{1}{3}, -\frac{19}{192}, 0, 0, -\frac{1}{3}, \frac{19}{192}, 0, 0, \frac{1}{12}, -\frac{13}{384}, -\frac{1}{12}, \frac{13}{384}, -\frac{1}{12}, \frac{13}{384}, \frac{1}{12}, -\frac{13}{384}, 0, ..., 0\right]^T$$

$$\mathbf{R}_2 := \left[0, 0, 0, 0, \frac{1}{3}, -\frac{19}{192}, 0, 0, -\frac{1}{3}, \frac{19}{192}, \frac{1}{12}, -\frac{13}{384}, \frac{1}{12}, -\frac{13}{384}, -\frac{1}{12}, \frac{13}{384}, -\frac{1}{12}, \frac{13}{384}, 0, ..., 0\right]^T$$

$$\mathbf{R}_3 := \left[\begin{array}{c} -\frac{848}{1121}, \frac{144}{1121}, \frac{1533}{4484}, -\frac{5231}{71744}, -\frac{709}{4484}, \frac{1495}{71744}, \frac{1533}{4484}, -\frac{5231}{71744}, -\frac{709}{4484}, \frac{1495}{71744}, \frac{109}{1121}, \\ -\frac{435}{17936}, \frac{109}{1121}, -\frac{435}{17936}, \frac{109}{1121}, -\frac{435}{17936}, \frac{109}{1121}, -\frac{435}{17936}, 0, ..., 0 \end{array}\right]^T$$

$$\mathbf{R}_4 := \left[0, 0, 0, 0, 0, 0, 0, 0, 0, 0, \frac{1}{4}, -\frac{1}{12}, -\frac{1}{4}, \frac{1}{12}, \frac{1}{4}, -\frac{1}{12}, -\frac{1}{4}, \frac{1}{12}, 0, ..., 0\right]^T$$

$$\mathbf{R}_5 := \left[\begin{array}{c} -\frac{848}{1121}, \frac{144}{1121}, -\frac{709}{4484}, \frac{1495}{71744}, \frac{1533}{4484}, -\frac{5231}{71744}, -\frac{709}{4484}, \frac{1495}{71744}, \frac{1533}{4484}, -\frac{5231}{71744}, \frac{109}{1121}, \\ -\frac{435}{17936}, \frac{109}{1121}, -\frac{435}{17936}, \frac{109}{1121}, -\frac{435}{17936}, \frac{109}{1121}, -\frac{435}{17936}, 0, ...0 \end{array}\right]^T$$

Figures 5.4 , ,5.5 and 5.6 visually show the symmetry that these formulas have.

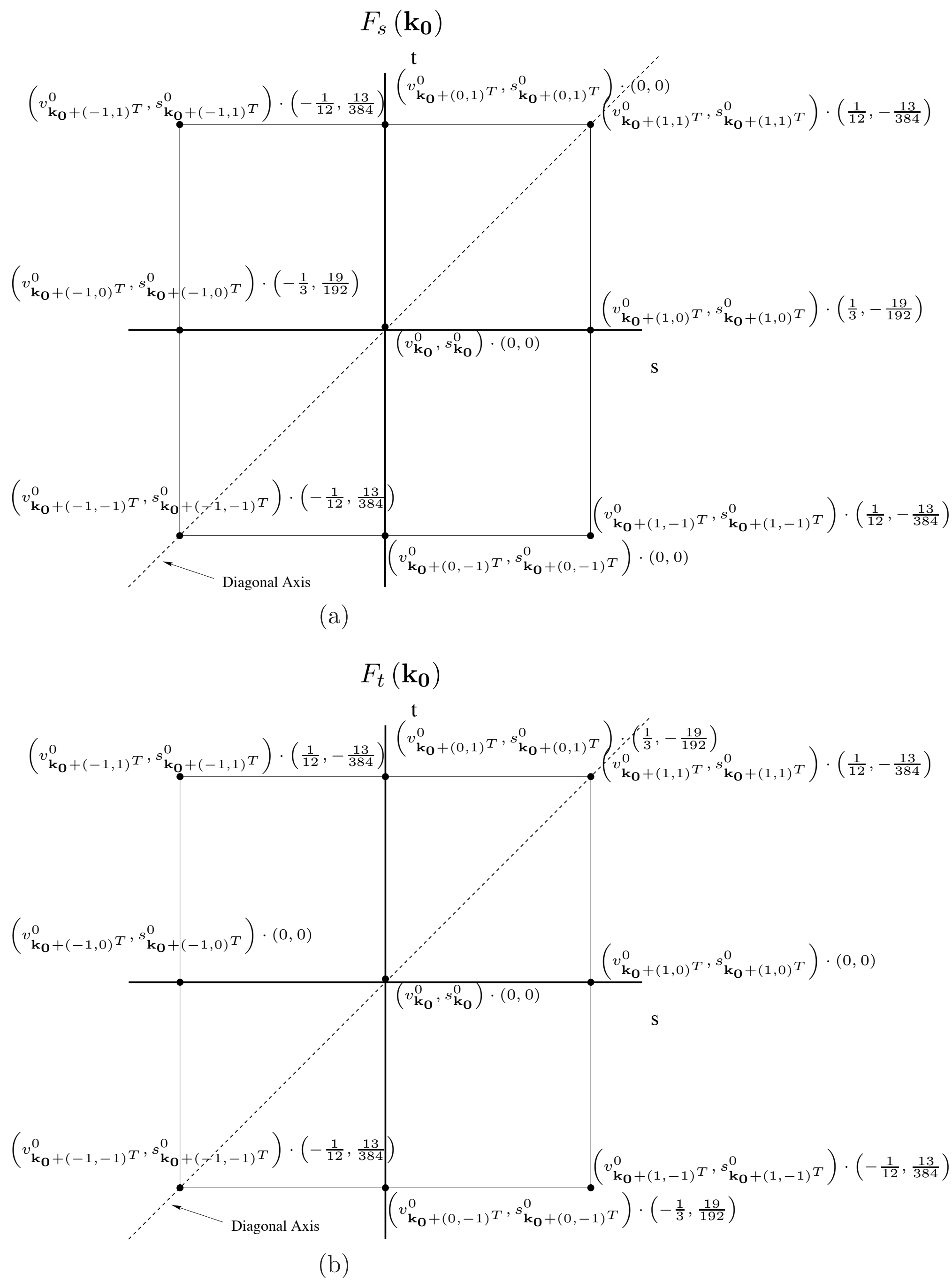

Figure 5.4. The above diagrams represent F_s and F_t. Note the symmetry between each diagram around the diagonal axis.

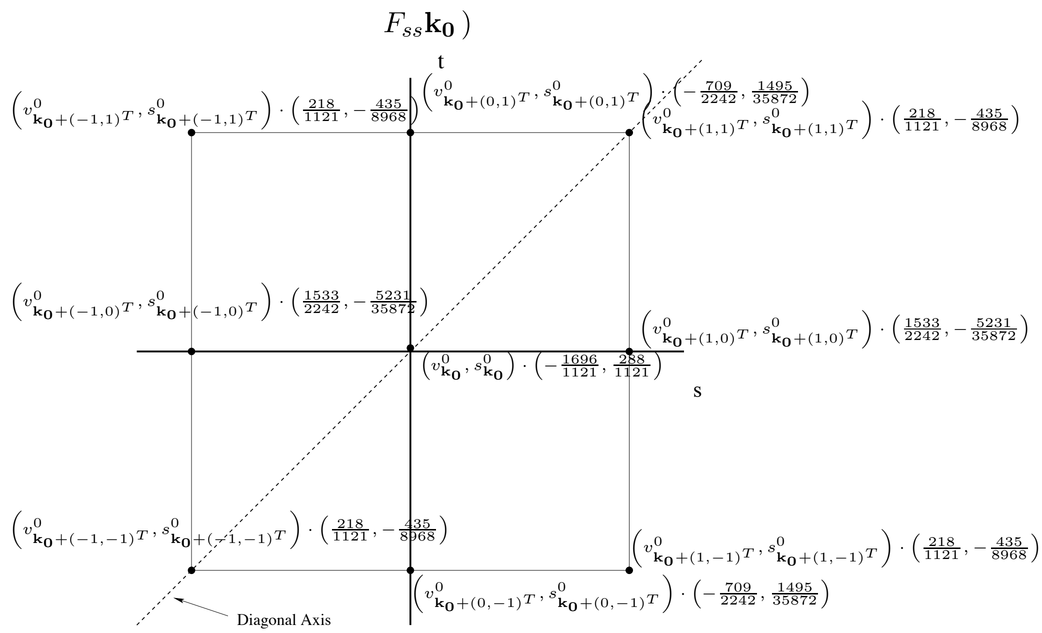

(a)

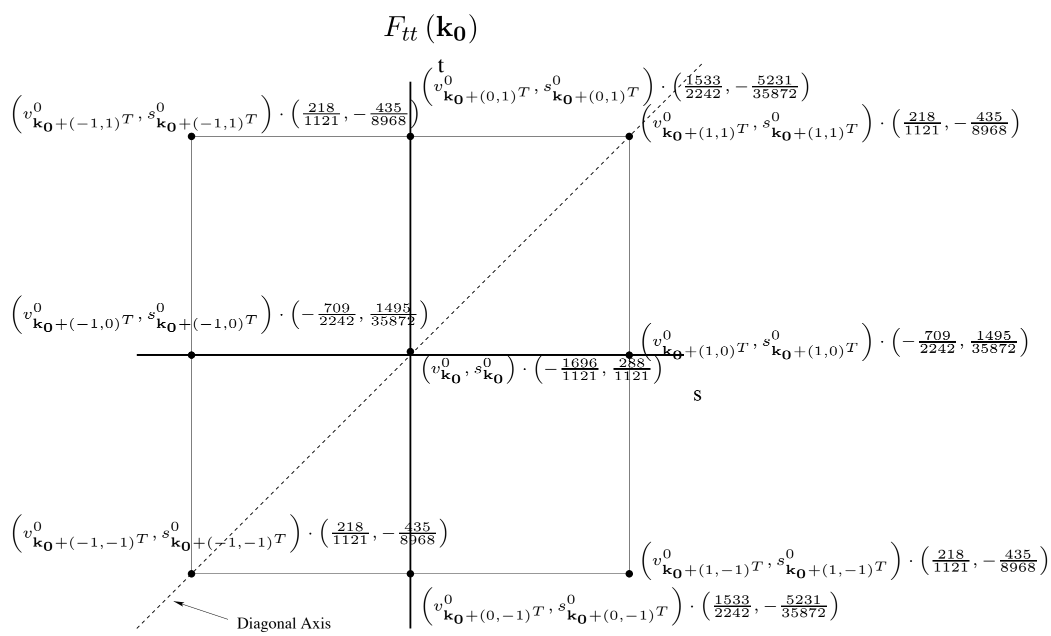

(b)

Figure 5.5. The above diagrams represent F_{ss} and F_{tt}. Note the symmetry between each diagram around the diagonal axis.

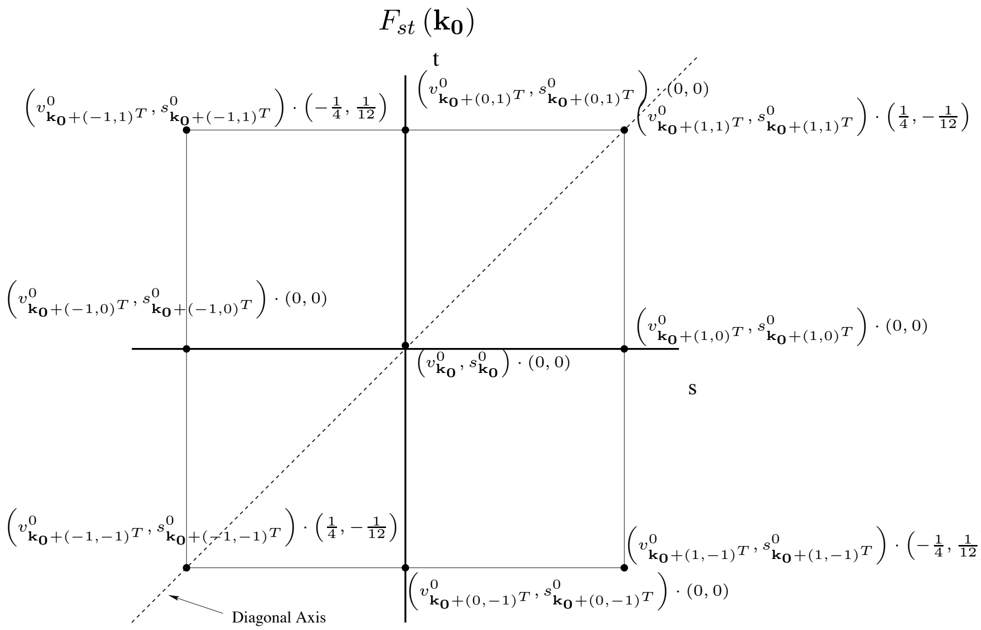

Figure 5.6. The above diagram represents F_{st}. Note the symmetry around the diagonal axis.

5.5. First Partial Derivatives: Approximating Extraordinary Case

The approximating extraordinary case is the most difficult to establish first partial derivative formulas. We will require an additional assumption. Before we get to that, we will first obtain right and left eigenvectors for the subdominant eigenvalue λ that has multiplicity 2.

5.5.1. Triangular Scheme

The template and subdivision matrix for the extraordinary vertex are the same as with the interpolatory extraordinary case except for the matrices Q_n and Q. See Figure 3.3 on p. 36 for the template and see (3.33 |p.38) for the subdivision matrix.

Here Q_n and Q will be denoted by

$$Q_n = \begin{bmatrix} w_{1,1} & w_{1,2} \\ w_{2,1} & w_{2,2} \end{bmatrix} \qquad Q = \begin{bmatrix} q_{1,1} & q_{1,2} \\ q_{2,1} & q_{2,2} \end{bmatrix} \tag{5.24}$$

where we will assume that

$$w_{1,1} + q_{1,1} = 1$$
$$w_{1,2} + q_{1,2} = 0$$

These restrictions on the templates are needed to ensure that the left eigenvector for 1 has the format

$$\widetilde{\mathbf{L}}_0 = [1, 0, 1, 0, ..., 1, 0]$$

Just as with the extraordinary interpolatory case, we have that λ is an eigenvalue of the 2×2 matrix $B + C\left(z + \frac{1}{z}\right)$ where $z := e^{\frac{2\pi i}{n}}$ [n equals the valence of the extraordinary vertex] and where B, C are from (3.4 |p.24).

In addition, as with the interpolatory triangular case, if we further restrict our subdivision matrix to a 1-ring neighborhood around the central extraordinary vertex we will arrive at the same pair of left and right eigenvectors of λ:

$$\widetilde{\mathbf{L}}_1 = \left(0,0,1,0,\cos\left(\frac{2\pi}{n}\right),0,\ldots,\cos\left(\frac{2\,(n-1)\,\pi}{n}\right),0\right) \tag{5.25}$$
$$\widetilde{\mathbf{L}}_2 = \left(0,0,0,0,\sin\left(\frac{2\pi}{n}\right),0,\ldots,\sin\left(\frac{2\,(n-1)\,\pi}{n}\right)\right)$$
$$\widehat{\mathbf{R}}_1 = \frac{2}{n}\begin{bmatrix} 0,0,1,d_2,\cos\left(\frac{2\cdot1\cdot\pi}{n}\right),d_2\cos\left(\frac{2\cdot1\cdot\pi}{n}\right),..., \\ \cos\left(\frac{2\cdot(n-1)\cdot\pi}{n}\right),d_2\cos\left(\frac{2\cdot(n-1)\cdot\pi}{n}\right) \end{bmatrix}^T$$
$$\widehat{\mathbf{R}}_2 = \frac{2}{n}\begin{bmatrix} 0,0,0,0,\sin\left(\frac{2\cdot1\cdot\pi}{n}\right),d_2\sin\left(\frac{2\cdot1\cdot\pi}{n}\right),..., \\ \sin\left(\frac{2\cdot(n-1)\cdot\pi}{n}\right),d_2\sin\left(\frac{2\cdot(n-1)\cdot\pi}{n}\right) \end{bmatrix}^T$$

for some $d_2 \in \mathbb{R}$.

As with the interpolatory case, the *initial* control vector net ($\mathbf{U}^0$) around the irregular vertex [again let us call it $\mathbf{v}_\mathbf{0}^0$] and the vector net after m subdivisions ($\mathbf{U}^m$) can be represented as a linear combination of (possibly generalized) left eigenvectors.

By letting $\left\{\widetilde{\mathbf{L}}_j : 0 \le j \le 2n+1\right\}$ be this set of $2n+2$ (possibly generalized) linearly independent left eigenvectors then $\mathbf{U}^0$ and $\mathbf{U}^m$ can be written as

$$\mathbf{U}^0 = \widetilde{\alpha}_0^{(0)}\widetilde{\mathbf{L}}_0 + \widetilde{\alpha}_1^{(0)}\widetilde{\mathbf{L}}_1 + \widetilde{\alpha}_2^{(0)}\widetilde{\mathbf{L}}_2 + \sum_{j=3}^{2n+1}\widetilde{\alpha}_j^{(0)}\widetilde{\mathbf{L}}_j \tag{5.26}$$
$$\mathbf{U}^m = \widetilde{\alpha}_0^{(0)}\widetilde{\mathbf{L}}_0 + \lambda^m\widetilde{\alpha}_1^{(0)}\widetilde{\mathbf{L}}_1 + \lambda^m\widetilde{\alpha}_2^{(0)}\widetilde{\mathbf{L}}_2 + o\left(\lambda^m\right)$$

where we have:

- $\widetilde{\alpha}_j^{(0)} \in \mathbb{R}^3 \quad j = 0,\ldots,2n+1$
- the left eigenvector for 1 is $\widetilde{\mathbf{L}}_0 = [1,0,1,0,...,1,0]$ and
- $\widetilde{\mathbf{L}}_1, \widetilde{\mathbf{L}}_2$ are the left eigenvectors for λ from (5.25 |p.128).

Hence

$$\lim_{m\to\infty}\mathbf{U}^m = \widetilde{\alpha}_0^{(0)}\widetilde{\mathbf{L}}_0 \tag{5.27}$$

$$\lim_{m\to\infty}\lambda^{-m}\left(\mathbf{U}^m - \widetilde{\alpha}_0^{(0)}\widetilde{\mathbf{L}}_0\right) = \widetilde{\alpha}_1^{(0)}\widetilde{\mathbf{L}}_1 + \widetilde{\alpha}_2^{(0)}\widetilde{\mathbf{L}}_2 \tag{5.28}$$

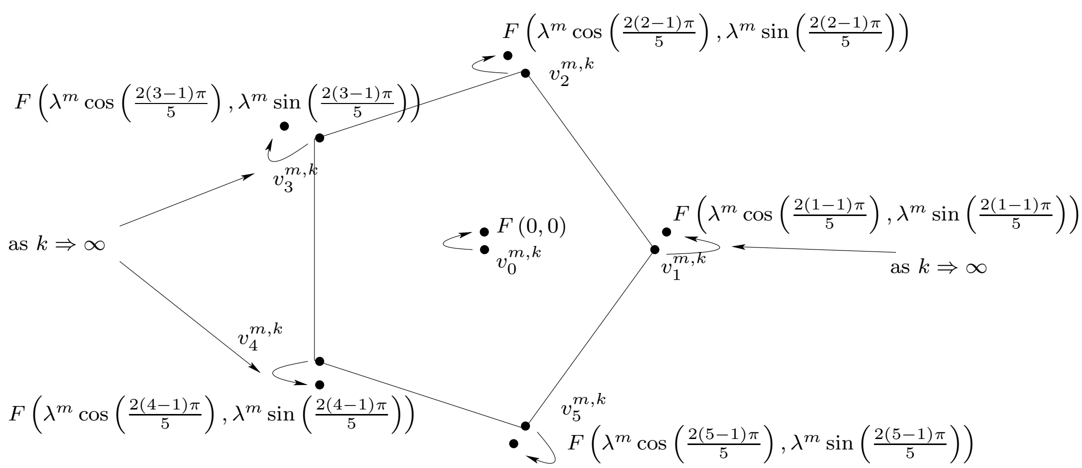

Figure 5.7. Representation of vertices approaching points on the limit surface that are parameterized as in (5.29 |p.129). Valence = 5.

Let us parametrize the limit surface F locally in a similar fashion as we did for the triangular interpolatory extraordinary case.

Since this is an approximating convergent scheme then we know that:

$$\lim_{m\to\infty} v_0^m \text{ is a point on the limit surface.}$$

Define $F(0,0) := \lim_{m\to\infty} v_0^m$ Now let us fix $m \in Z_+$. After we subdivide m times we get n new neighboring vertices around v_0^m. We shall denote them as v_j^m for $j = 1, 2, ..., n$. As we then continue to subdivide *beyond* m times we get updated vertices for these v_j^m and for v_0^m. Note that since this is an approximating scheme the updated vertices are not the same as the older vertices. Let us denote the updated vertices after k additional subdivisions as $v_j^{m,k}$ for $j = 0, 1, ..., n$. Again, for $j = 0, 1, ..., n$, $\lim_{k\to\infty} v_j^{m,k}$ are points on the limit surface.

For $j = 1, 2, ..., n$ we will parametrize these points as:

$$F\left(\lambda^m \cos\left(\frac{2(j-1)\pi}{n}\right), \lambda^m \sin\left(\frac{2(j-1)\pi}{n}\right)\right) := \lim_{k\to\infty} v_j^{m,k} \tag{5.29}$$

See Figure 5.7 for a visual representation in the case where valence = 5.

From (5.27 |p.128), $\lim_{m\to\infty} v_j^m = \widetilde{\alpha}_0^{(0)}$ for $j = 0, 1, ..., n$.

Thus we have:

$$\widetilde{\alpha}_0^{(0)} = \lim_{m\to\infty} v_0^m = F(0,0)$$

So from strictly looking at the odd components of each side of (5.28 |p.128) we have

(5.30)

$$\lim_{m\to\infty} \lambda^{-m} \left([v_0^m, v_1^m, v_2^m, ..., v_n^m] - [F(0,0), F(0,0), F(0,0), ..., F(0,0)] \right) =$$
$$\widetilde{\alpha}_1^{(0)} \left[0, 1, \cos\left(\frac{2\pi}{n}\right), \cos\left(\frac{4\pi}{n}\right), ..., \cos\left(\frac{2(n-1)\pi}{n}\right) \right]$$
$$+\widetilde{\alpha}_2^{(0)} \left[0, 0, \sin\left(\frac{2\pi}{n}\right), \sin\left(\frac{4\pi}{n}\right), ..., \sin\left(\frac{2(n-1)\pi}{n}\right) \right]$$

By assumption, the limit surface is C^1 at the parametrized point $F(0,0)$. Thus

(5.31)

$$\lim_{m\to\infty} \lambda^{-m} \left(\begin{array}{c} \left[\begin{array}{c} F(0,0), F\left(\lambda^m \cos\left(\frac{2(0)\pi}{n}\right), \lambda^m \sin\left(\frac{2(0)\pi}{n}\right)\right), \\ F\left(\lambda^m \cos\left(\frac{2(1)\pi}{n}\right), \lambda^m \sin\left(\frac{2(1)\pi}{n}\right)\right), \\ ..., F\left(\lambda^m \cos\left(\frac{2(n-1)\pi}{n}\right), \lambda^m \sin\left(\frac{2(n-1)\pi}{n}\right)\right) \end{array} \right] \\ -[F(0,0), F(0,0), F(0,0), ..., F(0,0)] \end{array} \right) =$$
$$F_s(0,0) \left[0, 1, \cos\left(\frac{2\pi}{n}\right), \cos\left(\frac{4\pi}{n}\right), ..., \cos\left(\frac{2(n-1)\pi}{n}\right) \right]$$
$$+F_t(0,0) \left[0, 0, \sin\left(\frac{2\pi}{n}\right), \sin\left(\frac{4\pi}{n}\right), ..., \sin\left(\frac{2(n-1)\pi}{n}\right) \right]$$

If we subtract (5.31) from (5.30) we obtain

$$\lim_{m\to\infty} \lambda^{-m} \left([v_0^m, v_1^m, v_2^m, ..., v_n^m] - \left[\begin{array}{c} F(0,0), F\left(\lambda^m \cos\left(\frac{2(0)\pi}{n}\right), \lambda^m \sin\left(\frac{2(0)\pi}{n}\right)\right), \\ F\left(\lambda^m \cos\left(\frac{2(1)\pi}{n}\right), \lambda^m \sin\left(\frac{2(1)\pi}{n}\right)\right), \\ ..., F\left(\lambda^m \cos\left(\frac{2(n-1)\pi}{n}\right), \lambda^m \sin\left(\frac{2(n-1)\pi}{n}\right)\right) \end{array} \right] \right) =$$
$$\left\{ \widetilde{\alpha}_1^{(0)} - F_s(0,0) \right\} \left[0, 1, \cos\left(\frac{2\pi}{n}\right), \cos\left(\frac{4\pi}{n}\right), ..., \cos\left(\frac{2(n-1)\pi}{n}\right) \right]$$
$$+ \left\{ \widetilde{\alpha}_2^{(0)} - F_t(0,0) \right\} \left[0, 0, \sin\left(\frac{2\pi}{n}\right), \sin\left(\frac{4\pi}{n}\right), ..., \sin\left(\frac{2(n-1)\pi}{n}\right) \right]$$

Now we come to the additional assumption mentioned earlier for this case. We will assume that

(5.32)

$$\lim_{m\to\infty}\lambda^{-m}\left(\left[v_0^m,v_1^m,v_2^m,...,v_n^m\right]-\left[\begin{array}{c} F\left(0,0\right),F\left(\lambda^m\cos\left(\frac{2(0)\pi}{n}\right),\lambda^m\sin\left(\frac{2(0)\pi}{n}\right)\right), \\ F\left(\lambda^m\cos\left(\frac{2(1)\pi}{n}\right),\lambda^m\sin\left(\frac{2(1)\pi}{n}\right)\right), \\ ...,F\left(\lambda^m\cos\left(\frac{2(n-1)\pi}{n}\right),\lambda^m\sin\left(\frac{2(n-1)\pi}{n}\right)\right)\end{array}\right]\right)=\mathbf{0}$$

Due to linear independence, this assumption leads to

$$F_s\left(0,0\right)=\widetilde{\alpha}_1^{(0)}$$
$$F_t\left(0,0\right)=\widetilde{\alpha}_2^{(0)}$$

For a particular subdivision scheme, this assumption could be verified through the use of a computer program. Unfortunately we don't know of any other method to characterize this assumption.

Recall that $\widetilde{\mathbf{L}}_i\widehat{\mathbf{R}}_j=\delta\left(i-j\right)$ for $i,j=1,2$. So from (5.26 |p.128) we derive

$$F_s\left(0,0\right)=\mathbf{U}^0\widehat{\mathbf{R}}_1$$
$$F_t\left(0,0\right)=\mathbf{U}^0\widehat{\mathbf{R}}_2$$

Theorem 5.7. *Suppose that an approximating triangular scheme is convergent with limiting surface F that is C^1 at points corresponding to extraordinary vertices. Let $F\left(0,0\right)$ be such a point. Assume (5.32 |p.131). Then for $\widehat{\mathbf{R}}_1,\widehat{\mathbf{R}}_2$ in (5.25 |p.128)*

$$F_s\left(0,0\right)=\mathbf{U}^0\widehat{\mathbf{R}}_1,\qquad F_t\left(0,0\right)=\mathbf{U}^0\widehat{\mathbf{R}}_2$$

5.5.2. Quadrilateral Scheme

The template and subdivision matrix for the extraordinary vertex are the same as with the interpolatory extraordinary case except for the matrices W_n,W and w. See Figure 4.3 on p. 67 for the template and see (4.21 |p.69) for the subdivision matrix.

Here W_n, W, and w will be denoted by

$$(5.33)\quad W_n := \begin{bmatrix} \widetilde{n}_{1,1} & \widetilde{n}_{1,2} \\ \widetilde{n}_{2,1} & \widetilde{n}_{2,2} \end{bmatrix} \qquad W := \begin{bmatrix} W_{1,1} & W_{1,2} \\ W_{2,1} & W_{2,2} \end{bmatrix} \qquad w := \begin{bmatrix} w_{1,1} & w_{1,2} \\ w_{2,1} & w_{2,2} \end{bmatrix}$$

where in addition to the assumption needed in the interpolatory case (4.18 |p.66) we must also assume that

$$\widetilde{n}_{1,1} + W_{1,1} + w_{1,1} = 1$$

These restrictions on the templates are needed to ensure that the left eigenvector for 1 has the format

$$\widetilde{\mathbf{L}}_0 = [1, 0, 1, 0, ..., 1, 0]$$

Just as with the extraordinary interpolatory case, we assume that the t_j are such that λ is an eigenvalue of the 4×4 matrix

$$\begin{bmatrix} J + M\left(z + \frac{1}{z}\right) & K\left(1 + z\right) \\ M\left(1 + \frac{1}{z}\right) & K \end{bmatrix}$$

where $z := e^{\frac{2\pi i}{n}}$ [n equals the valence of the extraordinary vertex] and where J, M, and K are from (4.2 |p.57).

In addition, as with the interpolatory quadrilateral case, if we further restrict our subdivision matrix to a 1-ring neighborhood around the central extraordinary vertex we will arrive at the same pair of left and right eigenvectors of λ as given in (4.23 |p.71) and (4.33 |p.82).

Again, like with the interpolatory case, the *initial* control vector net ($\mathbf{U}^0$) around the irregular vertex [again let us call it $\mathbf{v}_\mathbf{0}^0$] and the vector net after m subdivisions ($\mathbf{U}^m$) can be represented as a linear combination of (possibly generalized) left eigenvectors.

By letting $\left\{\widetilde{\mathbf{L}}_j : 0 \leq j \leq 4n+1\right\}$ be this set of $4n+2$ (possibly generalized) linearly independent left eigenvectors then $\mathbf{U}^0$ and $\mathbf{U}^m$ can be written as

$$\mathbf{U}^0 = \widetilde{\alpha}_0^{(0)}\widetilde{\mathbf{L}}_0 + \widetilde{\alpha}_1^{(0)}\widetilde{\mathbf{L}}_1 + \widetilde{\alpha}_2^{(0)}\widetilde{\mathbf{L}}_2 + \sum_{j=3}^{4n+1} \widetilde{\alpha}_j^{(0)}\widetilde{\mathbf{L}}_j \tag{5.34}$$

$$\mathbf{U}^m = \widetilde{\alpha}_0^{(0)}\widetilde{\mathbf{L}}_0 + \lambda^m\widetilde{\alpha}_1^{(0)}\widetilde{\mathbf{L}}_1 + \lambda^m\widetilde{\alpha}_2^{(0)}\widetilde{\mathbf{L}}_2 + o\left(\lambda^m\right)$$

where we have:

- $\widetilde{\alpha}_j^{(0)} \in \mathbb{R}^3 \quad j = 0, \ldots, 4n+1$
- the left eigenvector for 1 is $\widetilde{\mathbf{L}}_0 = [1, 0, 1, 0, ..., 1, 0]$ and
- $\widetilde{\mathbf{L}}_1, \widetilde{\mathbf{L}}_2$ are the left eigenvectors for λ from (4.23 |p.71).

Hence

$$\lim_{m\to\infty} \mathbf{U}^m = \widetilde{\alpha}_0^{(0)}\widetilde{\mathbf{L}}_0 \tag{5.35}$$

$$\lim_{m\to\infty} \lambda^{-m}\left(\mathbf{U}^m - \widetilde{\alpha}_0^{(0)}\widetilde{\mathbf{L}}_0\right) = \widetilde{\alpha}_1^{(0)}\widetilde{\mathbf{L}}_1 + \widetilde{\alpha}_2^{(0)}\widetilde{\mathbf{L}}_2 \tag{5.36}$$

Let us parametrize the limit surface F locally in a similar fashion as we did for the quadrilateral interpolatory extraordinary case.

Since this is an approximating convergent scheme

$$\lim_{m\to\infty} v_0^m \text{ is a point on the limit surface.}$$

Define $F(0,0) := \lim_{m\to\infty} v_0^m$ Now let us fix $m \in Z_+$. After we subdivide m times we get $2n$ new neighboring vertices around v_0^m. We shall denote the n vertices that share an edge with v_0^m as v_j^m for $j = 1, 2, ..., n$ and the n vertices that are *opposite* v_0^m in each quadrilateral as u_j^m for $j = 1, 2, ..., n$. As we then continue to subdivide beyond m times we get updated vertices for these v_j^m, u_j^m and for v_0^m. Note that since this is an approximating scheme the updated vertices are not the same as the older vertices. Let us denote the updated vertices after k additional subdivisions as $v_j^{m,k}$, $u_j^{m,k}$ respectively. Again for $j = 1, 2, ..., n$ $\lim_{k\to\infty} v_j^{m,k}$ and $\lim_{k\to\infty} u_j^{m,k}$ are points on the limit surface.

For $j = 1, 2, ..., n$ we will parametrize these points as:

$$\lim_{k\to\infty} v_j^{m,k} =: F\left(\lambda^m \cos\left(\frac{2(j-1)\pi}{n}\right), \lambda^m \sin\left(\frac{2(j-1)\pi}{n}\right)\right)$$

$$\lim_{k\to\infty} u_j^{m,k} =: F\left(\begin{array}{c} \frac{\lambda^m}{4\lambda-1}\left[\cos\left(\frac{2(j-1)\pi}{n}\right) + \cos\left(\frac{2(j)\pi}{n}\right)\right], \\ \\ \frac{\lambda^m}{4\lambda-1}\left[\sin\left(\frac{2(j-1)\pi}{n}\right) + \sin\left(\frac{2(j)\pi}{n}\right)\right] \end{array}\right)$$

From (5.35 |p.133),

$$\text{for } j = 0, 1, ..., n \quad \lim_{m\to\infty} v_j^m = \widetilde{\alpha}_0^{(0)}$$

$$\text{for } j = 0, 1, ..., n \quad \lim_{m\to\infty} u_j^m = \widetilde{\alpha}_0^{(0)}$$

Hence we have:

$$\widetilde{\alpha}_0^{(0)} = \lim_{m\to\infty} v_0^m = F(0,0)$$

So from just looking at strictly the odd components of each side of (5.36 |p.133) we obtain

$$\lim_{m\to\infty} \lambda^{-m} \left(\begin{array}{c} [v_0^m, v_1^m, v_2^m, ..., v_n^m, u_1^m, u_2^m, ..., u_n^m] - \\ [F(0,0), F(0,0), F(0,0), ..., F(0,0)] \end{array}\right) = \tag{5.37}$$

$$\widetilde{\alpha}_1^{(0)} \left[\begin{array}{c} 0, 1, \cos\left(\frac{2\pi}{n}\right), \cos\left(\frac{4\pi}{n}\right), ..., \cos\left(\frac{2(n-1)\pi}{n}\right), \\ \frac{1}{4\lambda-1}\left(1 + \cos\left(\frac{2\pi}{n}\right)\right), ..., \frac{1}{4\lambda-1}\left(\cos\left(\frac{2(n-1)\pi}{n}\right) + \cos\left(\frac{2(n)\pi}{n}\right)\right) \end{array}\right]$$

$$+\widetilde{\alpha}_2^{(0)} \left[\begin{array}{c} 0, 0, \sin\left(\frac{2\pi}{n}\right), \sin\left(\frac{4\pi}{n}\right), ..., \sin\left(\frac{2(n-1)\pi}{n}\right), \\ \frac{1}{4\lambda-1}\sin\left(\frac{2\pi}{n}\right), ..., \frac{1}{4\lambda-1}\left(\sin\left(\frac{2(n-1)\pi}{n}\right) + \sin\left(\frac{2(n)\pi}{n}\right)\right) \end{array}\right]$$

By assumption the limit surface is C^1 at the parametrized point $F(0,0)$. Thus

(5.38)

$$\lim_{m\to\infty}\lambda^{-m}\left(\begin{array}{c}\left[\begin{array}{c} F(0,0), F\left(\lambda^m\cos\left(\frac{2(0)\pi}{n}\right),\lambda^m\sin\left(\frac{2(0)\pi}{n}\right)\right), \\ F\left(\lambda^m\cos\left(\frac{2(1)\pi}{n}\right),\lambda^m\sin\left(\frac{2(1)\pi}{n}\right)\right),..., \\ F\left(\lambda^m\cos\left(\frac{2(n-1)\pi}{n}\right),\lambda^m\sin\left(\frac{2(n-1)\pi}{n}\right)\right), \\ F\left(\frac{\lambda^m}{4\lambda-1}\left[\cos\left(\frac{2(0)\pi}{n}\right)+\cos\left(\frac{2(1)\pi}{n}\right)\right],\frac{\lambda^m}{4\lambda-1}\left[\sin\left(\frac{2(0)\pi}{n}\right)+\sin\left(\frac{2(1)\pi}{n}\right)\right]\right),..., \\ F\left(\frac{\lambda^m}{4\lambda-1}\left[\cos\left(\frac{2(n-1)\pi}{n}\right)+\cos\left(\frac{2(n)\pi}{n}\right)\right],\frac{\lambda^m}{4\lambda-1}\left[\sin\left(\frac{2(n-1)\pi}{n}\right)+\sin\left(\frac{2(n)\pi}{n}\right)\right]\right)\end{array}\right] \\ -\left[F(0,0),F(0,0),F(0,0),...,F(0,0)\right]\end{array}\right)=$$

$$F_s(0,0)\left[\begin{array}{c}0,1,\cos\left(\frac{2\pi}{n}\right),\cos\left(\frac{4\pi}{n}\right),...,\cos\left(\frac{2(n-1)\pi}{n}\right), \\ \frac{1}{4\lambda-1}\left[\cos\left(\frac{2(0)\pi}{n}\right)+\cos\left(\frac{2(1)\pi}{n}\right)\right],...,\frac{1}{4\lambda-1}\left[\cos\left(\frac{2(n-1)\pi}{n}\right)+\cos\left(\frac{2(n)\pi}{n}\right)\right]\end{array}\right]$$

$$+F_t(0,0)\left[\begin{array}{c}0,0,\sin\left(\frac{2\pi}{n}\right),\sin\left(\frac{4\pi}{n}\right),...,\sin\left(\frac{2(n-1)\pi}{n}\right), \\ \frac{1}{4\lambda-1}\left[\sin\left(\frac{2(0)\pi}{n}\right)+\sin\left(\frac{2(1)\pi}{n}\right)\right],...,\frac{1}{4\lambda-1}\left[\sin\left(\frac{2(n-1)\pi}{n}\right)+\sin\left(\frac{2(n)\pi}{n}\right)\right]\end{array}\right]$$

Just as in the triangular approximating case, if we subtract (5.38) from (5.37) and if we assume

(5.39)

$$\lim_{m\to\infty}\lambda^{-m}\left(\begin{array}{c}\left[v_0^m,v_1^m,v_2^m,...,v_n^m,u_1^m,...,u_n^m\right]- \\ \left[\begin{array}{c} F(0,0), F\left(\lambda^m\cos\left(\frac{2(0)\pi}{n}\right),\lambda^m\sin\left(\frac{2(0)\pi}{n}\right)\right), \\ F\left(\lambda^m\cos\left(\frac{2(1)\pi}{n}\right),\lambda^m\sin\left(\frac{2(1)\pi}{n}\right)\right),..., \\ F\left(\lambda^m\cos\left(\frac{2(n-1)\pi}{n}\right),\lambda^m\sin\left(\frac{2(n-1)\pi}{n}\right)\right), \\ F\left(\begin{array}{c}\frac{\lambda^m}{4\lambda-1}\left[\cos\left(\frac{2(0)\pi}{n}\right)+\cos\left(\frac{2(1)\pi}{n}\right)\right], \\ \frac{\lambda^m}{4\lambda-1}\left[\sin\left(\frac{2(0)\pi}{n}\right)+\sin\left(\frac{2(1)\pi}{n}\right)\right]\end{array}\right),..., \\ F\left(\begin{array}{c}\frac{\lambda^m}{4\lambda-1}\left[\cos\left(\frac{2(n-1)\pi}{n}\right)+\cos\left(\frac{2(n)\pi}{n}\right)\right], \\ \frac{\lambda^m}{4\lambda-1}\left[\sin\left(\frac{2(n-1)\pi}{n}\right)+\sin\left(\frac{2(n)\pi}{n}\right)\right]\end{array}\right)\end{array}\right]\end{array}\right)=\mathbf{0}$$

then by linear independence

$$F_s(0,0) = \widetilde{\alpha}_1^{(0)}$$
$$F_t(0,0) = \widetilde{\alpha}_2^{(0)}$$

Again, as with the triangular case, this assumption could be verified for any particular subdivision scheme through the use of a computer program.

Recall that $\widetilde{\mathbf{L}}_i\widehat{\mathbf{R}}_j = \delta(i-j)$ for $i, j = 1, 2$. So from (5.34 |p.133) we derive

$$F_s(0,0) = \mathbf{U}^0\widehat{\mathbf{R}}_1$$
$$F_t(0,0) = \mathbf{U}^0\widehat{\mathbf{R}}_2$$

Theorem 5.8. *Suppose that an approximating quadrilateral scheme is convergent with limiting surface F that is C^1 at points corresponding to extraordinary vertices. Let $F(0,0)$ be such a point. Assume (5.39 |p.135). Then for $\widehat{\mathbf{R}}_1, \widehat{\mathbf{R}}_2$ in (4.33 |p.82)*

$$F_s(0,0) = \mathbf{U}^0\widehat{\mathbf{R}}_1, \qquad F_t(0,0) = \mathbf{U}^0\widehat{\mathbf{R}}_2$$

5.5.3. "Visual C^1" Templates

5.5.3.1. Triangular. In [**CJ08**], Chui/Jiang develop a template for an extraordinary vertex of a 1-ring triangular approximating scheme. Referring to Q_n and Q in (5.24 |p.127), they set

$$Q := \begin{bmatrix} a & -a \\ a & -a \end{bmatrix} \qquad Q_n := \begin{bmatrix} 1-a & a \\ x_3 & x_4 \end{bmatrix}$$

where $a = \frac{5}{8} - \left(\frac{3}{8} + \frac{1}{4}\cos\frac{2\pi}{n}\right)^2$ [the weight used in Loop's scheme [**Loo87**]] and x_3, $x_4 \in \mathbb{R}$.

Chui/Jiang found that the eigenvalues of the upper left block in M_0 in (3.42 |p.44) would be given by 1, $\frac{1}{8}$, and

$$\widetilde{\lambda}_\pm := \frac{5}{16} + \frac{x_4 - a}{2} \pm \frac{1}{16}\sqrt{64a^2 - 176a + 128ax_4 + 25 - 80x_4 + 64x_4^2 + 256ax_3}$$

Choices can be made for x_3 and x_4 such that the eigenvalues of the subdivision matrix $S1_n$ (3.33 |p.38) satisfy $\lambda_0 = 1$, $\lambda_1 = \lambda_2$, with $|\lambda_1 < 1|$ and $|\lambda_j| < |\lambda_1|$, $j = 3, 4, ...$

One such choice was to set $\widetilde{\lambda}_+ := \left(\frac{3}{8} + \frac{1}{4}\cos\frac{2\pi}{n}\right)^2$ [where we then obtain that $x_3 = \frac{3}{8}$] and $\widetilde{\lambda}_- = x_4$ for a sufficiently small value of x_4.

Meshes are formed by subdividing an initial control set of points in $\mathbb{R}^2$ whose coordinates are the 2 left eigenvectors of the subdominant eigenvalue λ. The extraordinary scheme is shown to be "visually" C^1 in the sense that these 2-D meshes shown in [**CJ08**] suggest the regularity and injectivity properties of the characteristic map.

As discussed earlier, the right eigenvectors of λ have the same formula as in the interpolatory triangular extraordinary case. However, the value of d_2 (3.46 |p.48)will differ since we would use t_1,t_2 and h values from the corresponding (regular) approximating triangular scheme.

Using the t_1, t_2 and h values from (5.20 |p.115) we obtain that $d_2 = 1$ no matter what the valence is for the extraordinary vertex.

So from (3.48 |p.115), (3.47 |p.48) and for $n = 5$

$$\widehat{\mathbf{R}}_1 = \frac{2}{5}\left[0, 0, 1, 1, \cos\left(\frac{2\pi}{5}\right), \cos\left(\frac{2\pi}{5}\right), ..., \cos\left(\frac{8\pi}{5}\right), \cos\left(\frac{8\pi}{5}\right)\right]^T$$

$$\widehat{\mathbf{R}}_2 = \frac{2}{5}\left[0, 0, 0, 0, \sin\left(\frac{2\pi}{5}\right), \sin\left(\frac{2\pi}{5}\right), ..., \sin\left(\frac{8\pi}{7}\right), \sin\left(\frac{8\pi}{7}\right)\right]^T$$

See Figure 5.8 for a visual representation of the two first partial derivatives.

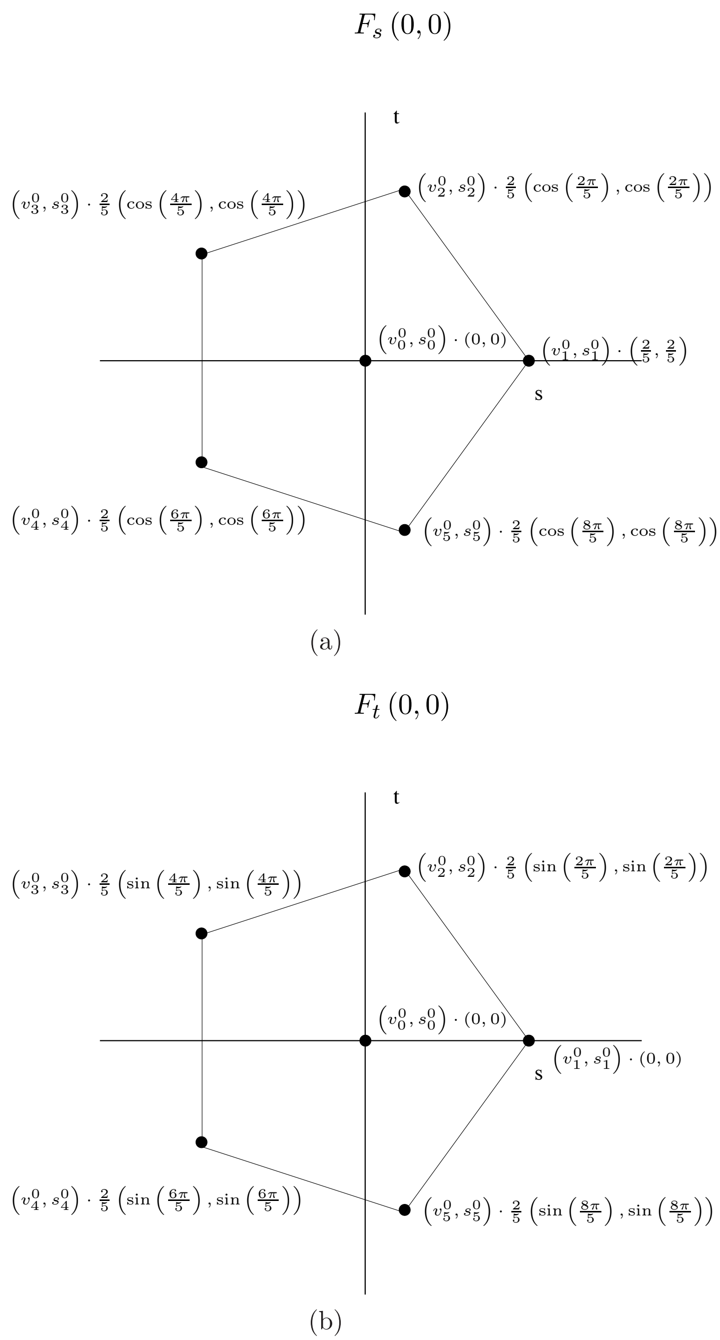

Figure 5.8. The above diagrams represent F_s and F_t for a specific triangular approximating scheme developed by Chui/Jiang in [**CJ08**]. Valence = 5.

5.5.3.2. Quadrilateral. To accompany the *regular* approximating quadrilateral template (5.7 |p.94), we propose the following specific template for an extraordinary vertex. Referring to the matrices in (5.33 |p.132), let

$$W_n = \begin{bmatrix} 1-\beta\left[t_9+t_{10}\right) & \frac{\beta}{4}\left[4t_3+h\left(-\frac{1}{2}+8t_4+8t_5+2t_6\right)\right] \\ \frac{\beta}{4}\left[-\frac{4}{h}t_{10}-\frac{2}{h}t_9-4t_8-4t_7\right] & \frac{\beta}{4}\left(t_6\right) \end{bmatrix}$$

$$W = \beta\begin{bmatrix} t_9 & -t_3-\frac{1}{4}\left(4t_3+h\left(-\frac{1}{2}+8t_4+8t_5+2t_6\right)\right) \\ t_7 & t_5 \end{bmatrix}$$

$$w = \beta\begin{bmatrix} t_{10} & t_3 \\ t_8 & t_4 \end{bmatrix}$$

where $\beta = 4$ if $n = 3$ else $\beta = \frac{16}{n}$. Note that if $n = 4$ then these revert to the matrices for the regular mask.

This template appears satisfactory for three reasons. The first is that the leading eigenvalues of the subdivision matrix $S1_n$ (4.21 |p.69) satisfy the conditions (4.36 |86) for valences 3 to (at least) 16. See Appendix D on p. 213 for a listing of the eigenvalues for each of these valences.

The second is the appearance of the 2-D meshes formed by performing 4 subdivisions on an initial control set of points in $\mathbb{R}^2$ whose coordinates are the two left eigenvectors of the subdominant eigenvalue λ. These meshes were first introduced in [**Rei95**] and were seen again in [**CJ08**]. The meshes shown in Appendix E on p. 218 suggest the regularity and injectivity of the characteristic map.

As discussed earlier, the right eigenvectors of λ have the same formula as in the *interpolatory* quadrilateral extraordinary case. However, the values of d_2, d_3, and d_4 (4.32 |p.81) will differ since we would use the values of t_1,t_2 and h (5.23 |p.123) from the corresponding (regular) approximating quadrilateral scheme.

Using such t_1, t_2 and h values we obtain for $n = 5$

$$d_2 = -.3124965340$$

$$d_3 = .2727224604 - .1981444659i$$

$$d_4 = -.1136337283 + .08255973628i$$

So from (4.33 |p.82) we have:

$$\widehat{\mathbf{R}}_1 = \begin{bmatrix} 0, 0, .2749, -.08597, .08492, -.02656, -.2224, .06954, -.2224, .06954, .08492, -.02656, \\ .074978, -.03127, -.02864, .01194, -.09266, .03864, -.02864, .01194, .07497, -.03125 \end{bmatrix}^T$$

$$\widehat{\mathbf{R}}_2 = \begin{bmatrix} 0, 0, 0, 0, .2614, -.08176, .1616, -.05053, -.1616, .05053, -.2614, .08176, \\ .05447, -.02270, .08816, -.03672, 0, 0, -.08816, .03672, -.05447, .02270 \end{bmatrix}^T$$

See Figure 5.9 on p. 141 for a visual representation of these two first partial derivatives.

See Figures 5.11 and 5.12 on p. 143 and p. 143 that show a subdivision surface for this quadrilateral scheme. The original polyhedron is shown in Figure 5.10 on p. 142. These figures suggest C^1 at the extraordinary vertices.

$F_s\,(0,0)$

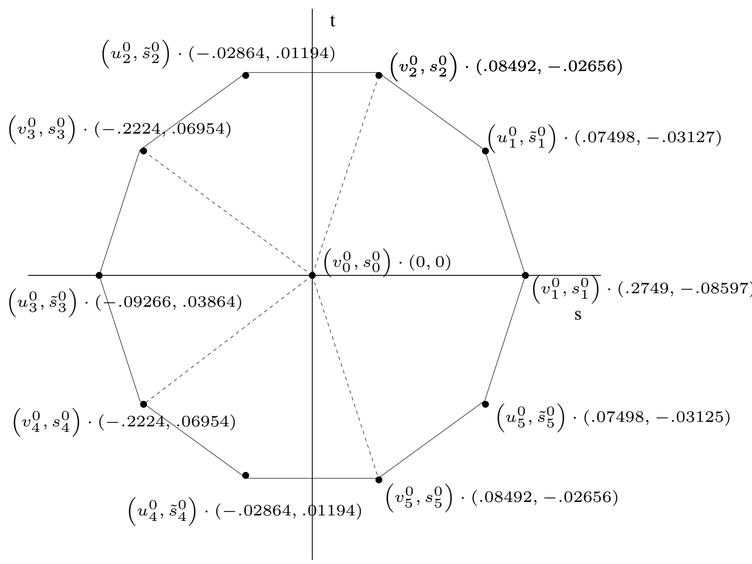

(a)

$F_t\,(0,0)$

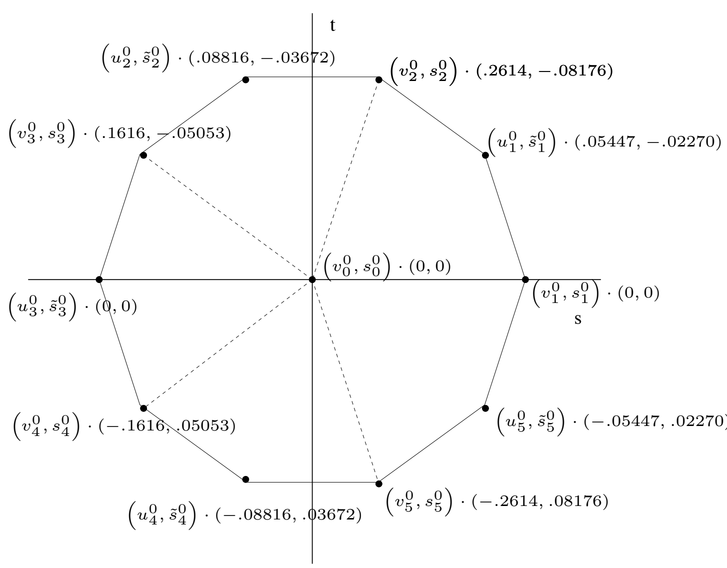

(b)

Figure 5.9. The above diagrams represent F_s and F_t for our specific quadrilateral approximating scheme. Valence = 5.

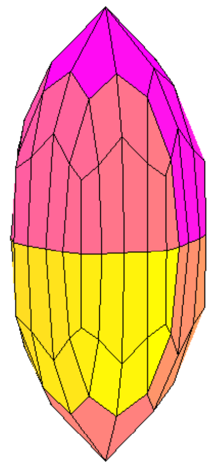

Figure 5.10. Approximating quadrilateral scheme: Original Polyhedron

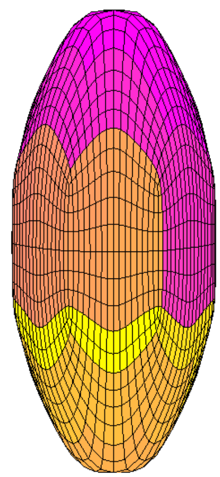

Figure 5.11. Approximating quadrilateral surface

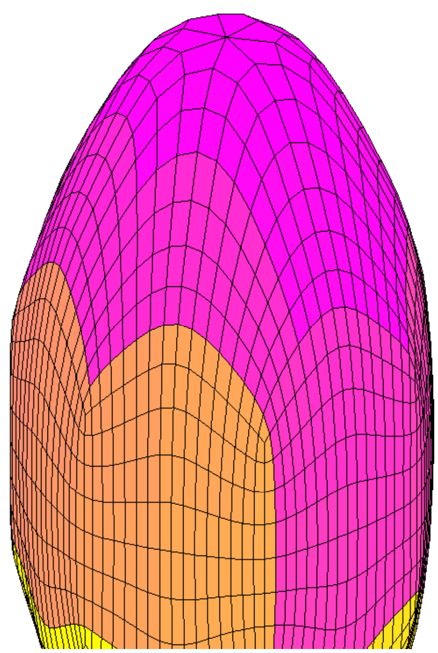

Figure 5.12. Approximating quadrilateral scheme: Closeup of subdivision surface

CHAPTER 6

Shape Parameters

6.1. Background

Parameters have been used to improve the smoothness of subdivision curves and surfaces at least as far back as 1987 when Dyn and Levin ([**DLG87**]) showed that for a certain range of parameter values a 4-point interpolatory subdivision curve is C^1. Later in 1998, Shenkman, Dyn and Levin [**SDL99**] demonstrated that the Butterfly scheme is C^1 at irregular vertices [valence 4 through 10] for a certain range of parameter values that are part of its mask. We have already mentioned the use of free variables [parameters] to arrive at a certain Sobolev smoothness for the surface generated by the regular mask [**CJ05**], [**JO03**].

We have found two articles in the literature that specifically use the term "shape parameter" that are different than how the term is used here [**GZC07**], [**MA10**]. In [**MA10**], Mustafa and Ashraf showed that for certain ranges of a "shape parameter" w that is part of the scalar mask, a 6-point ternary interpolatory subdivision scheme will generate either a C^0, C^1, or C^2 curve. In [**GZC07**] 3 "shape parameters" are introduced in a Doo-Sabin surface: one is for the scale of the type-V face and the other two perturb the normal vector of the type-V face. [The type-V face is a face that contains a vertex.]

Here we use the term "shape parameter" as initially used by Chui/Jiang in [**CJ03b**]. Our initial vector "net" is defined as collection of row vectors $\{\mathbf{v}_{\mathbf{k}}^0\}_{\mathbf{k}}$

$$\mathbf{v}_{\mathbf{k}}^0 := \left[v_{1,\mathbf{k}}^0, v_{2,\mathbf{k}}^0, ..., v_{n,\mathbf{k}}^0\right]$$

Each component is a "point" in 3-D where the first component is used for the position of the subdivision vertices and the remaining components provide up to $3\,(n-1)$ parameters for shape control. Throughout this paper, $n = 2$ and the initial shape control vertex is represented as $s^0_{\mathbf{k}}$ instead of as $v^0_{2,\mathbf{k}}$. We see how the limiting subdivision surface is influenced by $\{s^0_{\mathbf{k}}\}_{\mathbf{k}}$ in (2.9 |p.13).

In [**CJ06**] it was proposed that the shape control parameters be related to the vectors for the sum rule order of the subdivision mask. And in [**CJ08**] observations were made that for a 1-ring interpolatory triangular subdivision the corresponding shape parameter s^0_j for an initial "corner-type" vertex v^0_j could be defined as $-t_j v_j$ for some suitable $t_j \in (0, 2]$.

In the following we will discuss a geometric method to formulate these initial shape control parameters $\{s^0_{\mathbf{k}}\}_{\mathbf{k}}$.

6.2. Definition based on discrete normal

We are utilizing discrete normals to formulate our initial shape control parameters. Here we are extending what was done in the 1-D setting by Jiang/Smith in [**JS09**]. Discrete normals have in the past been used as part of the subdivision process. See [**Yan06**] and [**Yan05**] for the 1-D case and 2-D case respectively. In fact, the methods in [**JS09**] were in part based on the work done in [**Yan06**].

So we will have a geometric definition of the initial shape vertices (parameters). We will see that this definition

- can be fairly easily implemented using computer programming
- provides for surfaces that appear free of wavy artifacts
- has a foundation in differential geometry.

In [**JS09**] shape parameters were formulated for a C^2 3-point subdivision scheme that produces planar curves. To formulate a shape parameter at an initial vertex $\mathbf{v}_j$ of the polygon, the basic idea was to use a projection of one of the two neighboring edges onto a well-defined discrete unit normal at that vertex and then multiply the resulting vector by a scalar ω_j. Values of w_j ranging between $-.5$ and $+.3$ produced curves that appeared satisfactory.

Working with triangular surfaces, Yang in [**Yan05**] used projections of edges onto vertex (discrete) normals to determine a suitable new edge midpoint. Figure 6.1 shows one of the triangular edges that has vertices $v^0_{\mathbf{k}}$ and $p^0_{\mathbf{i}}$ at each end. Using a weighted average of the normals to each adjoining face, he constructs a discrete unit normal at the two end vertices. The new edge vertex then equals the sum of the midpoint of the edge and the sum of the projection of each half of the edge onto the two normals. That sum is then weighted by a free parameter ω. See (6.1) and Figure 6.1. Yang found that for ω between 0.2 and 0.4 the interpolatory surface generated by this "normal based subdivision" is G^1 smooth (i.e. it has tangent plane continuity).

$$
\begin{aligned}
v^0_{\mathbf{2k}+1} &= \frac{1}{2}\left(v^0_{\mathbf{k}} + p^0_{\mathbf{i}}\right) + \omega\left(d_v n_v + d_i n_i\right) \\
d_v &= \frac{1}{2}\left(v^0_{\mathbf{k}} - p^0_{\mathbf{i}}\right) \cdot n_v \\
d_i &= \frac{1}{2}\left(p^0_{\mathbf{i}} - v^0_{\mathbf{k}}\right) \cdot n_i
\end{aligned}
\tag{6.1}
$$

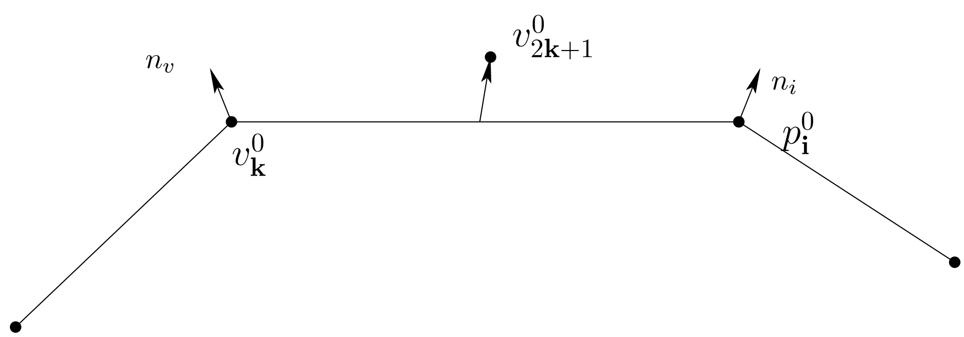

Figure 6.1. Shows the method used in [**Yan05**] to obtain a new edge vertex. Note that discrete normals are used.

With this method in mind, we will use specially calculated discrete normals at the initial vertices as a *basis* for the initial shape control parameters.

First we need to determine a "reasonable" definition for such a discrete normal for both our triangular case and our quadrilateral case.

6.3. Discrete Normal for Triangular Mesh Surfaces

In differential geometry, the *mean curvature normal* at a point P on a surface M is

$$\kappa_H \overrightarrow{\mathbf{n}}_P \tag{6.2}$$

where [[**O'N06**]]

- $\overrightarrow{\mathbf{n}}_P$ is a unit normal vector to M at P
- $\kappa_H := \frac{k_1+k_2}{2}$ and
- k_1, k_2 are the maximum and minimum values of the normal curvature of M at P.

The mean curvature normal is related to the Laplacian or the more general Laplace-Beltrami operator on M. If our surface is parametrized by a mapping $\mathbf{x}(s,t)$ such that $\mathbf{x}_s \cdot \mathbf{x}_t = 0$, $\mathbf{x}_s \cdot \mathbf{x}_s = 1$, and $\mathbf{x}_t \cdot \mathbf{x}_t = 1$ [s,t are then called *conformal* parameters [**DHKW92**]] we then have [see also [**DHKW92**]]

$$2\kappa_H \overrightarrow{\mathbf{n}} = \mathbf{x}_{ss} + \mathbf{x}_{tt} \tag{6.3}$$

where $\mathbf{x}_{ss} + \mathbf{x}_{tt}$ is a form of the Laplace-Beltrami operator on a surface.

In [**MDSB02**] the Laplace-Beltrami operator is denoted by $\mathbf{K}(P)$ where P is the point on the surface. We shall also use this notation for the Laplace-Beltrami operator. Recall that *here* our surface M is a complex of discrete triangular meshes. Let our point P be denoted by vertex $\mathbf{x}_i$. For *each* of the surrounding triangles we define an area as follows [**MDSB02**]:

- If the triangle is non-obtuse, then the area is the area of the quadrilateral bounded by the vertex $\mathbf{x}_i$, the two midpoints of each side of the triangle that has $\mathbf{x}_i$ as an endpoint and by the circumcenter of the triangle. Note that the circumcenter of a triangle is the point where the three perpendicular bisectors of each side meet. See Figure 6.2.

- If the triangle has an obtuse angle *and* if that obtuse angle is at the vertex $\mathbf{x}_i$, then the area in the triangle is the same as before except that we now use the *midpoint* of the side opposite the vertex [instead of the circumcenter].

- Finally if the non-obtuse angle is *not* at the vertex, then the area in the triangle is the area of the triangle whose three vertices are the vertex $\mathbf{x}_i$ and the two midpoints of each side of the triangle that has $\mathbf{x}_i$ as an endpoint.

Using the notation of [**MDSB02**] we will denote the sum of *all* these areas surrounding the vertex $\mathbf{x}_i$ by $\mathcal{A}_M$.

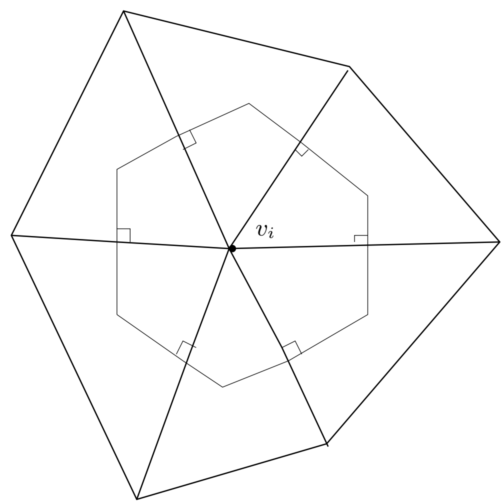

Figure 6.2. Method used in [**MDSB02**] to denote a quadrilateral area in an adjoining triangle if the triangle is non-obtuse. One corner of the quadrilateral is the *circumcenter* of the triangle.

So we have

$$\iint_{\mathcal{A}_M} \mathbf{K}(\mathbf{x})\, dA = \iint_{\mathcal{A}_M} \mathbf{x}_{ss} + \mathbf{x}_{tt}\, ds\, dt$$

and using Green's theorem in normal form [see [**Str10**]] that turns the Laplacian over a region into a line integral of the gradient over the boundary of the region:

$$\iint_{\mathcal{A}_M} \mathbf{x}_{ss} + \mathbf{x}_{tt}\, ds\, dt = \iint_{\mathcal{A}_M} \nabla \cdot \nabla_{s,t}\mathbf{x}\, ds\, dt = \int_{\partial\mathcal{A}_M} \nabla_{s,t}\mathbf{x} \cdot \mathbf{n}_{s,t}\, dl$$

where $\nabla_{s,t}\mathbf{x}$ is the gradient of the surface and $\mathbf{n}_{s,t}$ is the outer unit normal to the border $\partial\mathcal{A}_M$ with respect to the s, t parameter space.

In [**MDSB02**], Meyer et al derive that

$$\int_{\partial\mathcal{A}_M} \nabla_{s,t} \cdot \mathbf{n}_{s,t}\, dl = \frac{1}{2} \sum_{j \in N_1(i)} \left(\cot \alpha_{ij} + \cot \beta_{ij}\right)\left(\mathbf{x}_j - \mathbf{x}_i\right)$$

where $N_1(i)$ are all the subscripts of the 1-ring neighboring vertices surrounding $\mathbf{x}_i$ and α_{ij}, β_{ij} are the two angles *opposite* to the edge in the two triangles sharing the edge $\overline{\mathbf{x}_j\mathbf{x}_i}$. See Figure 6.3.

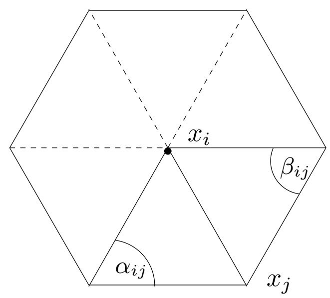

Figure 6.3. Diagram of angles opposite the common side $\overline{\mathbf{x}_j\mathbf{x}_i}$ as done in [**MDSB02**]

Hence

$$\iint_{\mathcal{A}_M} \mathbf{K}(\mathbf{x})\, dA = \frac{1}{2} \sum_{j \in N_1(i)} \left(\cot \alpha_{ij} + \cot \beta_{ij}\right)\left(\mathbf{x}_j - \mathbf{x}_i\right) \tag{6.4}$$

Using (6.4) the *discrete* mean curvature normal operator at a vertex $\mathbf{x}_i$ of a triangular mesh is then defined in [**MDSB02**] as

$$\mathbf{K}(\mathbf{x}_i) := \frac{1}{2\mathcal{A}_M} \sum_{j \in N_1(i)} \left(\cot \alpha_{ij} + \cot \beta_{ij}\right)\left(\mathbf{x}_i - \mathbf{x}_j\right) \tag{6.5}$$

Hence the discrete *unit* normal at the vertex $\mathbf{x}_i$ is

$$\frac{\mathbf{K}(\mathbf{x}_i)}{\|\mathbf{K}(\mathbf{x}_i)\|} \tag{6.6}$$

For triangular mesh surfaces we will be using the definition in (6.6) for the discrete unit normal at a vertex $\mathbf{x}_i$.

Note that from (6.3 |p.147) and (6.5), Meyer in [**MDSB02**] obtains a formula to define the *discrete mean curvature* at a vertex $\mathbf{x}_i$

$$\kappa_H := \frac{1}{\mathcal{A}_M} \sum_{j \in N_1(i)} \left[\frac{1}{8} (\cot \alpha_{ij} + \cot \beta_{ij}) \left\| \mathbf{x}_i - \mathbf{x}_j \right\|^2 \right] \kappa_{i,j}^N \tag{6.7}$$

where $\kappa_{i,j}^N$ is an estimate of the normal curvature in the direction of the edge $\mathbf{x}_i\mathbf{x}_j$ given by

(6.8)

$$\kappa_{i,j}^N = 2 \frac{(\mathbf{x}_i - \mathbf{x}_j) \cdot \mathbf{n}}{\left\| \mathbf{x}_i - \mathbf{x}_j \right\|^2} \quad \text{for } \mathbf{n} = \text{ the discrete unit normal in (6.6 |p.149)}$$

In [**MDSB02**] it was reported that (6.7 |p.150) had a low average percent error when compared to second-order accurate Finite Difference operators on discrete meshes for approximating curvature on simple surfaces where the curvature is known analytically.

In [**Xu04**] it is shown that under certain conditions the discrete Laplace-Beltrami operator in (6.5 |p.149) converges to the actual Laplace-Beltrami operator. Hence, under these same conditions, the discrete mean curvature normal converges to the actual mean curvature normal.

6.4. Discrete Normal for Quadrilateral Mesh Surfaces

As noted in [**LXZ08**] we could use the above methods for quadrilateral meshes if we subdivide each quadrilateral into two triangles. However, since a quadrilateral may not be located on a plane, two ways of subdividing a quadrilateral into triangles can lead to two different computational results [two different discrete normals] if we apply the methods from subsection 6.3. So in [**LXZ08**], Liu et al use a different computational method to define the discrete mean curvature normal in the case of quadrilateral mesh surfaces in $\mathbb{R}^3$.

In such a case, Liu first defines a bilinear parametric surface S_j that interpolates the four vertices, $\{p_i,\ p_j,\ p_{j+1},\ p_{j'}\}$, of the quadrilateral (see Figure 6.4):

(6.9)

$$S_j(s,t) := (1-s)(1-t)\,p_i + t(1-s)\,p_j + s(1-t)\,p_{j+1} + (st)\,p_{j'} \quad (s,t) \in [0,1]^2$$

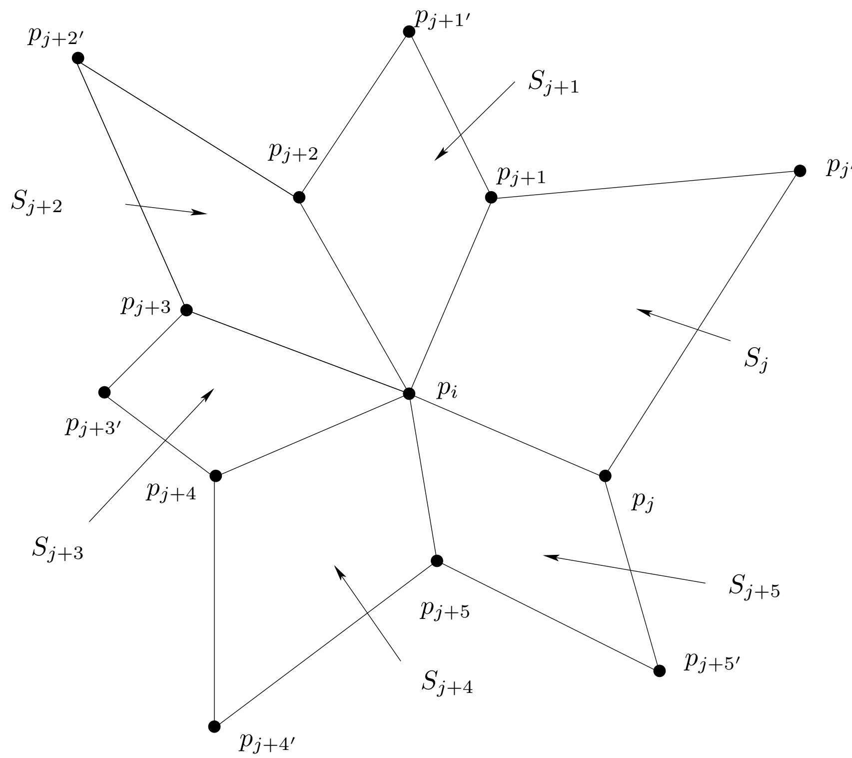

Figure 6.4. Diagram of quadrilaterals and their vertices around vertex p_i. S_j are from (6.9 |p.150).

Liu uses the formula in differential geometry

$$\lim_{diam(R)\to 0} \frac{2\nabla A}{A} = -\kappa_H \overrightarrow{\mathbf{n}}_P =: -H(P)$$

where

- $\kappa_H \overrightarrow{\mathbf{n}}_P$ [mean curvature normal] is from (6.2 |p.146)
- A is the area of a region R around point P
- ∇A is the gradient of A with respect to the (x, y, z) coordinates of P and
- $H(P)$ is notation for the mean curvature normal at P

From this starting point the *discrete mean curvature normal* at point p_i is derived to be

$$H(p_i) := \frac{2}{A(p_i)} \sum_j \left[\alpha_j (p_j - p_i) + \beta_{j+1} (p_{j+1} - p_i) + \gamma_{j'} (p_{j'} - p_i)\right] \tag{6.10}$$

where $A(p_i)$ is the total area of the quadrilaterals around p_i, and is given by

$$A(p_i) = \sum_j A_j$$

and where

$$\begin{aligned}
A_j &= \sqrt{\|S_s\|^2 \|S_t\|^2 - \langle S_s, S_t \rangle^2} \\
S_s &= \frac{1}{2}(p_{j+1} - p_i) + \frac{1}{2}(p_{j'} - p_j) \\
S_t &= \frac{1}{2}(p_j - p_i) + \frac{1}{2}(p_{j'} - p_{j+1}) \\
\alpha_j &= \frac{\|S_s\|^2 - \|S_t\|^2}{4A_j} \\
\beta_{j+1} &= \frac{\|S_t\|^2 - \|S_s\|^2}{4A_j} \\
\gamma_{j'} &= \frac{\|S_s - S_t\|^2}{4A_j}
\end{aligned}$$

In [**LXZ08**] it is shown that the discrete mean curvature normal given in (6.10 |p.151) converges to the actual mean curvature normal given certain conditions that include that the vertices interpolate a sufficiently smooth surface.

Hence for quadrilateral meshes we will use

$$\frac{H(p_i)}{\|H(p_i)\|}$$

as the discrete unit normal at vertex p_i.

6.5. Formulation of Shape Parameters for Triangular Meshes

We will now formulate our shape parameters for both the triangular and quadrilateral meshes. Examples will be given on sample meshes that indicate the feasibility of these formulations. A geometric interpretation will also be given.

First we will consider shape parameters of our 1-ring triangular scheme (either interpolatory or approximating).

For the triangular case (either interpolatory or approximating) we now will develop initial shape parameters that generate a "suitable" new edge point. Using the top template of Figure 2.1 on p. 15 along with the local averaging rule, we can derive the following formula for the new edge vertex (here denoted as $v^1_{\mathbf{2k+m}}$) [See Figure 6.5]:

(6.11)

$$v^1_{\mathbf{2k+m}} = 2b_{1,1}\left(\frac{v^0_{\mathbf{k}} + v^0_{\mathbf{l}}}{2}\right) + 2c_{1,1}\left(\frac{v^0_{\mathbf{i}} + v^0_{\mathbf{j}}}{2}\right) + b_{2,1}\left(s^0_{\mathbf{k}} + s^0_{\mathbf{l}}\right) + c_{2,1}\left(s^0_{\mathbf{i}} + s^0_{\mathbf{j}}\right)$$

where $\mathbf{i}, \mathbf{j}, \mathbf{k}, \mathbf{l}, \mathbf{m} \in \mathbb{Z}^2$.

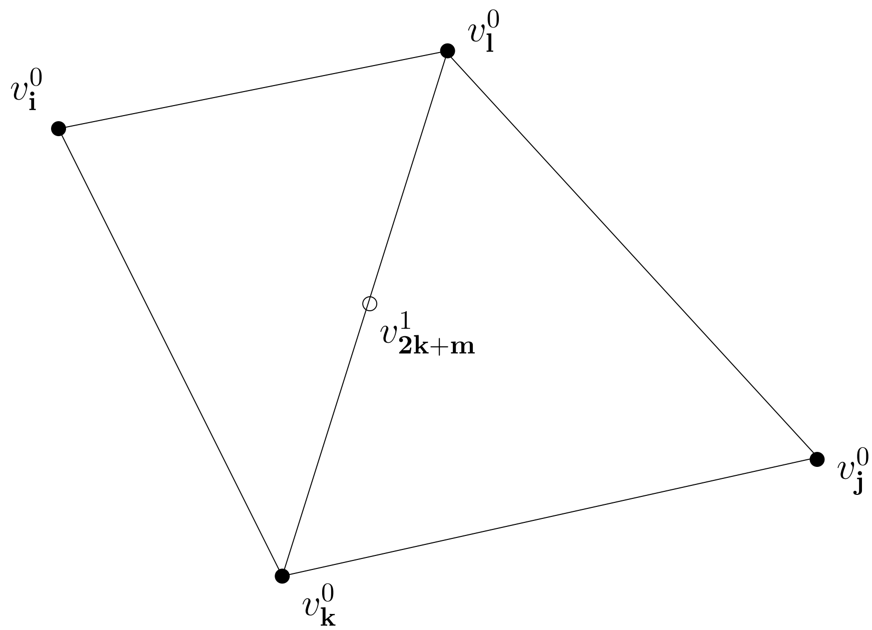

Figure 6.5. Diagram of new edge vertex for a triangular scheme

In [**Yan05**], Yang computed the new edge vertex in a triangular scheme as the sum of the midpoint of the two edge vertices plus projections of that same edge onto discrete unit normals of its two end vertices. Similarly, we will formulate the new edge vertex $v^1_{\mathbf{2k+m}}$ as equal to

- a "weighted midpoint" of the 4 vertices of the two triangles (the first two terms in (6.11)) plus

- a certain linear combination of projections of edges onto the *discrete* unit normals (6.6 |p.149) of the four surrounding vertices (the last two terms in (6.11)).

The shape parameters $\left\{s_{\mathbf{k}}^0,\ s_{\mathbf{l}}^0,\ s_{\mathbf{i}}^0,\ s_{\mathbf{j}}^0\right\}$ *will be* these linear combinations of edge projections onto the discrete unit normals of the respective corresponding vertices.

For the following we will be developing the shape parameter $s_{\mathbf{i}}^0$ corresponding to the vertex $v_{\mathbf{i}}^0$. We will assume that $v_{\mathbf{i}}$ has a valence $k_{\mathbf{i}}$ and so has $k_{\mathbf{i}}$ adjacent edges. This vertex has a discrete outer directed unit normal $\mathbf{n}_{\mathbf{i}}$ as defined by (6.6 |p.149). If we want to use projections of edges onto the unit normals, then we must use *all* $k_{\mathbf{i}}$ adjoining edges in our formulation of the shape parameter. Thus define

$$d_{\mathbf{i},\mathbf{j}} := \frac{1}{2}\left(v_{\mathbf{i}}^0 - v_{\mathbf{j}}^0\right) \cdot \mathbf{n}_{\mathbf{i}} \tag{6.12}$$

where $\left\{v_{\mathbf{j}}^0\right\}_{\mathbf{j}}$ are the $k_{\mathbf{i}}$ adjacent vertices to $v_{\mathbf{i}}$ and we use the factor $\frac{1}{2}$ as in (6.1 |p.146) from [**Yan05**].

We will average these projections. Hence we will use

$$\frac{1}{k_{\mathbf{i}}} \sum_{\mathbf{j}} d_{\mathbf{i},\mathbf{j}}$$

in our formula for the shape parameter $s_{\mathbf{i}}$.

The resulting vector that we obtain from projecting these averages onto the discrete unit normal $\mathbf{n}_{\mathbf{i}}$ is

$$\left[\frac{1}{k_{\mathbf{i}}} \sum_{\mathbf{j}} d_{\mathbf{i},\mathbf{j}}\right] \mathbf{n}_{\mathbf{i}} \tag{6.13}$$

Notice in (6.11 |p.153) that the shape parameters are either multiplied by $b_{2,1}$ or by $c_{2,1}$. Similarly [see (6.14)] when we *update* existing *regular* vertices in the triangular *approximating* scheme the shape parameters are either multiplied by $p_{2,1}$ or by $d_{2,1}$ from (2.10 |p.13). If the vertex to be updated is extraordinary (let's call it v_0^0) then the shape parameters are multiplied by $w_{2,1}$ and $\frac{1}{n}\, q_{2,1}$ from (5.24 |p.127). See (6.15).

$$v^1_{2\mathbf{k}} = p_{1,1} v^0_{\mathbf{k}} + d_{1,1} \begin{pmatrix} v^0_{\mathbf{k}+[1\ 0]^T} + v^0_{\mathbf{k}+[1\ 1]^T} + v^0_{\mathbf{k}+[0\ 1]^T} \\ +v^0_{\mathbf{k}+[-1\ 0]^T} + v^0_{\mathbf{k}+[-1\ -1]^T} + v^0_{\mathbf{k}+[0\ -1]^T} \end{pmatrix} + p_{2,1} s^0_{\mathbf{k}} + d_{2,1} \begin{pmatrix} s^0_{\mathbf{k}+[1\ 0]^T} + s^0_{\mathbf{k}+[1\ 1]^T} + s^0_{\mathbf{k}+[0\ 1]^T} \\ +s^0_{\mathbf{k}+[-1\ 0]^T} + s^0_{\mathbf{k}+[-1\ -1]^T} + s^0_{\mathbf{k}+[0\ -1]^T} \end{pmatrix} \tag{6.14}$$

$$v^1_0 = w_{1,1} v^0_0 + \frac{1}{n} q_{1,1} \begin{pmatrix} v^0_1 + v^0_2 + v^0_3 \\ +\ldots + v^0_{n-2} + v^0_{n-1} + v^0_n \end{pmatrix} + w_{2,1} s^0_0 + \frac{1}{n} q_{2,1} \begin{pmatrix} s^0_1 + s^0_2 + s^0_3 \\ +\ldots + s^0_{n-2} + s^0_{n-1} + s^0_n \end{pmatrix} \tag{6.15}$$

Since we want a new edge point (and in addition any *updated* vertex) to mainly reflect the average of the projections onto the unit normal we will now multiply our formula (6.13 |p.154) by the factor $\frac{1}{\gamma_{\mathbf{i}}}$ such that

- $\gamma_{\mathbf{i}}$ = the element of $\{p_{2,1}, d_{2,1}, b_{2,1}, c_{2,1}\}$ that has the *maximum absolute value* if the initial shape parameter ($s^0_{\mathbf{i}}$) is for a regular vertex that immediately adjoins *only* other regular vertices
- $\gamma_{\mathbf{i}}$ = the element of $\left\{p_{2,1}, d_{2,1}, \frac{1}{n} q_{2,1}, b_{2,1}, c_{2,1}\right\}$ that has the *maximum absolute value* if the initial shape parameter ($s^0_{\mathbf{i}}$) is for a regular vertex that also adjoins an extraordinary vertex of valence n
- $\gamma_{\mathbf{i}}$ = the element of $\{w_{2,1}, d_{2,1}, b_{2,1}, c_{2,1}\}$ that has the *maximum absolute value* if the initial shape parameter ($s^0_{\mathbf{i}}$) is for an extraordinary vertex of valence n

So now we have arrived at the following formula:

$$\left[\frac{1}{\gamma_{\mathbf{i}}\ k_{\mathbf{i}}}\sum_{\mathbf{j}} d_{\mathbf{i},\mathbf{j}}\right]\mathbf{n}_{\mathbf{i}}$$

Finally as in [**Yan05**] and [**JS09**] we want to multiply by a free variable $\omega_{\mathbf{i}}$ that we can vary to achieve differing shape results with our shape parameter. Hence we finally arrive at the following formulation for our shape parameter:

$$s_{\mathbf{i}}^0 := \left[\frac{\omega_{\mathbf{i}}}{\gamma_{\mathbf{i}}\ k_{\mathbf{i}}}\sum_{\mathbf{j}} d_{\mathbf{i},\mathbf{j}}\right]\mathbf{n}_{\mathbf{i}} \tag{6.16}$$

From (6.11 |p.153) and (6.16 |p.156) we see that our new edge vertex is a weighted average of the four surrounding vertices plus a displacement using the four surrounding discrete unit normals.

Similarly, from (6.14 |p.155), (6.15 |p.155) and (6.16 |p.156) we see that an updated vertex [approximating case] is a weighted average of the *old* vertex and its surrounding vertices plus a displacement using the surrounding discrete unit normals.

See Figure 6.6 that diagrams how the edge vertex is created [or a regular vertex is updated] for the triangular case. In these diagrams, $\xi_{\mathbf{x}}$ stands for $\frac{\omega_{\mathbf{x}}}{\gamma_{\mathbf{x}}\ k_{\mathbf{x}}}\sum_{\mathbf{j}} d_{\mathbf{x},\mathbf{j}}$ in the shape parameter formula (6.16 |p.156).

Now let us explore this definition of the shape parameter in terms of the definition of the discrete normal curvature in [**MDSB02**]. From (6.8 |p.150) and (6.12 |p.154) we see immediately that

$$\kappa_{i,j}^N = \frac{4d_{\mathbf{i},\mathbf{j}}}{\left\|v_{\mathbf{i}}^0 - v_{\mathbf{j}}^0\right\|^2}$$

Thus

$$d_{\mathbf{i},\mathbf{j}} = \frac{\kappa_{i,j}^N \left\|v_{\mathbf{i}}^0 - v_{\mathbf{j}}^0\right\|^2}{4} = \text{one fourth the product of the discrete normal curvature in the direction of the edge } \overline{v_{\mathbf{i}}^0 v_{\mathbf{j}}^0} \text{ and the square of the length of that adjoining edge.}$$

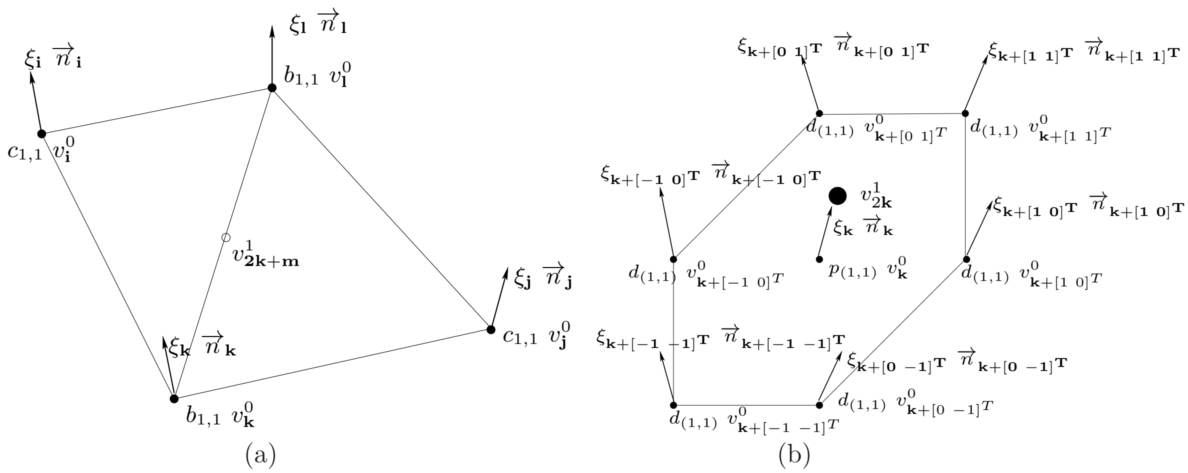

Figure 6.6. Two diagrams that show how the edge vertex is created [left side] or how a regular vertex is updated [right side] for the triangular case. In these diagrams, $\xi_{\mathbf{x}}$ stands for $\frac{\omega_{\mathbf{x}}}{\gamma_{\mathbf{x}}\ k_{\mathbf{x}}} \sum_{\mathbf{j}} d_{\mathbf{x},\mathbf{j}}$ in the shape parameter formula (6.16 |p.156).

.

From the definition of the dot product we also know that

$$\kappa^N_{i,j} = \frac{2\cos\theta_{\mathbf{i},\mathbf{j}}}{\|v_{\mathbf{i}} - v_{\mathbf{j}}\|}$$

where $\theta_{\mathbf{i},\mathbf{j}}$ is the angle between the discrete unit normal $\mathbf{n}_{\mathbf{i}}$ and the adjoining edge $v^0_{\mathbf{i}} - v^0_{\mathbf{j}}$.

So we also have that

$$d_{\mathbf{i},\mathbf{j}} = \frac{\cos\theta_{\mathbf{i},\mathbf{j}} \left\|v^0_{\mathbf{i}} - v^0_{\mathbf{j}}\right\|}{2} = \text{half the product of the cosine of the angle}$$
$$\text{between } \mathbf{n}_{\mathbf{i}} \text{ and the adjoining edge } v^0_{\mathbf{i}} - v^0_{\mathbf{j}}$$
$$\text{and the length of that adjoining edge.}$$

We can thus reformulate $s^0_{\mathbf{i}}$ (6.16 |p.156) as:

$$s^0_{\mathbf{i}} := \left[\frac{\omega_{\mathbf{i}}}{4\gamma_{\mathbf{i}}\ k_{\mathbf{i}}} \sum_{\mathbf{j}} \left\|v^0_{\mathbf{i}} - v^0_{\mathbf{j}}\right\|^2 \kappa^N_{i,j}\right] \mathbf{n}_{\mathbf{i}} \qquad \text{or}$$

$$s^0_{\mathbf{i}} := \left[\frac{\omega_{\mathbf{i}}}{2\gamma_{\mathbf{i}}\ k_{\mathbf{i}}} \sum_{\mathbf{j}} \left\|v^0_{\mathbf{i}} - v^0_{\mathbf{j}}\right\| \cos\theta_{\mathbf{i},\mathbf{j}}\right] \mathbf{n}_{\mathbf{i}}$$

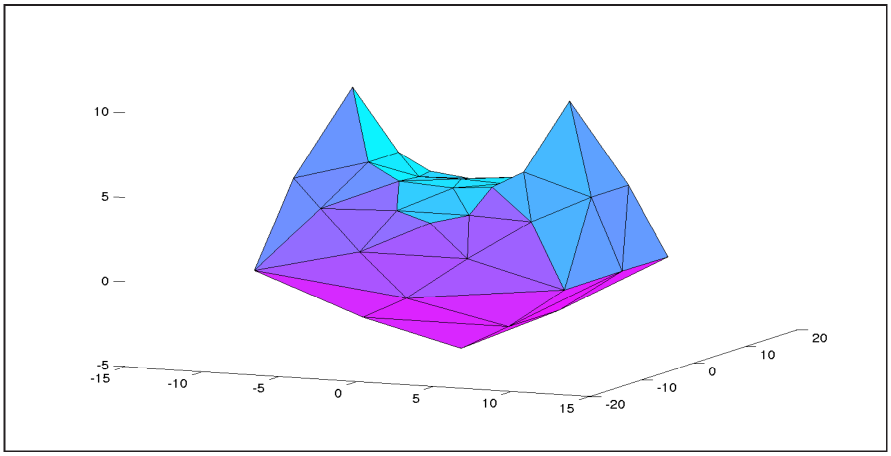

Figure 6.7. Original Triangular Polyhedron

So we can see that if a vertex $v_{\mathbf{i}}^0$ has larger discrete normal curvatures in the directions of its adjacent edges then the length or norm of $s_{\mathbf{i}}^0$ will increase. From (6.11 |p.153) this increased length will provide more displacement to "push out" further the new midpoint vertices along these edges.

In the same vein, if we have the same angles $\{\theta_{\mathbf{i,j}}\}_{\mathbf{j}}$ yet longer adjacent edges then the length or norm of $s_{\mathbf{i}}^0$ will increase. So again we will have more outward displacement of the midpoint vertices along these longer edges.

Note that with our definition of $s_{\mathbf{i}}^0$ we now have only *one* free variable for each individual initial shape parameter rather than three [since the shape parameter is a 3×1 vector]. Thus we can still vary the shape parameter to achieve different shapes but we now only have to deal with choosing one value for each initial shape parameter. So of course this leads to the question of what range of values for the free variable $\omega_{\mathbf{i}}$ might produce suitable surfaces that have fewer artifacts or waviness.

Figure 6.7 is the original triangular polyhedron. Figures 6.8, 6.9 and 6.10 show the result of using 3 different values for ω for all the initial shape vertices (interpolatory triangular scheme). Note how $w = .25$ appears smooth. We could speculate that values of ω between .2 and .4 provide smooth surfaces with that particular interpolatory triangular scheme. Further examples might be able to support that speculation.

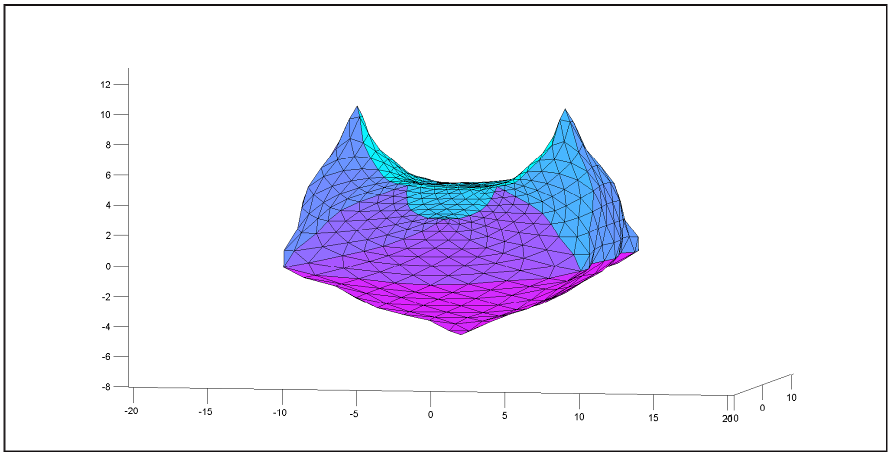

Figure 6.8. $\omega = .10$: Note that surface is very "bumpy"

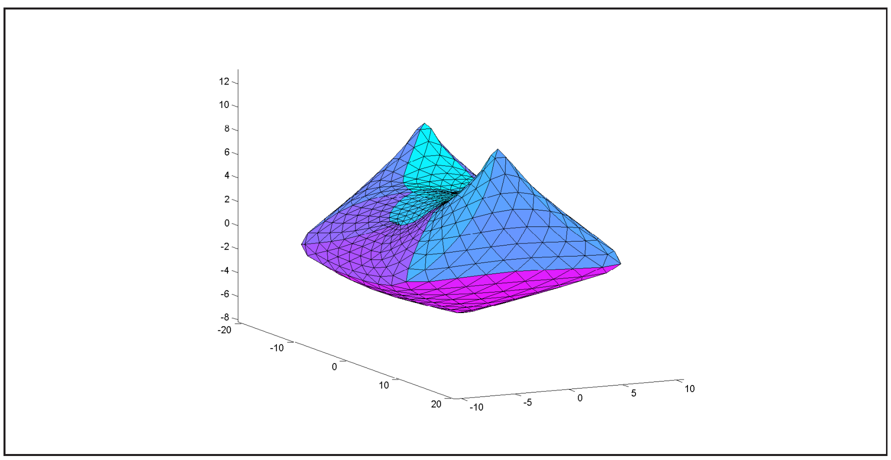

Figure 6.9. $\omega = .25$: Note that surface appears smooth

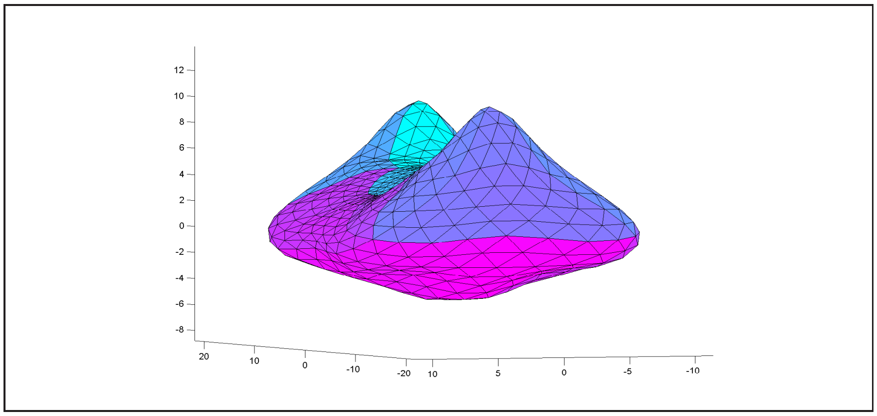

Figure 6.10. $\omega = .50$: Note that surface appears a little "bumpier" than with $\omega = .25$

6.6. Formulation of Shape Parameters for Quadrilateral Meshes

For a quadrilateral scheme [both interpolatory and approximating] we now will develop initial shape parameters that generate "suitable" new edge points, face points and updated existing vertices [approximating case only]. Using the bottom template from (2.1 |p.15) along with the local averaging rule, we can derive the following formulas for the new edge, face vertices and updated existing vertices (let's call them $v^1_{2\mathbf{p}+\mathbf{i}}$, $v^1_{2\mathbf{u}+\mathbf{v}}$ and $v^1_{2\mathbf{j}}$ respectively).

For a new edge vertex $v^1_{2\mathbf{p}+\mathbf{i}}$ the local averaging rule yields: [for both the interpolatory and the approximating cases]

(6.17)

$$v^1_{2\mathbf{p}+\mathbf{i}} = 2\,j_{1,1}\left(\frac{v^0_{\mathbf{p}}+v^0_{\mathbf{q}}}{2}\right)+4m_{1,1}\left(\frac{v^0_{\mathbf{k}}+v^0_{\mathbf{j}}+v^0_{\mathbf{m}}+v^0_{\mathbf{n}}}{4}\right)+j_{2,1}\left(s^0_{\mathbf{p}}+s^0_{\mathbf{q}}\right)+m_{2,1}\left(s^0_{\mathbf{k}}+s^0_{\mathbf{j}}+s^0_{\mathbf{m}}+s^0_{\mathbf{n}}\right)$$

where $\mathbf{p},\mathbf{i},\mathbf{j},\mathbf{k},\mathbf{m},\mathbf{n},\mathbf{q}\in\mathbb{Z}^2$

For a new face vertex $v^1_{2\mathbf{u}+\mathbf{v}}$ the local averaging rule yields: [for both the interpolatory and the approximating cases]

$$v^1_{2\mathbf{u}+\mathbf{v}} = 4k_{1,1}\left(\frac{v^0_{\mathbf{r}}+v^0_{\mathbf{s}}+v^0_{\mathbf{t}}+v^0_{\mathbf{w}}}{4}\right)+k_{2,1}\left(s^0_{\mathbf{r}}+s^0_{\mathbf{s}}+s^0_{\mathbf{t}}+s^0_{\mathbf{w}}\right) \tag{6.18}$$

where $\mathbf{r},\mathbf{s},\mathbf{t},\mathbf{u},\mathbf{v},\mathbf{w}\in\mathbb{Z}^2$

To update an existing *regular* vertex $v^0_{\mathbf{j}}$ [in the approximating case] the local averaging rule yields:

$$\begin{aligned} v^1_{2\mathbf{j}} = r_{1,1}v^0_{\mathbf{j}} &+ 4l_{1,1}\left(\frac{v^0_{\mathbf{j}+(1,0)^T}+v^0_{\mathbf{j}+(0,1)^T}+v^0_{\mathbf{j}+(-1,0)^T}+v^0_{\mathbf{j}+(0,-1)^T}}{4}\right)\\ &+ 4n_{1,1}\left(\frac{v^0_{\mathbf{j}+(1,1)^T}+v^0_{\mathbf{j}+(-1,1)^T}+v^0_{\mathbf{j}+(-1,-1)^T}+v^0_{\mathbf{j}+(1,-1)^T}}{4}\right)\\ &+ r_{2,1}s^0_{\mathbf{j}}\\ &+ l_{2,1}\left(s^0_{\mathbf{j}+(1,0)^T}+s^0_{\mathbf{j}+(0,1)^T}+s^0_{\mathbf{j}+(-1,0)^T}+s^0_{\mathbf{j}+(0,-1)^T}\right)\\ &+ n_{2,1}\left(s^0_{\mathbf{j}+(1,1)^T}+s^0_{\mathbf{j}+(-1,1)^T}+s^0_{\mathbf{j}+(-1,-1)^T}+s^0_{\mathbf{j}+(1,-1)^T}\right) \end{aligned} \tag{6.19}$$

where $\mathbf{j}\in\mathbb{Z}^2$

To update an existing *extraordinary* vertex v^0_0 [in the approximating case] we use the template given in (4.3 |p.67) and the corresponding matrices given in (5.33 |p.132). See Figure 6.11 to help clarify the notation in the following.

$$\begin{aligned}
v_0^1 &= \tilde{n}_{1,1} v_0^0 \\
&+ \frac{1}{n} W_{1,1} \begin{pmatrix} v_1^0 + v_2^0 + v_3^0 \\ +\ldots + v_{n-2}^0 + v_{n-1}^0 + v_n^0 \end{pmatrix} \\
&+ \frac{1}{n} w_{1,1} \begin{pmatrix} u_1^0 + u_2^0 + u_3^0 \\ +\ldots + u_{n-2}^0 + u_{n-1}^0 + u_n^0 \end{pmatrix} \\
&+ \tilde{n}_{2,1} s_0^0 \\
&+ \frac{1}{n} W_{2,1} \begin{pmatrix} s_1^0 + s_2^0 + s_3^0 \\ +\ldots + s_{n-2}^0 + s_{n-1}^0 + s_n^0 \end{pmatrix} \\
&+ \frac{1}{n} w_{2,1} \begin{pmatrix} \tilde{s}_1^0 + \tilde{s}_2^0 + \tilde{s}_3^0 \\ +\ldots + \tilde{s}_{n-2}^0 + \tilde{s}_{n-1}^0 + \tilde{s}_n^0 \end{pmatrix}
\end{aligned}$$

Similar to our triangular mesh case, we will formulate the new *edge* vertex $v_{\mathbf{2p+i}}^1$ as equal to a "weighted midpoint" of the 6 vertices of the adjoining quadrilaterals (the first two terms in (6.17 |p.161)) plus a certain linear combination of projections of the edges onto the discrete unit normals (from [**LXZ08**]) of the six surrounding vertices (the last two terms in (6.17 |p.161)). The shape parameters $\left(s_{\mathbf{k}}^0,\ s_{\mathbf{j}}^0,\ s_{\mathbf{m}}^0,\ s_{\mathbf{n}}^0\right)$ will then be these linear combinations of edge projections onto the discrete unit normals of the respective corresponding vertices.

The new *face* vertex $v_{\mathbf{2u+v}}^1$ will be equal to a "weighted midpoint" of the 4 vertices of the quadrilateral (the first term in (6.18 |p.161)) plus a certain linear combination of projections of the edges onto the discrete unit normals of these four surrounding vertices (the last term in (6.18 |p.161)). Again the shape parameters $(s_{\mathbf{r}},\ s_{\mathbf{s}},\ s_{\mathbf{t}},\ s_{\mathbf{w}})$ will be these linear combinations of edge projections onto the discrete unit normals of the respective corresponding vertices.

The updated existing *regular* vertex $v_{\mathbf{2j}}^1$ will be equal to a weighted average of the "old" vertex and the 8 surrounding vertices [regular case] (first 3 terms in (6.19 |p.161)) plus a certain linear combination of projections of

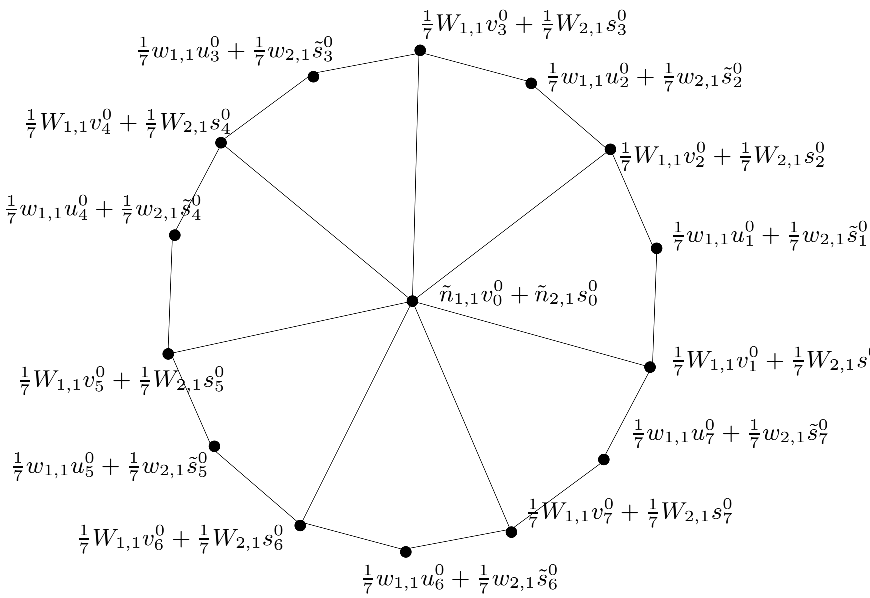

Figure 6.11. Diagram showing what an initial extraordinary central vertex and shape parameter and its surrounding vertices and their shape parameters are multiplied by to update the central vertex. Note that the u_k^0 and $\tilde{s}_k^0$ pertain to the vertices that are *opposite* the quadrilateral from the central vertex. Here valence = 7.

edges onto the discrete unit normals of the "old" vertex and and of these 8 surrounding vertices (last 3 terms in (6.19 |p.161)). The shape parameters $\begin{pmatrix} s^0_{\mathbf{j}},\ s^0_{\mathbf{j}+(1,0)^T},\ s^0_{\mathbf{j}+(0,1)^T},\ s^0_{\mathbf{j}+(-1,0)^T},\ s^0_{\mathbf{j}+(0,-1)^T}, \\ s^0_{\mathbf{j}+(1,1)^T},\ s^0_{\mathbf{j}+(-1,1)^T},\ s^0_{\mathbf{j}+(-1,-1)^T},\ s^0_{\mathbf{j}+(1,-1)^T} \end{pmatrix}$ *are* these linear combinations of edge projections onto the discrete unit normals of the respective corresponding vertices.

The shape parameter $s^0_{\mathbf{i}}$ (related to $v^0_{\mathbf{i}}$) is defined similarly as in the triangular case:

$$s^0_{\mathbf{i}} := \left[\frac{\omega_{\mathbf{i}}}{\gamma_{\mathbf{i}}\ k_{\mathbf{i}}} \sum_{\mathbf{j}} d_{\mathbf{i},\mathbf{j}} \right] \mathbf{n}_{\mathbf{i}} \tag{6.20}$$

where

- ω_i is our free variable and can vary in value as needed [we will generally want to keep it within the range from .2 to .4]

- $k_{\mathbf{i}}$ = valence of $v_{\mathbf{i}}^0$,
- $\mathbf{n_i}$ is the discrete unit normal at $v_{\mathbf{i}}^0$ as defined for a quadrilateral mesh in [**LXZ08**]
- $d_{\mathbf{i},\mathbf{j}} := \frac{1}{2}\left(v_{\mathbf{i}}^0 - v_{\mathbf{j}}^0\right) \cdot \mathbf{n_i}$ where $\left\{v_{\mathbf{j}}^0\right\}_{\mathbf{j}}$ are the adjacent vertices along edges to $v_{\mathbf{i}}^0$
  and
- $\gamma_{\mathbf{i}}$ = the element of $\{r_{2,1}, l_{2,1}, n_{2,1}, k_{2,1}, j_{2,1}, m_{2,1}\}$ that has the *maximum absolute value* if the initial shape parameter ($s_{\mathbf{i}}^0$) is for a regular vertex that immediately adjoins *only* other regular vertices
- $\gamma_{\mathbf{i}}$ = the element of $\left\{r_{2,1}, l_{2,1}, n_{2,1}, k_{2,1}, j_{2,1}, m_{2,1}, \frac{1}{n}W_{2,1}, \frac{1}{n}w_{2,1}\right\}$ that has the *maximum absolute value* if the initial shape parameter ($s_{\mathbf{i}}^0$) is for a regular vertex that also adjoins an extraordinary vertex of valence n
- $\gamma_{\mathbf{i}}$ = the element of $\{\tilde{n}_{2,1}, l_{2,1}, n_{2,1}, k_{2,1}, j_{2,1}, m_{2,1}\}$ that has the *maximum absolute value* if the initial shape parameter ($s_{\mathbf{i}}^0$) is for an extraordinary vertex of valence n

6.7. Illustration of Shape Parameter Definitions Using Matlab®,

With this definition of the shape parameter in place, we can use computer routines on various surfaces to test how well such a definition works. We will use the quadrilateral schemes developed in sections 4.6 (p. 83), 4.6.2 (p. 84), 5.4.2.1 (p. 122), and 5.5.3.2 (p. 139). Figures 6.13 through 6.24 show the result of using 3 different values for ω ($\omega = .25$, $\omega = .4$, $\omega = .8$) uniformly for all the initial shape vertices. Since interpolatory schemes retain all the vertices from every level of subdivision we would expect them to more quickly reflect differing values for ω. Note how $w = .25$ appears fairly smooth for both types of schemes but $\omega = .4$ starts to show a bit of waviness for the interpolatory scheme. The waviness increases significantly for $\omega = .8$. On the other hand, the approximating scheme remains smooth for both $\omega = .4$ and $\omega = .8$.

All figures were done with 3 subdivisions of the original polyhedron (Figure 6.12).

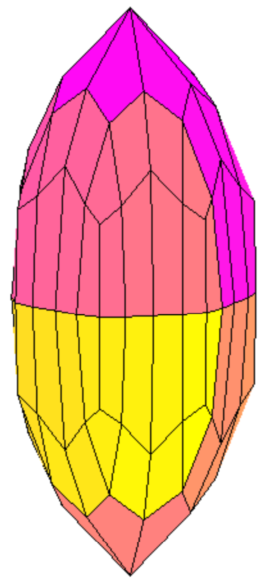

Figure 6.12. Original polyhedron used for the following figures

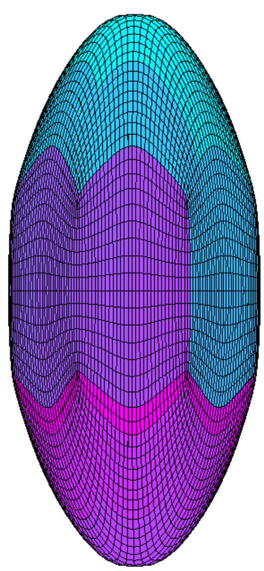

Figure 6.13. Approximating scheme with $\omega = .25$

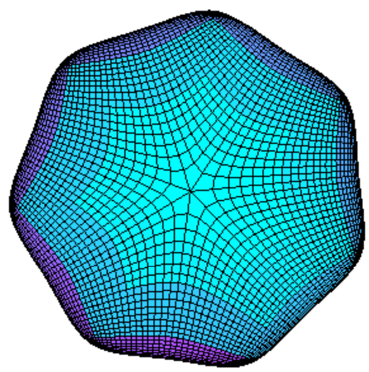

Figure 6.14. Top view for approximating scheme where $\omega = .25$

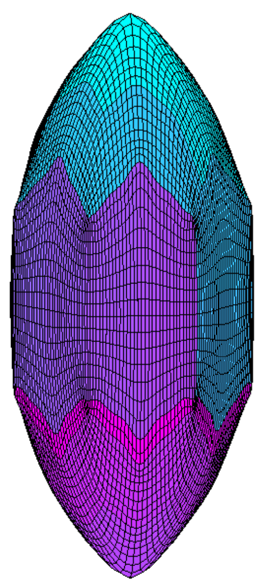

Figure 6.15. Interpolatory scheme with $\omega = .25$

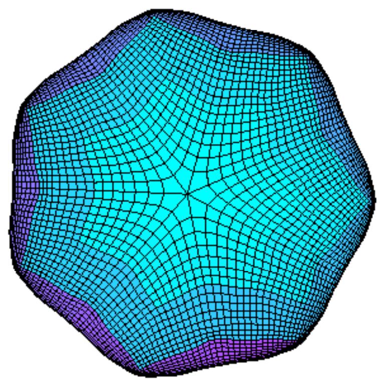

Figure 6.16. Top view for interpolatory scheme with $\omega = .25$

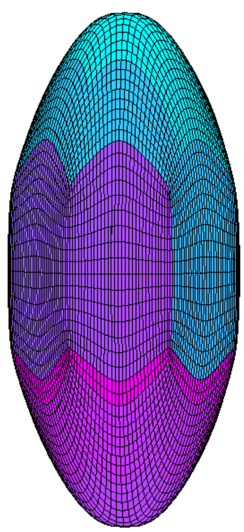

Figure 6.17. Approximating scheme with $\omega = .4$

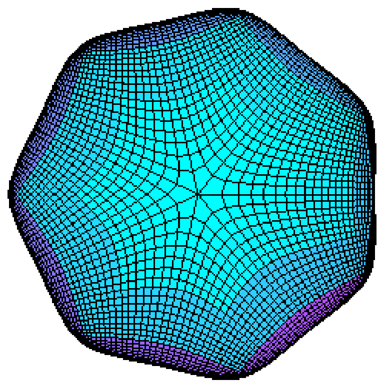

Figure 6.18. Top view of approximating scheme with $\omega = .4$

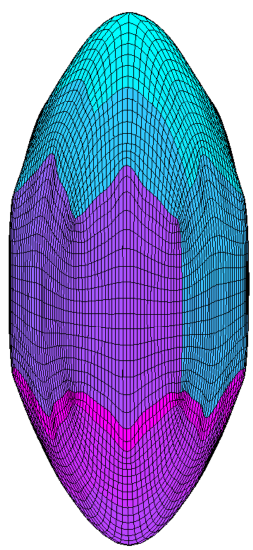

Figure 6.19. Interpolatory scheme with $\omega = .4$

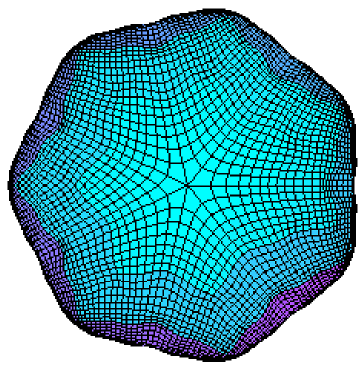

Figure 6.20. Top view of interpolatory scheme with $\omega = .4$

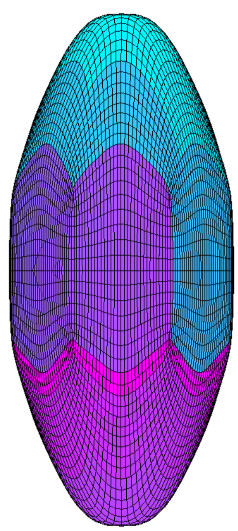

Figure 6.21. Approximating scheme with $\omega = .8$

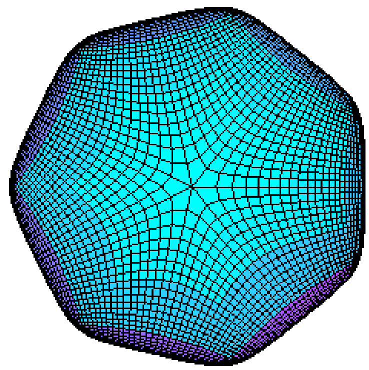

Figure 6.22. Top view of approximating scheme with $\omega = .8$

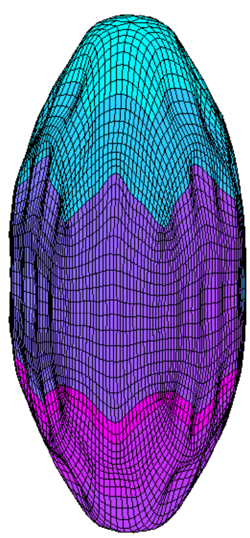

Figure 6.23. Interpolatory scheme with $\omega = .8$

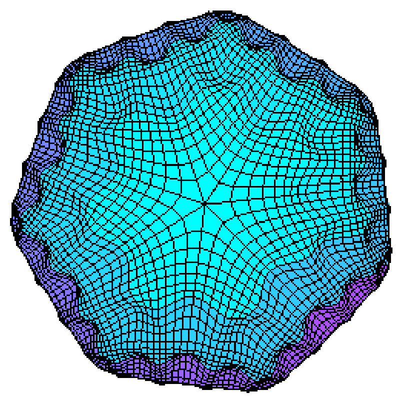

Figure 6.24. Top view of interpolatory scheme with $\omega = .8$

CHAPTER 7

Surface Normals and Curvature

Up to now we have obtained the first and second partial derivatives at a point $\mathbf{x}_0$ on the limit surface F that is locally parameterized as (s_0, t_0). In applications the geometric structures of interest are the unit surface normals, Gaussian curvature and perhaps the mean curvature. We can derive formulas for these directly from these first and second partial derivatives [**Gra93**].

7.1. Normal and Curvature Formulas

Having obtained the first partial derivatives at a point $\mathbf{x}_0$ on the limit surface F that is locally parameterized as (s_0, t_0), the unit surface normal at such a point

$$\mathbf{n}_{\mathbf{x}_0} = \pm \frac{D_1(s_0,t_0) \times D_2(s_0,t_0)}{\|D_1(s_0,t_0) \times D_2(s_0,t_0)\|} \tag{7.1}$$

where $\|\cdot\|$ is the Euclidean norm and

$$(x_1,x_2,x_3)^T \times (y_1,y_2,y_3)^T := (x_2y_3 - y_2x_3, x_3y_1 - y_3x_1, x_1y_2 - y_1x_2)^T$$

for $(x_1,x_2,x_3)^T, (y_1,y_2,y_3)^T \in \mathbb{R}^3$

We can also obtain the mean and Gaussian curvatures [**Gra93**]

If $\mathbf{x}_0$ corresponds to a regular vertex then the Gaussian curvature, $K_g(\mathbf{x}_0)$, equals

$$K_g(\mathbf{x}_0) = \frac{\begin{array}{c}\left[D_1^2(s_0,t_0) \cdot (D_1(s_0,t_0) \times D_2(s_0,t_0))\right]\left[D_2^2(s_0,t_0) \cdot (D_1(s_0,t_0) \times D_2(s_0,t_0))\right] \\ - \left[D_1D_2(s_0,t_0) \cdot (D_1(s_0,t_0) \times D_2(s_0,t_0))\right]^2\end{array}}{\left[(D_1(s_0,t_0) \cdot D_1(s_0,t_0))(D_2(s_0,t_0) \cdot D_2(s_0,t_0)) - (D_1(s_0,t_0) \cdot D_2(s_0,t_0))^2\right]^2}$$

If $\mathbf{x}_0$ corresponds to a regular vertex then the mean curvature, $K_h(\mathbf{x}_0)$, equals

$$K_h(\mathbf{x}_0) = \frac{\begin{array}{c}\left(D_1^2(s_0,t_0)\cdot\left(D_1(s_0,t_0)\times D_2(s_0,t_0)\right)\right)\left\|D_2(s_0,t_0)\right\|^2 \\ -2\left(D_1D_2(s_0,t_0)\cdot\left(D_1(s_0,t_0)\times D_2(s_0,t_0)\right)\right)\left(D_1(s_0,t_0)\cdot D_2(s_0,t_0)\right) \\ +\left(D_2^2(s_0,t_0)\cdot\left(D_1(s_0,t_0)\times D_2(s_0,t_0)\right)\right)\left\|D_1(s_0,t_0)\right\|^2\end{array}}{2\left(\left\|D_1(s_0,t_0)\right\|^2\left\|D_2(s_0,t_0)\right\|^2-\left(D_1(s_0,t_0)\cdot D_2(s_0,t_0)\right)^2\right)^{\frac{3}{2}}}$$

We have created several figures of normal vectors on both triangular and quadrilateral surfaces (both interpolatory and approximating.) These were created on Matlab® using the formula (7.1 |p.172) and using our derived formulas for the two first partial derivatives. For each particular surface we have created figures showing a surface normal vector corresponding to both a regular vertex and an extraordinary vertex. Hence all of our first partial derivative formulas were used. See Appendix F starting on p. 221 to view these figures. The black line extending from the figures is the surface normal. For visual purposes, we have deliberately made the normals longer than unit length. Note that the lines appear to be visually normal to the surface.

7.2. Achieving a specific normal at a point

There may be times when a specific normal is desired on a surface. (See Chapter 8 starting on p. 179.) First note that the first partial derivatives are a linear combination of the immediately surrounding control and shape vertices. Also recall that the parameter (ω) is the free variable in determining a shape vertex. So basically there are 2 methods that can be used to achieve a specific unit normal at a point corresponding to a vertex. They are:

- to adjust the needed surrounding parameter values (ω_j)
- to adjust the necessary surrounding initial control vertices

We will examine the first option. (The second option may be examined in future work. Notice that by changing or adjusting surrounding control vertices then by our definition of shape vertices the surrounding shape vertices will also change.)

So the goal is to discover surrounding parameter values that *minimally* differ from their default value (for instance, a default value of $\omega_k = .25$) and that at the same time will achieve the desired unit normal at our point on the surface.

Let us assume we have a point on the surface that corresponds to a vertex of valence n. For a triangular scheme the two first partial derivatives are composed of a linear combination of the n adjacent initial control and shape vertices For a quadrilateral scheme, they are composed of a linear combination of the $2n$ adjacent and opposing initial control and shape vertices. Let us denote the initial control vertices by $\{v_k^0\}_{k=1}^{n \text{ or } 2n}$ and the corresponding shape vertices by $\{\omega_k b_k^0\}_{k=1}^{n \text{ or } 2n}$ where b_k^0 is the initial shape control parameter defined in (6.16 |p.156) or (6.20 |p.163) except for the ω_k.

So we then have for *specific* $\alpha_k, \beta_k, \gamma_k, \eta_k$ from our first partial derivative formulas:

$$D_1(s_0, t_0) = \sum_{k=1}^{n \text{ or } 2n} \left(\alpha_k v_k^0 + \beta_k w_k b_k^0\right)$$
$$D_2(s_0, t_0) = \sum_{k=1}^{n \text{ or } 2n} \left(\gamma_k v_k^0 + \eta_k w_k b_k^0\right)$$

where here we will allow ω_k to vary as needed.

In order to achieve a specific unit normal $\mathbf{u} := (u_1, u_2, u_3)^T$ we must satisfy the following set of equalities:

$$(7.2) \qquad \begin{aligned} u_1 - \begin{bmatrix} 1 & 0 & 0 \end{bmatrix} \left(\frac{D_1(s_0,t_0) \times D_2(s_0,t_0)}{\|D_1(s_0,t_0) \times D_2(s_0,t_0)\|} \right) &= 0 \\ u_2 - \begin{bmatrix} 0 & 1 & 0 \end{bmatrix} \left(\frac{D_1(s_0,t_0) \times D_2(s_0,t_0)}{\|D_1(s_0,t_0) \times D_2(s_0,t_0)\|} \right) &= 0 \\ u_3 - \begin{bmatrix} 0 & 0 & 1 \end{bmatrix} \left(\frac{D_1(s_0,t_0) \times D_2(s_0,t_0)}{\|D_1(s_0,t_0) \times D_2(s_0,t_0)\|} \right) &= 0 \end{aligned}$$

that are *nonlinear* in our variables ω_k.

In addition, we want at the same time to keep our ω_k values as close as possible to whatever value we usually set the ω_k equal to. So, as an example, we want to minimize

$$\sum_{k=1}^{n \text{ or } 2n} (\omega_k - .25)^2 \tag{7.3}$$

Hence our problem becomes minimizing $\sum_{k=1}^{n \text{ or } 2n} (\omega_k - .25)^2$ while satisfying 3 nonlinear constraint equations (7.2).

We solved this problem by using the command *patternsearch* on Matlab®. This command in turn utilizes an Augmented Lagrangian Pattern Search (ALPS) algorithm to solve the nonlinear constraint [**Mat11**]. Here is some background and information on both *patternsearch* and ALPS.

The patternsearch algorithm is a direct search algorithm. The term "direct search" has been around since 1961 where it appeared in an article [**HJ61**] by R. Hooke and T.A. Jeeves . There it was described as a

> sequential examination of trial solutions involving comparison of each trial solution with the 'best' obtained up to that time together with a strategy for determining...what the next trial solution will be.

In [**LTT00**] Lewis discusses three basic categories of direct search methods that are used in solving the *unconstrained* minimization

$$\text{minimize } f(x) \quad \text{where } f : \mathbb{R}^n \to \mathbb{R}$$

These categories are:

- *pattern search methods*
- *simplex methods*
- *methods with adaptive sets of search directions*

Only the first method (pattern search) will be discussed here. Starting with some initial point in $\mathbb{R}^n$, the value of the function $f(x)$ is considered at a pattern of points that lie on a rational lattice. These surrounding points can be considered as steps leading *from* the initial point. For example, this rational lattice can be formed from the n unit coordinate vectors where the magnitude of the vectors (i.e. the magnitude of the steps) indicates the resolution of the lattice. Look at Figure 7.1 on p. 176 for a simple example where $n = 2$.

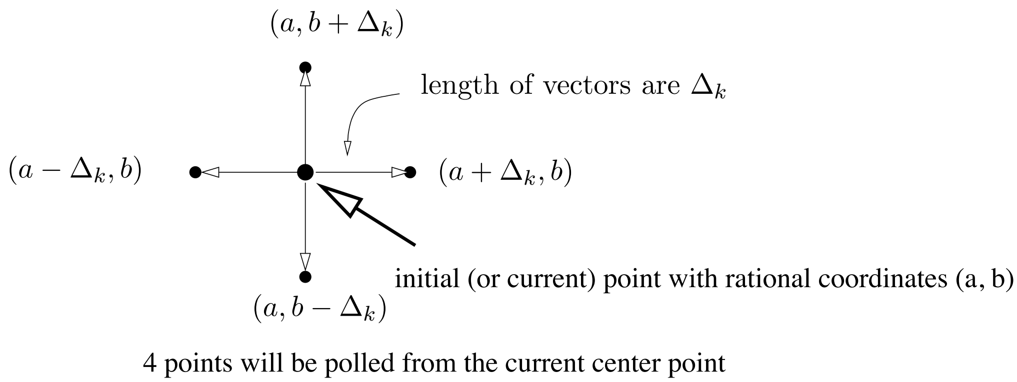

Figure 7.1. Current point with the arrows pointing to next 4 points to be polled. Length of the steps will change according to the algorithm.

A systematic strategy is employed for visiting the points in the lattice in the immediate vicinity of the current point in $\mathbb{R}^n$. This strategy of visiting points is called "polling." At each point visited (or polled) the function is evaluated or compared with previous values. If a point in that poll is found that has a smaller value for the function $f(x)$ then that point is labeled as the new current point. The mesh size is then increased (often by a factor of 2) and a new polling begins around that *new* current point. If the poll is unsuccessful (i.e. no smaller function value is found) then the mesh size is decreased (often by a factor of .5). This is the only time the mesh of the lattice is reduced. This feature is crucial to the convergence to the discovery of a minimum value [**LTT00**].

In our case, the function we want to minimize is subject to 3 nonlinear constraints (7.2 |p.174). So *patternsearch* must have an additional algorithm to accommodate such constraints. This algorithm is the Augmented Lagrangian Pattern Search algorithm (ALPS) that is discussed in both [**Mat11**] and [**KLT06**].

The algorithm uses what is called an *outer* iteration and each outer iteration contains an *inner* iteration. Assume that we have m nonlinear equality constraints ($c_i = 0$ for $i = 1...m$) and the function to be minimized is $f(x)$ where $c_i : \mathbb{R}^n \to \mathbb{R}$ and $f : \mathbb{R}^n \to \mathbb{R}$. At each (*outer*) iteration k

the new function to be minimized becomes

$$\Phi_k\left(x;\lambda^{(k)},\mu_k\right) := f\left(x\right) + \sum_{i=1}^{m} \lambda_i^{(k)} c_i\left(x\right) + \frac{1}{2\mu_k}\sum_{i=1}^{m} c_i\left(x\right)^2$$

where $\lambda_i^{(k)}$ are (nonnegative) Lagrange multiplier estimates and μ_k is a positive penalty parameter. Note that this is an unconstrained function and so a direct search method such as patternsearch is used to to find the solutions

$$\mathbf{x}_k = \arg\min \Phi_k\left(x;\lambda,\mu\right) \tag{7.4}$$

This minimization requires its own iterations (the *inner* iterations) and a stopping criterion is the first unsuccessful polling for a mesh size less than δ_k (a stopping tolerance that is calculated with each outer iteration). Stopping criteria for the *outer* iterations are that our mesh has become suitably small and that the nonlinear equality constraints are met using $\mathbf{x}_k$ from (7.4 |p.177):

$$\begin{aligned} \delta_k &< \delta^* \quad \text{[a small predetermined positive number]} \\ \left\|c_i\left(\mathbf{x}_k\right)\right\|_{i=1}^{m} &< \eta^* \quad \text{[another preset small positive number]} \end{aligned}$$

At each outer iteration $\lambda_i^{(k)}$ and μ_k are updated.

If $\left\|c_i\left(\mathbf{x}_k\right)\right\|_{i=1}^{m} < \eta_k$ [small number determined at each outer iteration] then the $\lambda_i^{(k)}$ are updated by

$$\lambda_i^{(k+1)} = \lambda_i^{(k)} + \frac{c_i\left(\mathbf{x}_k\right)}{\mu_k}$$

and μ_k stays the same ($\mu_{k+1} = \mu_k$).

Otherwise keep the Lagrangian multiplier estimates the same ($\lambda_i^{(k+1)} = \lambda_i^{(k)}$) and reduce the penalty parameter μ_k :

$$\mu_{k+1} = \tau_k \mu_k$$

for some small τ_k that is calculated with each outer iteration.

The solutions to (7.4 |p.177) at the final outer iteration are the output of this algorithm. The convergence of this algorithm is shown in [**KLT06**].

In Appendix G we show several figures using our various subdivision schemes. Each figures shows a "desired" normal that is obtained using the above algorithm in the Matlab® routine *patternsearch*. This normal is shown using a solid line. Also shown as a dashed or broken line is the normal we would have obtained at that point if we had not been trying to obtain a specific normal. The caption shows the angle (in degrees) between the two normals and the value of the minimized function in (7.3 |p.175). Note that generally the larger the minimized function value is then the poorer the final surface appears. Also note how approximation schemes yield surfaces with fewer artifacts than the comparable interpolatory schemes.

CHAPTER 8

Applications Involving Surface Normals

Here we shall consider two uses of surface normals in the field of computer graphics.

The first is in lighting and shading. Surface normals have been and still are used in computer graphics to light and shade figures. Lighting and shading, however, are not identical. Lighting refers to the interaction between sources of light and the materials that the light(s) shine on. In this process, some light is absorbed and some is reflected [**Avi89**]. On the other hand, shading refers to where and how the lighting methods are applied. It is used to determine the color of *all* the pixels. Shading can be done per polygon (flat shading), per vertex (Gouraud shading) or per pixel (Phong shading, Ray tracing) [**FvDFH95**]. So shading and lighting are *not* independent since the lighting model that is used *does* affect the shading of a pixel.

The second application of surface normals that we will consider involves creating the appearance of a "rough" surface without explicitly changing the geometry of the underlying model. This process is called *bump mapping* and was developed by J.F. Blinn in [**Bli78**].

But first we will look at lighting and shading.

8.1. Lighting and Shading Models

We shall first look at two lighting models that use the surface normal:

- Lambert model
- Phong model

These are not the only lighting models. For instance, the Torrance-Sparrow model [**TS92**] and Anisotropic lighting [**IB02**] also use surface normals.

After first looking at these two models, we will then look at three shading methods that use surface normals:

- Flat shading
- Gouraud shading
- Phong shading

8.1.1. Lambert Lighting Model

Before discussing the Lambert model, note that light also gets reflected off objects in the environment instead of just emanating from an outside light source. This indirect lighting is called "ambient" lighting. In lighting models this ambient lighting is added onto the other types of light reflection considered by the particular model. By adding this ambient lighting unlit areas do not appear completely black. The formula for this ambient illumination is: [**FvDFH95**]

$$I_a k_a$$

where I_a is the ambient light intensity, k_a is the material's ambient reflectance coefficient, and $I_a,\ k_a \in [0,1]$.

Now we shall go on to the Lambert lighting model. This model uses Lambert's cosine law. This law states that the intensity of reflected light from a surface that *only* reflects in a diffuse way [such a chalk] is directly proportional to the cosine of the angle θ between the vector to the light source and the surface normal. [**FvDFH95**] This type of reflection is called a "diffuse" reflection. Here the intensity of the reflected light depends only on the direction of the light sources and is *not* dependent on the position of the viewer. If a light source is directly "over" the unit surface normal then the reflection will be the most intense. The larger the angle the light source makes with the unit surface normal then the less intense will be the reflected light.

The formula for the intensity of the diffuse reflection (I_d) is: [**FvDFH95**]

$$I_d = I_L\ k_d\ max\,(\mathbf{n}\cdot\mathbf{L}, 0) \tag{8.1}$$

where

- $I_L =$ light source intensity $\in [0,1]$

- k_d = the material's diffuse reflectance coefficient $\in [0, 1]$
- $\mathbf{n}$= surface unit normal
- $\mathbf{L}$ = unit vector pointing toward the light source

See upper diagram in Figure 8.1.

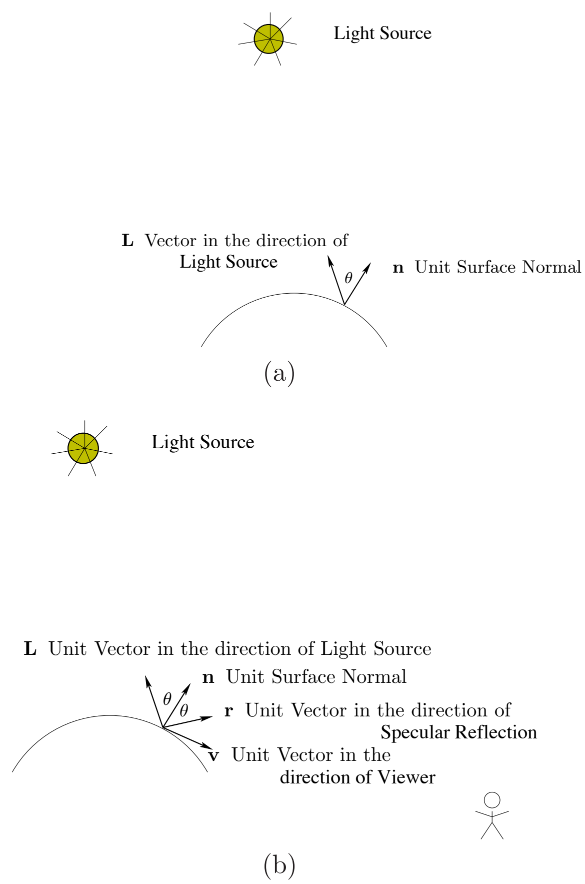

Figure 8.1. The top diagram represents the Lambert Illumination Model. Note that the position of a viewer is *not* part of the model. The bottom diagram represents the Phong Illumination Model. Here we have two additional components: a vector $\mathbf{r}$ that reflects the light source vector across the unit normal $\mathbf{n}$ and a vector $\mathbf{v}$ that points to a viewer. Thus specular highlights are made that depend on the position of a viewer.

8.1.2. Phong Lighting Model

In this model developed by Bui Tuong Phong in 1975, light received by a surface is *also* considered to be reflected in *one* direction [**Pho75**]. Note that this is in addition to having a diffuse reflection component *and* an ambient reflection component. This type of reflection is called a "specular" reflection. Metallic or polished surfaces conform to this model. Bright spots on the surface exhibit these reflections. Here the intensity of the reflected light depends on the relationship between the viewer, the light sources and the surface.

One formula for the intensity of the specular reflection (I_s) is [**FvDFH95**]:

$$I_s = I_L \ k_s \ max\,(\mathbf{r} \cdot \mathbf{v}, 0)^n$$

where

- $I_L =$ light source intensity $\in [0, 1]$
- $k_s =$ specular reflectance coefficient $\in [0, 1]$
- $\mathbf{v}=$ unit vector in the direction of the viewer
- $\mathbf{r} =$ unit vector in the direction of the specular reflection $= \frac{2(\mathbf{n} \cdot \mathbf{L})\mathbf{n} - \mathbf{L}}{||2(\mathbf{n} \cdot \mathbf{L})\mathbf{n} - \mathbf{L}||}$ for $\mathbf{n}$ and $\mathbf{L}$ in (8.1 |p.180)
- $n =$ an index that conveys how imperfect the surface is [Note that when $n = \infty$ then the surface is a perfect mirror and all reflected light emerges along the direction reflected by this "mirror" [**Wat00**].]

See lower diagram in Figure 8.1.

An alternative lighting model [Blinn-Phong model] was developed in 1977 by J. Blinn [**Bli77**]. Here the formula for the intensity of the specular reflection (I_s) is:

$$I_s = I_L \ k_s \ (\mathbf{n} \cdot \mathbf{h})^n$$

where

- $I_L =$ light source intensity $\in [0, 1]$
- $k_s =$ specular reflectance coefficient $\in [0, 1]$
- $\mathbf{n}=$ surface unit normal
- $\mathbf{h} := \frac{\mathbf{L}+\mathbf{v}}{||\mathbf{L}+\mathbf{v}||}$
- $n =$ an index that conveys how imperfect the surface is

Since the angle between **h** and **n** is *always* less than 90°, this alternative avoids a problem in the regular Phong model that occurs when the angle between **r** and **v** is greater than 90° [**McK11**].

Now we proceed onto the three types of shading that we will consider.

8.1.3. Flat Shading

Flat shading is a fast way to color the pixels of each polygon. Here an illumination method is applied at one of the vertices of the polygon or at the center of the polygon. The color that is so obtained is then applied to *all* the pixels of that particular polygon. The obvious disadvantage is that the surface appears faceted since there is no variation in shade across the polygon. The advantage is that is it relatively inexpensive to implement.

8.1.4. Gouraud Shading

Gouraud shading reduces the faceted appearance of the flat shading method [**Gou71**]. Here an illumination method is applied to each of the vertices of the polygon. Thus an RGB color is calculated for each of the polygonal vertices. These colors are then interpolated across each polygon. See Figure 8.2 showing the interpolation across a scanline of a surface triangle.

Gouraud shading does not deal effectively with specular highlights and so is usually reserved for calculating diffuse reflections. However, it is computationally less expensive than Phong shading discussed below [**Wat00**].

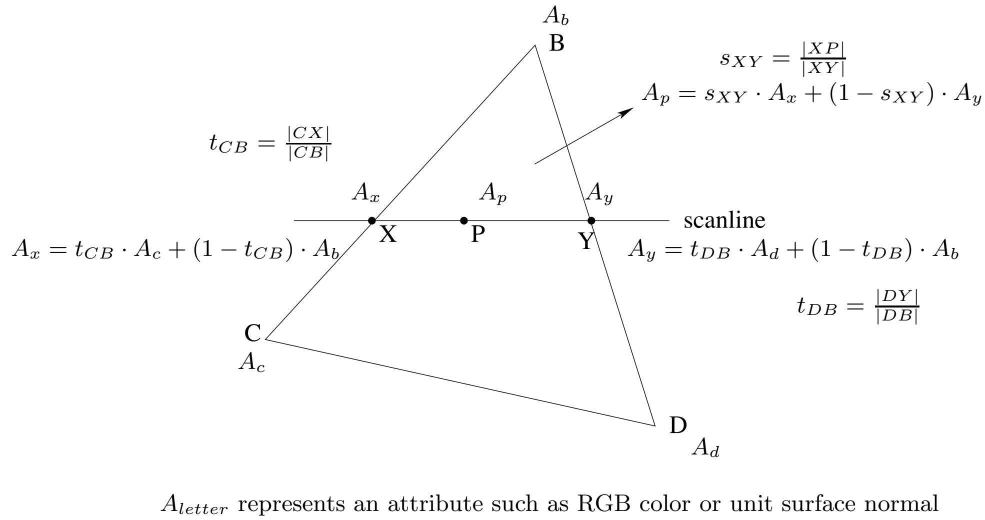

Figure 8.2. This diagram represents the interpolation of an attribute such as RGB color [Gouraud shading] and Unit Surface Normal [Phong Shading]. Given any scanline across a surface polygon, the endpoint attributes (A_x, A_y) are first interpolated and *then* the attribute on the scanline (A_p) is interpolated using the previously obtained interpolated values at the two endpoints.

8.1.5. Phong Shading

In Phong shading, the unit surface normals are calculated at each vertex and then interpolated across the surface of the polygon similar to how Gouraud shading interpolates a color across the surface. Then at *each* pixel of the polygon, the interpolated surface normal is used to implement the Phong lighting method. So we see that the illumination is applied per pixel.

Phong shading provides a more realistic image than does Gouraud shading. Specular reflection will show up that might be missed with the Gouraud method. Highlights are produced that are much less dependent on the underlying polygons. However, Phong shading is more expensive to implement than Gouraud shading since more calculations are required to interpolate the surface normal and to evaluate the illumination at each pixel [**Wat00**].

In the Gouraud method and particularly in the Phong method, we have an advantage in that we can use the methods described in this paper and thus calculate the precise unit surface normals at each vertex instead of *approximating* the surface unit normal with a discrete normal calculation. Future work could include comparing the difference in the shading of the image using our exact surface unit normal versus using a discrete approximation.

8.1.6. Perspective Corrected Interpolation

Both Gouraud and Phong shading use linear interpolation of some attribute (RGB color and unit surface normal respectively). However, the linear interpolation of some attribute in 3D space between two points of *varying* distances from the viewer does *not* translate into a linear interpolation in 2D screen space. For instance, a point in 3D space that is *not* at the center of the interpolation line could be projected onto 2D screen space at the *center* of the 2D projection of the 3D line. This will cause a distortion of that attribute in our 2D image.

Many graphics rendering programs place a "virtual" camera at the origin of 3D space and have it look out into either the $-z$ or $+z$ direction. The z value of a 3D point tells us the distance that point is away from the virtual camera. In [**Low02**] Low determined how we can interpolate in *screen space* and yet correct for perspective. The formula is given in (8.2).

If Z_1 is the z coordinate for attribute A_1 at one end of an edge in 3D space and Z_2 is the z coordinate for attribute A_2 at the *other* end of that edge in 3D space then we can interpolate between these two attributes in **2D space** [say using variable s] as follows:

$$A_s1 = \frac{\left(\frac{A_1}{Z_1} + s\left(\frac{A_2}{Z_2} - \frac{A_1}{Z_1}\right)\right)}{\left(\frac{1}{Z_1} + s\left(\frac{1}{Z_2} - \frac{1}{Z_1}\right)\right)} \qquad s \in [0,1] \tag{8.2}$$

8.2. Bump Mapping

Now we're moving onto the second application of surface normals that we will consider. This application is called "bump mapping." In [**FvDFH95**] we can find a summary of the process of bump mapping developed by J.F.

Blinn in [**Bli78**]. This process involves slightly changing the surface normal *before* using the normal in the lighting and shading model. The surface itself is not actually changed because of this new surface normal. What *does* change is the way the surface will be illumined. This process models a slight roughness in a surface that if it *truly* were there *would* alter the surface normal.

So a bump map is an array of displacements, each of which is used to model moving a point on the surface slightly. Say we have a point on the surface represented by $\overline{P}$. Using our first partial derivatives given in this paper, we can calculate the surface normal at this point. Let's call it $\overline{N}$.

$$\overline{N} = \overline{P_s} \times \overline{P_t}$$

where $\overline{P_s}$ and $\overline{P_t}$ are the two first partial derivatives at $\overline{P}$.

Note that this surface normal is unnormalized.

This point $\overline{P}$ can then be displaced by adding to it the normalized surface normal scaled by a selected bump-map value B. The new point $\overline{P}'$ is:

$$\overline{P}' = \overline{P} + \frac{B\overline{N}}{|\overline{N}|}$$

Blinn then provides an approximation for the new [not yet normalized] normal of this "new" surface point. Let's call this normal $\overline{N}'$.

$$\overline{N}' = \overline{N} + \frac{B_u\left(\overline{N} \times \overline{P_t}\right) - B_v\left(\overline{N} \times \overline{P_s}\right)}{|\overline{N}|}$$

where B_u and B_v are partial derivatives of the bump-map entry B with respect to a parameterization of the bump-map using axes labeled u and v. Blinn notes that bilinear interpolation can be used to obtain bump-map values at any certain (u, v) and that finite differences can be used to derive B_u and B_v.

This new normal $\left(\overline{N}'\right)$ is then normalized and substituted as the surface normal in the lighting and shading process to give the illusion of texturizing.

Two very convincing color plates are displayed in [**FvDFH95**] demonstrating the realistic texture provided by bump mapping.

8.3. Potential to Use Matrix-valued Schemes for these Applications

These two general applications, shading and texturizing with a bump map, can be readily applied if our computer graphic surfaces are generated using a 1-ring triangular or quadrilateral matrix-valued subdivision scheme described in this thesis. Given a *particular* matrix-valued subdivision scheme, we can initially compute the coefficients that form the linear combination of surrounding control and shape vertices. Recall that these coefficients come from the orthogonal right eigenvectors. See, for example, (4.28 |p.79), (5.16 |p.111), and (5.21 |p.119). These linear combinations of surrounding vertices (both control and shape) provide us with *precise* first partial derivatives that in turn give us *precise* unit surface normals. We can then shade or texturize our generated surface using these exact unit normals.

We can obtain these precise unit normals at vertices of the *original* control mesh without even having to further subdivide. The formulas for the first partial derivatives involve the immediate surrounding vertices at whatever refinement level of subdivision we have attained. So for first partial derivatives at *initial* vertices, we only need the surrounding *initial* vertices (again both control and shape). We want to emphasize that the coefficients that multiply these surrounding vertices only need to be calculated *one* time for any particular matrix-valued subdivision scheme.

So, to summarize, any computer graphic application that requires unit normals can benefit from these formulas that readily provide such unit normals as long as the surface is being generated by a 1-ring matrix-valued scheme described here.

CHAPTER 9

Conclusions and Future Work

Surface subdivision schemes are used in computer graphics to generate visually smooth surfaces of arbitrary topology. Knowing precise unit surface normals on these smooth surfaces can be useful for certain applications in computer graphics. We have seen two applications (shading and texturizing with a bump map) that require knowledge of the unit surface normal at a wide array of surface points. In this dissertation we have provided formulas for such normals for both triangular and quadrilateral 1-ring subdivision schemes at both regular surface points and extraordinary surface points. Both interpolatory and approximating schemes have been considered. Hence, a computer graphics surface designer can use our subdivision schemes to readily compute unit surface normals as needed.

We derived these unit surface normals at points on the limit surface as follows. Starting with 1-ring subdivision schemes (triangular and quadrilateral), we were able to obtain formulas for the two first partial derivatives at points on the limit surface that "correspond" to vertices of the *initial* control net or that "correspond" to vertices of any *subsequent* refinement of that initial control net. Then, by normalizing the cross product, we obtained the unit normals.

In addition, at points on the limit surface that correspond to so-called *regular* control net vertices, we have been able to derive the three *second* partial derivatives. Hence, we can then obtain Gaussian or mean curvature values at such points on the limit surface.

Since we are using subdivision schemes that have matrix-valued masks, every vertex of our original polyhedron (and of its successive refinements) has a corresponding "shape" vertex. These shape vertices are aptly named because they play a role in changing the shape of our ultimate limit surface. More specifically, the first and second partial derivative formulas for a particular point consist of linear combinations of "surrounding" vertices *and* their corresponding shape vertices. In this dissertation, for various 1-ring subdivision schemes, we derived the coefficients involved in these linear combinations. Given any particular subdivision scheme we only need to calculate these coefficients one time. From there, we can readily obtain the partial derivatives. And so we can use the appropriate formulas from Differential Geometry to obtain the unit normals and, if desired, the Gaussian or mean curvatures.

With the use of Matlab® to not only generate the refinements for an initial triangular polyhedron (Fig. 6.7|ṗ.158) and an initial quadrilateral polyhedron (Fig. 6.12|ṗ.165) but also to calculate the surface normals using our derivative formulas, we saw that the unit surface normals so obtained *visually* appear to be normal to the surface at both regular and extraordinary vertices.

We proposed a definition of the *initial* shape vertices that correspond to our initial vertex control net. Up to now there have been preliminary suggestions as to how to define the initial shape vertices [**CJ06**], [**CJ08**]. Taking the lead from Yang in [**Yan05**] and [**Yan06**] who used discrete normals to obtain new edge points, we defined an initial shape vertex as the average of the adjacent edge projections onto the discrete surface unit normal where this result is then multiplied by a scalar ω.

There is an advantage and a disadvantage to defining the initial shape vertex this way. The advantage is that there is only one variable to be decided upon when defining the shape vertex. That variable is the ω value we want for that particular shape vertex. The disadvantage is related to the advantage. There is a lack of flexibility in only having one free variable. Future work could involve using *different* values for the ω variable at different areas of the surface. Here we uniformly used one value of ω throughout the surface. Artifact was seen in some of the ω values chosen (particularly in interpolating schemes). Future work could include testing ω values that vary depending on the curvature of the surface.

We know that the shape vertices will affect the shape of the limiting surface. Here, we examined how to obtain a specific unit surface normal by changing *just* the surrounding shape vertices. Since the initial control net of vertices of the polyhedron was *not* changed, we saw quite a bit of waviness in the interpolatory schemes when we created a unit normal that widely differed from its original direction. Approximating schemes showed less artifact.

Future work could include *also* changing the surrounding control net vertices to achieve a certain unit surface normal. This could result in surfaces with less artifact (particularly in the interpolatory case). However, there could be a significant increase in computation time.

Another factor to consider is the *reason* we are wanting to alter a surface normal to become some specified vector. If the reason is to change the texture of a surface (in computer graphics), we saw that this can be achieved using a bump map without actually altering the shape of the surface. Nonetheless, surface normals are still used in bump mapping and our formulation of the first partial derivatives can be directly utilized in the bump map algorithm discussed in section 8.2 on p. 185.

Other future work could involve comparing the lighting and shading achieved using our precise surface normals as opposed to using approximate discrete surface normals. Is there a significant enough improvement in the image to compensate for a possible increase in computational cost?

Another avenue of future work would be to program the algorithm for the determination of C^k convergence discussed in subsection 5.1.1 on p. 90.

References

[Asp03] N. Aspert, *Non-linear subdivision of univariate signals and discrete surfaces*, Ph.D. thesis, EPFL, 2003.

[Avi89] J. Avison, *The world of physics*, 2nd ed., Nelson Thornes, 1989.

[Bli77] J. Blinn, *Models of light reflection for computer synthesized pictures*, SIGGRAPH Comput. Graph. **11** (1977), 192–198.

[Bli78] J.F. Blinn, *Simulation of wrinkled surfaces*, SIGGRAPH Comput. Graph. **12** (1978), 286–292.

[CC78] E. Catmull and J. Clark, *Recursively generated b-spline surfaces on arbitrary topological surfaces*, Computer-Aided Design **10** (1978), 350–355.

[CDM91] A.S. Cavaretta, W. Dahmen, and C.A. Micchelli, *Stationary subdivision*, Mem. Am. Math. Soc. **93** (1991), 1–186.

[CDV10] C. Chui and J. De Villiers, *Wavelet subdivision methods: Gems for rendering curves and surfaces*, CRC Press, 2010.

[Cha74] G. Chaikin, *An algorithm for high speed curve generation*, Comput. Graph Image Process. **3** (1974), 346–349.

[Chu98] C.K. Chui, *Multivariate splines*, Regional Conference Series in Applied Mathematics, vol. 54, SIAM, 1998.

[CJ03a] C.K. Chui and Q. Jiang, *Multivariate balanced vector-valued refinable functions*, Modern Development in Multivariate Approximation Theory (W. Haussmann, K. Jetter, M. Reimer, and J. Stöckler, eds.), vol. 145, Birkhaüser Verlag, 2003.

[CJ03b] ———, *Surface subdivision schemes generated by refinable bivariate spline function vectors*, Appl. Comput. Harmonic Analysis **15** (2003), 147–162.

[CJ05] ———, *Matrix-valued symmetric templates for interpolatory surface subdivisions i. regular vertices*, Appl. Comput. Harmonic Analysis **19** (2005), 303–339.

[CJ06] ———, *Matrix-valued subdivision schemes for generating surfaces with extraordinary vertices*, Computer Aided Geometric Design **23** (2006), 419–438.

[CJ08] ———, *From extension of loop's approximation scheme to interpolatory subdivisions*, Computer Aided Geometric Design **25** (2008), 96–115.

[CJR02] D-R. Chen, R-Q. Jia, and S.D. Riemenschneider, *Convergence of vector subdivision schemes in sobolev spaces*, Applied and Computational Harmonic Analysis **12** (2002), 128–149.

[DGL90] N. Dyn, J.A. Gregory, and D. Levin, *A butterfly subdivision scheme for surface interpolation with tension control*, ACM Transactions on Graphics **9** (1990), 160–169.

[DHKW92] U. Dierkes, S. Hildebrandt, A. Kuster, and O. Wohlrab, *Minimal surfaces i*, Springer-Verlag, 1992.

[DLG87] N. Dyn, D. Levin, and J. Gregory, *A 4-point interpolatory subdivision scheme for curve design*, Computer Aided Geometric Design **4** (1987), 257–268.

[DLG91] ———, *Analysis of uniform binary subdivision schemes for curve design*, Constructive Approximation **7** (1991), 127–148.

[DLM90] N. Dyn, D. Levin, and C. Micchelli, *Using parameters to increase smoothness of curves and surfaces generated by subdivision*, Computer Aided Geometric Design **7** (1990), 129–140.

[dR47] G. de Rahm, *Un peu de mathématiques à propos d'une courbe plane*, Elemente der Math **2** (1947), 73–76,89–97.

[dR56] ______, *Sur une courbe plane*, J. Math. Pure. Appl. **35** (1956), 25–42.

[DS78] D. Doo and M. Sabin, *Behaviour of recursive subdivision surfaces near extraordinary points*, Computer-Aided Design **10** (1978), 356–360.

[Dyn92] N. Dyn, *Subdivision schemes in cagd*, Advances in Numerical Analysis, Univ. Press, 1992, pp. 36–104.

[FvDFH95] J. Foley, A. van Dam, S. Feiner, and J. Hughes, *Computer graphics: Principles and practice in c*, 2nd ed., Addison-Wesley, 1995.

[Gou71] H. Gouraud, *Continuous shading of curved surfaces*, IEEE Trans. Comput. **20** (1971), 623–629.

[Gra93] A. Gray, *Modern differential geometry of curves and surfaces*, CRC Press, 1993.

[GZC07] W. Guan, J. Zheng, and J. Cai, *Including and optimizing shape parameters in doo-sabin subdivision surfaces for interpolation*, Proceedings of the 2007 ACM symposium on Solid and physical modeling (New York, NY, USA), SPM '07, ACM, 2007, pp. 439–444.

[HJ61] R. Hooke and T.A. Jeeves, *Direct search solution of numerical and statistical problems*, J. Assoc. Comput. Mach. **8** (1961), 212–229.

[IB02] J. Isidoro and C. Brennan, *Per-pixel strand based anisotropic lighting*, Direct3D ShaderX: Vertex and Pixel Shader Tips and Tricks (Wolfgang Engel, ed.), Wordware, 2002.

[Jia99] R-Q. Jia, *Characterization of smoothness of multivariate refinable functions in sobolev spaces*, Trans. Amer. Math. **351** (1999), 4089–4112.

[Jia02] ______, *Cascade algorithms in wavelet analysis*, Wavelet Analysis: Twenty Years' Developments: Proceedings of the International Conference of Computational Harmonic Analysis (D-X. Zhou, ed.), World Scientific Publishing, 2002, pp. 196–230.

[JJ02] R-Q. Jia and Q. Jiang, *Approximation power of refinable vectors of functions*, Wavelet Analysis and Applications (D. Ding, D. Huang, R-Q. Jia, W. Lin, and J. Wang, eds.), American Mathematical Society and International Press, 2002, pp. 153–176.

[JJ03] R.Q. Jia and Q.T. Jiang, *Spectral analysis of the transition operator and its applications to smoothness analysis of wavelets*, SIAM J. of Matrix Anal. and Appl. **24** (2003), 1071–1109.

[JJL02] R-Q. Jia, Q. Jiang, and S.L. Lee, *Convergence of cascade algorithms in sobolev spaces and integrals of wavelets*, Numerische Mathematik **91** (2002), 453–473.

[JO01] Q. Jiang and P. Oswald, *Matlab 5 routines for sobolev smoothness*, Software at http://www.cs.umsl.edu/ jiang/Jsoftware.htm, 2001.

[JO03] Q.T. Jiang and P. Oswald, *Triangular $\sqrt{3}$-subdivision schemes: the regular case*, J. Comp. Appl. Math. **156** (2003), 47–75.

[JS09] Q. Jiang and J. Smith, *Tangents and curvatures of matrix-valued subdivision curves and their applications to curve design*, preprint, 2009.

[Kei03] F. Keinert, *Wavelets and multiwavelets (studies in advanced mathematics)*, Chapman and Hall/CRC, 2003.

[KLT06] T. Kolda, R. Lewis, and V. Torczon, *A generating set direct search augmented lagrangian algorithm for optimization with a combination of general and linear constraints*, Tech. report, Sandia National Laboratory, 2006.

[Kob96] L. Kobbelt, *Numeralgo/na11 for box-spline*, Software at http://www.netlib.no/netlib/numeralgo/na11, 1996.

[Kob98] M. Kobayashi (ed.), *Wavelets and their applications: case studies*, SIAM, 1998.

[Kob00] L. Kobbelt, $\sqrt{3}$-*subdivision*, Proceedings of the ACM SIGGRAPH Computer Graphics 2000 (2000), 103–112.

[LMB04] G. Li, W. Ma, and H. Bao, *$\sqrt{2}$ subdivision for quadrilateral meshes*, Visual Computer **20** (2004), 180–198.

[Loo87] C. Loop, *Smooth subdivision surfaces based on triangles*, Master's thesis, Department of Mathematics, University of Utah, 1987.

[Loo01] ______, *Triangle mesh subdivision with bounded curvature and the convex hull property*, Technical Report MSR-TR-2001-24, Microsoft Research (2001).

[Low02] K. Low, *Perspective-correct interpolation*, retrieved from http://www.cs.unc.edu/ lowk/research/writings/lowk_perp_interp.pdf, 2002.

[LTT00] R. Lewis, V. Torczon, and M. Trosset, *Direct search methods: then and now*, Journal of Computational and Applied Mathematics **124** (2000), 191–207.

[LXZ08] D. Liu, G. Xu, and Q. Zhang, *A discrete scheme of laplace-beltrami operator and its convergence over quadrilateral meshes*, Computers and Mathematics with Applications **55** (2008), 1081–1093.

[MA10] G. Mustafa and P. Ashraf, *A new 6-point ternary interpolating subdivision scheme and its differentiability*, Journal of Information and Computing Science **5** (2010), no. 3, 199–210.

[Mat11] MathWorks, *Global optimization toolbox 3 user's guide*, retrieved from http://www.mathworks.com/help/pdf doc/gads/gads tb.pdf, 2011.

[McK11] J. McKesson, *Learning 3d graphics programming*, retrieved from http://www.arcsynthesis.org/gltut/index.html, 2011.

[MDSB02] M. Meyer, M. Desbrun, P. Schröder, and A. Barr, *Discrete differential geometry operators for triangulated 2-manifolds*, Visualization and Mathematics III (H-C. Hege and K. Polthier, eds.), Springer, 2002, pp. 35–54.

[Mel02] R. Melrose, *Sobolev spaces*, retrieved from http://www.math.mit.edu/ rbm/18.155-F02/Lecture-notes/node11.html, 2002.

[O'N06] B. O'Neill, *Elementary differential geometry*, rev. second ed., Elsevier, 2006.

[Pho75] B. Phong, *Illumination for computer generated pictures*, Commun. ACM **18** (1975), 311–317.

[PR98] J. Peters and U. Reif, *Analysis of algorithms generalizing B-spline subdivisions*, Siam J. Numer. Anal. **35** (1998), 728–748.

[PR08] ______, *Subdivision surfaces*, Springer-Verlag, 2008.

[Rei95] U. Reif, *A unified approach to subdivision algorithms near extraordinary vertices*, Computer Aided Geometric Design **12** (1995), 153–174.

[RP06] U. Reif and J. Peters, *Structural analysis of subdivision surfaces-a summary*, Topics in Multivariate Approximation and Interpolation (K. Jetter et al., eds.), Elsevier, 2006, pp. 149–190.

[SDL99] P. Shenkman, N. Dyn, and D. Levin, *Normals of the butterfly subdivision scheme surfaces and their applications*, Journal of Comp. and Appl. Math. **102** (1999), 157–180.

[She98] Z. Shen, *Refinable function vectors*, SIAM J. Math. Anal. **29** (1998), 235–250.

[Str96] V. Strela, *Multiwavelets: Theory and applications*, Ph.D. thesis, MIT, 1996.

[Str10] G. Strang, *Calculus*, second ed., Wellesley-Cambridge, 2010.

[TS92] K. E. Torrance and E. M. Sparrow, *Theory for off-specular reflection from roughened surfaces*, Radiometry (L. Wolff, Shafer S., and G. Healey, eds.), Jones and Bartlett Publishers, Inc., 1992, pp. 32–41.

[VZ01] L. Velho and D. Zorin, *4-8 Subdivision*, Computer Aided Geometric Design **18** (2001), 397–427.

[Wat00] A. Watt, *3d computer graphics*, 3rd ed., Addison-Wesley, 2000.

[Xu04] G. Xu, *Convergence of discrete laplace-beltrami operators over surfaces*, Comput. Math. Appl **48** (2004), 347–360.

[Yan05] X. Yang, *Surface interpolation of meshes by geometric subdivision*, Computer Aided Design **37** (2005), 497–508.

[Yan06] ———, *Normal based subdivision scheme for curve design*, Computer Aided Geometric Design **23** (2006), 243–260.

[Zor00a] D. Zorin, *A method for analysis of $\mathcal{C}^1$-continuity of subdivision surfaces*, Siam J. Numer. Anal. **37** (2000), 1677–1708.

[Zor00b] ———, *Subdivision zoo*, ACM SIGGRAPH 2000 Conference Course Notes (2000), 65–102.

Appendix A

Eigenvalues are listed for varying valences of the Quadrilateral Interpolatory Scheme (see 4.35 on p. 84). The eigenvalues are listed for a $4n+2 \times 4n+2$ subdivision matrix around the extraordinary vertex of valence n. The subdominant eigenvalue λ of multiplicity 2 is listed in bold where $\lambda = \frac{10+2\cos\left(\frac{2\pi}{n}\right)+\sqrt{38+40\cos\left(\frac{2\pi}{n}\right)+2\cos\left(\frac{4\pi}{n}\right)}}{32}$.

The eigenvalues are listed in increasing modulus with the exception of 2 complex conjugate eigenvalues that are listed last. Note that their modulus is less than λ.

Valence 3

0.065949, 0.065949, 0.077245, 0.12832, 0.13327, 0.13327, 0.15240,0.15240, 0.25000, **0.41010, 0.41010**, 1, 0.073007-0.057712 I ,0.073007+0.057712 I

Valence 5

0.063740, 0.063740, 0.073791, 0.073791, 0.077245, 0.11365, 0.11365, 0.11911, 0.11911, 0.12832, 0.13790, 0.13790, 0.18377, 0.18377, 0.25000, 0.34011, 0.34011, **0.54999, 0.54999**, 1, 0.073007-0.057712 I, 0.073007+0.057712 I

Valence 6

0.062500, 0.065949, 0.065949, 0.076467, 0.076467, 0.077244, 0.10782, 0.10782, 0.11494, 0.11494, 0.12832, 0.13327, 0.13327, 0.14062, 0.15240, 0.15240, 0.25000, 0.25000, 0.25000, 0.41010, 0.41010, **0.57968, 0.57968**, 1, 0.073007-0.057712 I, 0.073007+0.057712 I

Valence 7

0.063130, 0.063130, 0.068222, 0.068222, 0.077244, 0.078550, 0.078550, 0.10443, 0.10443, 0.11189, 0.11189, 0.12832, 0.12883, 0.12883, 0.13532, 0.13532, 0.13922, 0.13922, 0.20022, 0.20022, 0.25000, 0.31216, 0.31216, 0.46186, 0.46186, **0.59851, 0.59851**, 1, 0.073007-0.057712 I, 0.073007+0.057712 I

Valence 8

0.062500, 0.064438, 0.064438, 0.070312, 0.070312, 0.077244, 0.080203, 0.080203, 0.10227, 0.10227, 0.10958, 0.10958, 0.12500, 0.12500, 0.12500,

0.12500, 0.12832, 0.13640, 0.13640, 0.14062, 0.17090, 0.17090, 0.25000,
0.25000, 0.25000, 0.36572, 0.36572, 0.50000, 0.50000,
0.61111, 0.61111, 1, 0.073007-0.057712 I, 0.073007+0.057712 I

Valence 9
0.062880, 0.062880, 0.065949, 0.065949, 0.072165, 0.072165, 0.077245,
0.081542, 0.081542, 0.10082, 0.10082, 0.10778, 0.10778, 0.11827, 0.11827,
0.12179, 0.12179, 0.12832, 0.13327, 0.13327, 0.13977, 0.13977, 0.15240,
0.15240, 0.21019, 0.21019, 0.25000, 0.29734, 0.29734, 0.41010, 0.41010,
0.52843, 0.52843, **0.61994, 0.61994**,
1, 0.073007-0.057712 I, 0.073007+0.057712 I

Valence 10
0.062500, 0.063740, 0.063740, 0.067480, 0.067480, 0.073791, 0.073791,
0.077244, 0.082645, 0.082645, 0.09978, 0.09978, 0.10635, 0.10635,
0.11365, 0.11365, 0.11911, 0.11911, 0.12832, 0.13025, 0.13025, 0.13790,
0.13790, 0.14002, 0.14002, 0.14062, 0.18377, 0.18377, 0.25000, 0.25000,
0.25000, 0.34011, 0.34011, 0.44634, 0.44634, 0.54999,
0.54999, **0.62634, 0.62634**, 1, 0.073007-0.057712 I,
0.073007+0.057712 I

Valence 11
0.062755, 0.062755, 0.064805, 0.064805, 0.068945, 0.068945, 0.075215,
0.075215, 0.077244, 0.083570, 0.083570, 0.099029, 0.099029, 0.10517,
0.10517, 0.11030, 0.11030, 0.11685, 0.11685, 0.12748, 0.12748, 0.12832,
0.13134, 0.13134, 0.13562, 0.13562, 0.14005, 0.14005, 0.16550, 0.16550,
0.21686, 0.21686, 0.25000, 0.28820, 0.28820, 0.37764, 0.37764, 0.47587,
0.47587, 0.56662, 0.56662, **0.63113, 0.63113**, 1,
0.073007-0.057712 I, 0.073007+0.057712 I

Valence 12
0.062500, 0.063359, 0.063359, 0.065949, 0.065949, 0.070312, 0.070312,
0.076467, 0.076467, 0.077244, 0.084354, 0.084354, 0.09846, 0.09846,
0.10419, 0.10419, 0.10782, 0.10782, 0.11494, 0.11494, 0.12500, 0.12500,
0.12500, 0.12500, 0.12832, 0.13327, 0.13327, 0.13872, 0.13872, 0.14062,
0.15240, 0.15240, 0.19313, 0.19313, 0.25000, 0.25000,

0.25000, 0.32361, 0.32361, 0.41010, 0.41010, 0.50000,
0.50000, 0.57968, 0.57968, **0.63480, 0.63480**, 1,
0.073007-0.057712 I, 0.073007+0.057712 I

Valence 13

0.062682, 0.062682, 0.064148, 0.064148, 0.067102, 0.067102, 0.071575,
0.071575, 0.077244, 0.077570, 0.077570, 0.085028, 0.085028, 0.098013,
0.098013, 0.10337, 0.10337, 0.10592, 0.10592, 0.11330, 0.11330, 0.12023,
0.12023, 0.12280, 0.12280, 0.12832, 0.13098, 0.13098, 0.13701, 0.13701,
0.14022, 0.14022, 0.14270, 0.14270,
0.17568, 0.17568, 0.22163, 0.22163, 0.25000, 0.28200, 0.28200, 0.35575,
0.35575, 0.43797, 0.43797, 0.51984, 0.51984, 0.59009, 0.59009,
0.63767, 0.63767, 1, 0.073007-0.057712 I, 0.073007+0.057712 I

Valence 14

0.062500, 0.063130, 0.063130, 0.065030, 0.065030, 0.068222, 0.068222,
0.072732, 0.072732, 0.077244, 0.078550, 0.078550, 0.085612, 0.085612,
0.097663, 0.097663, 0.10266, 0.10266, 0.10443, 0.10443, 0.11189, 0.11189,
0.11655, 0.11655, 0.12084, 0.12084, 0.12832, 0.12883, 0.12883, 0.13515,
0.13515, 0.13532, 0.13532, 0.13922, 0.13922, 0.14062, 0.16254, 0.16254,
0.20022, 0.20022, 0.25000, 0.25000, 0.25000, 0.31216, 0.31216, 0.38453,
0.38453, 0.46186, 0.46186, 0.53627, 0.53627, 0.59851, 0.59851,
0.63996, 0.63996, 1, 0.073007-0.057712 I, 0.073007+0.057712 I

Valence 15

0.062638, 0.062638, 0.063740, 0.063740, 0.065949, 0.065949, 0.069298,
0.069298, 0.073791, 0.073791, 0.077245, 0.079422, 0.079422, 0.086122,
0.086122, 0.097380, 0.097380, 0.10205, 0.10205, 0.10324, 0.10324, 0.11066,
0.11066, 0.11365, 0.11365, 0.11911, 0.11911, 0.12683, 0.12683, 0.12832,
0.12957, 0.12957, 0.13327, 0.13327, 0.13790, 0.13790, 0.14032, 0.14032,
0.15240, 0.15240, 0.18377, 0.18377, 0.22520, 0.22520, 0.25000, 0.27753,
0.27753, 0.34011, 0.34011, 0.41010, 0.41010, 0.48236, 0.48236, 0.54999,
0.54999, 0.60540, 0.60540, **0.64181, 0.64181**, 1,
0.073007-0.057712 I, 0.073007+0.057712 I

Valence 16

0.062500, 0.062982, 0.062982, 0.064438, 0.064438, 0.066872, 0.066872, 0.070312, 0.070312, 0.074762, 0.074762, 0.077245, 0.080203, 0.080203, 0.086575, 0.086575, 0.097150, 0.097150, 0.10152, 0.10152, 0.10227, 0.10227, 0.10958, 0.10958, 0.11130, 0.11130, 0.11756, 0.11756, 0.12500, 0.12500, 0.12500, 0.12500, 0.12832,
0.13143, 0.13143, 0.13640, 0.13640, 0.13955, 0.13955, 0.14062, 0.14443, 0.14443, 0.17090, 0.17090, 0.20575, 0.20575, 0.25000, 0.25000, 0.25000, 0.30376, 0.30376, 0.36572, 0.36572, 0.43273, 0.43273, 0.50000, 0.50000, 0.56153, 0.56153, 0.61111, 0.61111, **0.64333, 0.64333** , 1,
0.073007-0.057712 I, .073007+0.057712 I

Appendix B

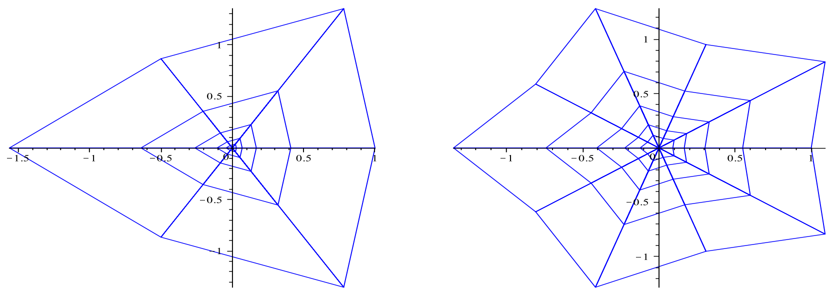

Figure 9.1. “Characteristic” map for Interpolatory Quadrilateral Scheme (4.35 |p.84) for valences 3 and 5. Note that it “appears” regular and injective.

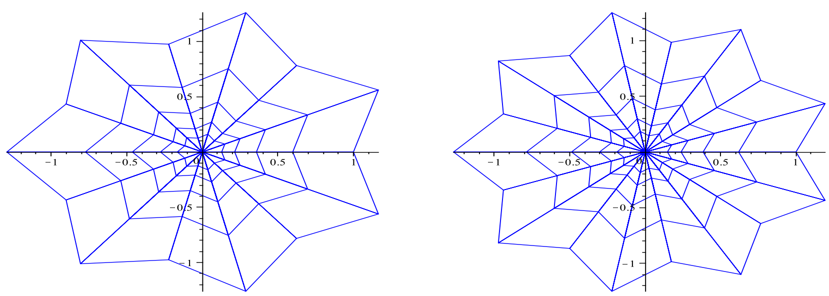

Figure 9.2. “Characteristic” map for Interpolatory Quadrilateral Scheme (4.35 |p.84) for valences 7 and 9. Note that it “appears” regular and injective.

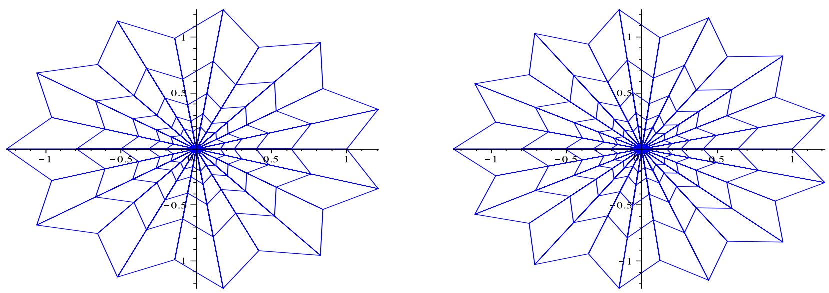

Figure 9.3. "Characteristic" map for Interpolatory Quadrilateral Scheme (4.35 |p.84) for valences 11 and 13. Note that it "appears" regular and injective.

Appendix C

The following is the proof of Theorem 5.1 on p. 96:

Proof. Let $\Phi_0 := \left[\begin{smallmatrix} M_{221} \\ 0 \end{smallmatrix}\right]$. Note that $M_{221} \in C^1(\mathbb{R}^2)$ and that $M_{221} \in \pi_3^2$ (accuracy order 4). Define

$$\begin{aligned} F_m(\mathbf{x}) &:= \sum_{\mathbf{k}\in\mathbb{Z}^2} \mathbf{v}_{\mathbf{k}}^m \Phi_0(2^m\mathbf{x}-\mathbf{k}) \\ &= \sum_{\mathbf{k}\in\mathbb{Z}^2} v_{\mathbf{k}}^m M_{221}(2^m\mathbf{x}-\mathbf{k}) \\ &= \sum_{\mathbf{k}\in\mathbb{Z}^2} \mathbf{v}_{\mathbf{k}}^0 Q_P^m \Phi_0(\mathbf{x}-\mathbf{k}) \quad \text{from (5.2 |p.90)} \end{aligned}$$

So for $j = 1, 2$, and using the derivative notation from (2.1 |p.8):

$$D_j F_m(\mathbf{x}) = \sum_{\mathbf{k}\in\mathbb{Z}^2} \mathbf{v}_{\mathbf{k}}^0 D_j \left\{ Q_P^m \Phi_0(\mathbf{x}-\mathbf{k}) \right\} \tag{9.1}$$

$$\begin{aligned} \lim_{m\to\infty} D_j F_m(\mathbf{x}) &= \sum_{\mathbf{k}\in\mathbb{Z}^2} \mathbf{v}_{\mathbf{k}}^0 \lim_{m\to\infty} D_j \left\{ Q_P^m \Phi_0(\mathbf{x}-\mathbf{k}) \right\} \\ &= \sum_{\mathbf{k}\in\mathbb{Z}^2} \mathbf{v}_{\mathbf{k}}^0 D_j \Phi(\mathbf{x}-\mathbf{k}) \quad \text{by the } C^1 \text{ convergence} \\ &= D_j F(\mathbf{x}) \end{aligned}$$

Now we will get a representation of $D_1 F_m(\mathbf{x})$ in terms of surrounding vertices.

$$\begin{aligned} D_1 F_m(\mathbf{x}) &= \sum_{\mathbf{k}\in\mathbb{Z}^2} v_{\mathbf{k}}^m D_1 \left\{ M_{221}(2^m\mathbf{x}-\mathbf{k}) \right\} \\ &= \sum_{\mathbf{k}\in\mathbb{Z}^2} v_{\mathbf{k}}^m 2^m \left\{ M_{121}\left(2^m\mathbf{x}-\mathbf{k}+\left(\frac{1}{2},0\right)^T\right) - M_{121}\left(2^m\mathbf{x}-\mathbf{k}-\left(\frac{1}{2},0\right)^T\right) \right\} \end{aligned}$$

by (5.11 |p.95)

Thus for $\mathbf{k}_0 \in \mathbb{Z}^2$ we have:

$$D_1F_m(\mathbf{k}_0) = \sum_{\mathbf{k}\in\mathbb{Z}^2} v_{\mathbf{k}}^m 2^m \left\{ M_{121}\left(2^m\mathbf{k}_0 - \mathbf{k} + \left(\frac{1}{2},0\right)^T\right) - M_{121}\left(2^m\mathbf{k}_0 - \mathbf{k} - \left(\frac{1}{2},0\right)^T\right)\right\}$$

$$= 2^m \left\{ \frac{1}{8} \left(\begin{array}{c} 3v^m_{2^m\mathbf{k}_0+(1,0)^T} - 3v^m_{2^m\mathbf{k}_0+(-1,0)^T} + v^m_{2^m\mathbf{k}_0+(1,1)^T} \\ -v^m_{2^m\mathbf{k}_0+(0,1)^T} + v^m_{2^m\mathbf{k}_0+(0,-1)^T} - v^m_{2^m\mathbf{k}_0+(-1,-1)^T} \end{array} \right) \right\}$$

where we use Figure 9.4 on p. 206 showing values of M_{121} when the first coordinate equals $\pm\frac{1}{2}$. Note that these values were obtained by using the software in [**Kob96**].

Now we take the limit as our subdivisions go to infinity:

$$\lim_{m\to\infty} D_1F_m(\mathbf{k}_0) = \lim_{m\to\infty} \left[2^m \left\{ \frac{1}{8} \left(\begin{array}{c} 3v^m_{2^m\mathbf{k}_0+(1,0)^T} - 3v^m_{2^m\mathbf{k}_0+(-1,0)^T} + v^m_{2^m\mathbf{k}_0+(1,1)^T} \\ -v^m_{2^m\mathbf{k}_0+(0,1)^T} + v^m_{2^m\mathbf{k}_0+(0,-1)^T} - v^m_{2^m\mathbf{k}_0+(-1,-1)^T} \end{array} \right) \right\} \right]$$

And so by (9.1 |p.204)

$$D_1F(\mathbf{k}_0) = \lim_{m\to\infty} \left[2^m \left\{ \frac{1}{8} \left(\begin{array}{c} 3v^m_{2^m\mathbf{k}_0+(1,0)^T} - 3v^m_{2^m\mathbf{k}_0+(-1,0)^T} + v^m_{2^m\mathbf{k}_0+(1,1)^T} \\ -v^m_{2^m\mathbf{k}_0+(0,1)^T} + v^m_{2^m\mathbf{k}_0+(0,-1)^T} - v^m_{2^m\mathbf{k}_0+(-1,-1)^T} \end{array} \right) \right\} \right]$$

Similarly we will get a representation of $D_2F_m(\mathbf{x})$ in terms of a limit of surrounding vertices.

$$D_2F_m(\mathbf{x}) = \sum_{\mathbf{k}\in\mathbb{Z}^2} v_{\mathbf{k}}^m D_2\left\{M_{221}(2^m\mathbf{x} - \mathbf{k})\right\}$$

$$= \sum_{\mathbf{k}\in\mathbb{Z}^2} v_{\mathbf{k}}^m 2^m \left\{ M_{211}\left(2^m\mathbf{x} - \mathbf{k} + \left(0,\frac{1}{2}\right)^T\right) - M_{211}\left(2^m\mathbf{x} - \mathbf{k} - \left(0,\frac{1}{2}\right)^T\right)\right\}$$

by (5.11 |p.95)

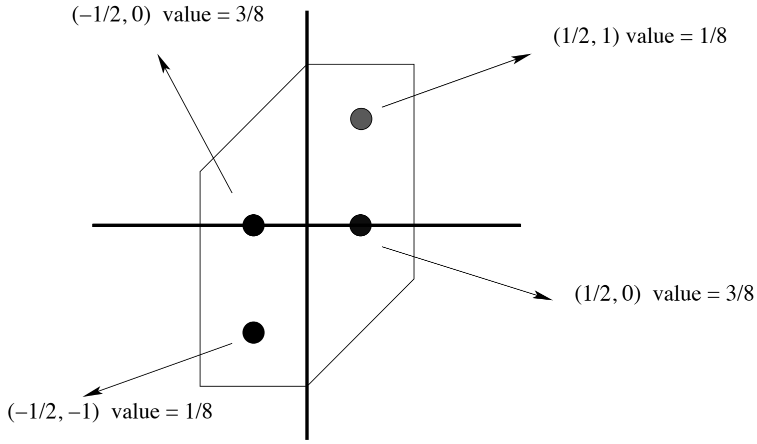

Figure 9.4. Values of M_{121} where first coordinate $=\pm\frac{1}{2}$

Thus for $\mathbf{k}_0 \in \mathbb{Z}^2$ we have:

$$D_2F_m(\mathbf{k}_0) = \sum_{\mathbf{k}\in\mathbb{Z}^2} v_{\mathbf{k}}^m 2^m \left\{ M_{211}\left(2^m\mathbf{k}_0 - \mathbf{k} + \left(0, \frac{1}{2}\right)^T\right) - M_{211}\left(2^m\mathbf{k}_0 - \mathbf{k} - \left(0, \frac{1}{2}\right)^T\right)\right\}$$

$$= 2^m \left\{ \frac{1}{8} \begin{pmatrix} v^m_{2^m\mathbf{k}_0+(1,1)^T} - v^m_{2^m\mathbf{k}_0+(1,0)^T} + v^m_{2^m\mathbf{k}_0+(-1,0)^T} \\ -v^m_{2^m\mathbf{k}_0+(-1,-1)^T} + 3v^m_{2^m\mathbf{k}_0+(0,1)^T} - 3v^m_{2^m\mathbf{k}_0+(0,-1)^T} \end{pmatrix} \right\}$$

where we use Figure 9.5 on p. 212 showing values of M_{121} when the *second* coordinate equals $\pm\frac{1}{2}$. Again recall that these values were obtained by using the software in [**Kob96**]. Now we take the limit as our subdivisions go to infinity:

$$\lim_{m\to\infty} D_2F_m(\mathbf{k}_0) = \lim_{m\to\infty} \left[2^m \left\{ \frac{1}{8} \begin{pmatrix} v^m_{2^m\mathbf{k}_0+(1,1)^T} - v^m_{2^m\mathbf{k}_0+(1,0)^T} + v^m_{2^m\mathbf{k}_0+(-1,0)^T} \\ -v^m_{2^m\mathbf{k}_0+(-1,-1)^T} + 3v^m_{2^m\mathbf{k}_0+(0,1)^T} - 3v^m_{2^m\mathbf{k}_0+(0,-1)^T} \end{pmatrix} \right\} \right]$$

And so by (9.1 |p.204)

$$D_2F(\mathbf{k}_0) = \lim_{m\to\infty} \left[2^m \left\{ \frac{1}{8} \begin{pmatrix} v^m_{2^m\mathbf{k}_0+(1,1)^T} - v^m_{2^m\mathbf{k}_0+(1,0)^T} + v^m_{2^m\mathbf{k}_0+(-1,0)^T} \\ -v^m_{2^m\mathbf{k}_0+(-1,-1)^T} + 3v^m_{2^m\mathbf{k}_0+(0,1)^T} - 3v^m_{2^m\mathbf{k}_0+(0,-1)^T} \end{pmatrix} \right\} \right]$$

$\square$

The following is the proof of Corollary 5.1 on p. 96:

Proof. It follows the proof of Theorem 5.1.

$$F_m(\mathbf{x}) := \sum_{\mathbf{k}\in\mathbb{Z}^2} \mathbf{v}_{\mathbf{k}}^{m} \Phi_0\left(2^m \mathbf{x} - \mathbf{k}\right) \rightarrow$$

$$F_{m+n}(\mathbf{x}) := \sum_{\mathbf{k}\in\mathbb{Z}^2} \mathbf{v}_{\mathbf{k}}^{m+n} \Phi_0\left(2^{m+n} \mathbf{x} - \mathbf{k}\right) \rightarrow$$

for $j = 1, 2$ $$D_j F_{m+n}(\mathbf{x}) = \sum_{\mathbf{k}\in\mathbb{Z}^2} 2^{m+n} \mathbf{v}_{\mathbf{k}}^{m+n} D_j \Phi_0\left(2^{m+n} \mathbf{x} - \mathbf{k}\right)$$

$$= 2^n \sum_{\mathbf{k}\in\mathbb{Z}^2} 2^{m} \mathbf{v}_{\mathbf{k}}^{m+n} D_j \Phi_0\left(2^{m+n} \mathbf{x} - \mathbf{k}\right) \rightarrow$$

$$\lim_{m\to\infty} D_j F_{m+n}(\mathbf{x}) = 2^n \lim_{m\to\infty} \sum_{\mathbf{k}\in\mathbb{Z}^2} 2^{m} \mathbf{v}_{\mathbf{k}}^{m+n} D_j \Phi_0\left(2^{m+n} \mathbf{x} - \mathbf{k}\right) \rightarrow$$

$$D_j F(\mathbf{x}) = 2^n \lim_{m\to\infty} \sum_{\mathbf{k}\in\mathbb{Z}^2} 2^{m} \mathbf{v}_{\mathbf{k}}^{m+n} D_j \Phi_0\left(2^{m+n} \mathbf{x} - \mathbf{k}\right) \rightarrow$$

$$D_j F\left(\mathbf{k}_0 + \frac{\mathbf{i}}{2^n}\right) = 2^n \lim_{m\to\infty} \sum_{\mathbf{k}\in\mathbb{Z}^2} 2^{m} \mathbf{v}_{\mathbf{k}}^{m+n} D_j \Phi_0\left(2^{m+n} \left[\mathbf{k}_0 + \frac{\mathbf{i}}{2^n}\right] - \mathbf{k}\right) \rightarrow$$

$$D_j F\left(\mathbf{k}_0 + \frac{\mathbf{i}}{2^n}\right) = 2^n \lim_{m\to\infty} \sum_{\mathbf{k}\in\mathbb{Z}^2} 2^{m} \mathbf{v}_{\mathbf{k}}^{m+n} D_j \Phi_0\left(2^{m+n} \mathbf{k}_0 + 2^m \mathbf{i} - \mathbf{k}\right) \rightarrow$$

$$D_1 F\left(\mathbf{k}_0 + \frac{\mathbf{i}}{2^n}\right) = 2^n \lim_{m\to\infty} \sum_{\mathbf{k}\in\mathbb{Z}^2} 2^{m} v_{\mathbf{k}}^{m+n} D_1 M_{221}\left(2^{m+n} \mathbf{k}_0 + 2^m \mathbf{i} - \mathbf{k}\right) \quad \text{for } j = 1$$

$$D_2 F\left(\mathbf{k}_0 + \frac{\mathbf{i}}{2^n}\right) = 2^n \lim_{m\to\infty} \sum_{\mathbf{k}\in\mathbb{Z}^2} 2^{m} v_{\mathbf{k}}^{m+n} D_2 M_{221}\left(2^{m+n} \mathbf{k}_0 + 2^m \mathbf{i} - \mathbf{k}\right) \quad \text{for } j = 2$$

The rest of the proof follows from using (5.11 |p.95) and the methods in last parts of Theorem 5.1. □

The following is the proof of Theorem 5.2 on page 98:

Proof. Let $\Phi_0 := \left[\begin{smallmatrix} M_{313} \\ 0 \end{smallmatrix}\right]$. Note that $M_{313} \in C^2\left(\mathbb{R}^2\right)$ and that $M_{313} \in \pi_5^2$ (accuracy order 6). Define

$$\begin{aligned}
F_m(\mathbf{x}) &:= \sum_{\mathbf{k}\in\mathbb{Z}^2} \mathbf{v}_{\mathbf{k}}^m \Phi_0\left(2^m\mathbf{x}-\mathbf{k}\right) \\
&= \sum_{\mathbf{k}\in\mathbb{Z}^2} v_{\mathbf{k}}^m M_{313}\left(2^m\mathbf{x}-\mathbf{k}\right) \\
&= \sum_{\mathbf{k}\in\mathbb{Z}^2} \mathbf{v}_{\mathbf{k}}^0 Q_P^m \Phi_0\left(\mathbf{x}-\mathbf{k}\right) \quad \text{from } (5.2\ |\text{p.}90) \rightarrow
\end{aligned}$$

$$D^{(i,j)^T} F_m(\mathbf{x}) = \sum_{\mathbf{k}\in\mathbb{Z}^2} \mathbf{v}_{\mathbf{k}}^0 D^{(i,j)^T}\left\{Q_P^m \Phi_0\left(\mathbf{x}-\mathbf{k}\right)\right\} \quad \text{for } (i,j)^T = (2,0)^T, (1,1)^T, (0,2)^T$$

where we are using the derivative notation in (2.2 |p.9)

Hence we can derive due to the C^2 convergence:

(9.2)

$$\begin{aligned}
\lim_{m\to\infty} D^{(i,j)^T} F_m(\mathbf{x}) &= \sum_{\mathbf{k}\in\mathbb{Z}^2} \mathbf{v}_{\mathbf{k}}^0 \lim_{m\to\infty} D^{(i,j)^T}\left\{Q_P^m \Phi_0\left(\mathbf{x}-\mathbf{k}\right)\right\} \\
&= \sum_{\mathbf{k}\in\mathbb{Z}^2} \mathbf{v}_{\mathbf{k}}^0 D^{(i,j)^T} \Phi\left(\mathbf{x}-\mathbf{k}\right) \\
&= D^{(i,j)^T} F(\mathbf{x}) \quad \text{for } (i,j)^T = (2,0)^T, (1,1)^T, (0,2)^T
\end{aligned}$$

Now we will get a representation of $D^{(2,0)^T} F_m(\mathbf{x})$ in terms of surrounding vertices.

$$\begin{aligned}
D^{(1,0)^T} F_m(\mathbf{x}) &= \sum_{\mathbf{k}\in\mathbb{Z}^2} v_{\mathbf{k}}^m D^{(1,0)^T}\left\{M_{313}\left(2^m\mathbf{x}-\mathbf{k}\right)\right\} \\
&= \sum_{\mathbf{k}\in\mathbb{Z}^2} v_{\mathbf{k}}^m 2^m \left\{\begin{array}{c} M_{213}\left(2^m\mathbf{x}-\mathbf{k}+\left(\frac{1}{2},0\right)^T\right) \\ -M_{213}\left(2^m\mathbf{x}-\mathbf{k}-\left(\frac{1}{2},0\right)^T\right) \end{array}\right\} \quad \text{by } (5.11\ |\text{p.}95)
\end{aligned}$$

Hence

$$D^{(1,0)^T}\left[D^{(1,0)^T}F_m(\mathbf{x})\right]=\sum_{\mathbf{k}\in\mathbb{Z}^2}v_{\mathbf{k}}^m 2^{2m}\left\{\begin{array}{c}\left[\begin{array}{c}M_{113}\left(2^m\mathbf{x}-\mathbf{k}+(1,0)^T\right)\\-M_{113}\left(2^m\mathbf{x}-\mathbf{k}-\left(\frac{1}{2},0\right)^T+\left(\frac{1}{2},0\right)^T\right)\end{array}\right]\\-\left[\begin{array}{c}M_{113}\left(2^m\mathbf{x}-\mathbf{k}+\left(\frac{1}{2},0\right)^T-\left(\frac{1}{2},0\right)^T\right)\\-M_{113}\left(2^m\mathbf{x}-\mathbf{k}-(1,0)^T\right)\end{array}\right]\end{array}\right\}$$

Let $\mathbf{k}_0\in\mathbb{Z}^2$.

$$\begin{aligned}D^{(1,0)^T}\left[D^{(1,0)^T}F_m(\mathbf{k}_0)\right]&=\sum_{\mathbf{k}\in\mathbb{Z}^2}v_{\mathbf{k}}^m 2^{2m}\left\{\begin{array}{c}\left[\begin{array}{c}M_{113}\left(2^m\mathbf{k}_0-\mathbf{k}+(1,0)^T\right)\\-M_{113}\left(2^m\mathbf{k}_0-\mathbf{k}-\left(\frac{1}{2},0\right)^T+\left(\frac{1}{2},0\right)^T\right)\end{array}\right]\\-\left[\begin{array}{c}M_{113}\left(2^m\mathbf{k}_0-\mathbf{k}+\left(\frac{1}{2},0\right)^T-\left(\frac{1}{2},0\right)^T\right)\\-M_{113}\left(2^m\mathbf{k}_0-\mathbf{k}-(1,0)^T\right)\end{array}\right]\end{array}\right\}\\&=2^{2m}\left\{\frac{1}{6}\left(\begin{array}{c}-8v^m_{2^m\mathbf{k}_0+(0,0)^T}+4v^m_{2^m\mathbf{k}_0+(1,0)^T}+4v^m_{2^m\mathbf{k}_0+(-1,0)^T}\\-2v^m_{2^m\mathbf{k}_0+(1,1)^T}+v^m_{2^m\mathbf{k}_0+(2,1)^T}+v^m_{2^m\mathbf{k}_0+(0,1)^T}\\-2v^m_{2^m\mathbf{k}_0+(-1,-1)^T}+v^m_{2^m\mathbf{k}_0+(0,-1)^T}+v^m_{2^m\mathbf{k}_0+(-2,-1)^T}\end{array}\right)\right\}\end{aligned}$$

by Figure 9.6 that shows values of M_{113} where both coordinates are integers.

Hence

$$\lim_{m\to\infty}D^{(2,0)^T}F_m(\mathbf{k}_0)=$$

$$\lim_{m\to\infty}2^{2m}\left\{\frac{1}{6}\left(\begin{array}{c}-8v^m_{2^m\mathbf{k}_0+(0,0)^T}+4v^m_{2^m\mathbf{k}_0+(1,0)^T}+4v^m_{2^m\mathbf{k}_0+(-1,0)^T}\\-2v^m_{2^m\mathbf{k}_0+(1,1)^T}+v^m_{2^m\mathbf{k}_0+(2,1)^T}+v^m_{2^m\mathbf{k}_0+(0,1)^T}\\-2v^m_{2^m\mathbf{k}_0+(-1,-1)^T}+v^m_{2^m\mathbf{k}_0+(0,-1)^T}+v^m_{2^m\mathbf{k}_0+(-2,-1)^T}\end{array}\right)\right\}$$

and so by (9.2 |p.208)

$$D^{(2,0)^T}F(\mathbf{k}_0)=$$

$$\lim_{m\to\infty}2^{2m}\left\{\frac{1}{6}\left(\begin{array}{c}-8v^m_{2^m\mathbf{k}_0+(0,0)^T}+4v^m_{2^m\mathbf{k}_0+(1,0)^T}+4v^m_{2^m\mathbf{k}_0+(-1,0)^T}\\-2v^m_{2^m\mathbf{k}_0+(1,1)^T}+v^m_{2^m\mathbf{k}_0+(2,1)^T}+v^m_{2^m\mathbf{k}_0+(0,1)^T}\\-2v^m_{2^m\mathbf{k}_0+(-1,-1)^T}+v^m_{2^m\mathbf{k}_0+(0,-1)^T}+v^m_{2^m\mathbf{k}_0+(-2,-1)^T}\end{array}\right)\right\}$$

Using a symmetric argument [this time starting with $\Phi_0 := \left[\begin{smallmatrix} M_{313} \\ 0 \end{smallmatrix}\right]$] we can derive

$$D^{(0,2)^T} F(\mathbf{k}_0) =$$

$$\lim_{m\to\infty} 2^{2m} \left\{ \frac{1}{6} \left(\begin{array}{c} -8v^m_{2^m\mathbf{k}_0+(0,0)^T} + 4v^m_{2^m\mathbf{k}_0+(0,1)^T} + 4v^m_{2^m\mathbf{k}_0+(0,-1)^T} \\ -2v^m_{2^m\mathbf{k}_0+(1,1)^T} + v^m_{2^m\mathbf{k}_0+(1,2)^T} + v^m_{2^m\mathbf{k}_0+(1,0)^T} \\ -2v^m_{2^m\mathbf{k}_0+(-1,-1)^T} + v^m_{2^m\mathbf{k}_0+(-1,0)^T} + v^m_{2^m\mathbf{k}_0+(-1,-2)^T} \end{array} \right) \right\}$$

Now we will get a representation of $D_2D_1F_m(\mathbf{x})$ in terms of surrounding vertices. Let $\Phi_0 := \left[\begin{smallmatrix} M_{222} \\ 0 \end{smallmatrix}\right]$. Note that $M_{222} \in C^2(\mathbb{R}^2)$ and that $M_{222} \in \pi_4^2$ (accuracy order 5).

$$\begin{aligned} D_1F_m(\mathbf{x}) &= \sum_{\mathbf{k}\in\mathbb{Z}^2} v^m_{\mathbf{k}} D_1 \left\{ M_{222}(2^m\mathbf{x}-\mathbf{k}) \right\} \\ &= \sum_{\mathbf{k}\in\mathbb{Z}^2} v^m_{\mathbf{k}} 2^m \left\{ \begin{array}{c} M_{122}\left(2^m\mathbf{x}-\mathbf{k}+\left(\frac{1}{2},0\right)^T\right) \\ -M_{122}\left(2^m\mathbf{x}-\mathbf{k}-\left(\frac{1}{2},0\right)^T\right) \end{array} \right\} \text{ by (5.11 |p.95)} \end{aligned}$$

Hence

$$D_2D_1F_m(\mathbf{x}) = \sum_{\mathbf{k}\in\mathbb{Z}^2} v^m_{\mathbf{k}} 2^{2m} \left\{ \begin{array}{c} \left[\begin{array}{c} M_{112}\left(2^m\mathbf{x}-\mathbf{k}+\left(\frac{1}{2},0\right)^T+\left(0,\frac{1}{2}\right)^T\right) \\ -M_{112}\left(2^m\mathbf{x}-\mathbf{k}-\left(\frac{1}{2},0\right)^T+\left(0,\frac{1}{2}\right)^T\right) \end{array} \right] \\ -\left[\begin{array}{c} M_{112}\left(2^m\mathbf{x}-\mathbf{k}+\left(\frac{1}{2},0\right)^T-\left(0,\frac{1}{2}\right)^T\right) \\ -M_{112}\left(2^m\mathbf{x}-\mathbf{k}-\left(\frac{1}{2},0\right)^T-\left(0,\frac{1}{2}\right)^T\right) \end{array} \right] \end{array} \right\}$$

Let $\mathbf{k}_0 \in \mathbb{Z}^2$.

$$D_2D_1F_m(\mathbf{k}_0) = \sum_{\mathbf{k}\in\mathbb{Z}^2} v_{\mathbf{k}}^m 2^{2m} \left\{ \begin{array}{c} \left[\begin{array}{c} M_{112}\left(2^m\mathbf{k}_0 - \mathbf{k} + \left(\frac{1}{2},0\right)^T + \left(0,\frac{1}{2}\right)^T\right) \\ -M_{112}\left(2^m\mathbf{k}_0 - \mathbf{k} - \left(\frac{1}{2},0\right)^T + \left(0,\frac{1}{2}\right)^T\right) \end{array} \right] \\ - \left[\begin{array}{c} M_{112}\left(2^m\mathbf{k}_0 - \mathbf{k} + \left(\frac{1}{2},0\right)^T - \left(0,\frac{1}{2}\right)^T\right) \\ -M_{112}\left(2^m\mathbf{k}_0 - \mathbf{k} - \left(\frac{1}{2},0\right)^T - \left(0,\frac{1}{2}\right)^T\right) \end{array} \right] \end{array} \right\}$$

$$= 2^{2m} \left\{ \frac{1}{2} \left(\begin{array}{c} 2v_{2^m\mathbf{k}_0+(0,0)^T}^m - v_{2^m\mathbf{k}_0+(1,0)^T}^m - v_{2^m\mathbf{k}_0+(-1,0)^T}^m \\ +v_{2^m\mathbf{k}_0+(1,1)^T}^m - v_{2^m\mathbf{k}_0+(0,1)^T}^m \\ +v_{2^m\mathbf{k}_0+(-1,-1)^T}^m - v_{2^m\mathbf{k}_0+(0,-1)^T}^m \end{array} \right) \right\}$$

by Figure 9.7 on p. 213 showing values of M_{112} at $\left(\frac{1}{2},\frac{1}{2}\right)$ and $\left(-\frac{1}{2},-\frac{1}{2}\right)$.

Thus we have

$$\lim_{m\to\infty} D_2D_1F_m(\mathbf{k}_0) = \lim_{m\to\infty} 2^{2m} \left\{ \frac{1}{2} \left(\begin{array}{c} 2v_{2^m\mathbf{k}_0+(0,0)^T}^m - v_{2^m\mathbf{k}_0+(1,0)^T}^m - v_{2^m\mathbf{k}_0+(-1,0)^T}^m \\ +v_{2^m\mathbf{k}_0+(1,1)^T}^m - v_{2^m\mathbf{k}_0+(0,1)^T}^m \\ +v_{2^m\mathbf{k}_0+(-1,-1)^T}^m - v_{2^m\mathbf{k}_0+(0,-1)^T}^m \end{array} \right) \right\}$$

and so by (9.2 |p.208)

$$D_2D_1F(\mathbf{k}_0) = \lim_{m\to\infty} 2^{2m} \left\{ \frac{1}{2} \left(\begin{array}{c} 2v_{2^m\mathbf{k}_0+(0,0)^T}^m - v_{2^m\mathbf{k}_0+(1,0)^T}^m - v_{2^m\mathbf{k}_0+(-1,0)^T}^m \\ +v_{2^m\mathbf{k}_0+(1,1)^T}^m - v_{2^m\mathbf{k}_0+(0,1)^T}^m \\ +v_{2^m\mathbf{k}_0+(-1,-1)^T}^m - v_{2^m\mathbf{k}_0+(0,-1)^T}^m \end{array} \right) \right\}$$

$\square$

.

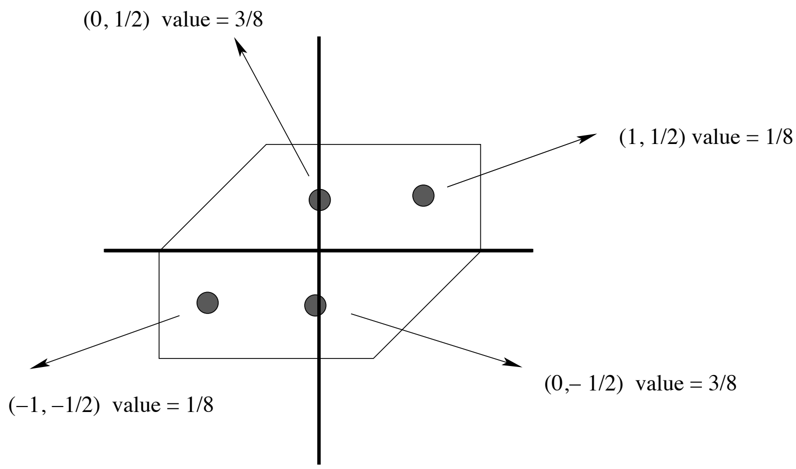

Figure 9.5. Box spline M_{211}: showing values where second coordinate $=\pm\frac{1}{2}$

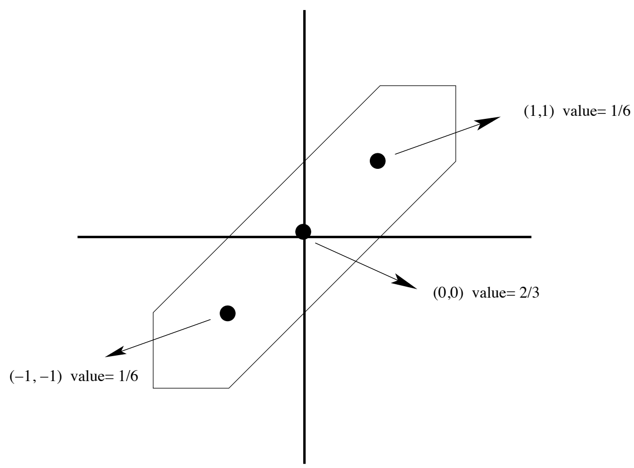

Figure 9.6. Box spline M_{113} with values shown at integer coordinates

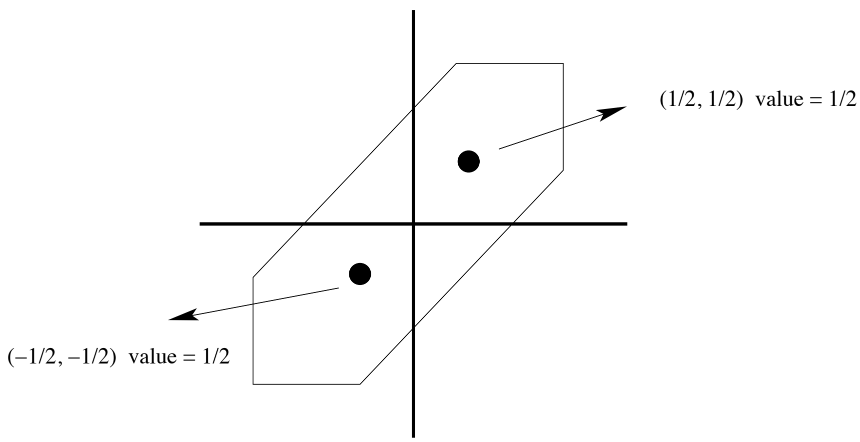

Figure 9.7. Box spline M_{112} with values shown at $\left(\frac{1}{2}, \frac{1}{2}\right)$ and $\left(-\frac{1}{2}, -\frac{1}{2}\right)$

Appendix D

Eigenvalues are listed for varying valences of Quadrilateral Approximating Scheme (5.5.3.2 |p.139). The subdominant eigenvalue λ is listed in bold, and eigenvalues are listed in increasing order. Note that complex eigenvalue(s) are listed last and that their modulus is less than the subdominant eigenvalue.

Valence 3

0., 0., 0., 0.093750, 0.093750, 0.15240, 0.15240, 0.25000, **0.41010, 0.41010**, 1., -0.051460-0.0000027064 I, 0.060722+0.0000027064 I, 0.10011-0.000001 I

Valence 5

0., 0., 0., 0., 0., 0.074441, 0.074441, 0.11365, 0.11365, 0.14432, 0.14432, 0.18377, 0.18377, 0.25000, 0.34011, 0.34011, **0.54999, 0.54999**, 1., -0.051460-0.0000027064I, 0.060722+0.0000027064 I, 0.10011-0.000001 I

Valence 6

0., 0., 0., 0., 0., 0., 0.062500, 0.093750, 0.093750, 0.10782, 0.10782, 0.15240, 0.15240, 0.15625, 0.15625, 0.25000, 0.25000, 0.25000, 0.41010, 0.41010, **0.57968, 0.57968**, 1., -0.051460-0.0000027064 I, 0.060722+0.0000027064 I, 0.10011-0.000001 I

Valence 7

0., 0., 0., 0., 0., 0., 0., 0.10443, 0.10443, 0.13532, 0.13532, 0.20022, 0.20022, 0.25000, 0.31216, 0.31216, 0.46186, 0.46186, **0.59851, 0.59851**, 1., -0.051460-0.0000027064I, 0.060722+0.0000027064 I, 0.068682+0. I, 0.068682+0. I, 0.10011-0.000001 I, 0.11109+0. I, 0.11109+0. I, 0.16396+0.000001I, 0.16396+0.000001 I

Valence 8

0, 0., 0., 0., 0., 0., 0., 0., 0.062500, 0.080806, 0.080806, 0.10227, 0.10227, 0.12500, 0.12500, 0.12500, 0.12500, 0.16919, 0.16919, 0.17090, 0.17090, 0.25000, 0.25000, 0.25000, 0.36572, 0.36572, 0.50000, 0.50000, **0.61111, 0.61111**, 1., -0.051460-0.0000027064I, 0.060722+0.0000027064 I, 0.10011-0.000001 I

Valence 9

0., 0., 0., 0., 0., 0., 0., 0., 0., 0.093750, 0.093750, 0.10082, 0.10082, 0.11827, 0.11827, 0.15240, 0.15240, 0.21019, 0.21019, 0.25000, 0.29734, 0.29734, 0.41010, 0.41010, 0.52843, 0.52843, **0.61994, 0.61994**, 1., -0.051460-0.0000027064 I, 0.060722+0.0000027064 I, 0.066266-0.0000012706 I, 0.066266-0.0000012706I, 0.10011-0.000001 I, 0.13585-7.2936$\times$ 10^(-7) I, 0.13585-7.2936$\times$10^(-7) I, 0.17288+0.000001 I, 0.17288+0.000001 I

Valence 10

0., 0., 0., 0., 0., 0., 0., 0., 0., 0., 0.062500, 0.074441, 0.074441, 0.09978, 0.09978, 0.10568, 0.10568, 0.11365, 0.11365, 0.14002, 0.14002, 0.14432, 0.14432, 0.17556, 0.17556, 0.18377, 0.18377, 0.25000, 0.25000, 0.25000, 0.34011, 0.34011, 0.44634, 0.44634, 0.54999, 0.54999, **0.62634, 0.62634**, 1., -0.051460-0.0000027064 I, 0.060722+0.0000027064 I, 0.10011-0.000001 I

Valence 11

0., 0., 0., 0., 0., 0., 0., 0., 0., 0., 0., 0.099029, 0.099029, 0.11030, 0.11030, 0.13134, 0.13134, 0.16550, 0.16550, 0.21686, 0.21686, 0.25000, 0.28820, 0.28820, 0.37764, 0.37764, 0.47587, 0.47587, 0.56662, 0.56662, **0.63113, 0.63113**, 1., -0.051460-0.0000027064I, 0.060722+0.0000027064 I, 0.065032-0.0000010 I, 0.065032-0.0000010 I, 0.084069-0.000001I, 0.084069-0.000001 I, 0.10011-0.000001 I, 0.11611-0.0000029 I, 0.11611-0.0000029 I, 0.15096+0.000004 I, 0.15096+0.000004I, 0.17759+0.000002 I, 0.17759+0.000002 I

Valence 12
0., 0., 0., 0., 0., 0., 0., 0., 0., 0., 0., 0., 0.062500, 0.070872, 0.070872, 0.093750, 0.093750, 0.09846, 0.09846, 0.10782, 0.10782, 0.12500, 0.12500, 0.12500, 0.12500, 0.15240, 0.15240, 0.15625, 0.15625, 0.17913, 0.17913, 0.19313, 0.19313, 0.25000, 0.25000, 0.25000, 0.32361, 0.32361, 0.41010, 0.41010, 0.50000, 0.50000, 0.57968, 0.57968, **0.63480, 0.63480**, 1., -0.051460-0.0000027064I, 0.060722+0.0000027064 I, 0.10011-0.000001 I

Valence 13
0., 0., 0., 0., 0., 0., 0., 0., 0., 0., 0., 0., 0., 0.064316, 0.064316, 0.078219, 0.078219, 0.098013, 0.098013, 0.10284, 0.10284, 0.10592, 0.10592, 0.12023, 0.12023, 0.13253, 0.13253, 0.14270, 0.14270, 0.16050, 0.16050, 0.17568, 0.17568, 0.18034, 0.18034, 0.22163, 0.22163, 0.25000, 0.28200, 0.28200, 0.35575, 0.35575, 0.43797, 0.43797, 0.51984, 0.51984, 0.59009, 0.59009, **0.63767, 0.63767**, 1., -0.051460-0.0000027064I, 0.060722+0.0000027064 I, 0.10011-0.000001 I

Valence 14
0., 0., 0., 0., 0., 0., 0., 0., 0., 0., 0., 0., 0., 0., 0.062500, 0.097663, 0.097663, 0.10443, 0.10443, 0.11655, 0.11655, 0.13532, 0.13532, 0.16254, 0.16254, 0.20022, 0.20022, 0.25000, 0.25000, 0.25000, 0.31216, 0.31216, 0.38453, 0.38453, 0.46186, 0.46186, 0.53627, 0.53627, 0.59851, 0.59851, **0.63996, 0.63996**, 1., -0.051460-0.0000027064I, 0.060722+0.0000027064 I, 0.068682+0. I, 0.068682+0. I, 0.086041+3.$\times$ 10^(-7) I, 0.086041+3.10$\times$ 10^(-7) I, 0.10011-0.000001 I, 0.11109+0. I, 0.11109+0. I, 0.13892+3.$\times$ 10^(-7) I, 0.13892+3.10$\times$ 10^(-7) I, 0.16396+0.000001 I, 0.16396+0.000001 I, 0.18132-0.000001 I, 0.18132-0.000001 I

Valence 15

0., 0., 0., 0., 0., 0., 0., 0., 0., 0., 0., 0., 0., 0., 0., 0.063862, 0.063862, 0.074441, 0.074441, 0.093750, 0.093750, 0.097380, 0.097380, 0.10324, 0.10324, 0.11365, 0.11365, 0.11847, 0.11847, 0.12957, 0.12957, 0.14432, 0.14432, 0.15240, 0.15240, 0.16682, 0.16682, 0.18209, 0.18209, 0.18377, 0.18377, 0.22520, 0.22520,
0.25000, 0.27753, 0.27753, 0.34011, 0.34011, 0.41010, 0.41010, 0.48236, 0.48236, 0.54999, 0.54999, 0.60540, 0.60540, **0.64181, 0.64181**, 1., -0.051460-0.0000027064 I, 0.060722+0.0000027064I, 0.10011-0.000001 I

Valence 16

0., 0., 0., 0., 0., 0., 0., 0., 0., 0., 0., 0., 0., 0., 0., 0., 0., 062500, 0.067256, 0.067256, 0.080806, 0.080806, 0.097150, 0.097150, 0.10108, 0.10108, 0.10227, 0.10227, 0.11130, 0.11130, 0.12500, 0.12500, 0.12500, 0.12500, 0.14443, 0.14443, 0.14892, 0.14892, 0.16919, 0.16919, 0.17090, 0.17090, 0.18274, 0.18274, 0.20575, 0.20575,
0.25000, 0.25000, 0.25000, 0.30376, 0.30376, 0.36572, 0.36572, 0.43273, 0.43273, 0.50000, 0.50000, 0.56153, 0.56153, 0.61111, 0.61111,
0.64333, 0.64333, 1., -0.051460-0.0000027064I, 0.060722+0.0000027064 I, 0.10011-0.000001 I

Appendix E

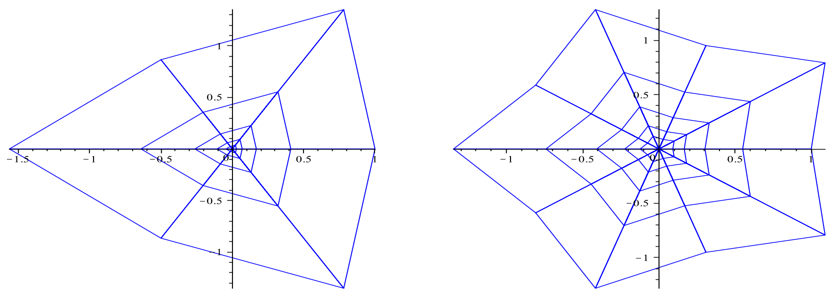

Figure 9.8. "Characteristic" maps for Approximating Quadrilateral Scheme (5.5.3.2 |p.139) for valences 3 and 5. Note that they "appear" regular and injective.

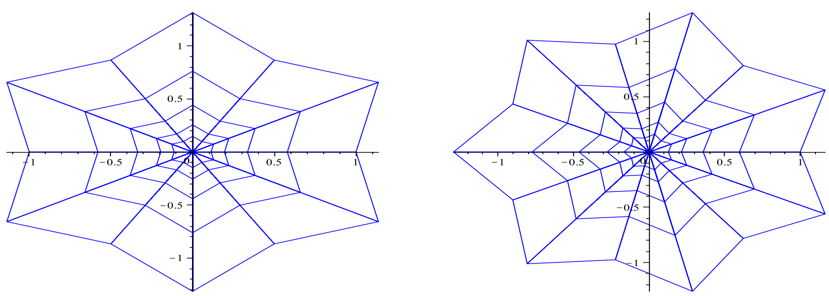

Figure 9.9. "Characteristic" maps for Approximating Quadrilateral Scheme (5.5.3.2 |p.139) for valences 6 and 7. Note that they "appear" regular and injective.

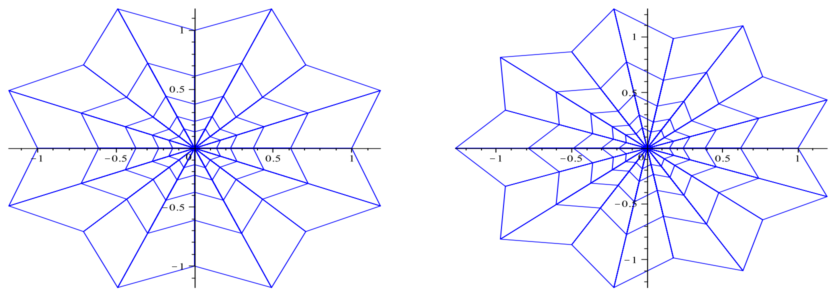

Figure 9.10. “Characteristic” maps for Approximating Quadrilateral Scheme (5.5.3.2 |p.139) for valences 8 and 9. Note that they “appear” regular and injective.

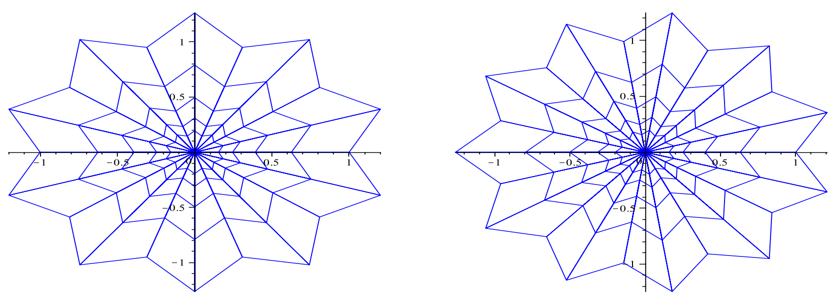

Figure 9.11. “Characteristic” maps for Approximating Quadrilateral Scheme (5.5.3.2 |p.139) for valences 10 and 11. Note that they “appear” regular and injective.

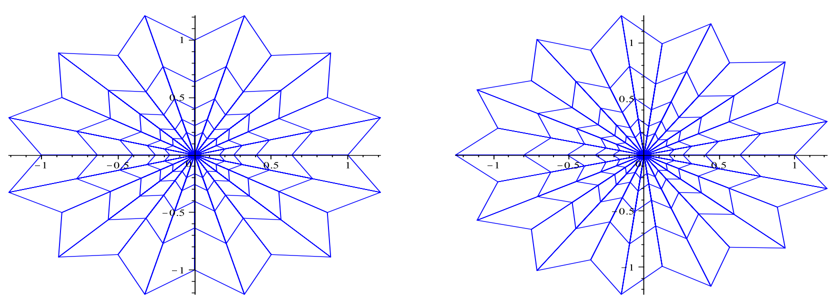

Figure 9.12. “Characteristic” maps for Approximating Quadrilateral Scheme (5.5.3.2 |p.139) for valences 12 and 13. Note that they “appear” regular and injective.

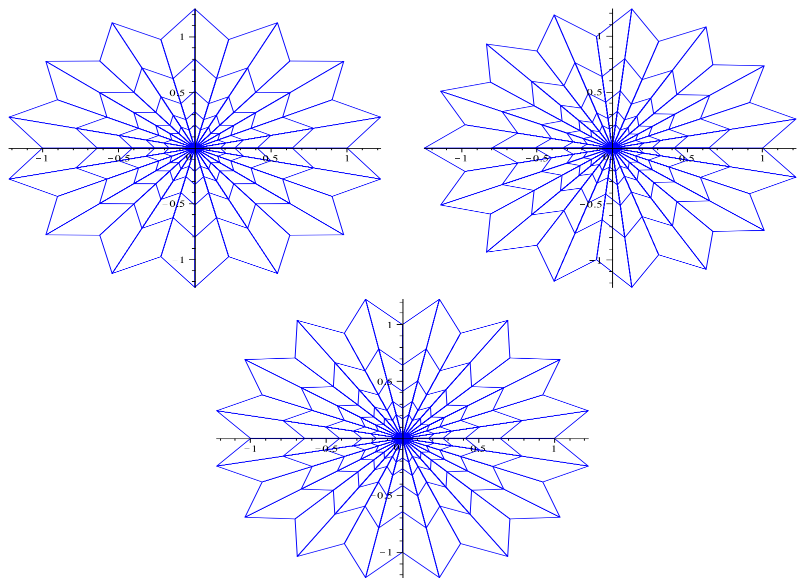

Figure 9.13. “Characteristic” maps for Approximating Quadrilateral Scheme (5.5.3.2 |p.139) for valences 14, 15, and 16. Note that they “appear” regular and injective.

Appendix F

Here are figures showing normals at both regular and extraordinary vertices for approximating and interpolatory quadrilateral and triangular schemes. The normal vector in each figure is indicated by the black line. Please observe that these normal vectors visually affirm the formulas that went into their calculation.

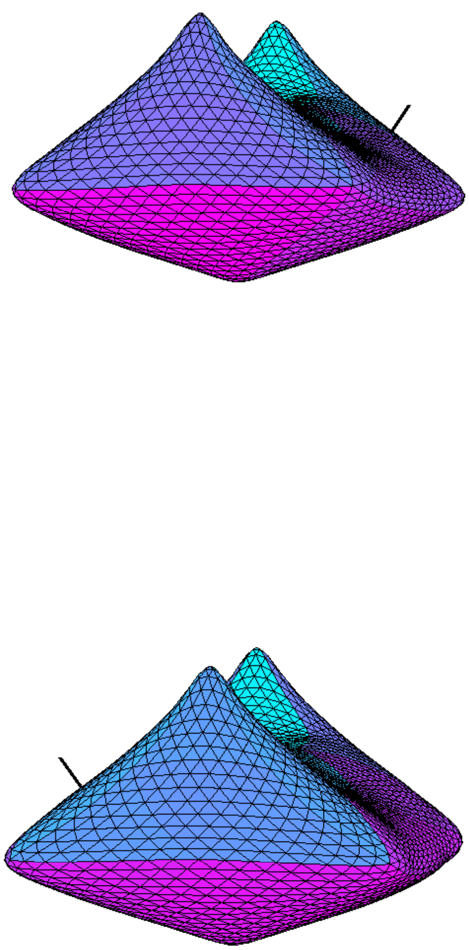

Figure 9.14. Interpolatory triangular scheme: Two different views of same normal vector at a regular vertex

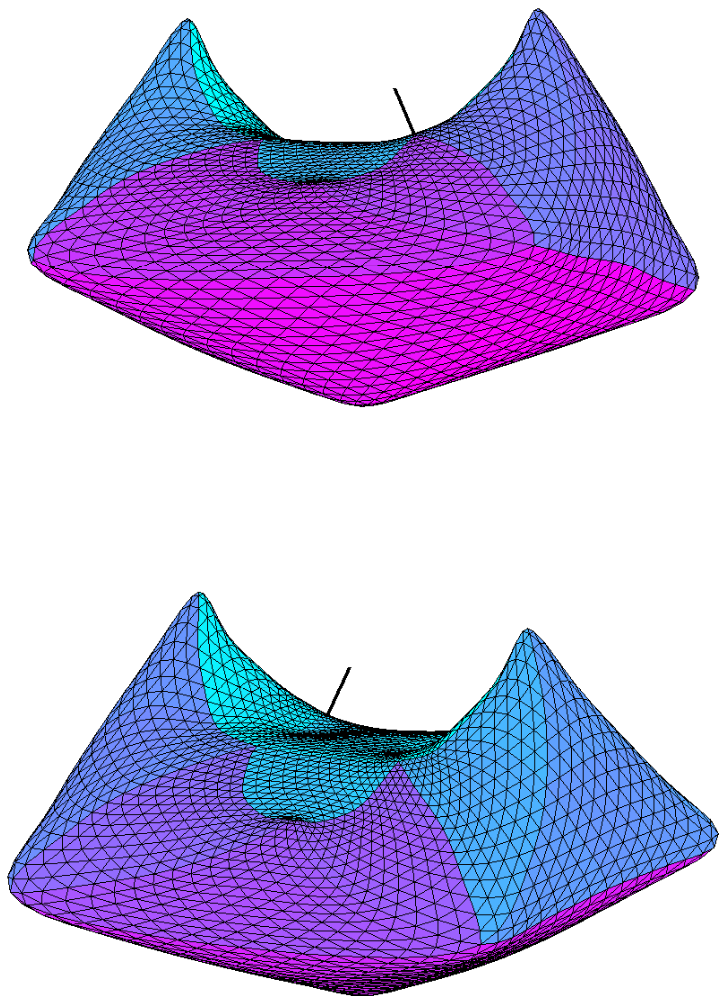

Figure 9.15. Interpolatory triangular scheme: Normal at vertex of valence 5

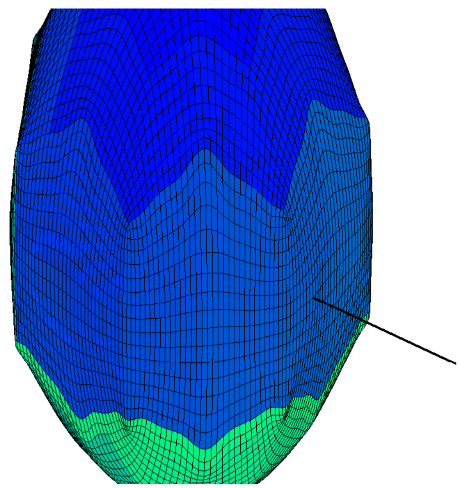

Figure 9.16. Interpolatory quadrilateral scheme: Normal at regular vertex

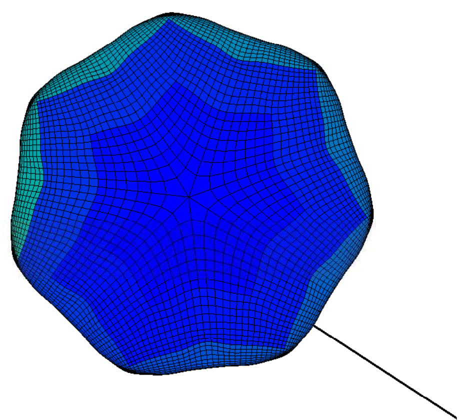

Figure 9.17. Interpolatory Quadrilateral Scheme: "Top View" of same normal at regular vertex

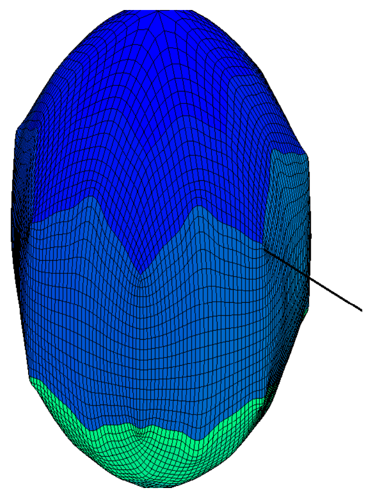

Figure 9.18. Interpolatory Quadrilateral Scheme: Normal at vertex of valence 3

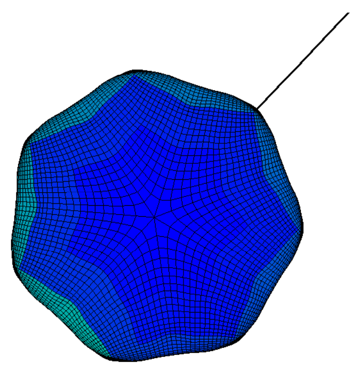

Figure 9.19. Interpolatory Quadrilateral Scheme: "Top View" of same normal at vertex of valence 3

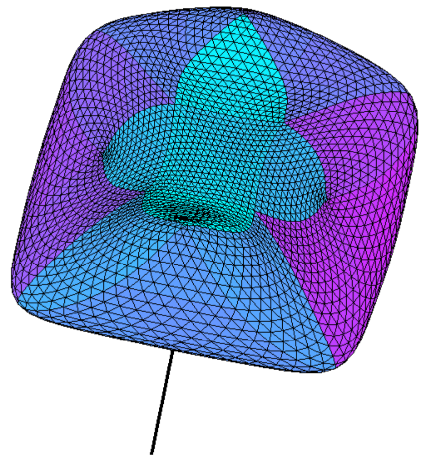

Figure 9.20. Approximating triangular scheme; Normal at regular vertex

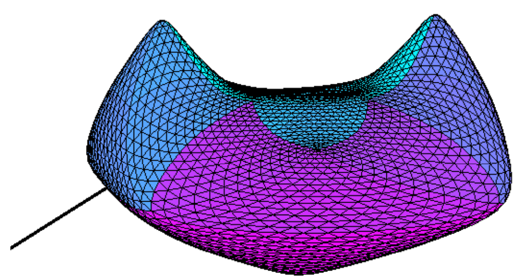

Figure 9.21. Approximating triangular scheme: Another view of normal at regular vertex

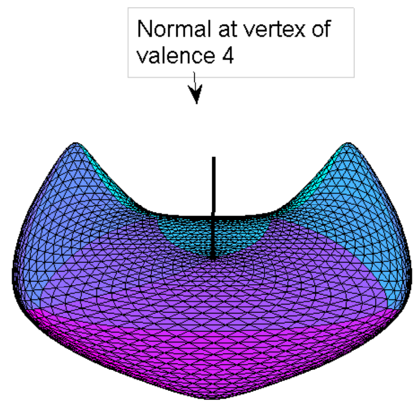

Figure 9.22. Approximating triangular scheme: Normal at vertex of valence 4

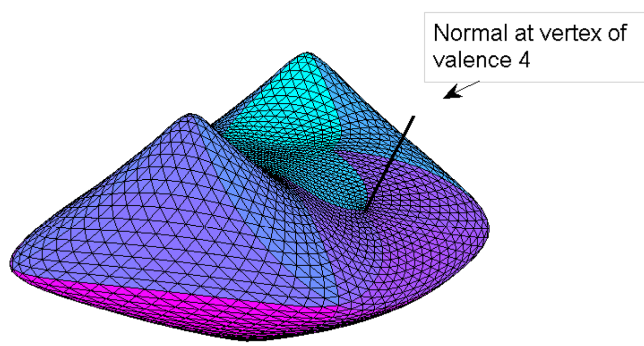

Figure 9.23. Approximating triangular scheme: Another view of normal at vertex of valence 4

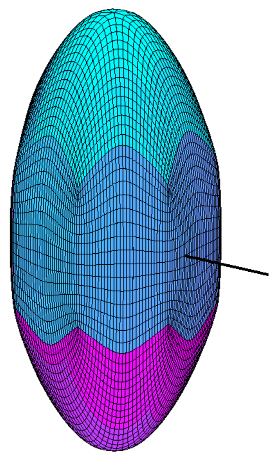

Figure 9.24. Approximating quadrilateral scheme: Normal at a regular vertex

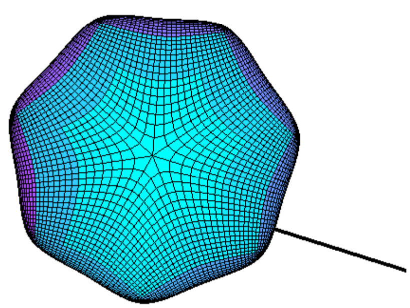

Figure 9.25. Approximating quadrilateral scheme: "Top view" of same normal at regular vertex

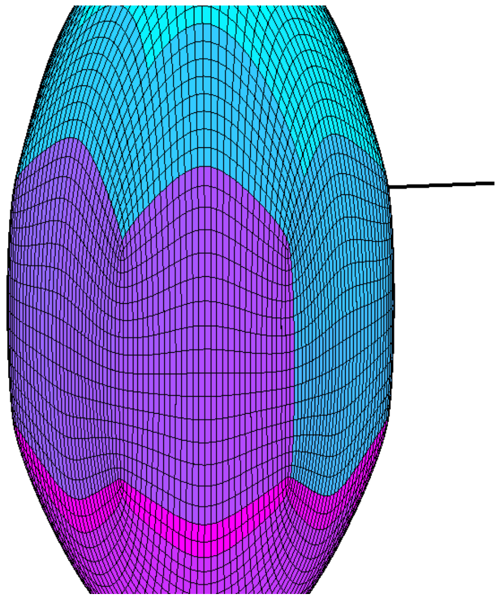

Figure 9.26. Approximating quadrilateral scheme: Normal at vertex of valence 3

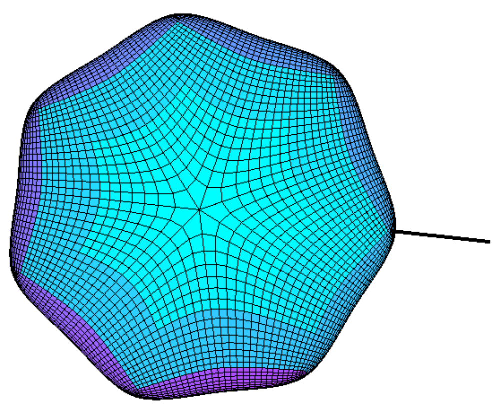

Figure 9.27. Approximating quadrilateral scheme: "Top view" of same normal at vertex of valence 3

Appendix G

Here are shown figures with a specified normal vector [solid line] and the "usual" normal [broken line] the surface would have had if we had not done the calculations from section 7.2 on p. 173. Brief descriptions are given along with the value of the minimized function $f(x) = \sum (x - .25)^2$ (7.3 |p.175).

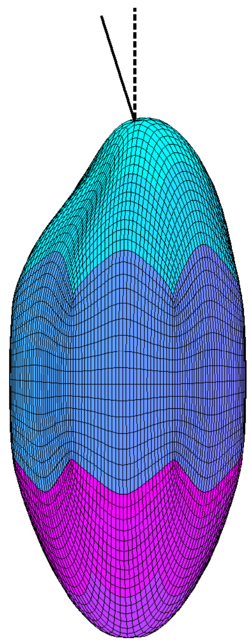

Figure 9.28. Approximating quadrilateral scheme: Larger angle (19.88°) between desired normal [solid line] and the "usual" normal [broken line]. $\sum (\omega_k - .25)^2 = 39.34$ Note how the figure is forced into a lopsided shape due to the direction of the normal at the top.

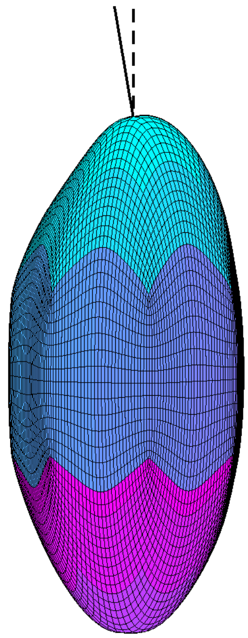

Figure 9.29. Approximating quadrilateral scheme: Smaller angle (9.93°) between desired normal [solid line] and "usual" normal [broken line]. $\sum (\omega_k - .25)^2 = 10.65$ Note there is a lesser lopsided look to the figure.

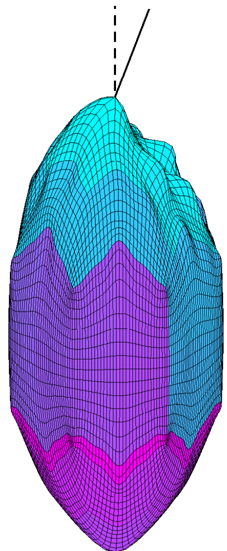

Figure 9.30. Interpolatory quadrilateral scheme: Larger angle (19.94°) between desired normal [solid line] and "usual" normal [broken line]. $\sum(\omega_k - .25)^2 = 19.0319$ Note the large amount of artifact and bumpiness for the interpolating figure to accommodate the new position of the normal at the top.

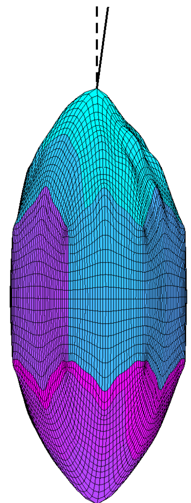

Figure 9.31. Interpolatory quadrilateral scheme: Smaller angle (9.97°) between desired normal [solid line] and “usual” normal [broken line]. $\sum(\omega_k - .25)^2 = 5.165$ Less bumpiness than with the larger angle, but artifact is still present with the interpolatory figure accommodating the new normal at the top.

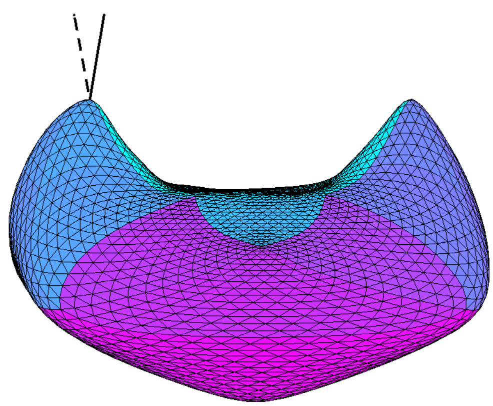

Figure 9.32. Approximating triangular scheme: Larger angle (19.97°) between desired normal [solid line] and “usual” normal [broken line]. $\sum(\omega_k - .25)^2 = 1.4468$ Note that the left “tower” bulges a bit more due to the new direction of the normal at top.

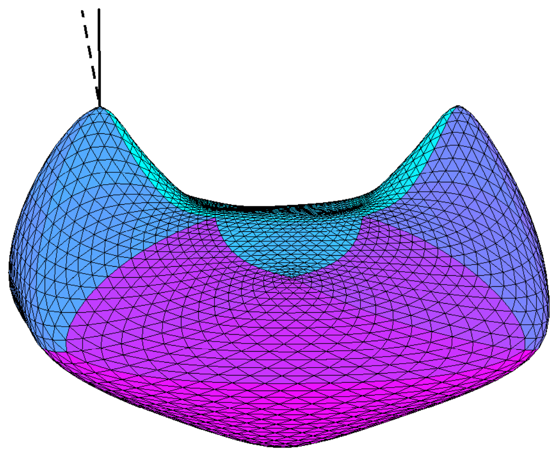

Figure 9.33. Approximating triangular scheme: Smaller angle (9.79°) between desired normal [solid line] and "usual" normal [broken line]. $\sum(\omega_k - .25)^2 = .2794$ Note there is less bulging of the left "tower".

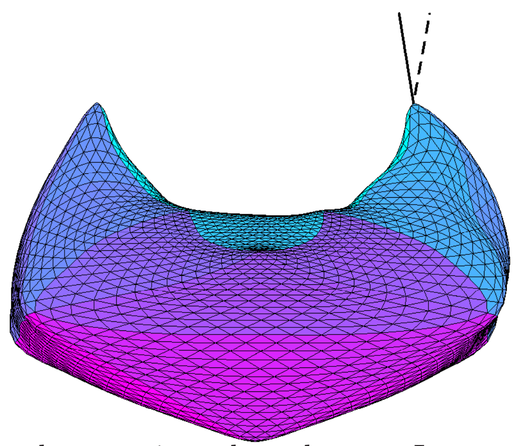

Figure 9.34. Interpolatory triangular scheme: Larger angle (19.46°) between desired normal [solid line] and "usual" normal [broken line]. $\sum(\omega_k - .25)^2 = 1.2749$ Note "bulges" in right "tower" to accomodate new direction of normal at the top.

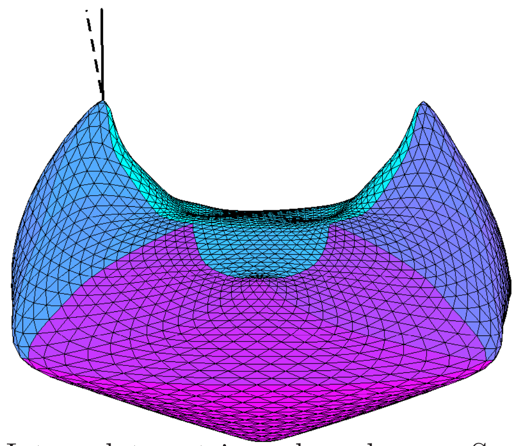

Figure 9.35. Interpolatory triangular scheme: Smaller angle (9.53°) between desired normal [solid line] and "usual" desired normal [broken line] $\sum(\omega_k - .25)^2 = .2468$ Note that there is much less bulging of the left "tower" to accomodate the direction of unit normal at the top.